Faculty of Science

Department of Imaging and Applied Physics

Microstructural Design and Properties of High Performance Recycled Cellulose Fibre Reinforced Polymer Eco-Nanocomposites

Hatem Rashed Alamri

This thesis is presented for the degree of

Doctor of Philosophy

of

Curtin University

July 2012

DECLARATION

To the best of my knowledge and belief this thesis contains no material previously published by any other person except where due acknowledgment has been made.

This thesis contains no material which has been accepted for the award of any other degree or diploma in any university.

Hatem Alamri

Signature

Date: 13th July 2012

ABSTRACT

In recent years, cellulose fibre-reinforced polymer composites have been gaining a great attention in several engineering applications due to their desirable properties, which include low density, low cost, renewability and recyclability as well as good mechanical properties. Moreover, cellulose fibres are environmentally friendly, non-toxic and renewable materials. Therefore, manufacturing industries especially packaging, building construction, automotive and furniture have been encouraged to use cellulose fibres in their applications instead of the more expansive and non-renewable synthetic fibres. However, one of the major drawbacks that has limited the use of cellulose fibres as reinforcement in polymer composites is their susceptibility to moisture absorption due to the hydrophilic nature of cellulose fibres. Moisture absorption can result in a reduction of mechanical properties and dimensional stability of composites. Several studies in plant fibre reinforced polymer composites have reported an enhancement in mechanical properties, fibre-matrix interfacial bonding and fibre resistance to moisture via various chemical or physical treatments. In this project, a novel approach has been used to enhance the resistance of cellulose fibre reinforced polymer composites to water absorption and to improve the mechanical properties by introducing a nano-filler that provides good resistance to water diffusion and enhances fibre-matrix interfacial bonding for better mechanical properties.

In this study, epoxy eco-nanocomposites reinforced with both recycled cellulose fibres (RCF) and different nano-fillers such as nanoclay platelets (Cloisite 30B), halloysite nanotubes (HNT) and silicon carbide nanoparticles (n-SiC) were synthesized. The influence of RCF/nano-filler dispersions on physical, thermal, mechanical and fracture properties was investigated in terms of water absorption, flexural strength, flexural modulus, impact strength, fracture toughness, impact toughness and thermal stability. The effect of water soaking on the mechanical properties of composites was also investigated. Different analytical methods such as wide angle X-ray scattering (WAXS), synchrotron radiation diffraction (SRD), transmission electron microscopy (TEM), Fourier transforms infrared spectroscopy (FTIR) and scanning electron microscopy (SEM) were used to examine the nano and microstructures of these materials.

First, multi layered recycled cellulose fibre (RCF) reinforced epoxy composites were fabricated with fibre loadings of 19, 28, 40, 46 and 52wt%. Results indicated that flexural strength, flexural

modulus, facture toughness and impact strength increased as the fibre content increased. Water absorption and diffusion coefficient were found to increase with an increase in fibre content. Mechanical properties such as flexural strength, modulus and fracture toughness were found to decrease after water treatment due to the degradation of bonding at the fibre–matrix interfaces. The thermal stability of samples was determined using thermo-gravimetric analysis (TGA). Results indicated that the presence of cellulose fibres led to a reduction in the maximum decomposition temperature (T_{max}) of epoxy. However, composites with cellulose fibre showed better thermal stability than neat epoxy at high temperature ($\geq 600\ ^{o}$C). SEM observations showed a variety of toughness mechanisms such as crack bridging, fibre pullouts and fibre fracture and matrix cracking on the fracture surface of RCF/epoxy composites, which led to good fracture properties for samples reinforced by RCF layers.

Second, epoxy-based nanocomposites reinforced with organo-clay platelets (Cloisite 30B), halloysite nanotubes (HNT) and nano-silicon carbide (n-SiC) were prepared by mixing the epoxy resin with three different filler loadings (1, 3 and 5 wt%) using a high speed mechanical mixer for 10 minutes with rotation speed of 1200 rpm. WAXS results showed that nanoclay platelets were intercalated by the epoxy resin. The d-space of the peak (001) of nanoclay increased from 1.85 to 3.4 nm after mixing with epoxy. TEM results showed a major intercalated structure with some exfoliated regions. Based on TEM results, the basal spacing of (001) varied from 2.65 to 7.98 nm. SRD results of HNT and n-SiC showed no change in the peak position after mixing with epoxy. TEM results of epoxy filled with nanoclay, HNT and n-SiC indicated that the dispersion of nano-filler was quite homogenous with some particle agglomerations that found to increase as filler content increased due to an increase in matrix viscosity. The addition of nano-fillers enhanced the mechanical properties of epoxy matrix. Maximum improvements in flexural strength, modulus and fracture toughness were achieved at 1 wt% of nano-filler loading, while the addition of 5 wt% of nano-filler displayed the maximum impact strength and toughness. The presence of nano-filler was found to have insignificant effect on the thermal stability of neat epoxy. Water absorption was found to decrease as the filler content increased. After six months of water treatment, there was a reduction in flexural strength and modulus, but an improvement in fracture toughness and impact strength. SEM results showed that nanocomposites had rougher fracture surfaces than that of neat epoxy. Several toughness mechanisms such as crack deflection, crack pinning, particle debonding, plastic void growth, plastic deformation and particle pullouts were observed.

Finally, epoxy-based nanocomposites filled with nano-filler (*i.e.* nanoclay, HNT and n-SiC) were successfully used as a matrix for fabrication of multi-layers RCF/nano-filler reinforced epoxy eco-nanocomposites. The presence of nano-fillers was found to have insignificant or modest effect on flexural strength, modulus and fracture toughness when compared to unfilled RCF/epoxy composites. Impact strength and impact toughness increased due to the presence of nano-fillers. The addition of nano-fillers increased the rate of the degradation by decreasing the maximum decomposition temperatures by about 8-9 ^{o}C compared to unfilled RCF/epoxy composites. However, the thermal stability of nano-filler filled RCF/epoxy eco-nanocomposites was found to increase at high temperature (≥ 500 ^{o}C). The presence of nano-fillers led to a significant decrease in maximum absorbed water compared to unfilled RCF/epoxy composites. Exposure to water for six months severely reduced the mechanical properties of wet composites when compared to dry composites. However, the addition of nano-fillers enhanced the mechanical properties of nano-filler reinforced RCF/epoxy eco-nanocomposites compared to unfilled RCF/epoxy composites in wet condition. SEM results showed that water absorption led to degradation in cellulose fibres and weakening of the bonding at fibres-matrix interfaces. Enhanced barrier and mechanical properties of nanocomposites were more pronounced for composites filled with n-SiC as compared to those filled with nanoclay platelets and halloysite nanotubes.

The success in this project indicated that this approach of 'designing for recycling' or 'eco-design' to develop environmentally friendly composite materials is achievable. Moreover, this project may provide a great momentum for a 'cradle to grave' approach in the eco-design of fully 'green' or biodegradable and environmentally friendly composite materials through the use of nanoclay and recycled cellulose fibres as reinforcement for bio-resins.

ACKNOWLEDGEMENTS

LIST OF PUBLICATION INCLUDED AS PART OF THE THESIS

(Listed in order as found on this thesis)

Alamri, H., and I. M. Low. 2012. Mechanical properties and water absorption behaviour of recycled cellulose fibre reinforced epoxy composites. *Polymer Testing* 31(5): 620-628.

Alamri, H., I. M. Low, and Z. Alothman. 2012. Mechanical, thermal and microstructural characteristics of cellulose fibre reinforced epoxy/organoclay nanocomposites. *Composites Part B: Engineering* 43: 2762-2771.

Alamri, H., and I. M. Low. 2012. Microstructural, mechanical, and thermal characteristics of recycled cellulose fibre-halloysite-epoxy hybrid nanocomposites. *Polymer Composites,* 33(4): 589-600.

Alamri, H., and I. M. Low. 2012. Characterization of epoxy hybrid composites filled with cellulose fibres and nano-SiC. *Journal of Applied Polymer Science* 126: 221-231.

Alamri, H., and I. M. Low. 2012. Effect of water absorption on the mechanical properties of nano-filler reinforced epoxy nanocomposites. *Materials and Design* 42: 214-222.

Alamri, H., and I. M. Low. 2012. Effect of water absorption on the mechanical properties of n-SiC filled recycled cellulose fibre reinforced epoxy eco-nanocomposites. *Polymer Testing,* 31(6): 810-818.

Alamri, H., and I. M. Low. 2013. Effect of water absorption on the mechanical properties of nanoclay filled recycled cellulose fibre reinforced epoxy hybrid nanocomposites. *Composites Part A: Applied Science and Manufacturing* 44: 23-31.

STATEMENT OF CONTRIBUTION OF OTHERS
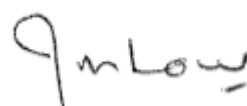
Hatem Alamri's input into this study and the associated papers included the execution of all the experimental work as well as a dominant contribution to the intellectual input involved in the project. Other scientists made some contributions to the current work, as is almost always the case in the physical sciences. These contributions were significant enough to warrant co-authorship on the resulting journal articles. These are specific below:

I.M. Low, provided project supervision and manuscript editing.

Z. Alothman, provided specialist technical advice and instrument usage (Thermogravimetric analysis TGA at King Saud University)

Hatem Alamri

Prof. It-Meng Low

LIST OF PUBLICATIONS BY THE CANDIDATE RELEVANT TO THE THESIS BUT NOT FORMING PART OF IT

Conference Papers

Presented as a poster

Alamri, H., and I.M. Low. 2009. Physical and mechanical characteristics of nano-clay–cellulose fibre- reinforced epoxy nanocomposites. *Proc. 16th AINSE Conference on Nuclear and Complementary Techniques of Analysis (NCTA)*, Sydney, Australia, 25-27 Nov.

Alamri, H., and I.M. Low. 2010. Characterization and properties of recycled cellulose fibre-reinforced epoxy-hybrid clay nanocomposites. *Proc. 7th Pacific Rim International Conference on Advanced Materials and Processing (PRICM 7)*, Cairns, Australia, 1-8 Aug, 4 pages.

Alamri, H., and I.M. Low. 2010. Mechanical characteristics of nano-filler–cellulose fibre-reinforced epoxy nanocomposites. *Proc. 7th Asian-Australasian Conference on Composite Materials (ACCM-7)*, Taipei, Taiwan, 15-18 Nov, 4 pages.

Oral presentation

Alamri, H., and I.M. Low. 2010. Mechanical and fracture properties of nano-filler–cellulose fibre-reinforced epoxy nanocomposites. *Proc. 6th Australasian Congress on Applied Mechanics (ACAM-6)*, Perth, Australia, 12-15 Dec, 9 pages.

Alamri, H., and I.M. Low. 2012. Effect of HNT addition on enhancing barrier and mechanical properties of RCF/epoxy composites in fully wet environment. *Proc. 8th Asian-Australasian Conference on Composite Materials (ACCM-8)*, Kuala Lumpur, Malaysia, 6-8 Nov, 6 pages.

Book-Chapters

Alamri, H., A. Alhuthali, and I. M. Low. 2010. Mechanical properties and moisture absorption behaviour of cellulose-fibre reinforced polymer composites. In *Green composites: Properties, design and life cycle assessment*, ed. F. Willems and P. Moens, 175-196. New York, USA: Nova Publishers.

Alhuthali, A., **H. Alamri**, and I. M. Low. 2011. Physical, flammability and mechanical properties of polymer eco-nanocomposites. In *Fibre reinforced composites*, ed. Quingzheng (George) Cheng, 105-124. Hauppauge, New York, USA: Nova Science Publishers Inc.

Journal Papers

Alamri, H., and I. M. Low. 2010. Characterization and properties of recycled cellulose fibre-reinforced epoxy-hybrid clay nanocomposites. *Materials Science Forum* 654-656: 2624-2627.

TABLE OF CONTENTS

LIST OF FIGURES

LIST OF TABLES

LIST OF ABBREVIATIONS

CMC	Ceramic-Matrix Composites
CrI	Crystallinity Index
DSC	Differential Scanning Calorimetry
DTA	Differential Thermal Analysis
FTIR	Fourier Transforms Infrared Spectroscopy
HNT	Halloysite Nanotube
MMC	Metal-Matrix Composites
n-SiC	Nano-Silicon Carbide
PMC	Polymer-Matrix Composites
RCF	Recycled Cellulose Fibre
SAXS	Small Angle X-Ray Scattering
SEM	Scanning Electron Microscopy
SiC	Silicon Carbide
SRD	Synchrotron Radiation Diffraction
TEM	Transmission Electron Microscopy
T_g	Glass Transition Temperature
TGA	Thermogravimetric Analysis
T_{max}	Maximum Decomposition Temperature
WAXS	Wide Angle X-Ray Scattering
XRD	X-Ray Diffraction

1. INTRODUCTION

1.1 Background

Epoxy has unique properties such as comparatively high strength, high modulus, excellent heat and chemical resistance, and low shrinkage (Shih 2007; Deng *et al.* 2008). For these reasons, it is increasingly being used as a matrix for fibre-reinforced polymer composites. Epoxy has found wide applications in the manufacture of adhesives, aerospace and electronic structures as well as coatings. On the other hand, majority of the epoxy systems are characterized by low fracture toughness and low impact strength (Shih 2007; Deng *et al.* 2008). The main disadvantages of the industrial use of epoxy resins include their brittleness and relatively high cost (Gañan *et al.* 2005). Two different approaches have recently been reported in the literature to substantially enhance the properties and reduce the cost of the composite compared to that for the neat epoxy resin.

In the first approach, brittle polymers are modified using nano-sized inorganic particles. Nano-particles embedded in polymer matrix have attracted increasing interest because of the unique mechanical, optical, electrical and magnetic properties compared to neat polymers (Sinha Ray and Okamoto 2003; Chatterjee and Islam 2008; Shukla *et al.* 2008). Polymer nanocomposites represent a new category of organic-inorganic hybrid material made up of nanometer-scale inorganic particles dispersed in a matrix of organic polymer (Alexandre and Dubois 2000; Luo and Daniel 2003; McNally *et al.* 2003). The nanometer size of nano-particles is largely responsible for the unique properties of polymer nanocomposites because of their comparative large surface area per unit volume. Such properties are the results of the phase interactions that take place between the polymer matrix and the nano-particles at the interfaces since many essential chemical and physical interactions are governed by surfaces (McNally *et al.* 2003; Pavlidou and Papaspyrides 2008; Yong and Hahn 2009). These properties include thermal (thermal stability, coefficient of thermal expansion, flammability, decomposition), mechanical (strength, toughness, modulus), and physical (optical, shrinkage, dielectric, permeability) properties (Ma *et al.* 2003; Sinha Ray and Okamoto 2003; Lu and Mai 2007).

The interest in polymer nanocomposites comes from the fact that the addition of only a few percent (5 wt% or less) of the nano-additives into a polymeric matrix would have a great effect

on the properties of the matrix (Alexandre and Dubois 2000; Cauvin *et al.* 2010; Zainuddin *et al.* 2010). Compared to conventional filled-polymers with micron-sized particles, polymer nanocomposites possess superior specific strength and stiffness, good fire retardant and enhanced barrier properties (Liu *et al.* 2005b; Zainuddin *et al.* 2010; Kiliaris and Papaspyrides 2010). Other superior properties include abrasive wear resistance, creep and fatigue performance, and functional properties. Owing to these enhanced mechanical, thermal and physical properties, polymer nanocomposites find wide application in packages, automotive, adhesives, microelectronics and the like (Yasmin *et al.* 2003; Zhao and Li 2008; Zainuddin *et al.* 2010). In 1990, the Toyota research group carried out the first study on the polymer nanocomposites. These researchers synthesized polymer nanocomposites based on nylon-6/ montmorillonite clay via the in-situ polymerization method. When 5 wt% clay was added to Nylon-6 polymer, the tensile modulus increased by 68% and the flexural modulus by 224% (Okada *et al.* 1990; Kojima *et al.* 1993). This research was the fore-runner of the global trend researches in different types of polymer nanocomposites made of different combination of nano-fillers and matrix polymers (Zhao and Li 2008; Pavlidou and Papaspyrides 2008; Deng *et al.* 2008; Chen and Evans 2009).

Kaynak and colleagues (2009) investigated mechanical and flammability properties of nanoclay (Na- montmorillonite) based epoxy nanocomposites. The research findings revealed an enhancement in fracture toughness and flexural strength. The maximum value was attained at 0.5% nanoclay loading. The addition of nanoclay also enhanced thermal stability and reduced flammability of nanocomposites compared to neat epoxy. In another experiment, Ha and co-workers (2010) investigated the effect of silane treated clay on the fracture toughness of clay/epoxy nanocomposites. It was reported that fracture toughness increased by 82% for nanocomposites with treated clay over untreated clay/epoxy nanocomposites. This improvement in fracture behaviors was due to the excellent dispersion of the treated clay into epoxy matrix and to the enhancement in interfacial adhesive strength between resin and clay layers. Zhao *et al.* (2005) investigated the mechanical, thermal and flammability properties of polyethylene/clay nanocomposites. Results showed an increase in the tensile strength, flexural strength and flexural modulus due to the presence of organoclay. Moreover, the enhanced thermal stability and flammability of nanocomposites was also attributed to the addition of nanoclay. Becker *et al.* (2004) and Kim *et al.* (2005) reported that the moisture barrier properties of epoxy nanocomposites tended to improve as a result of the addition of nanoclay platelets. Ye *et al.*

(2007) observed significant improvement in impact strength of halloysite (HNT)/epoxy nanocomposites at only 2.3 wt% HNT loading. The tremendous improvement in impact strength was as a result of particle (bridging, pull-out, and breaking) and crack deflection, as well as micro-cracking. Tang *et al.* (2011) studied the mechanical properties of treated halloysite reinforced epoxy nanocomposites. It was reported that the fracture toughness of epoxy significantly increased by 78.3% due to the presence of 10 wt% of intercalated HNTs. Additionally, Du *et al.* (2006) and Ismail *et al.* (2008) reported an enhancement in thermal and flammability properties of HNT-filled polymer nanocomposites. Chen *et al.* (2008) investigated the mechanical properties of silica-epoxy nanocomposites. They reported that the tensile modulus and fracture toughness increased by 25% and 30%, respectively, due to the addition of only 10 wt% nano-silica. Likewise, a significant increase in fracture toughness of epoxy nanocomposites as a result of adding nano-silica has also been reported by Blackman *et al.* (2007) and Johnsen *et al.* (2007). Moreover, Wetzel *et al.* (2006) reported an increase in flexural strength (up to 15%), flexural modulus (up to 40%) and fracture toughness (up to 120%) for epoxy nanocomposites reinforced with aluminium oxide (Al_2O_3). Liao *et al.* (2011) and Majewski *et al.* (2006) both reported an increase in thermal stability of polymer/n-SiC nanocomposites compared to unfilled polymer.

The second approach involves the use of cellulose fibres as reinforcements in the polymeric matrices for making low cost engineering materials. Some of natural fibres used in this approach include flax, sisal, hemp, jute, kenaf and wood. Cellulose fibres have a lot of desirable properties such as low cost, low density, recyclability, and renewability. In addition, they possess excellent mechanical properties like high toughness, flexibility high specific modulus, and specific strength (Dhakal *et al.* 2007; Low *et al.* 2007; Marsh 2003). For these reasons, cellulose fibre reinforced polymer composites have become very popular in various engineering applications such as automobile, building, furniture. Besides, there is much pressure on manufacturing industries especially packaging, construction and automotive industries to utilize new materials in substituting the non-renewable reinforcing materials for instance glass fibre emerging from consumers and new environmental legislation due to increased sensitivity on environmental pollution (Dhakal *et al.* 2007). Natural fibres are environmental friendly materials (green composites). Thus, they have become a preferred compound as a replacement for the conventional petroleum-based fibre reinforced composites like carbon, aramid fibres, and glass fibres (Low *et al.* 2007; Marsh 2003).

Recycled cellulose fibre (RCF) obtained from cellulosic waste products such as cardboard, printed paper as well as recycled newspaper and magazine have many advantages in comparison with natural cellulose fibres (Alamri and Low 2012b). RCF are abundantly available throughout the world, very friendly to the environment and cheap. Thus, RCF- based polymer composites can be classified as desirable performing composites on the basis of their economic and environmental advantages (Alamri and Low 2012b; Wang *et al.* 2007). Composites reinforced with RCF represent a new class of materials that are likely to replace wood and other plant composites in the future. This new class of composites may be used in manufacturing of furniture and automotive and in housing (Alamri and Low 2012b; Wang *et al.* 2007).

There is significant amount of work can be found in the literature on the effect of the addition of cellulose fibres on mechanical, physical and thermal properties of the polymer systems (Low *et al.* 2007; Shih 2007; Dhakal *et al.* 2007; Liu and Hughes 2008; Low *et al.* 2009; De Rosa *et al.* 2010; Mohan and Kanny 2011). For instance, Shih (2007) investigated the mechanical properties of waste water bamboo husk fibre/epoxy composites. Chemically treated water bamboo husk and untreated powder obtained from water bamboo husks were used to reinforced epoxy matrix composites. Results indicated that the additional of treated fibre and untreated powder enhanced the mechanicals properties of composites. Liu and Hughes (2008) carried out a research study to determine the fracture toughness of epoxy matrix reinforced with woven flax fibres. According to their research findings, there was a 2-4 fold increase in the fracture toughness of the epoxy matrix due to the addition of flax fibres in comparison with pure epoxy samples. They concluded that this significant improvement in facture toughness was related to the increase in fibre volume fraction. Another study by Maleque *et al.* (2007) showed an increase in flexural strength and impact strength by 38 and 40%, respectively, when banana woven fabric was added to the epoxy matrix. De Rosa *et al.* (2010) studied the mechanical and thermal properties of phormium tenax leaf fibre reinforced epoxy composites. In that study, the epoxy matrix was reinforced using 20% loading of short and long fibres. The researchers observed that after the addition of long fibre, tensile and flexural strengths of pure epoxy increased by 25% and 32%, respectively. Moreover, tensile and flexural modulus was found to be two times higher than those measured for neat epoxy. However, when short fibres were added, there was a significant reduction in tensile strength by approximately 40%, with very little impact on the flexural strength of the material. This reduction in strength was attributed to the poor distribution of the fibre, resulting in matrix-

rich regions and fibre disorders. Also, the plant fibres were found to favourably enhance the thermal stability of the composites. Low *et al*. (2009) have reported a considerable increase in facture toughness, modulus, flexural strength, impact toughness, and impact strength of recycled cellulose fibre reinforced epoxy composites.

However, cellulose fibres are hydrophilic in nature and hence have a poor resistance to water absorption. High moisture absorption is one of the major drawbacks of cellulose fibres, which restricts the use of cellulose fibre reinforced polymer composites in many outdoor applications. Water absorption can lead to swelling of the fibre forming voids and micro-cracks at the fibre-matrix interface region, which can result in a reduction of mechanical properties and dimensional stability of composites (Dhakal *et al.* 2007; Low *et al.* 2007).

Therefore, in order to promote the wider use of these materials in high performance applications, it is essential to consider the effect of moisture absorption and water uptake on their physical and mechanical properties. Many studies on epoxy-based composites have claimed that moisture and water absorption can strongly affect and reduce the mechanical and thermal properties of epoxy resins (Low *et al.* 2009; Dhakal *et al.* 2007; Athijayamani *et al.* 2009; Reddy *et al.* 2010). Other studies reported that the rate of water absorption and moisture diffusion in polymer-nanocomposites is significantly reduced by adding nanoclay, and the great reduction of water uptake was found by adding 5 wt% of nanoclay (Liu *et al.* 2008; Lu and Mai 2007; Becker *et al.* 2004; Zhao and Li 2008; Kim *et al.* 2005). Hence, the variation in the permeability of moisture as a function of nano-particle content will be investigated in this project.

In this work, the effect of recycled cellulose-fibre sheets and nano-fillers (*i.e.* nanoclay platelets, halloysite nanotubes and nano-silicon carbide) as well as both recycled cellulose fibre and nano-particle dispersion on the microstructure, mechanical, thermal and barrier properties of epoxy resin was investigated and discussed in terms of wide angle X-ray scattering (WAXS), synchrotron radiation diffraction (SRD), Fourier transforms infrared spectroscopy (FTIR), transmission electron microscopy (TEM), scanning electron microscopy (SEM), flexural strength, flexural modulus, impact strength, fracture toughness, impact toughness, thermo-gravimetric analysis

(TGA) and water absorption. Moreover, the effect of water absorption on the mechanical properties of these composites was also investigated and discussed.

1.2 Project Significance and Objectives

1.2.1 Significance

This project focused on the technology advances in cost-effective materials design and evaluation. It combined a novel processing methodology with new materials design concept for improved mechanical properties and moisture resistance.

Natural fibres have been used as reinforcing agents in composites throughout history as they are light, cheap, tough or impact resistant and have excellent strength and modulus properties. However, the wider application has been limited by their susceptibility to swelling in water and rotting (Bledzki and Gassan 1999; Kim and Seo 2006; Arbelaiz *et al.* 2005).

Similarly, in the last decade significant amount of work has focused on the improvement of mechanical properties of adding nano-particle into pure epoxy resin system. Moreover, nano-particle-filled polymer nanocomposites have shown excellent improvement in reducing moisture. However, their engineering applications have been limited due to the lack of interfacial adhesion between polymer resin and nano-particles (Kim *et al.* 2005; Liu *et al.* 2008; Morgan and Harris 2004). This project will provide a solution to these problems and has a potential to revolutionize the wide-spread use of renewable eco-composites.

In this project an innovative process will be used to synthesize multi-layers recycled cellulose fibre/nano-filler reinforced epoxy eco-nanocomposites. This combination consists of a three-phase composite, in which the main reinforcing phase is the cellulose fibre sheets for toughness and damage tolerance and the matrix consists of epoxy nanocomposites filled with nano-filler for strength and moisture resistance. Therefore, thin layers of RCFs measuring about 2 μm will be used to construct multi-layered epoxy composites reinforced with cellulose fibres and different nano-filler such as nanoclay platelets, halloysite nanotubes and nano-silicon carbide. This approach is aimed at production of composites with uniform fibre/nano-filler dispersion into the matrix, controlled microstructure and increased fibre volume fractions as a result of improved

fibre packing. This novel structure will provide unique mechanical properties and good moisture resistance. Therefore this project will build essential links to the use of natural fibres and nano-fillers as reinforced composites for polymer resins. In addition, this project will provide new design concepts for developing materials with multi-functional properties, and that will also give a significant impact on the future potential application of the technology.

1.2.2 Objectives

The main objective of this project was to study, design, produce, and characterize a new class of polymer eco-nanocomposites reinforced with nano-sized fillers (i.e. nanoclay platetlets, halloysite nanotubes and nano-silicon carbide) and recycled cellulose fibre sheets. This project aimed to obtain fundamental knowledge regarding the cost-effectiveness and optimum design of eco-nanocomposites reinforced with nano-fillers and recycled cellulose fibres. The approach of 'designing for recycling' or 'eco-design' will lead to the development of environmentally-friendly composite materials which are eco-efficient and sustainable.

The specific objectives of this project were as follows:

• To obtain a fundamental understanding on the processing-nanostructure-property relationships of eco-composites

• To study the optimum content of nano-sized fillers and cellulose fibre for achieving the desired mechanical and thermal properties.

• To investigate the roles of nano-fillers and fibre interfacial properties on the efficiency of strengthening, toughening and thermal stability.

• To explore the influence of nano-fillers on water absorption behavior of epoxy resin and cellulose fibre reinforced epoxy composites

• To examine the effect of water absorption on the mechanical properties of various epoxy eco-composites, epoxy nanocomposites and epoxy eco-nanocomposites

• To identify the underlying mechanisms of enhanced physico-mechanical properties of eco-nanocomposites with nano-fillers and micro-fibre dispersions

1.3 Research Plan

Based on the significant and objectives mentioned in the previous section, the following research plan was proposed:

(1) Fabrication of RCF reinforced epoxy composites, nano-filler (i.e. nanoclay, HNT and n-SiC) reinforced epoxy nano-composites and RCF/nano-filler reinforced epoxy eco-nano-composites.

(2) Characterization of nano-filler dispersion, morphology and micro-structure by wide angle X-ray diffraction (WAXRD), synchrotron radiation diffraction (SRD), Fourier transform infrared (FTIR) and Transmitted electron microscopy (TEM).

(3) Investigation of the influence of RCF, nano-fillers (i.e. nanoclay, HNT and n-SiC) or RCF and nano-filler dispersion on mechanical, moisture barrier and thermal properties of the produced composites.

(4) Determination of the effect of moisture absorption on the mechanical properties of produced composites.

(5) Observation of the fracture surface, failure mechanism and crack path features by scanning electron microscopy (SEM).

2. LITERATURE REVIEW

2.1 Natural Fibres

Based on their sources, natural fibres are divided into mineral, animal and plant fibres. The physical, thermal and chemical properties of these fibres are also vastly different (Bismarck *et al.* 2005). Mineral fibres such as those derived from geological materials like quartz and asbestos are tough, highly temperature resistant and their uses include ceiling tiles and high temperature gaskets (Yeoman and Paisley 2005). Animal fibres (i.e. hair, silk and wool) are generally made up of proteins. Such fibres find their main use in textile industry. In recent times, animal fibres have been used in bioengineering and orthopaedic applications for producing biodegradable and biomedical composite materials (Cheung *et al.* 2009). Plant fibres are mainly made up of cellulose fibres as the main component and depending on the plant parts from where they are obtained, and they are further categorized into bast or stem fibres such as flax, hemp, ramie, jute and kenaf; leaf or hard fibres such as banana, sisal and pineapple; seed fibres as in cotton and kapok; fruit fibres such as coir from coconut; wood fibres; stalk fibres; grass fibres and so on (Figure 2.1) (John and Thomas 2008; John *et al.* 2009).
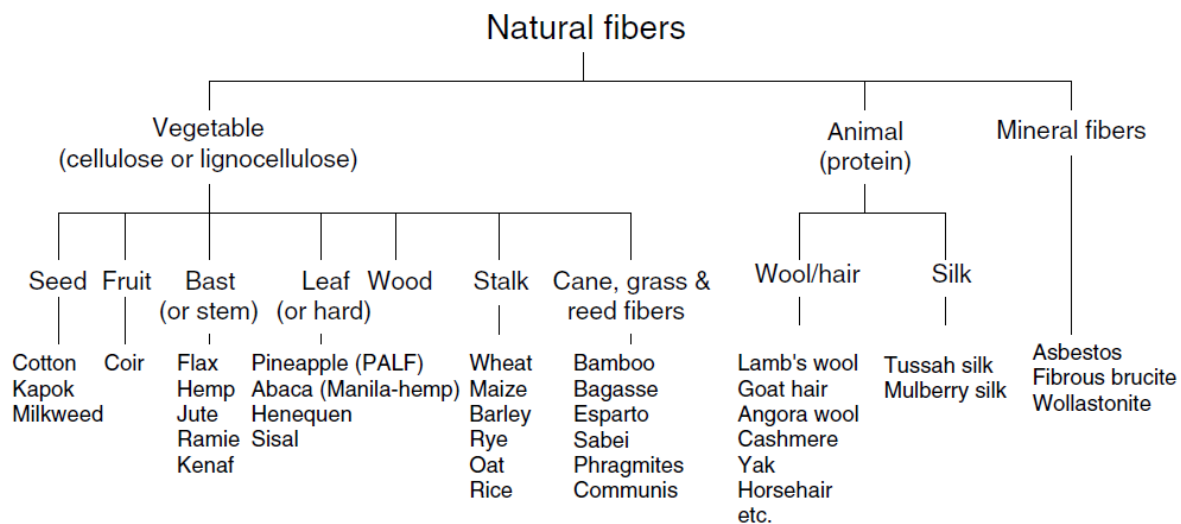
Figure 2.1. Categorization of natural fibres (Bismarck *et al.* 2005)

Several methods that can be used to separate the fibres from the other plant parts include retting, scrapping and pulping. Plant fibres are available all over the world. However, such countries like India, China, Bangladesh, Tanzania, Brazil, Mexico and Philippines produce abundant quantities of plant fibres (Taj *et al.* 2007). Moreover, agro-fibre based products such as paper, cardboard,

waste wood can also be recycled to obtain large quantities of cellulose fibres. The easy availability in adequate quantities and the good mechanical properties of cellulose fibres have made them very desirable materials for reinforcing composites especially in the manufacture of reinforced polymers due to their breaking length mechanical properties (Riedel and Nickel 2005). Classification of the plant fibres according to their uses in various applications depends on their different properties such as stiffness, tensile strength, thermal stability, the adhesive quality between the fibre and the matrix, the cost factors relating to the materials as well as in their manufacture. These factors also determine their roles in different applications (Nickel and Riedel 2003). These properties are further dependant on different factors like the nature of the plant, its age, its place of growth, and the method of fibre extraction. Table 2.1 displays the properties of some plant fibres.

Table 2.1. Properties of some nature fibres. (Mallick 2007)

Properties	Hemp	Jute	Sisal	Flax
Density (g/cm^3)	1.48	1.46	1.33	1.4
Tensile strength (MPa)	550-900	400-800	600-700	800-1500
Tensile modulus (GPa)	70	10-30	38	60-80
Elongation to failure (%)	1.6	1.8	2-3	1.2-1.6

2.1.1 Structure and Chemical Constituents of Natural Fibres

Actually plant fibres are themselves composite materials made by nature and their structure as well as their chemical composition are quite complex. They are essentially rigid, crystalline cellulose fibrils that are dispersed in a matrix made of lignin and/or hemicellulose (Mallick 2007; Bismarck *et al.* 2005). With the exception of cotton, most plant fibres are composed of cellulose, hemicelluloses, lignin, pectin, waxes, and a few water-soluble compounds. The physical properties of the fibres are governed by the cellulose, hemicelluloses and lignin that are its basic constituents (John and Thomas 2008). Depending on the type of plant fibres, cellulose forms about 30-90 wt% of the fibres and lignin about 3-40 wt%, while the moisture content is

about 6-20 wt% (Mallick 2007; De Rosa *et al.* 2010; Bismarck *et al.* 2005). Table 2.2 exhibits the chemical compositions of some important plant fibres.

Table 2.2. Chemical compositions of selected plant fibres. (De Rosa *et al.* 2010)

Type of fibre	Cellulose (wt%)	Hemicellulose (wt%)	Lignin (wt%)	Pectin (wt%)	Wax (wt%)
Bast Fibre					
Hemp	70.2-74.4	17.9-22.4	3.7-5.7	0.9	0.8
Jute	61-71.5	12-20.4	11.8-13	0.2	0.5
Flax	64.1-71.9	16.7-20.6	2-2.2	1.8-2.3	1.7
Kenaf	31.57	21.5	8-19	3-5	
Leaf Fibre					
Sisal	65.8-78	8-14	10-14	0.8-10	2
Pineapple	70-82		5-12.7		
Banana	63.64	10-19	5		
Seed fibre					
Cotton	82.7-90	5.7		0-1	0.6
Fruit fibre					
Coir	32-43	0.15-0.25	40-45	3-4	

These plant fibres are made up of hollow cellulose fibrils held together by a matrix made up of lignin and hemicelluloses. The cells in these fibres do not have a homogenous membrane in their cell walls (Figure 2.2). Instead, the cell walls are complex and layered structures with the thin primary layer set during the growth of the cell that is encloses a secondary wall and is made of fibres that are not regularly arranged. The secondary wall is actually a three layered structure, whose solid middle layer is the most important in determining the mechanical properties of the fibre (John and Thomas 2008). This middle layer consists of a series of cellular microfibrils that have a helically coiled structure that are made up of long chain cellulose molecules, with microfibrillar angles between the axis of the fibre and the microfibrils. This angle varies according to the type of fibre. Most microfibrils are made up of 30-100 cellulose molecules and

11

have a diameter of about 10 to 30 nm These extended chain formations supply the mechanical strength to the fibre (Bismarck *et al.* 2005; John and Thomas 2008). The noncrystalline regions of the cell wall are complex structures made up of hemicelluloses, lignin and sometimes pectin. Hydrogen bonds link the hemicelluloses to the cellulose microfibrils in a network of cross-linked molecules that are called the cellulose-hemicellulose network and form the backbone of the fibre cell (Stamboulis *et al.* 2001; Bismarck *et al.* 2005). The lignin network, on the other hand, is hydrophobic in nature and influences the properties by operating as a coupling agent and thus enhancing the strength of the cellulose-hemicellulose network. The properties of the fibres have many variable determinants such as the structure, the microfibrillar angle, dimensions of the cell, its defects, as well as the chemical composition of fibres (Bismarck *et al.* 2005; John and Thomas 2008).

It is usually found that there is a proportionate increase in the tensile strength and Young's modulus to the increase in the cellulose content and the microfibrillar angle has a direct influence on the stiffness of the fibres. Microfibrils oriented spiral to the fibre axis make the fibre flexible and those which are parallel oriented renders the fibres rigid with a high tensile strength (John and Thomas 2008).
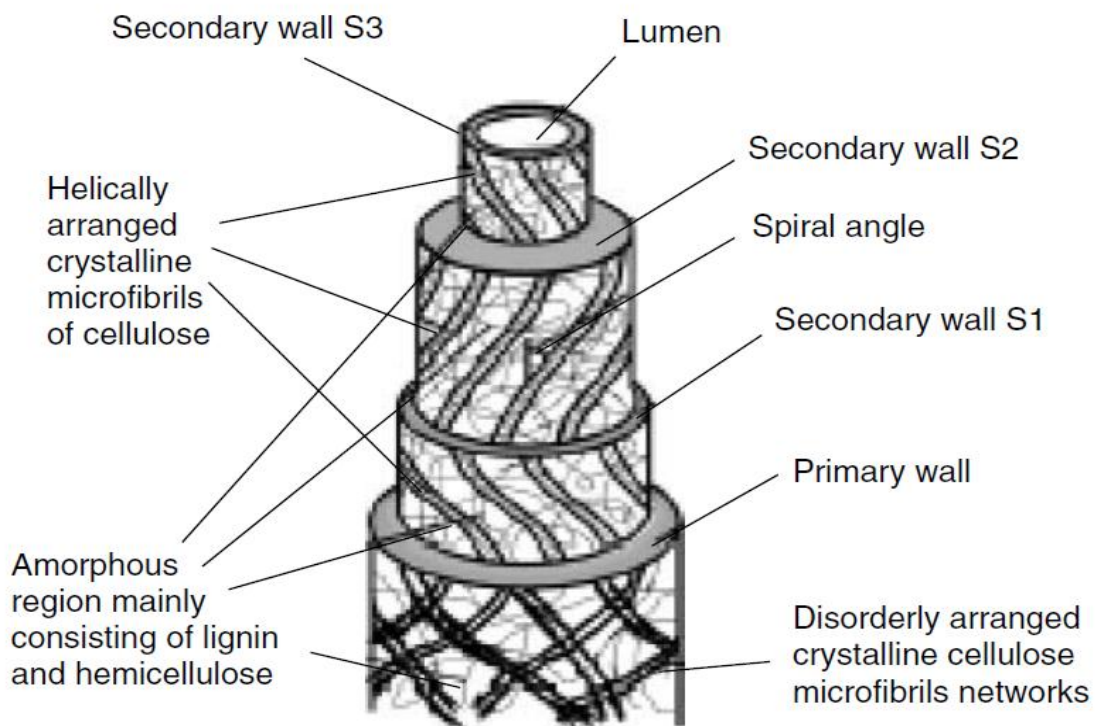
Figure 2.2. Structure of biofibre. (Bismarck *et al.* 2005)

Cellulose forms the main constituent of most of the natural plant fibres. It is hydrophilic nature polymer, comprising of D-anhydroglucose with the formula $C_6H_{11}O_5$ with repeating glucose units linked by 1,4-β-D glycosidic bonds, where each glucose molecule is bonded to the next one through 1 and 4 carbon atoms (Figure 2.3) (John and Thomas 2008; Mohanty *et al.* 2005). Each of these repeated units comprises of three hydroxyl groups. These hydroxyl groups and their ability to hydrogen bonds are the most influential in guiding the arrangement of the crystalline packing and also in managing the physical properties of cellulose materials (Bismarck *et al.* 2005). The degree of polymerization (DP) in the cellulose molecules is about 10,000 and these cellulose molecules are disposed in the microfibrils with diameters ranging from 10 nm to 20 nm (Rösler *et al.* 2007; Bismarck *et al.* 2005; John and Thomas 2008). Solid cellulose has a microcrystalline structure with highly crystalline as well as amorphous regions with slender rod-like crystalline microfibrils (Bismarck *et al.* 2005). Natural cellulose, also called cellulose I has a monoclinic sphenodic crystalline form. Although cellulose is highly resistant even to strong alkali up to 17.5 wt%, it dissolves easily in water-soluble sugars. The resistance of cellulose to oxidizing agents is also quite high (John and Thomas 2008). In the solid state, there are four main different allomorphic forms of cellulose (cellulose I, II, III, IV) (Mittal *et al.* 2011). Each type displays distinctive X-ray diffraction patterns. Cellulose I is the most abundant crystalline form, which occurs naturally with two structures, cellulose I_α (triclinic) and cellulose I_β (monoclinic) (Mittal *et al.* 2011; Wada *et al.* 2004). Cellulose II is modified cellulose. It is formed from cellulose I via mercerization (alkali treatment) or regeneration (recrystallization from a solution) (Mittal *et al.* 2011; Wada *et al.* 2004). These treatments change the chain structure of cellulose I from parallel to anti-parallel forming cellulose II (Ford *et al.* 2010; Wada *et al.* 2004). Cellulose III and IV can be both derived from either cellulose I or cellulose II by treatment with liquid ammonia and heating, respectively. Cellulose III_I and IV_I are obtained from cellulose I while cellulose III_{II} and IV_{II} are produced from cellulose II (Mittal *et al.* 2011; Ford *et al.* 2010). Bledzki and Gassan (1999) stated that the cell geometry of each type of cellulose is the determinant factor of its mechanical properties and each type of cellulose has different cell geometry. The content of the cellulose matter in the raw material determines the pulp yield of during chemical pulping. Thus cellulose content is a vital factor in the fibre.
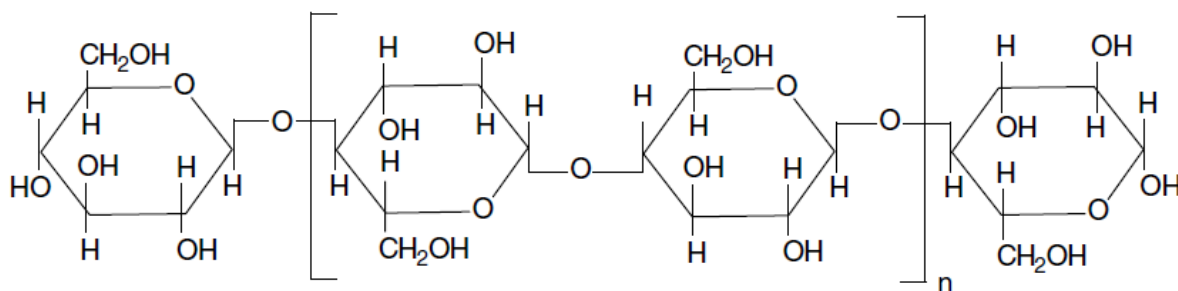
Figure 2.3. The structure of cellulose. (Mohanty *et al.* 2005)

(b) Hemicellulose

Hemicelluloses are misnamed because they are not celluloses at all but polysaccharides with a blend of 5-ring and 6-ring carbon ring sugars. These sugars include glucose, and monomers like galactose, mannose, arabinose and xylose (Saari *et al.* 2010). The polymer chains are non-crystalline in nature consisting of short and branched chains, with DP about 50 to 300 and pendant side groups that make it amorphous (Bismarck *et al.* 2005). The differences between hemicelluloses and cellulose are in three significant features: hemicelluloses are made up of different types of sugar units while celluloses are made up of only 1,4-β-D-glucopyranose units; the extensive chain branching and pendant side groups make hemicelluloses amorphous while the celluloses are strictly linear polymer. Although hemicelluloses have 50-300 DP or degree of polymerization, the DP of celluloses is 10-100 times higher. Another difference between them is that hemicelluloses form the matrix part of the composite whereas the celluloses microfibrils are dispersed in them (John and Thomas 2008). Moreover, hemicelluloses are easily hydrolyzed in acids, are hydrophyllic in nature and dissolved by alkali (John and Thomas 2008). Stamboulis *et al.* (2001) found that the main structural constituents of fibre cells are the cellulose hemicelluloses networks that are made up of cross-linking molecules of hemicellulose bonding with cellulose microfibrils through hydrogen bonds.

(c) Lignin

After cellulose, lignin has the most importance in natural fibres. Rigidity and the length of plant fibres are provided by lignin. This complex hydrocarbon polymer is composed of aliphatic as well as aromatic components. Its properties include its completely non-crystalline and hydrophobic character, its resistance to most solvents and not easily fragmented into monomeric units. It is envisioned as a complex copolymer with high molecular weight, a three-dimensional

14

structure and composed of aliphatic and aromatic compounds belonging to the hydroxyl, methoxyl and carbonyl groups (John and Thomas 2008; Bismarck *et al.* 2005). Each building unit of lignin is made up of five hydroxyl and five methoxyl groups. The structural units are thought to be derived from 4-hydroxy-3-methoxy phenylpropane. Due to the non-availability of any conventional method to isolate lignin in a native state from the fibre of which it is part, the study of its chemistry is difficult (Bismarck *et al.* 2005; John and Thomas 2008) . There are more possible cross-linking sites available in lignin than in either cellulose or hemicellulose and that is considered to be the main chemical difference between them. These cross-linking sites are responsible for the non-crystalline structure of login and they are feasible on the propane chain, through the C4 oxygen and at the free aromatic ring carbons. Lignin that is extracted from fibres can be used as an alternative for phenol in the matrix material. Bledzki & Gassan (1999) also stated that isotropic lignin displayed significantly lower mechanical properties than those of cellulose.

Lignin is a thermoplastic polymer that starts to melt at about 170°C and has glass transition temperature of about 90°C. Lignin is resistant to hydrolysis by acids but dissolves in hot alkali, can be easily oxidized and readily condenses with phenol (Bismarck *et al.* 2005). Lignin can only be removed through pulping methods that involve polluting bleaching process that are not environment friendly in procedures like in the manufacture of paper.

(d) Pectin

Hetero-polysaccharides are collectively known as pectins. These complex polysaccharide chains comprise of polymer form of glucuronic acid and residues of rhannose. Pectins provide flexibility to the plants (John and Thomas 2008). Pectin can dissolve in water only if they are partially neutralized with alkali like ammonium hydroxide (Bledzki and Gassan 1999).

(e) Waxes

Waxes can be removed from the plant fibres by organic solutions. These materials form the last part of the plant fibre. They are mostly alcoholic in their structure and show resistance to water and acids such as palmitic, oleoginic and stearic acids (Bledzki and Gassan 1999; John and Thomas 2008).

2.2 Matrix

The matrix is the primary constituent phase in composites. It is usually more ductile and less hard phase. Matrix plays a major role and provides several important functions in fibre reinforced composites. It keeps the fibres in their place and also transfers the stresses to the fibres and distributes these forces between fibres uniformly. Moreover, it also has a protective function and shields the fibres from unfavourable and destructive forces like chemicals, moisture and mechanical degradation (Mallick 2007). The efficiency of such load transferring and distribution can only be availed through a quality bonding of the fibres and the matrix which makes composites can withstand compression, flexural force and tensile loads. Furthermore, the processing capability of the matrix is responsible for both the quality and the imperfections in the final material (Mallick 2007).

2.2.1 Classification of Composites Based on Matrix Material

Composite materials can be classified into three main groups according to their matrix composition: composites that possess a metallic matrix (MMC), those that have a ceramic matrix (CMC) and those that have a polymer matrix (PMC)

(a) Metal-matrix composites (MMC)

The metallic matrix used in the MMCs could be combined with ceramics such as oxides or carbides, or in the form of a metallic dispersed stage using metals like lead, tungsten or molybdenum. Metal matrixes provide better comparative mechanical properties such as high strength, fracture toughness and stiffness compared to the unreinforced materials. Light metals such as aluminium, titanium and magnesium are more often used for their lightness as the matrix material and fibres of carbon, silicon carbide, aluminium oxide, boron or refractory materials like tungsten as the fibre components (Rösler *et al.* 2007). Although these composites need a large processing temperature, they can be operated at higher temperatures than the polymer based composites. Moreover, shaping and strengthening of such metallic composites is possible using many different types of mechanical and thermal treatments (Mallick 2007; Rösler *et al.* 2007).

(b) Ceramic-matrix composites (CMC)

Ceramic matrix composite materials are made up of ceramic oxides or carbides in a dispersed phase with a ceramic matrix. Such materials possess a low density but are able to withstand high temperatures in a stable condition. Their other properties include high modulus, high hardness, high thermal shock resistance and corrosion resistance. Unlike the metallic composites, CMCs are brittle and have a low fracture toughness due to which they crack very easily. Reinforcing ceramic matrix is the major reason to increase its fracture toughness (Mallick 2007).

(c) Polymer-matrix composites (PMC)

Polymer matrix composites consist of fibrous reinforcing dispersed phase embedded in a polymer resin matrix. Because of their properties in room temperature, their low-cost and simple of fabrication procedures, they are widely used in many applications. But the usage of non-reinforced polymers in structure materials is constrained because of their poor mechanical properties. Such polymers are usually categorised into thermoplastic resins like polypropylene, polyethylene, polyphenylene sulfone, polyamide and so on, and the thermoset resins that include polyesters, phenolics, polyurethanes and epoxies (Mallick 2007).

2.2.2 Polymers

Polymers consist of long molecular chains with one or more repeating units of atoms. The atoms are bonded together with strong covalent bonds (Figure 2.4). Such polymeric substances are also called plastics and made up of many different lengths of polymer molecules that have similar chemical structure. When these molecules are seen in their solid state, they are found to be frozen in space. The molecules are randomly distributed in amorphous polymers or in a combination of random and folded orderly chains as in semi-crystalline polymers as shown in Figure 2.5. When seen at the sub-microscopic scale, even the orderly polymers are shown to possess unstable areas where there is random excitation. This excitation or movements only increase with the rise in temperature (Mallick 2007; Rösler *et al.* 2007). The structure of polymers is more complex when compared to metals and ceramics because of their linear structure and not point-like atoms (Rösler *et al.* 2007).

The advantages of polymers are their low cost, simple processing properties and their resistance to chemicals. Their main disadvantages are their low strength, modulus and low temperature use

limits. Polymers also exhibit low conductivity to heat and electricity due to their covalent bonds (Chawla 1998).
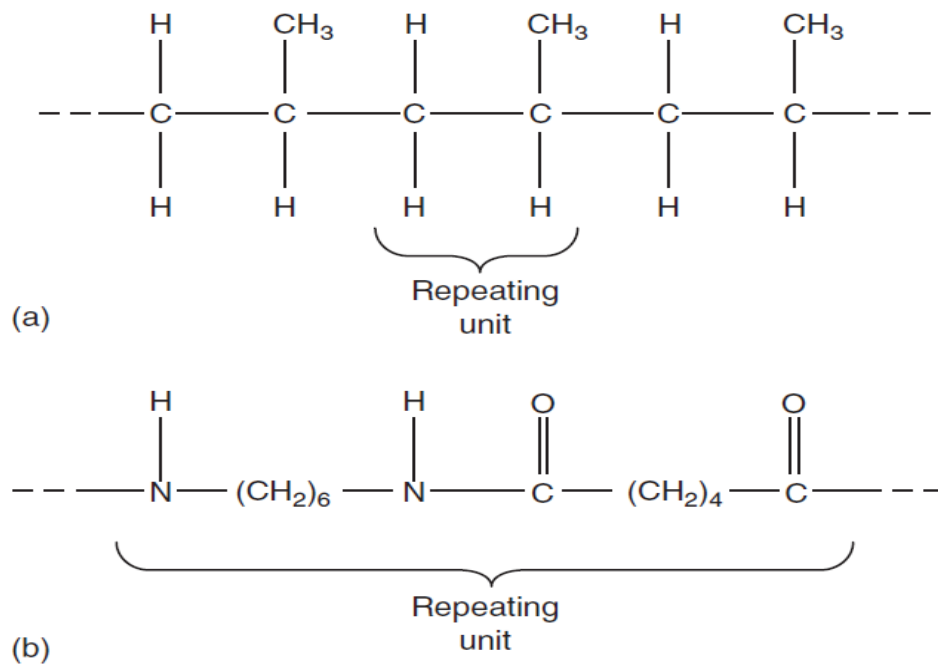
Figure 2.4. Examples of repeating units in polymer molecules. (a) A polypropylene molecule. (b) A nylon 6,6 molecule. (Mallick 2007)

Figure 2.5. Arrangement of molecules in (a) amorphous polymers and (b) semicrystalline polymers. (Mallick 2007)

The thermal behaviour of the polymers is used in classifying polymers into either thermoplastics or thermosets. This thermal behaviour is due to the physical and chemical microstructure of these polymers. Thermoplastics are made up of chain monomers with strong covalent bonds and weak inter-chain Van der Waals bonds (Figure 2.6a). The Van der Waal bonds can be easily dissolved using high temperature and allows for easy softening and moulding of the material. The desired shape formed during the heat treatment, is retained even after cooling and this material can be reshaped many times with hardly any impairment to its properties. Also, they score over the thermoset polymers in having an almost unlimited storage or shelf life at normal temperatures, being easily repaired or joined by welding or by solvent bonding and need less time for their fabrication. They can also be recycled and reprocessed and have a higher strain-to-failure property that offer a greater resistance to the micro-cracking of the matrix. However, their poor creep resistance and thermal stability rank them lower than thermoset polymers (Mallick 2007). A lot of research is being conducted to surmount the problems that arise from the difficulty of fabricating some types of fibres-thermoplastic materials due to their higher viscosity (Mazumdar 2002).

 Thermosets, on the other hand, possess chains that are bonded by cross linking network type of covalent bonds (Figure 2.6b). Unlike the thermoplastic polymers, these bonds cannot be re-melted by heated once the polymerisation reaction takes place during the curing process and as a result, they cannot be recycled. As the name implies, the plastic is permanently set by the application of heat. But there are also some thermosets that are cured by using chemical reactions at room temperature (Mazumdar 2002). Although the resins or thermosetting plastics are in a liquid form at first, they are hardened using heat or chemicals. Generally epoxy, polyester, vinyl-ester, phenolics, cyanate esters, bismaleimides, and polyimides are the resins used in thermoset composites in place of the matrix in fibre-reinforced composites. Thermoset resins usually have very low viscosity before the curing stage. Therefore, fabrication of fibre reinforced polymer composites happen before the polymerization reaction starts for achieving a tolerable wet-out between the matrix and the fibres without the need to either of high temperature or pressure (Mallick 2007). The advantages of thermoset polymers over the thermoplastic polymers are their higher hardness, strength, higher stability in their shape and thermal properties, and also offer higher resistance to electrical, chemical and solvent forces. Such polymers display less creep and stress relaxation too. However, their disadvantages can be

summarized as longer fabrication period, shorter storage life, and lower strain-to-failure, impact strength and fracture resistance (Mallick 2007).
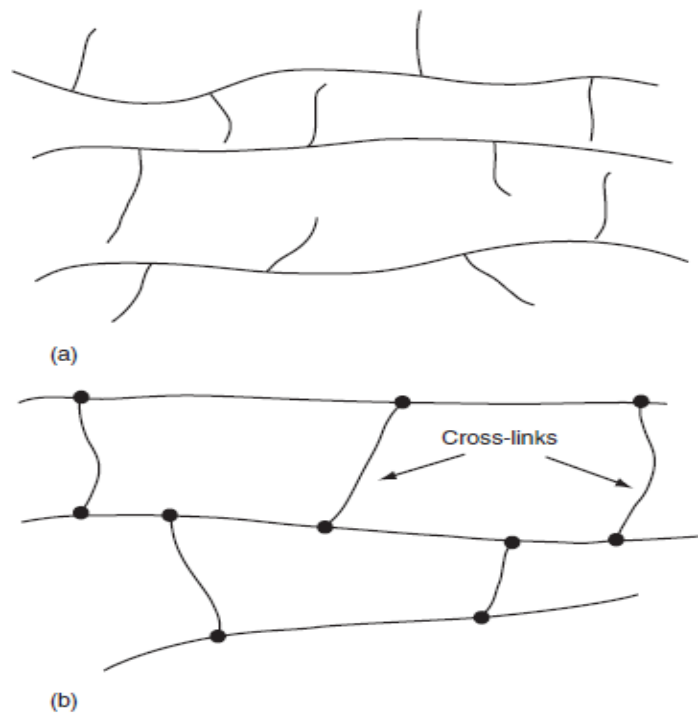
Figure 2.6. Schematic representation of (a) thermoplastic polymer and (b) thermoset polymer. (Mallick 2007)

(b) Structure of polymers

Polymers are made up of chainlike molecules where carbon atoms forming the backbone of the chain. Artificial polymers are processed through polymerization that can be carried out in two ways: condensation polymerization and addition polymerization. Each of these processes produces a different type of polymer with varied configurations in their molecular chains (Chawla 1998). The first type consists of long single chains of atoms in which atoms or monomers are joined together end to end forming linear polymers. The second type are branched polymers in which some of the side groups are cross linked to branch chains by bonds. These branches when connected would be able to form a three dimensional network made up of these cross-linked polymers (Callister 2003). Still another type is the ladder polymers in which the cross-linked branches are placed in repeated order as shown in Figure 2.7. In fact, this linking variety clarifies the diversity in the polymeric materials properties. It also gives these materials wider range of applications.

20
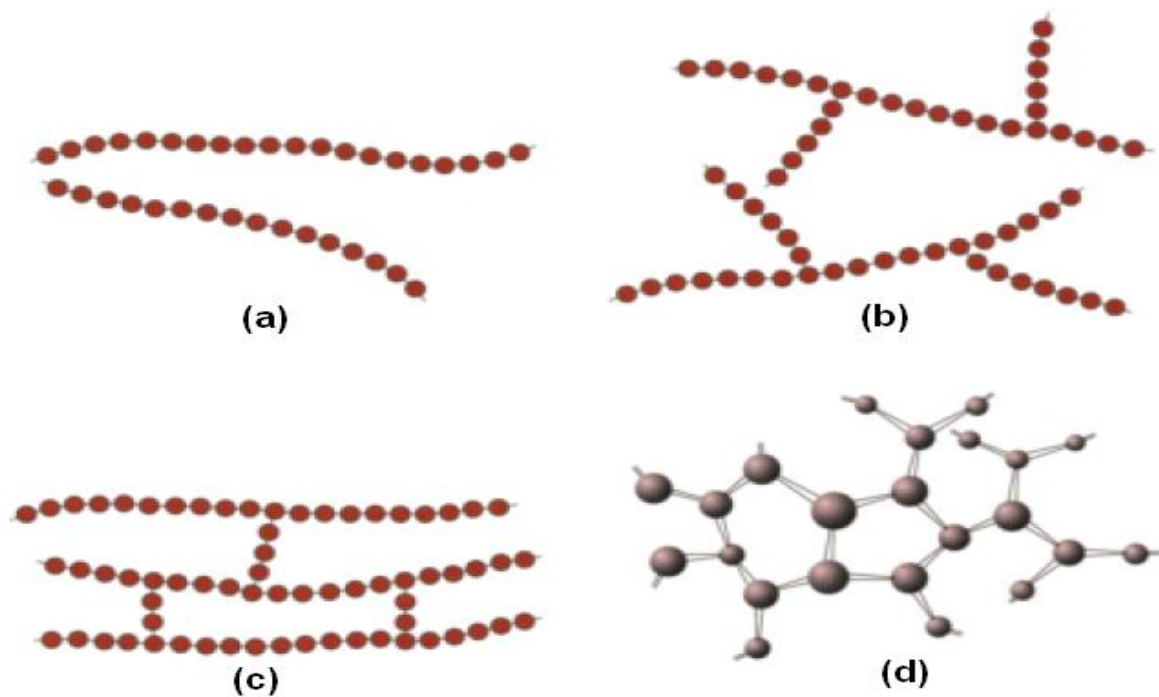
Figure 2.7 a) linear polymer chain. b) branched polymer chain c) crosslinked polymer chain d) ladder polymer chain. (Callister 2003)

Polymer can also be classified by monomer composition to homopolymer and copolymer. Homopolymer is a polymer consists of only one type of repeat units or monomers. However, polymer is called copolymer when it consists of different types of monomers. The monomers are arranged in different ways in the copolymers as shown in Figure 2.8 (Callister 2003).
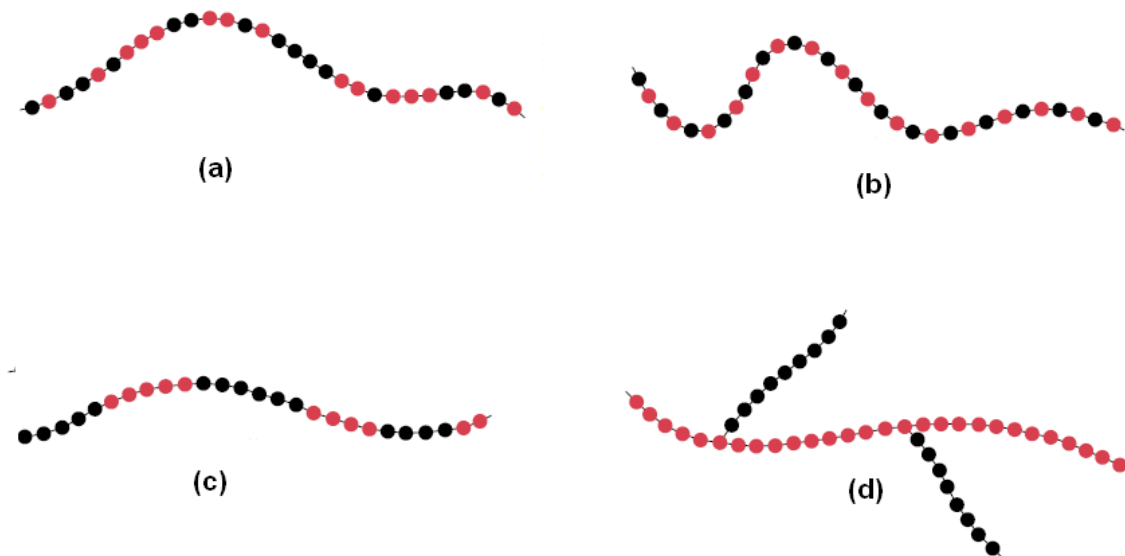
Figure 2.8. Schematic representation of (a) Random Copolymers, (b) Alternating Copolymers, (c) Block Copolymers, and (d) Graft Copolymers. Black and red circles represent the different monomer units (Callister 2003).

(c) Epoxy resin

Epoxy resins are one of the most popular resins available commercially that come in a large variety. Their advantages include characteristics like low shrinkage, good mechanical properties, resistance to environmental degradation and a high level of adhesive quality that can be applied to a large number of substrates. Epoxies have wide application range from aerospace to sporting materials and the most widely used resins because of their varied grades and performance levels that suit the different requirements of each application (Ray and Rout 2005). Their advantages also lies in the fact that they are capable of being processed mixed with other materials or epoxies to suit the particular performance specifications (Mazumdar 2002).

This family of polymers has a base structure of epoxide group of molecules that are chemically made up of two carbon atoms and one oxygen atom in the form of a three-member ring (Figure

2.9). These polymerizable thermosetting resins having one or more epoxide groups can be cured through chemical reactions involving amines, anhydrides, phenols, carboxylic acids, or alcohols (Mallick 2007; Mazumdar 2002). When cured with a hardening catalyzing agent, these epoxies turn into crosslink polymers that exhibit higher mechanical and thermal properties (Low and Mai 1992). The variation of hardener can lead to different cure characteristics and different properties to the final product. The epoxies can be cured using a wide range of temperatures from the normal room temperature up to elevated temperatures depend on the type of the curing agent (Mazumdar 2002; Low and Mai 1992). The finished products would have varied use temperatures depending on their cure temperatures. For example, hardeners that require high temperatures during curing produce materials with greater resistance to temperatures and superior mechanical properties (Mallick 2007; Mazumdar 2002; Low and Mai 1992).
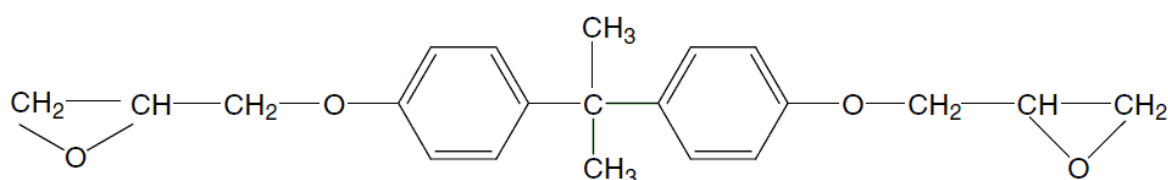
Figure 2.9. Chemical structure of a typical epoxy. (Ray and Rout 2005)

The advantages of epoxy resins over the other thermoset matrices are: superior resistance to moisture and chemicals, elevated strength and modulus properties, lower shrinking when cured, higher maximum use temperatures and their excellent adhesion with the fibres. However, they are brittle and have higher manufacturing costs and longer cure times. Table 2.3 displays the typical properties of cast epoxy resins (Mallick 2007; Mazumdar 2002).

Table 2.3. Typical properties of cast epoxy resin at 23 ^{o}C. (Mallick 2007)

Properties	Values
Density (g/cm^3)	1.2-1.3
Tensile strength, MPa (psi)	55-130 (8,000-19,000)
Tensile modulus, GPa (10^{6}psi)	2.75-4.10 (0.4-0.595)
Poisson's ratio	0.2-0.33
Coefficient of thermal expansion, 10^{-6} m/m per ^{o}C (10^{-6} in./in. per ^{o}F)	50-80 (28-44)
Cure shrinkage, %	1-5

2.3 Natural Fibres Reinforced Polymer Composites

Natural fibres are used as fillers to reinforce the polymer matrix of the natural fibre filled polymer composites. Generally, natural fibres such as bamboo, wood, kenaf, cotton, coconut husk, oil palm, jute, areca fruit and so on. Right from Neolithic times, the usage of fibres and plant fibre composites have been widespread. Their history spreads back to the Neolithic era in the regions now known as Syria, Turkey, Iraq, and Iran. Carbon dating of hemp and linen remains found in these regions places them 8000 – 6000 B.C (Bismarck *et al.* 2005). They were mostly used in the production of energy, shelters, clothes, tools and weapons. Fibres like straw were also used as strengthening materials in the construction of walls in Egypt about 3000 years ago (Zaman *et al.* 2011). The designs and shapes of these composites were simple and placed in layers to produce the required arrangement. Although more creative designs were introduced early in the last century, they still had limitations due to the shape and weight of the structural fibres. These were mostly in the form of two-dimensional sheets that were also fabricated into tubes and pipes. Their usage was mainly in the electrical arena with fibre materials like cotton or paper reinforcing sheets made of phenol- or melamine-formaldehyde resins (Bismarck *et al.* 2005; Zaman *et al.* 2011).

Later on, with the advent of durable materials like metals in construction, natural fibre composites became less popular. It was only in 1940 that the first engineering fibre composites were manufactured. These consisted of stronger materials like continuous filament glass fibre and tough and rigid unsaturated polyester resins and began to be manufactured on extensively (Bader 2001). These fibres still have their uses in the reinforcing thermosetting and thermoplastic composites that are needed by industries such as automotive, aeronautics and aerospace. Since then, such cellulose fibre materials are mostly used in the manufacture of rope, clothing, carpets and other decorative products (Haghighat *et al.* 2005; Bismarck *et al.* 2005).

In the environment conscious present times, natural fibre dispersed polymer composites are being given a lot of importance for research, not only because they are pose no harm to the environment but also because they can be easily reproduced as replacements for the non-renewable reinforcing materials like glass fibre, carbon fibre, Kevlar fibre and so on. More stringent environmental safety regulations and consumer demands in the automotive, construction, and packaging industries have made research on natural fibre composites more significant (Moeini *et al.* 2009; Bachtiar *et al.* 2008; Wambua *et al.* 2003). Inorganic fibres such as glass fibres cannot be renewed or recycled and use large amounts of energy to manufacture, pose serious health risks due to their harmful gas emissions and negative biodegradability

although they can be produced at low cost and offer moderate strength properties useful in structural materials (De Rosa *et al.* 2010; Wambua *et al.* 2003; Harish *et al.* 2009). At the same time, the natural fibre composites offer exceptional mechanical properties, low density, low cost and good chemical resistance. The more conventional glass and other reinforcing materials can be replaced or substituted by natural fibres such as hemp, jute, wood, and even waste cellulose products in the automotive, construction or packaging industries due to their desirable qualities such as stiffness, impact resistance, flexibility and modulus (De Rosa *et al.* 2010; Bachtiar *et al.* 2008; Wambua *et al.* 2003; Nair *et al.* 2010). Also their ready availability in large quantities, their biodegradability and renewable nature are much appreciated in these industries. Additional properties like low density, low cost, less equipment abrasion, less irritation of skin and respiration, damping of vibrations and recovery of more energy have made these composites more welcome in various industries as good alternatives to the traditional synthetic fibre composites (Nair *et al.* 2010; Wambua *et al.* 2003).

The global automotive industry that is being pressurized by stringent legislation and strong consumer demands for more environment-friendly cars is looking to the natural fibre composites as good alternatives. Stamboulis *et al.* (2001) argue that the price-performance ratio and low weight materials that have the added advantage of being environmentally friendly has made the natural fibre composites being used in large volume engineering markets like the construction and automotive industries. The statistics for natural fibres in the automotive industry in 1999 stood at 75% for flax, 10% jute, 8% hemp, 5% kenaf and 2.5% sisal (Brouwer 2001).

With the 2006 European Union legislation, that 80% of a vehicle must be reusable or recyclable rising to 85% by 2015, the European car manufacturers have started using thermoplastic and thermoset natural fibre composites in the door panels, seat backs, head-liners, package trays, dashboards, and other interior components (Holbery and Houston 2006). The same is the case with the Japanese automotive industry where the requirements are even higher at 88% of vehicle components to be recovered including by incineration by 2005 and 95% by 2015. The impact of the vehicles on the environment throughout their life-cycle right from the raw materials, manufacture, and usage of the vehicle to its ultimate disposal is being studied very carefully and research is being carried out for alternative and more desirable materials that are not harmful to the environment (Holbery and Houston 2006). It is here that natural fibre composites score high because apart from being biodegradable, they also possess the desired reinforcement properties to improve the mechanical properties of the components. Other industries that use natural fibre

composites are in the manufacture of panels, furniture and denser beams used in outdoor railings and decking (Baroulaki *et al*. 2006; Marsh 2003; Sanadi *et al*. 1994).

Polymers such as unsaturated polyesters, epoxides and polyurethanes are beginning to be used as matrices for the cellulose fibres. Out of these, epoxy resins have shown better adhesive properties to the natural fibres. The resulting materials have noteworthy mechanical properties for use in the manufacture of structural materials because of their higher grades of strength, stiffness and low distortion properties (Buehler and Seferis 2000).

2.3.1 Properties of Cellulose Fibres-Polymer Composites

An enormous attention has been focused on cellulose fibre reinforced polymer due to the desirable properties of cellulose fibres over traditional fibres. Therefore, a number of investigation have been carried out on several types of cellulose fibres such as kenaf, hemp, flax, bamboo, jute and waste cellulose products to study the effect of these fibres on the properties of composites materials. This section outlines the mechanical, thermal, and moisture properties of cellulose fibres reinforced polymers.

(a) Mechanical properties

Maleque *et al.* (2007) have investigated the mechanical properties of pseudo-stem banana fibre-epoxy composite. The hand lay-up method was used to fabricate the pseudo-stem banana woven-fabric-reinforced epoxy composite. It was reported that there was an increase in flexural strength from 53.38 MPa to 73.58 MPa when banana woven fabric was added to the epoxy matrix. The impact strength of the pseudo-stem banana woven fabric reinforced epoxy composite was found to be approximately 40% higher than that of pure epoxy. The results also showed that the tensile strength of the banana fibre significantly enhance the tensile strength of the material by 90% when compared to pure epoxy.

Liu and Hughes (2008) investigated the fracture toughness of epoxy matrix composites reinforced with woven flax fibre. Woven flax fibre-epoxy composites were prepared by a vacuum infusion process. It was found that the fracture toughness of the composites was increased by 2-4 times due to the presence of flax fibre compared to pure epoxy samples. The authors concluded that this significant improvement in facture toughness was related to the fibre volume fraction.

De Rosa *et al.* (2010) carried out the mechanical properties of phormium tenax leaf fibre reinforced epoxy composites. Quasi-unidirectional long fibres and short fibres were used to reinforce epoxy matrix with a 20% loading of natural fibre. It was observed that the long fibres increased tensile strength and flexural strength of pure epoxy by 25% and 32%, respectively. Moreover, tensile and flexural modulus was found to be two times higher than those measured for pure epoxy samples. However, the addition of short fibres dramatically decreased tensile strength by around 40% and had a significant effect on the flexural strength. The authors explained that in the case of short fibre composites, the stress was not uniform along the fibre, which resulted in the lack of stress transmission between the matrix and fibre causing reduction in mechanical properties. However, long fibre reinforced polymer exhibited better stress transmission along the composites, which provided better mechanical properties. Figure 2.10 shows flexural strength and flexural modulus of pure epoxy and epoxy composites reinforced by short and long fibres.
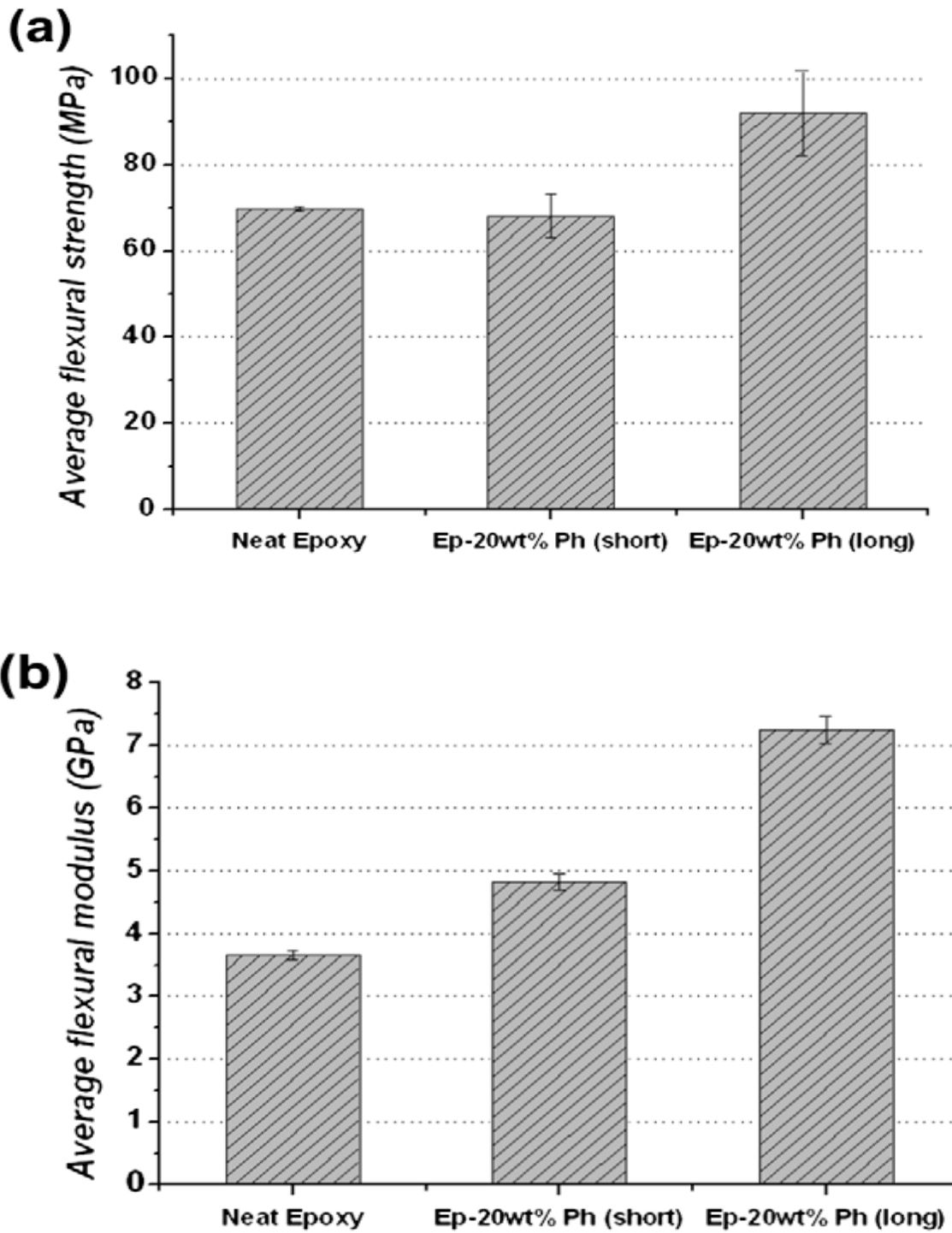
Figure 2.10. Flexural properties of short and long phormium fibre/epoxy composites: (a) flexural strength and (b) flexural modulus. (De Rosa *et al*. 2010)

Fibre-matrix adhesion is an essential factor that influences the mechanical properties of cellulose fibre/polymer composites. To overcome this problem, many types of fibre surface treatments have been carried out to modify the surface tension and polarity of cellulose fibres for better

fibre-matrix adhesion (Wang *et al.* 2007; Rong 2001; Gañan *et al.* 2005; Gassan and Bledzki 1999).

Wang *et al.* (2007) have investigated the effects of fibre treatment on the mechanical properties for flax-thermoplastic composites. They used four types of chemical treatments on flax fibres, namely mercerization, silane treatment, benzoylation, and peroxide treatment. Improvement in tensile strength was observed in the samples with silane and peroxide treatment over the samples with untreated fibres.

Rong (2001) studied the mechanical properties of treated sisal fibre reinforced epoxy composites. Three types of fibre treatments were used: alkalization, acetylation, cyanoethylation. An overall improvement of flexural strength and modulus properties was reported for all treated fibre-epoxy samples as shown in Figure 2.11. The authors pointed out that fibre treatment can improve the mechanical properties of cellulose fibre/polymer composites by improving matrix-fibre interface adhesion.
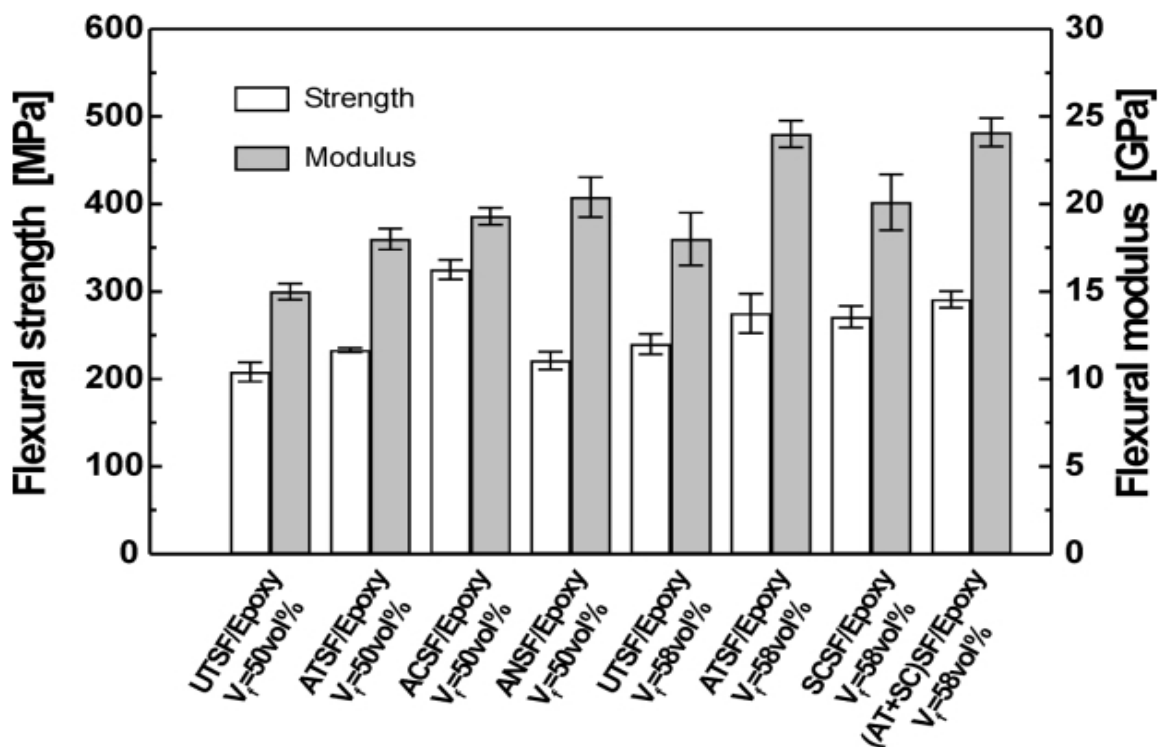
Figure 2.11. Comparison of flexural properties of untreated and treated sisal fibre - epoxy composites. (Rong 2001)

Fibre volume fraction is another critical factor that influences the mechanical properties of cellulose fibre/polymer composites. Hughes *et al.* (2002) investigated the variation of fracture toughness with fibre volume fraction of hemp and jute fibre reinforced polyester composites.

The results are shown in Figure 2.12, which illustrates that fracture toughness increases as fibre volume fraction increases. The fracture toughness of polyester matrix composites reinforced with glass, hemp and jute fibre (at fibre volume fraction = 0.2) was found to be 9.01, 3.51 and 2.56 ($MNm^{-3/2}$) respectively, while the fracture toughness of the virgin polyester was 0.62 ($MNm^{-3/2}$). Moreover, the critical strain energy release rate (G_{IC}) was measured and found to be increased from 0.1 (kJm^{-2}) for polymer to 0.97 and 1.84 (kJm^{-2}) for polymer reinforced with jute and hemp respectively.
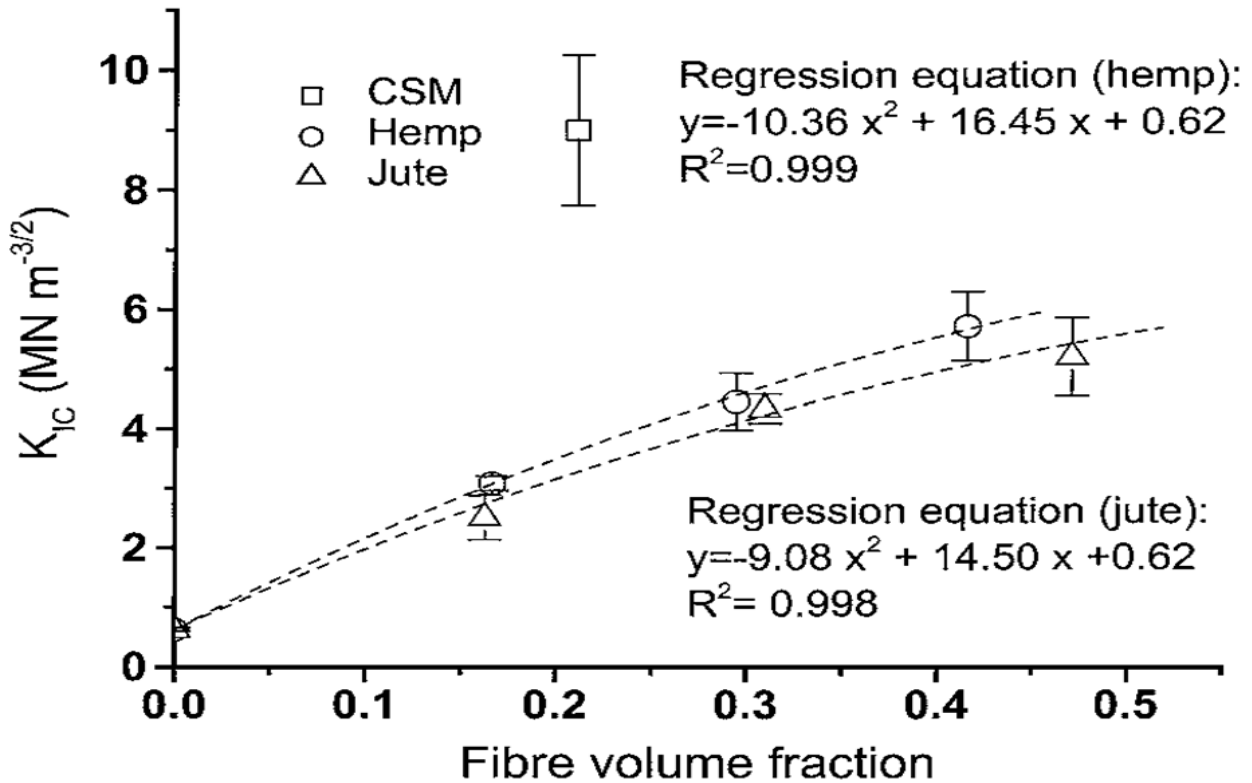
Figure 2.12. Facture toughness as a function of fibre volume fraction. (Hughes *et al.* 2002)

(b) Thermal properties

Albano *et al.* (1999) studied the thermal stability of thermoplastic polymers reinforced with plants fibres. Polypropylene (PP) systems were reinforced with treated and untreated sisal fibres. Results of initial and maximum degradation temperatures are summarized in Table 2.4. It can be seen that treated fibres displayed better thermal properties than untreated fibre. In all cases, the present of sisal fibres increased the thermal stability of PP matrix by shifting the maximum decomposition temperature (T_{max}) to higher values. In the other hand, the addition of sisal fibres accelerated the initial decomposition process of PP matrix.

Table 2.4. Initial and maximum degradation temperatures of raw materials and composites.

(Albano *et al.* 1999)

Sample	T_i (K)	T_{max} (K)
Untreated sisal	503	638
Treated sisal	523	658
PP	603	713
PP/untreated sisal	563	724
PP/treated sisal	583	733

In another interesting study, Gañan *et al.* (2005) carried out the influence of different chemical treatments of the fibres on the thermal behaviour of epoxy matrix reinforced with 30% sisal fibres. Thermogravimetric analysis indicated that chemical treatments enhanced the thermal stability of sisal fibre by increasing the maximum degradation peak temperatures of sisal fibre from 335°C to 390°C. This improvement was related to the modification of the chemical structure of the fibres. The study also revealed that the addition of treated fibres to the epoxy matrix was found to enhance the epoxy degradation slightly compared to untreated fibre composites. Finally, author stated that natural fibres governor the thermal stability of polymer composites.

The thermal properties of composites of poly (L-lactide) reinforced with different contents (1%, 5%, 10%, 20%, and 30%) of hemp fibres was investigated by Masirek *et al.* (2007). The thermogravimetric analysis of the composites, carried out in nitrogen atmosphere, showed that the addition of cellulose fibre accelerated the starting degradation of the hemp/PLA composites. The maximum degradation rate for neat PLA was at about 375°C, while it was shifted to lower temperatures in the range of (320°C- 338°C) for PLA/hemp composites, which is close to the typical degradation peak temperature of plain hemp. This result showed agreement with the previous study about the condition of cellulose fibre on polymer composites thermal stability. Table 2.5 display onset (T_{onset}) and derivative peak (T_D) temperatures of PLA and hemp fibre/PLA composites.

Table 2.5. TGA data of PLA and PLA/hemp fibre composites in nitrogen atmosphere. (Masirek *et al.* 2007)

composites	T_{onset} in N_2 (^{o}C)	T_D in N_2 (^{o}C)
PLA	342	375
99/1 PLA/hemp	322	338
95/5 PLA/hemp	295	323
90/10 PLA/hemp	301	322
80/20 PLA/hemp	289	322
70/30 PLA/hemp	305	331

De Rosa *et al.* (2010) investigated the thermal behaviour of epoxy composites reinforced with untreated phormium tenax lead fibres. Results showed that the incorporation of plant fibres increased the thermal stability of epoxy matrix. Figure 2.13 represents the DTG curve of epoxy resin, phormium tenax fibres and epoxy/ phormium fibre composite. It can be seen that the most mass of cellulose fibres and neat epoxy decomposed at temperatures of 337 ^{o}C and 335 ^{o}C respectively, while cellulose fibre/epoxy composites decomposed at 347 ^{o}C. Authors concluded that this enhancement in thermal properties was due to the improvement of fibre/matrix interface.
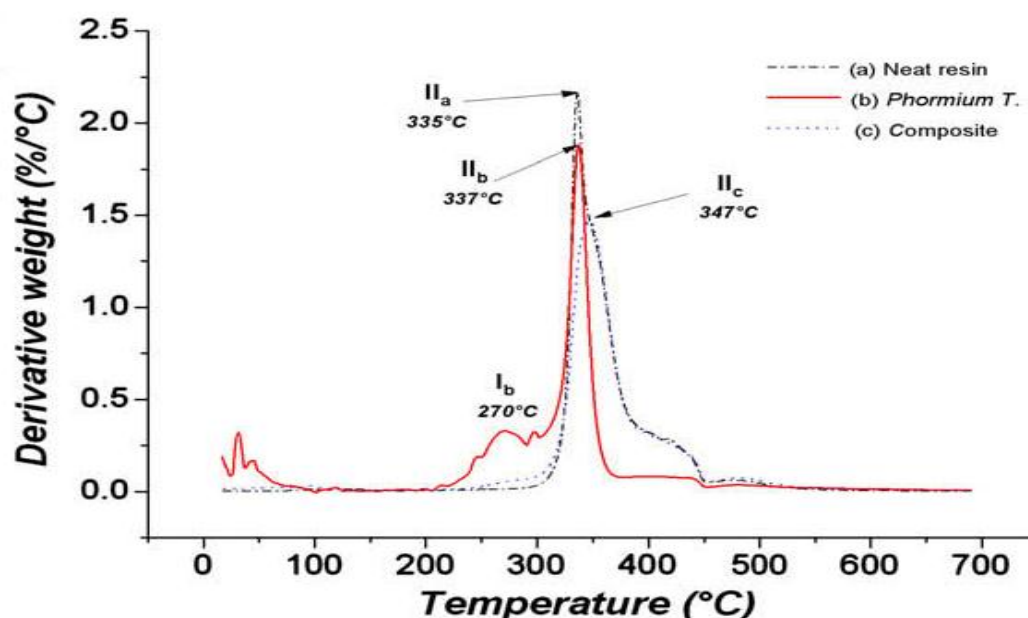
Figure 2.13. DTG curve of epoxy resin, phormium tenax fibres and epoxy/ phormium fibre composite. (De Rosa *et al.* 2010)

The use of nature plant fibres as reinforcements in polymer composites to replace traditional fibres like glass is currently generated much attention because of the advantages, including cost effectiveness, low density, high specific strength, as well as their availability as renewable resources (Low *et al.* 2007; Marsh 2003; Dhakal *et al.* 2007). However, one of the major drawbacks that have limited the use of plant fibre as reinforcement in polymer composites is their susceptibility to moisture absorption, which in turn can lead to swelling of the fibre forming voids and micro-cracks at the fibre-matrix interface region, which results in a reduction of mechanical properties and dimensional stability of composites (Dhakal *et al.* 2007; Wang *et al.* 2007). Cellulose fibres are hydrophilic in nature and they tend to absorb or attract much of water depending on the environmental condition. The chemical reason for this is due the presence of hydroxyl groups in the cellulose structure which attracts water molecules, and bind with them through hydrogen bonding (Han and Drzal 2003; Fraga *et al.* 2006; Kim and Seo 2006; Doan *et al.* 2007). A study on moisture behaviour of plant fibre/polymer composites was done by Dhakal *et al.* (2007). Unsaturated polyester was reinforced with 2, 3, 4 and 5 layers of hemp fibre. It was found that moisture absorption increased as fibre content increased as seen in Figure 2.14. Composite reinforced with 5 layers showed higher moisture absorption with higher maximum water uptake due to the higher cellulose content among other composites. Authors explained that hemp fibre swells after exposed to moisture creating micro-crack within the matrix-fibre interface. These micro-cracks make water molecules diffuse easily inside the composites which result in high moisture absorption.
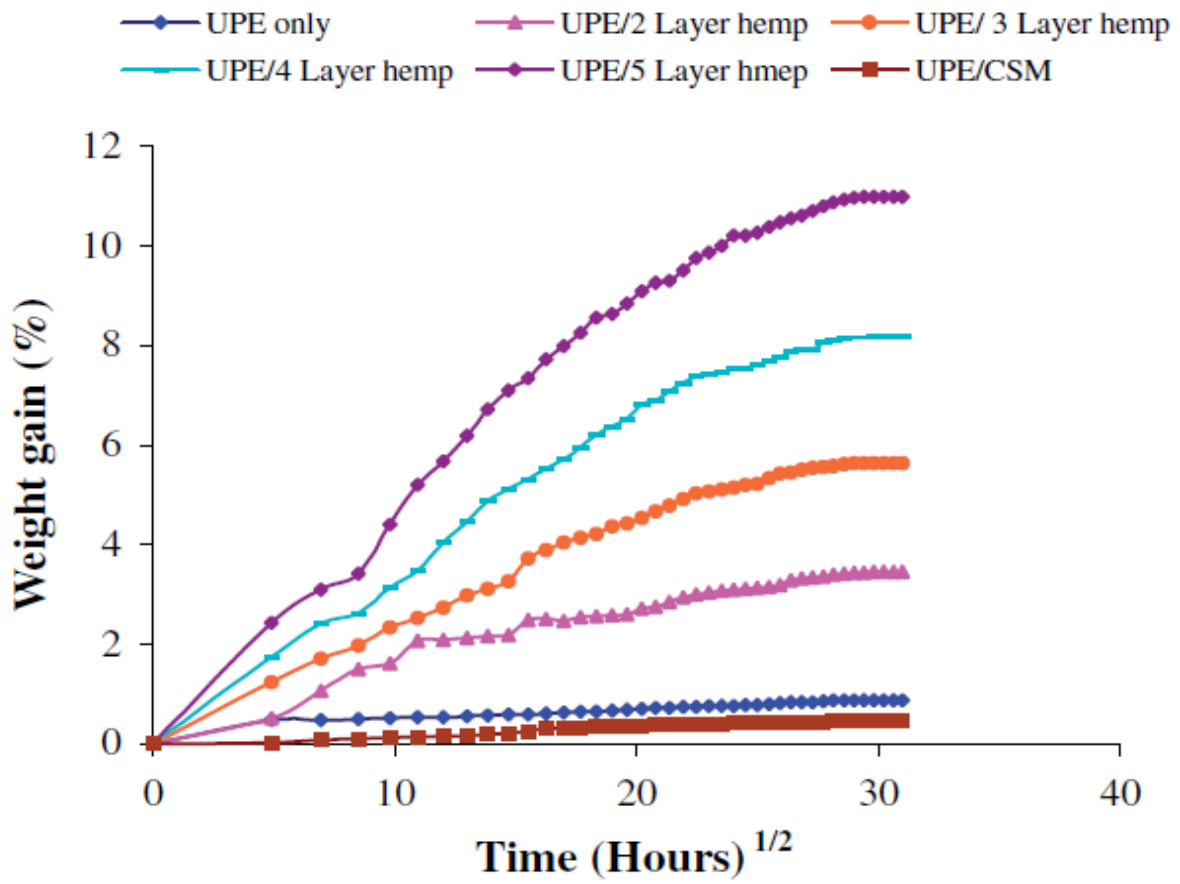
Figure 2.14. Water absorption behaviour at room temperature of unsaturated polyester matrix reinforced with different hemp fibre loading. (Dhakal *et al.* 2007)

Similar result was reported by Athijayamani *et al.* (2009). They studied the effect of fibre content on the moisture absorption behaviour of cellulose fibre/polyester composites. Results are shown in Figure 2.15 indicated that water uptake increased as fibre load increased. Moreover, it can be seen from the Figure that water absorption of composites increased as exposure time to moisture increased.
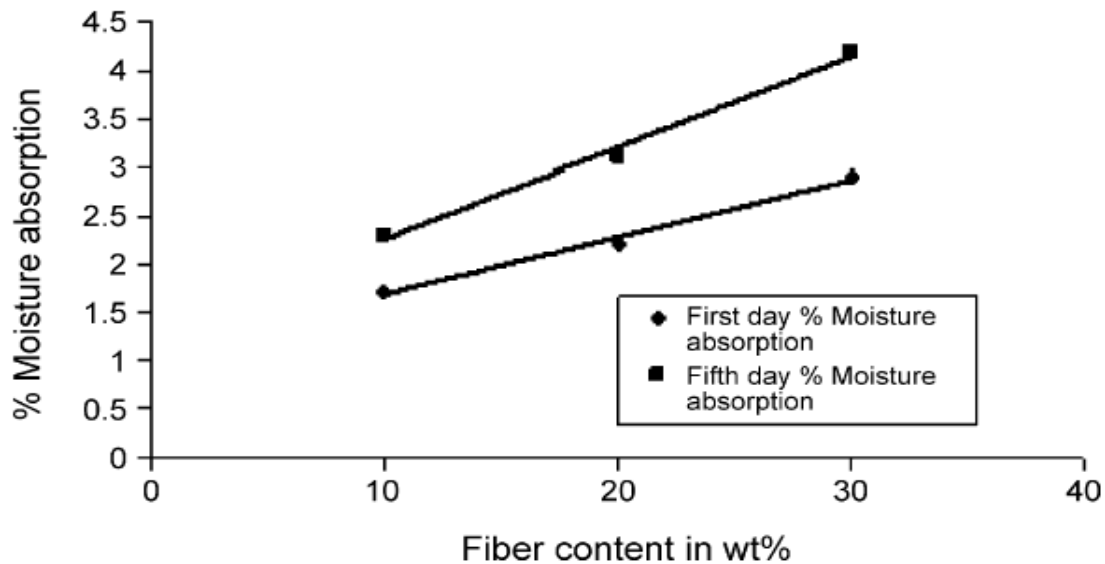
Figure 2.15. Moisture absorption of cellulose fibre/polyester composites as a function of fibre content. (Athijayamani *et al.* 2009)

Because of the hydrophilic nature of cellulose fibres, composites reinforced with cellulose fibres always tend to absorb much water than other types of composites. Rashdi *et al.* (2009) Also indicated in their study on kenaf fibre reinforced unsaturated polyester composites that as fibre load increased moisture absorption increased due to the high content of cellulose.

2.4 Polymer-Clay Nanocomposites

Polymer nanocomposite materials possess two phases consisting of inorganic particles of nanometre scale in the range between 1 and 100 nm that are dispersed in a matrix of polymeric material. These nano-particles demonstrate remarkable properties because of their comparative large surface area per unit volume. Such properties are the results of the phase interactions that take place between the polymer matrix and the nano-particles at the interfaces (Yong and Hahn 2009; Pavlidou and Papaspyrides 2008; Choudalakis and Gotsis 2009). The interest in polymer nanocomposites comes from the fact that the addition of nanosized fillers into a polymeric matrix would have a great effect on the properties of the matrix. Therefore, in the last couple decades, polymer nanocomposite materials have attracted increasing research and development attention because of their unique characteristics in terms of mechanical properties, thermal stability, barrier properties and flame retardancy (Kiliaris and Papaspyrides 2010; Pavlidou and Papaspyrides 2008; Mallick 2007). A large number of nano-fillers are available for combination with the polymers in the formation of nanocomposites. Table 2.6 displays six such materials that can be utilized for this purpose (Wypych and Satyanarayana 2005).

Table 2.6. Examples of layered host crystals used in polymer nanocomposites. (Wypych and Satyanarayana 2005)

Chemical nature	Examples
Element	Graphite
Metal chalcogenides	$(PbS)_{1.18}$ $(TiS_2)_2$, MoS_2
Carbon oxides	Graphite oxide
Metal phosphates	$Zr(HPO_4)_2$
Clay and layered silicates	Montmorillonite, hectroite, saponite, fluoromica, fluorohectorite, vermiculite, kaolinite, magadiite
Layered double hydroxides	$Mg_6Al_2(OH)_{16}CO_3$ nH_2O; M=Mg. Zn

Polymer-clay nanocomposites have been unique among composites and they have been preferred in many application for their unique mechanical, thermal, electrical and barrier properties (Hussain *et al.* 2006). In these nanocomposites the polymers is reinforced with high aspect ratio layered silicate sheets having about 1 nanometre thickness and a range of lengths between 100 and 300 nm. As the high aspect ratio provides a larger contact surface area, small concentrations of clay are enough to provide the necessary physical interactions between the

polymer and the filler silicate sheets. This makes them extremely compatible as filler materials (Mallick 2007; Pavlidou and Papaspyrides 2008; Kiliaris and Papaspyrides 2010). In 1990, the Toyota research group carried out the first study on the polymer nanocomposites. These researchers synthesized polymer nanocomposites based on nylon-6/ montmorillonite clay via the in-situ polymerization method. When 4.7 wt% clay was added to Nylon-6 polymer, the tensile modulus increased by 68% and the flexural modulus by 124% (Okada *et al.* 1990; Kojima *et al.* 1993). This research was the fore-runner of the global trend in polymer-clay research (Gao 2004). Many types of polymers including engineering polymers such as polypropylene, polyethylene, polystyrene, polyvinylchloride, polylactide, polycaprolactone, phenolic resin, poly p-phenylene vinylene, polypyrrole, rubber, starch, polyurethane, polyvinylpyridine as well as common polymers like nylons and the focus of this research epoxy-resins are developed for producing such nanocomposites (Gao 2004).

2.4.1 Clay Structure

Nanoclay can be found in nature as a common material and is made up of minerals with a fine grain structure that demonstrate a varied array of plasticity according to the amount of water it contains and becomes hardened when dried or fired. Clays are chemically known as hydrous aluminium silicate with the formula $Al_2O_3.SiO_2.H_2O$. They are usually found contaminated with small amounts of potassium, sodium, calcium, magnesium, or iron. The clay mineral has a basic crystal structure consisting of layers, a sandwich of an aluminium oxide or magnesium oxide sheet with one or two silicon dioxide sheets. The thickness of the sheets is usually on the older of 1 nm whereas the lateral aspect can range from 30 to 200 nm or even more. Both tetrahedral and octahedral types of sheets can be found in all clay minerals that unite in sharing the apical oxygen atoms from the tetrahedral sheets as shown in Figure 2.16. The classification of the clay minerals is based on the manner in which the tetrahedral and octahedral sheets are arranged into layers. When a single tetrahedral sheet is linked to a single octahedral sheet, a 1:1 layered structure is produced such as in kaolinite. When a single octahedral sheet is attached to tetrahedral sheets on both sides a 2:1 layered structure results such as in 2:1 phyllosilicates. The silicate layers in the 2:1 layered structures that are drawn towards each other by the Van de Waals forces (Hussain *et al.* 2006; Pavlidou and Papaspyrides 2008; Kiliaris and Papaspyrides 2010).
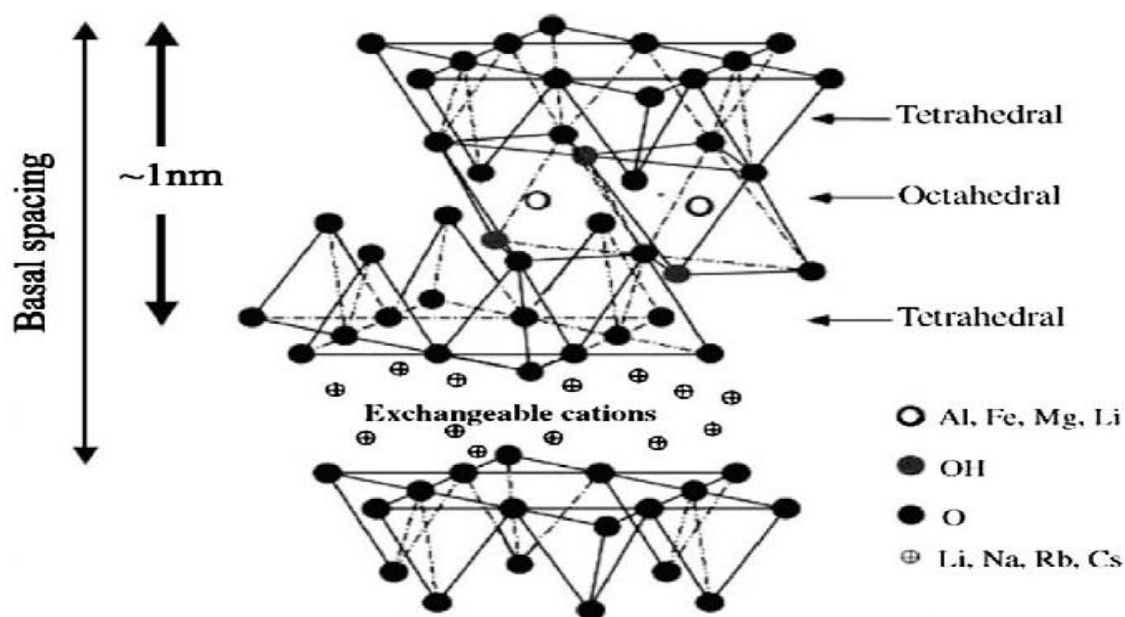
Figure 2.16. The structure for montmorillonite 2:1 layered silicates. (Choudalakis and Gotsis 2009)

Montmorillnite (MMT) is one of the most popular layered silicates being studied for its properties. This silicate has a 2:1 layer crystal structure that consists of a sandwich with an aluminium octahedron layer between two of silicon tetrahedron layers. The physical aspects of the MMT provide unique properties that render them highly suitable for inclusion as fillers in composites. The high aspect ratio sheets that are the produced by the 2:1 layer structure have a thickness of 1 nm and lengths ranging from 30 nm to several microns. When a clay platelet is diffused properly into the polymeric matrix without breaking, the aspect ratio of MMT increases to around 1000 with surface area is about 750 m^2/g (Hussain *et al.* 2006). Therefore, small quantities of silicates possess large surface areas that can be effectively utilized for interaction and thus are considered effective as fillers. The efficiency of the polymer chains in transferring stress into the filler particles increases dramatically due to the large surface area available for the interaction. Moreover, these high aspect ratio particles can also find use in the enhancement of barrier properties of polymer membranes by increasing the tortuosity of the material (Pavlidou and Papaspyrides 2008; Kiliaris and Papaspyrides 2010). Major clay mineral groups and the ideal structural chemical compositions of these minerals can be seen in Table 2.7.

Table 2.7. Common clay minerals used in polymer nanocomposites (Hussain *et al.* 2006)

Structure type	Group	Mineral examples	Ideal composition	Basal spacing (Å)
		Montmorillonite	$[(Al_{3.5-2.8}Mg_{0.5-0.2})(Si_8)O_{20}(OH)_4]\,Ex_{0.5-1.2}$	
2:1(TOT)	Smectite	Hectorite	$[(Mg_{5.5-4.8}Li_{0.5-1.2})\,(Si_8)O_{20}(OH)_4]\,Ex_{0.5-1.2}$	12.4-17
		Saponite	$[(Mg_6)(Si_{7.5-6.8}Al_{0.5-1.2})\,O_{20}(OH)_4]\,Ex_{0.5-1.2}$	
2:1(TOT)	lllite	lllite	$[(Al_4)(Si_{7.5-6.5}Al_{0.5-1.5})O_{20}(OH)_4]K_{0.5-1.5}$	10
2:1(TOT)	Vermiculite	Vermiculite	$[(Al_4)(Si_{6.8-6.2}Al_{1.2-1.8})O_{20}(OH)_4]Ex_{1.2-1.8}$	9.3-14
1:1(TO)	Kaolin-serpenite	Kaolinite,dickite, nacrite	$Al_4Si_4O_{10}(OH)_8$	7.14

2.4.2 Structure of Polymer-Clay Nanocomposites

There are three categories of polymer-clay composites: conventional composites, intercalated nanocomposites and exfoliated nanocomposites (Figure 2.17).
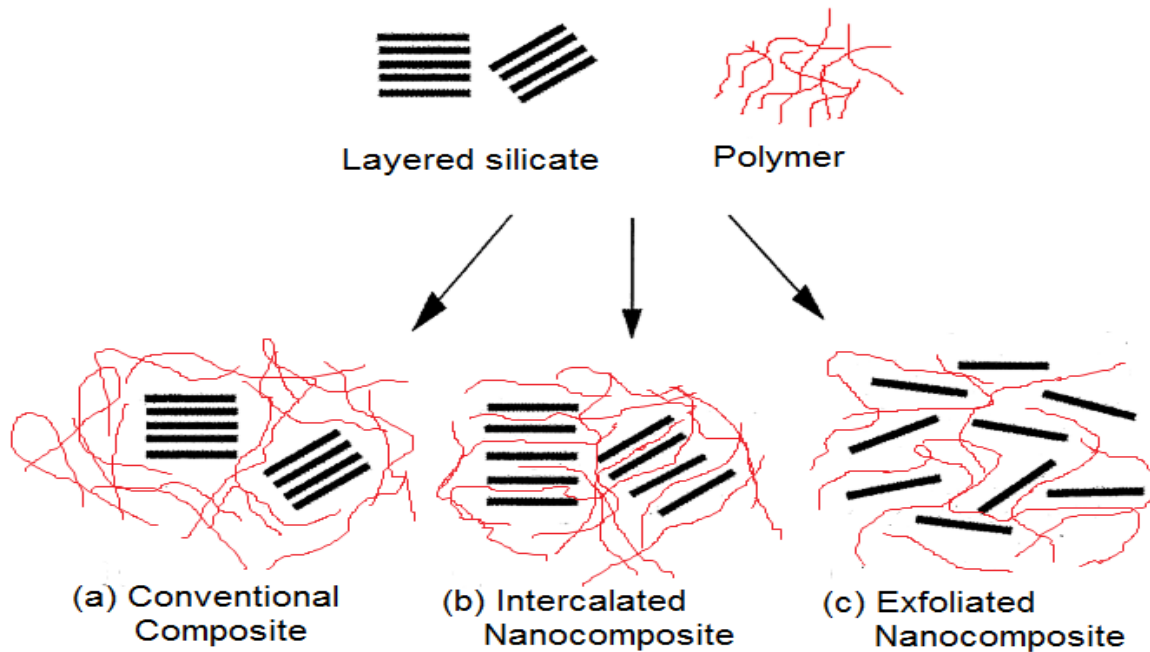
Figure 2.17. The three categories of polymer-clay composites. (Alexandre & Dubois. 2000)

Conventional composites: are those composites in which the polymer matrix is not introduced into the conventional clay filler that has the structure of combined layers and perform as microscale fillers. The properties of these composites and those of the traditional microcomposites are comparable (Beyer 2002; Kiliaris and Papaspyrides 2010).

Intercalated nanocomposites: In this composite, the polymer chains are inserted into the gallery gaps of the silicate layers in a diffuse and regularly repeating fashion (Auad *et al.* 2007). As a result of this, there is a complete loss of the registry in the clay layers that are well diffused in a continuous polymer matrix. Intercalated structures are not found suitable in applications that have strength as a requirement.

Exfoliated nanocomposites: The silicate layers in this type of nanocomposites are dispersed in the polymer matrix individually in an exfoliated microstructure. They have larger inter-spaces than in the intercalated nanocomposites and the amount of clay necessary for such composites is also comparatively less (Krishnamoorti and Yurekli 2001; Sinha Ray and Okamoto 2003). They

are also known as delaminated polymer-clay nanocomposites and are the most desirable as they provide better strength, stiffness and barrier characteristics while using less mineral content than the conventional polymer composites. The enhancement of these properties is due to the larger surface area and aspect ratio that provide for greater contact between the polymer and the clay components (Kiliaris and Papaspyrides 2010). It is seen that the degree of exfoliation is directly proportional to the improvement in these properties.

2.4.3 Synthesis of Polymer-Clay Nanocomposites

A large number of different methods are available for the synthesis of polymer/clay nanocomposites. But for the hydrophobic clay must first be organically modified to allow the organic polymer to be integrated between the silicate layers so that it changes into organo-clay or polymer-compatible clay. This pre-treatment is achieved through the ion exchange method in which the clay reacts with organic cations like alkyl ammonium or phosphonium ions. For the actual synthesis of the nanocomposite, three methods are popularly used: in situ polymerization, solution induced intercalation and melt processing or melt blending. Each of these methods has its own positive as well as negative aspects which are being well-researched in recent times (Gao 2004; Zanetti and Costa 2004; Pavlidou and Papaspyrides 2008; Kiliaris and Papaspyrides 2010).

(a) In situ polymerization

This type of polymerization technique was the very first used in the synthesis of polymer/clay nanocomposites based polyamide 6 (Okada *et al.* 1990). This method involves the swelling of the treated organoclay using monomers in liquid or solution form. The polymerization reaction occurs when the monomer migrates into the galleries within the intercalated sheets of the silicate (Figure 2.18). In this type of reaction, the initiators such as curing agents or high temperature have to be supplied before the swelling process to initiate the polymerization process (Pavlidou and Papaspyrides 2008). This method was first carried out by the Toyota research group in the production of clay/nylon-6 nanocomposites (Gao 2004).
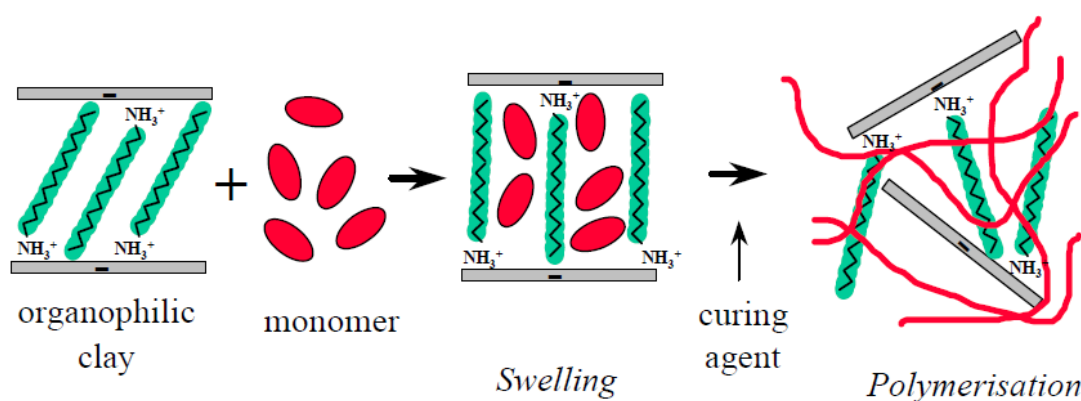
Figure 2.18. In situ polymerization method. (Kornmann 2000)

The advantages of in situ polymerization are that it can be used in the production of well-exfoliated nanocomposites and has been used in a wide range of polymeric systems (Patel *et al.* 2006). But processing through this method is time consuming and some types of polymers need a solvent when synthesised through this method. These problems must be tackled successfully to make use of this method at a large scale industrial level (Pavlidou and Papaspyrides 2008).

Alexander *et al.* (2002) used this method in the synthesis of polyethylene/hectorite nanocomposites. They found that there was an increase of up to 259% in Young's modulus for an 11.4 wt% clay sample when compared to an unfilled sample. The exfoliation structure of layered silicates was confirmed by the XRD analysis and TEM observation. Imai *et al.* (2002) used in-situ polymerization to prepare Poly(ethylene terephthalate) (PET) based polymer/layered silicate nanocomposites (PLSNs). The results showed that the intercalations of the PLSNs prepared by this method were poorly diffused. Compared to neat PET, the PLSNs displayed an 85% enhancement in their flexural modulus.

(b) Solution induced intercalation

Although this process is somewhat similar to the in-situ polymerization method, it differs in the use of polar solvents in the synthesis of intercalated polymer/clay nanocomposites. The swelling process of the organoclay is carried out using the polar solvents like chloroform, toluene or water (Figure 2.19) (Beyer 2002; Rai and Singh 2004). After that, a dissolved polymer is added to the solution that intercalates into the layers of the silicate galleries. Methods like vaporization under vacuum or precipitation are used to eliminate the solvent from the finished material (Pavlidou and Papaspyrides 2008).
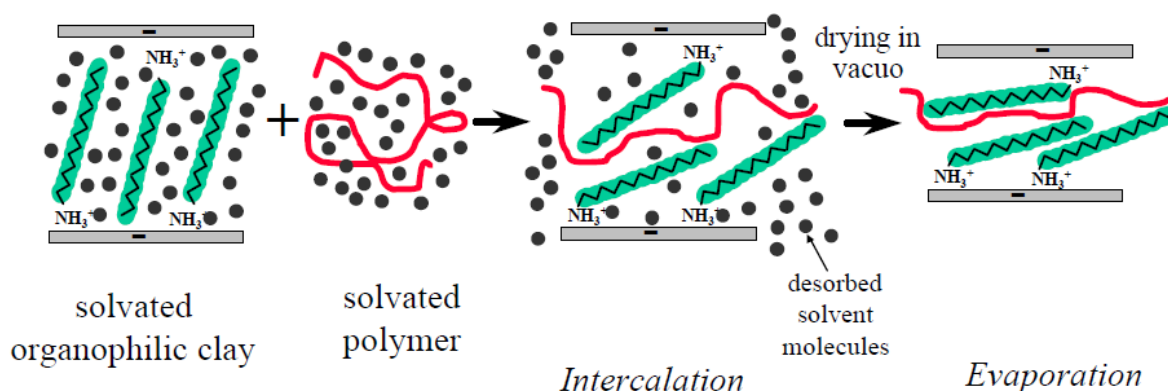
Figure 2.19. Solution induced intercalation method. (Kornmann 2000)

The driving force of this method is the compensation of the decrease in the conformational entropy of the resultant intercalated polymer chain by desorption of the solvent molecules. On the positive side, polymers with low or no polarity can be synthesized using this method, but commercial production on a large scale is difficult because of the need for solvents that are expensive and also the removal of those solvents from the finished products. Health and safety issues are also another negative aspect of this method (Beyer 2002; Gao 2004).

Krishnamoorti *et al.* (2001) prepared polystyrene-polyisoprene block copolymer through solution mixing method and toluene that was used as a solvent could only be separated by extensive drying in a vacuum oven at 100^oC. X-ray diffraction analysis of the resultant PLSN structure showed it to be a mixture of intercalated and exfoliated silicate layers.

(c) Melt processing

Melt processing involves the mechanical blending of the molten polymer and the organoclay to enhance the interactions between them and then annealing the mixture at a temperature that is placed at or above the melting point of the polymer to form the intercalated nanocomposite (Figure 2.20) (Kornmann 2000; Beyer 2002).
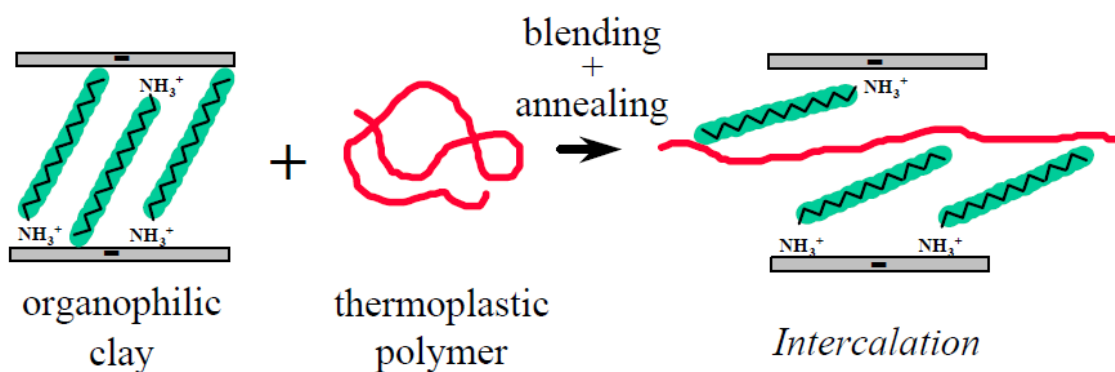
Figure 2.20. Melt processing method. (Kornmann 2000)

The thrust of this method is in the significant enthalpic involvement between the organoclay and the polymer throughout the blending and the annealing processes (Beyer 2002). Although this method is not as highly efficient in the intercalation as the in situ process (shown by the presence of partially exfoliated layered structures in the finished product), it is useful in the production of nanocomposites at the industry level by the traditional polymer processing methods like extrusion, injection moulding and so on. In fact, this technology serves to accelerate the commercial manufacture of clay/polymer nanocomposites (Gao 2004). The main positive aspects of the melt intercalation process over the in situ and the solution induced methods are that it does not involve environmentally harmful chemical solvents or reagents and quite compatible with the conventional extrusion or injection moulding methods, thus rendering it economical to the polymer industries as it reduces capital expenditure (Kiliaris & Papaspyrides 2010). Cho and Paul (2001) made a study of Nylon 6-organoclay nanocomposites that they processed through direct melt compounding making use of a conventional twin screw extruder. Their results proved that when the twin screw extruder is used, there is a good exfoliated dispersion of the organoclay into the Nylon 6 matrix but when a single screw extruder is used for the preparation, there was poor exfoliation. Peltola *et al.* (2006) investigated the influence of the rotational screw speed on polypropylene based organically modified silicate (montmorillonite). They employed a twin screw extruder at three different speeds: 200, 500 and 1000 rpm. The authors found a proportional increase in intercalation and some increase in exfoliation to the increase in the screw speed.

Although more fabrication techniques are being developed such as solid intercalation, co-vulcanization, and the sol-gel method, these are still in the early stage and still to be widely accepted (Gao 2004).

2.4.4 Characterisation of Polymer-Clay Nanocomposites

Morphology of polymer-clay nanocomposites can be demonstrated through two main and complementary techniques (Kiliaris & Papaspyrides 2010). The first is the X-ray diffraction (XRD) method that is quite a simple and convenient method of evaluating the d-spacing of the nanoclay galleries (Patel *et al.* 2006; Bahramian and Kokabi 2009). It is also quite easy to prepare the sample and the process consume only a few hours (Bahramian and Kokabi 2009). The second method is the Transmission electron microscopy (TEM) that is a major and effective in the analysis of submicron level particles and their structures. A direct determination of the spatial distribution of the layers of the composites is possible through this method and it becomes a complementary procedure to the XRD method. The main drawback of this method is the extensive skills needed for the preparation of the samples as well as in their analysis (Patel *et al.* 2006; Bahramian and Kokabi 2009; Kiliaris and Papaspyrides 2010). Other than these two, there are also useful methods such as scanning electron microscopy (SEM) and the small-angle X-ray scattering (SAXS) (Hussain *et al.* 2006).

(a) X-ray diffraction (XRD)

The most popular method used for the study of the structure of nanocomposites is X-ray diffraction because it is both simple and accessible. It is possible to examine the position, shape and the intensity of the basal reflections from the dispersed silicate layers to identify whether the nanocomposite is intercalated or exfoliated. The total absence of peaks in the XRD curves indicate the extensive layer separation that is seen as a result of the exfoliation of the original silicate layers dispersed in the polymer matrix (Patel *et al.* 2006). However, in intercalated nanocomposites, the intercalation of the polymer chains increases the interlayer spacing of the clay, producing a shift of the diffraction peak towards lower angle values and effect in the appearance of a new basal reflection that corresponds to the larger gallery height (Figure 2.21) (Alexandre and Dubois 2000; Pavlidou and Papaspyrides 2008). The basal spacing of the intercalated silicates can be related to the position of the peak with respect to the angle 2Θ using the Bragg equation (Alexandre and Dubois 2000):

$$n\lambda = 2d \sin \theta \qquad\qquad 2.1$$

Where λ corresponds to the wavelength of the X-ray radiation used in the diffraction experiment, d is the space between diffraction lattice planes and θ is half the measured diffraction angle (Pavlidou and Papaspyrides 2008).
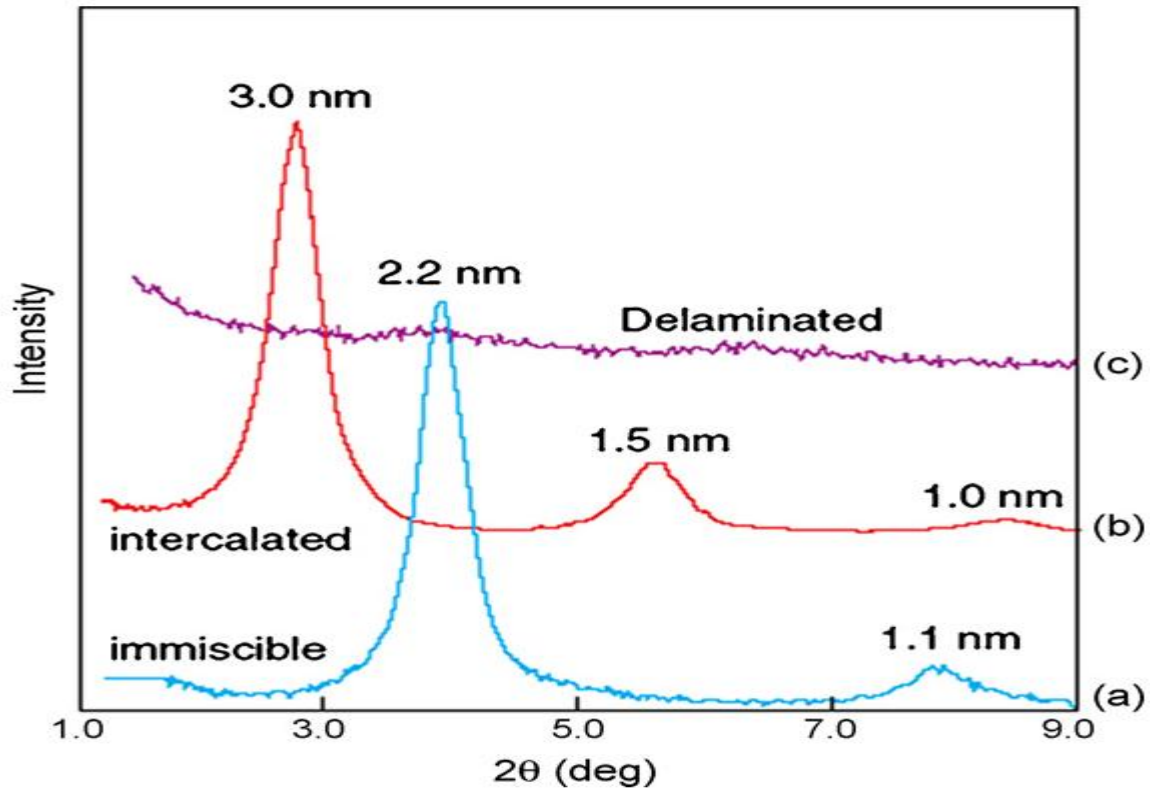
Figure 2.21. Typical XRD patterns of polymer/layered silicates: (a) PE + organoclay→ conventional composites, (b) PS + organoclay→ intercalated nanocomposite, (c) siloxane + organoclay→ delaminated or exfoliated nanocomposite. (Pavlidou and Papaspyrides 2008)

XRD can no doubt offer a convenient method of establishing the interlayer spacing of the layers in the initial layered silicates or in intercalated nanocomposites that are within 1-4 nm, it cannot be used to find out the spatial distribution of the silicate layers or any structural variations in the nanocomposites. Moreover, as some layered silicates do not display distinct basal reflections at first, the peak broadening and intensity decreases are not so easy to determine in a systematic manner. It follows that, the results of studies that make use of only XRD to examine the formation and structure of nanocomposites, cannot be considered as conclusive. It is in this area that XRD and TEM complement each other and together they provide the most effective devices to study nanocomposite structures (Sinha Ray and Okamoto 2003; Hussain *et al.* 2006; Pavlidou and Papaspyrides 2008).

(b) Transmission electron microscopy (TEM)

Transmission electron microscopy (TEM) is a major method of studying the characteristics of nanocomposites at the nanoscale and can present valuable data regarding the morphology, structure and spatial distribution of the dispersed phase in a limited area of the nanocomposite (Morgan and Gilman 2003; Sinha Ray and Okamoto 2003; Hussain *et al.* 2006; Tjong 2006). High energy electron beams are transmitted through a very thin specimen, no thicker than 10 nm, which interact with the material it passes through and produce two-dimensional images (Stadtländer 2007; Cao 2004; Ramesh 2009). Morgan and Gilman (2003) recommended that since XRD alone is insufficient, TEM images should be used to substantiate the results of XRD to determine whether the sample is exfoliated or intercalated.

TEM scores over XRD in its facility of confirming the presence of exfoliation in a polymer/clay nanocomposites specimen whereas XRD is highly influenced by features such as the orientation of the sample, the order of the layered silicates as well as its concentration (Morgan and Gilman 2003). Figure 2.22 illustrates the TEM micrographs of an intercalated and an exfoliated nanocomposite.
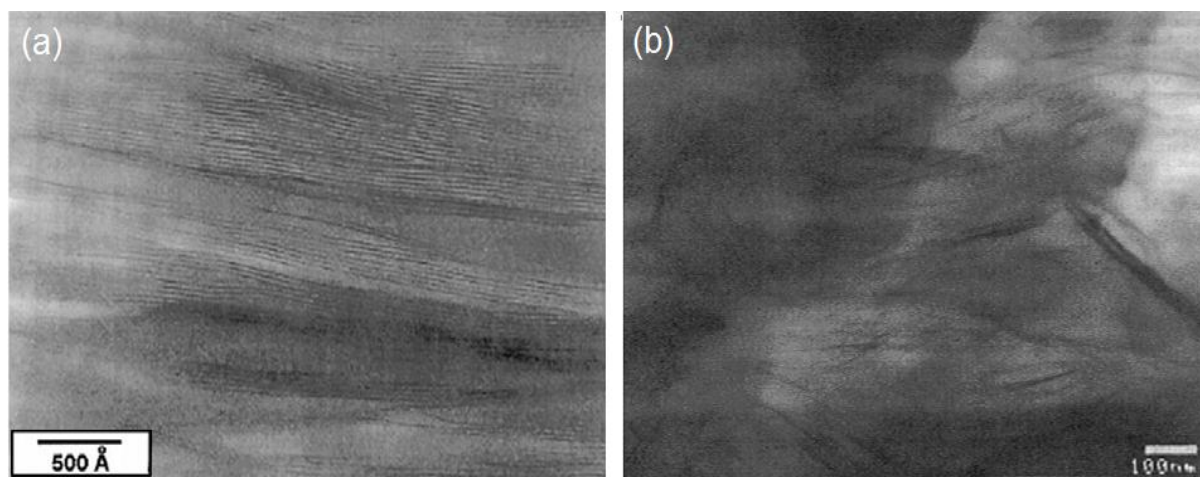
Figure 2.22. TEM micrographs of poly(styrene)-based nanocomposites: (a) intercalated nanocomposite and (b) exfoliated nanocomposite. (Pavlidou and Papaspyrides 2008)

As mentioned earlier TEM requires extensive skills in preparing the specimen and analyzing it. Also, because the magnification level in TEM is extremely high, the operator has to select a representative image for the complete sample from only a very small portion of the actual

specimen (Stadtländer 2007; Sinha Ray and Okamoto 2003). The TEM image may show many variations in the levels of intercalation and exfoliation and great attention must be paid to the selection of the representative sample that can be guaranteed as valid (Sinha Ray and Okamoto 2003).

(c) Scanning electron microscopy (SEM)

As the name signifies, scanning electron microscopy (SEM) scans the surface of the specimen using a high-energy electron beam and provides an image of it (Ramesh 2009). The electrons in the beam strike and penetrate the surface of the specimen, producing several interactions that create a number of signals on the surface layer. A three-dimensional image can be created from these signals that include a large amount of data concerning the topography and the chemical composition of the surface of the specimen (Cao 2004).

All scanning electron microscopy are generally made up of a column, a specimen chamber, detectors and the viewing system. The function of the column is to generate the beam of electrons. The interaction of this beam with the sample takes place in the specimen chamber, the detectors monitor the various signals that are produced by the interaction and the viewing system creates the image from the detector signals (Malik and Singh 2010).

The preparation of SEM samples involves various steps like cleaning of the surface of the sample, stabilizing it using a fixative, rinsing, dehydrating, drying and mounting the specimen on metal holders, as well as covering the surface with an electrically conductive material (Stadtländer 2007; Ramesh 2009). This last stage of coating is done with a view of rendering the specimen highly conductive to the electrons in the beam and preventing the build-up of high voltages. Such coating is usually made up of 20 nm to 30 nm layers of conductive metals like gold, gold-palladium or platinum (Stadtländer 2007).

2.4.5 Properties of Polymer-Clay Nanocomposites

As compared to the conventional composite materials, nanocomposites are more advantageous due to their enhanced properties of mechanical, thermal, solvent resistance and fire resistance. Because of this, a lot of research is being conducted in the creation of polymer-clay composites that utilize a variety of polymers. In this section, a number of studies on polymer nanocomposites are investigated from the available literature. These studies showed

improvements in the mechanical, thermal and barrier properties of polymer nanocomposites when small amounts (≤10 wt %) of nanoclay are added to them.

(a) Mechanical properties

One of the most important advantages of using nanoclay platelet for reinforcement polymers is that nanoclay platelet has high aspect ratios, high modulus, high surface area and high strengths which result in the enhancement of polymer mechanical properties when nanoclay is dispersed well into polymer system (Pavlidou and Papaspyrides 2008; Kiliaris and Papaspyrides 2010). In fact, the combination of well-dispersed nanoclay layers with good interfacial interactions between matrix and filler are the major reasons for the superior properties of nanocomposites (Manfredi *et al.* 2008). The first major report in the improving of the mechanical properties of polymers/clay nanocomposites was done by Toyota researchers in 1990. They studied the properties of nylon 6-clay nanocomposites through in situ polymerization. It was reported that with the addition of only 4.7 wt% of exfoliated clay, the tensile strength, tensile modulus, flexural strength and flexural modulus increased by 41%, 68%, 60% and 124% respectively over neat polymer (Okada *et al.* 1990; Kojima *et al.* 1993).

Qi *et al.* (2006) studied the effect of different nanoclay additives on the mechanical properties of a series of clay/epoxy nanocomposites. In situ polymerisation method was used to prepare the nanocomposites with four types of nanoclays, namely, montmorillonite (MMT-Na+), Cloisite 30B, Nanomer I.30E and CPC. Table 2.8 summarizes the tensile properties.

It was found that an increase in nanoclay content led to an increase in the tensile modules. At the maximum addition of nanoclay 10%, the maximum improvement in the tensile modules of the nanocomposites was found to be 26.9% for MMT-Na+/epoxy, 15.1% for MMT-30B/epoxy, and 12.2% for MMT-I.30E/Epoxy. The improved modulus was explained by the strong stiffening effect of the clay fillers which themselves have a higher modulus than epoxy. However, it was observed that the addition of nanoclay significantly reduced the failure strength and failure strain. This was explained by the poor dispersion of the nanolcay particles in the resin due to the increased viscosity of the system after adding nanoclay.

Table 2.8. Tensile properties of epoxy nanocomposites with different nanoclay loads and types.
(Qi *et al.* 2006)

Nanocomposites	Elastic modulus (GPa)	Ultimate failure strength (MPa)	Ultimate failure Strains (%)
Neat DGEBA	2.71 ± 0.11	72.06 ± 1.37	4.21 ± 0.36
2%MMT-Na$^+$/DGEBA	2.79 ± 0.07	68.04 ± 4	3.83 ± 0.39
5%MMT-Na$^+$/DGEBA	2.92 ± 0.17	57.2 ± 2.22	2.9 ± 0.3
10%MMT-Na$^+$/DGEBA	3.44 ± 0.29	57.68 ± 3.69	2.61 ± 0.35
2%MMT-30B/DGEBA	3.11 ± 0.09	62.19 ± 2.56	2.94 ± 0.19
5%MMT-30B/DGEBA	3.10 ± 0.08	58.35 ± 5.87	2.6 ± 0.47
10%MMT-30B/DGEBA	3.12 ± 0.23	57.31 ± 6.97	2.4 ± 0.2
2%MMT-I.30E/DGEBA	2.68 ± 0.26	64.58 ± 6.56	4.02 ± 0.33
5%MMT-I.30E/DGEBA	2.82 ± 0.12	59.94 ± 9.01	2.67 ± 0.64
10%MMT-I.30E/DGEBA	3.04 ± 0.11	58.23 ± 4.39	2.51 ± 0.38
2%MMT-CPC/DGEBA	2.57 ± 0.15	49.03 ± 2.72	2.52 ± 0.21
5%MMT-CPC/DGEBA	2.79 ± 0.08	50.14 ± 2.80	2.51 ± 0.26

It was also reported that fracture toughness increased with increased nanoclay content as seen in Table 2.9. The addition of 10% nanoclay increased the fracture toughness by 58.3% for MMT-Na+/epoxy, 25% for MMT-30B/epoxy and 41.6% for MMT-I.30E/epoxy. The reason for this

increase in fracture toughness was due to the intercalation structure of the resulting nanocomposites.

Table 2.9. Fracture toughness of nanocomposites as a function of clay content. (Qi *et al.* 2006)

Epoxy	Nanoclay	Clay content (wt%)	Fracture toughness (K_{IC}) (MPa m$^{1/2}$)
DGEBA	----------------	0	0.60
DGEBA	MMT-Na$^+$	2	0.63
DGEBA	MMT-Na$^+$	5	0.91
DGEBA	MMT-Na$^+$	10	0.95
DGEBA	MMT-30B	2	0.71
DGEBA	MMT-30B	5	0.72
DGEBA	MMT-30B	10	0.75
DGEBA	MMT-I.30B	2	0.64
DGEBA	MMT-I.30B	5	0.92
DGEBA	MMT-I.30B	10	0.85
DGEBA	MMT-CPC	2	0.83
DGEBA	MMT-CPC	5	0.99

It was concluded that poor mechanical properties could possible linked to the existed voids within the samples and formation of clay agglomerates due to the viscosity of the system and to the poor dispersion of nanoclay particles respectively.

Kaynak *et al.* (2009) investigated the flexural strength and fracture toughness of nanoclay (Na-montmorillonite) based epoxy nanocomposites. Nanocomposites were prepared via in-situ intercalative polymerization. Three different chemical treatments were used to modify the nanoclay. The results showed significant improvements in flexural strength and fracture toughness with maximum value at 0.5% nanoclay load, after which the values decreased as the nanoclay content increased.

Ha *et al.* (2008) investigated the dependence of fracture toughness of surface-modified MMT/epoxy nanocomposite with various clay contents (0%wt, 2%wt, 4%wt, 6%wt and 10%wt). The authors used a clay modified (3-aminopropyltriethoxysilane) to produce nanocomposites with well-dispersed nanoclay. The fracture toughness data is given in Figure 2.23. It can be seen that the addition of nanoclay decreased the fracture toughness for all the samples. However, the sample with 6%wt of clay content showed better toughness. It was

reported that this reduction was due to the presence of voids within nanocomposites as well as increased debonding between the nanoclay and polymer.
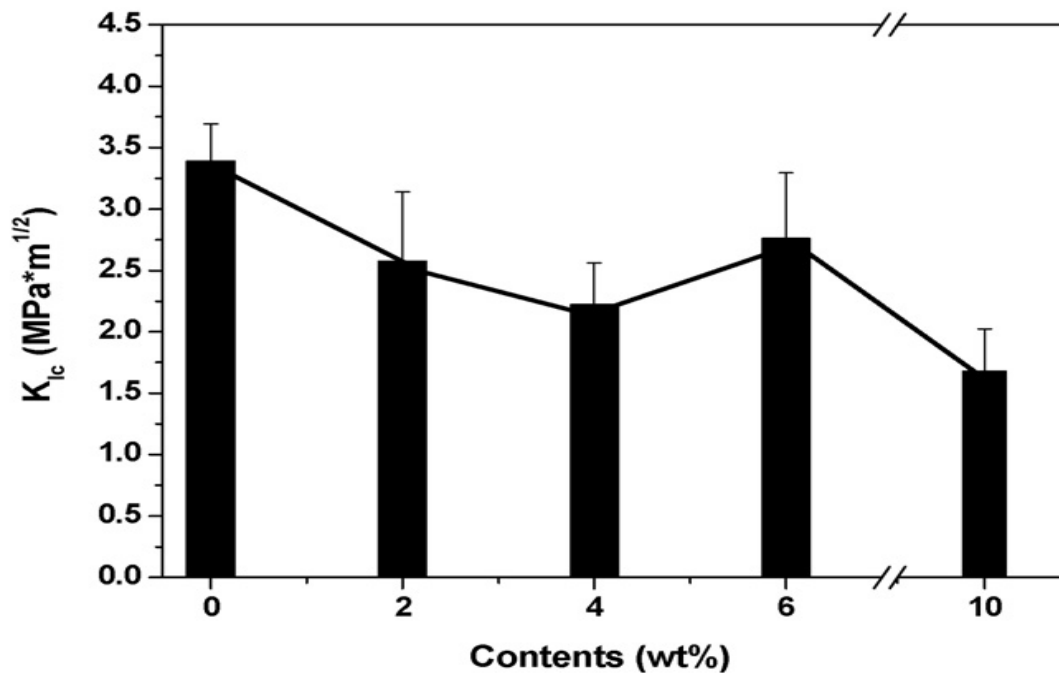
Figure 2.23. Fracture toughness versus various clay contents. (Ha *et al.* 2008)

Two years later, Ha and co-workers (2010) investigated the effects of clay silane treatment on the fracture toughness of clay/epoxy nanocomposites. Unlike the previous study, it was reported that fracture toughness increased by 82% for nanocomposites with clay silane treatment over untreated clay/epoxy nanocomposites. This improvement in fracture behaviors was due to the excellent dispersion of the treated clay into epoxy matrix and enhancement in interfacial adhesive strength between resin and clay layers.

Le Pluart *et al.* (2005) reported an increase in fracture toughness by 50% when 10 wt% of nanoclay was added to the epoxy matrix. In similar study, Brunner *et al.* (2006) investigated the fracture toughness of modified nanoclay based epoxy nanocomposites. The results showed that 10 wt% of nanoclay improved fracture toughness and energy release rate by 50% and 20% respectively over neat epoxy. Daud *et al.* (2009) investigated the effects of the addition of nanoclay on the mechanical properties of three-phase glass fibre reinforced composites (GFRP) consisting of traditional woven glass fibre and polyamide-6 (PA6) matrix. Nanocomposites were prepared via melt mixing method. The authors found an increase up to 30% in both flexural strength and compressive strength for the GFRP sample with 5 wt% nanoclay

Zainuddin *et al.* (2010) investigated the flexural properties of clay–epoxy nanocomposites. Nanocomposites were fabricated with 1–3 wt% loading of montmorillonite layered silicate via magnetic stirring mixing for 5 hours. The results showed that mixed intercalation and exfoliation structure was achieved by a 2% wt load of nanoclay. As shown in Figure 2.24, the flexural strength and modulus could be increased to a maximum of up to 8.7% and 17.4% respectively for samples reinforced by only 2% wt of nanoclay over neat epoxy. The authors stated that the poor dispersion of nanoclay led to poor mechanical properties.
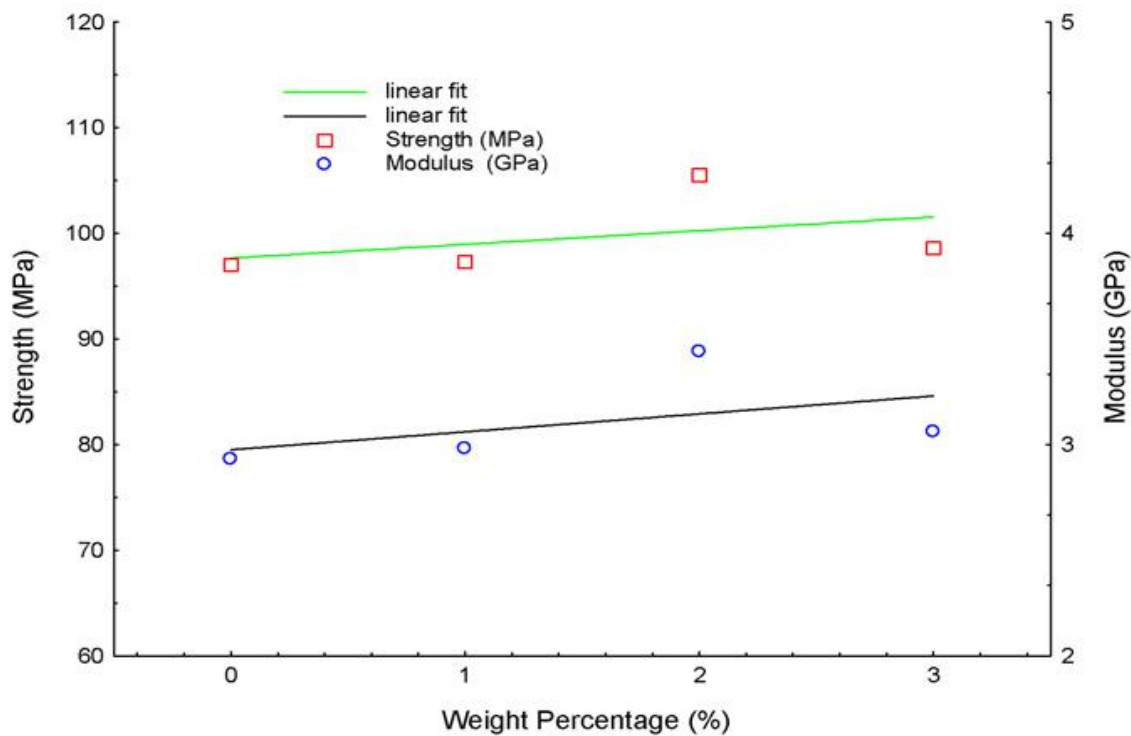
Figure 2.24. Flexural strength and flexural modulus of epoxy and nanocomposite as a function of clay content. (Zainuddin *et al.* 2010)

Manfredi *et al.* (2008) found that flexural strength, flexural modulus and impact strength were increased by 20%, 29% and 23% respectively for composites made with the addition of 5 wt% of nanoclay. Ratna and co-worker (2003) proved that the impact strength of nanocomposites was increased by about 57% with a clay content of 5% over neat polymer.

Yasmin *et al.* (2006) investigated the influence of nanoclay content on the mechanical properties of clay/epoxy nanocomposites. The team used shear mixing to fabricate nanocomposites with 1-10 wt% of nanoclay. The results showed that the addition of nanoclay significantly improved the

elastic modulus of neat epoxy. It was also found that as the clay content increased, the elastic modulus also increased gradually for both types of clay (Nanomer I.28E and Cloisite 30B). Authors concluded that the improvement in mechanical properties was due to the better dispersion of the nano-particles as well as effective interfacial adhesion.

(b) Thermal properties

One of the highly interesting properties of polymer-layered silicate nanocomposites is their increased thermal stability. Thermogravimetric analysis (TGA) is the general method used to study the thermal stability of polymeric materials. The mass lost by the polymer when it undergoes degradation at high temperatures is ascribed to the creation of volatile products and is considered as a function of temperature. Non-oxidative decomposition occurs when the material is heated under a flow of an inert gas like helium or nitrogen, while the use of air or oxygen allows analysis of oxidative decomposition reactions. It is seen that, as a rule, the integration of nanoclay in the polymer matrix was found to enhance the thermal stability of the samples, because the nanoclay platelets act as insulators to the heat as well as a barrier to the production of volatile products (Pavlidou and Papaspyrides 2008; Yeh *et al.* 2006). In the early 90s, Toyota researchers reported a remarkable improvement in thermal and flammability properties in polymers on the addition of nanoclay. The Toyota team found that the heat distortion temperature of nylon 6 increased from $65^{o}C$ to $152^{o}C$ for nylon 6 nanoclay composites by the addition of only 4.7 wt% of nanoclay contents (Okada *et al.* 1990; Kojima *et al.* 1993). Later on, a number of studies have reported similar improvements in thermal stability for nanocomposites prepared with various types of polymer matrices and nanoclay.

Phang and his team (2005) studied the thermal properties of PA12/organoclay nanocomposites. They reported a slight improvement in the thermal stability with additions of less than 2 wt% of nanoclay, while, a significant enhancement was observed for nanocomposites with only 5 wt% nanoclay.

Wang *et al.* (2006) reported that the addition of nanoclay improved the thermal stability of nanocomposites by increasing the onset temperature of degradation (T_{onset}) and the temperatures at maximum mass loss rate (T_{peak}). T_{onset} and T_{peak} of neat polymer increased by 22 and $23^{o}C$, respectively at a 3 wt% silicate loading. The authors indicated that the dispersion quality of organoclay and its content can influence the thermal properties.

In the same year, Yeh *et al.* (2006) investigated the thermal stability by TGA under nitrogen atmosphere of epoxy modified with different percentages (1%, 3%, 5% , 7%) of MMT clay. The TGA curves showed that the decomposed temperature at weight loss 5 wt% (T_d) of epoxy increases gradually with increase nanoclay content as can be seen in Figure 2.25. By adding only 7 wt% of clay into epoxy system, T_d increased from 304 °C to 343 °C. This significant enhancement on thermal properties was attributed to the presence of silicate layers acting as barriers to reduce the permeability of volatile degradation products out of the polymer/clay nanocomposites samples.
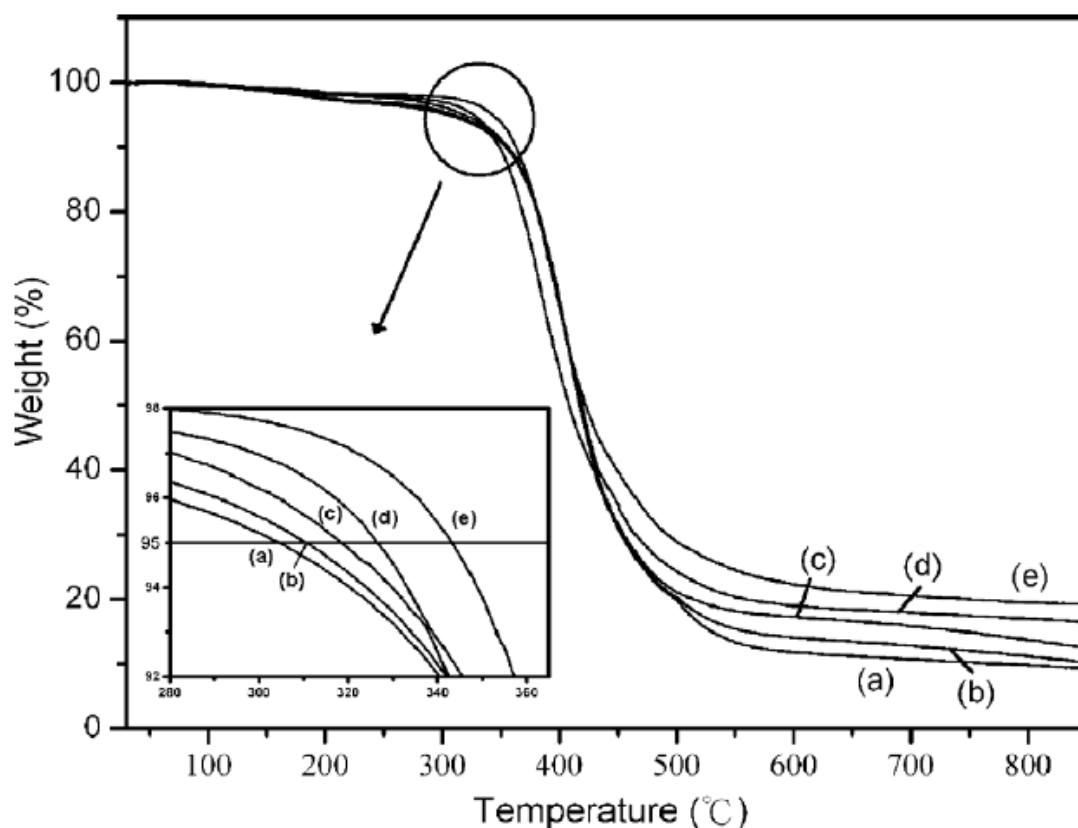
Figure 2.25. Weight% versus temperature curves of: (a) epoxy, (b) CLMA1, (c) CLMA3, (d) CLMA5, and (e) CLMA7. (Yeh *et al.* 2006)

Hwang *et al.* (2010) investigated the thermal properties of polybutylene terephthalate (PBT)/clay nanocomposites. Different amounts of nanoclay and two speeds of twin-screw extruders were used to prepare the nanocomposites. The results demonstrated that the presence of nanoclay increased the temperature of thermal decomposition of the nanocomposites samples over the

55

neat PBT as shown in Figure 2.26. However, Figure 2.27 shows that the melting temperature of nanocomposites slightly increased only after adding 0.5 and 1.0 wt% nanoclay.
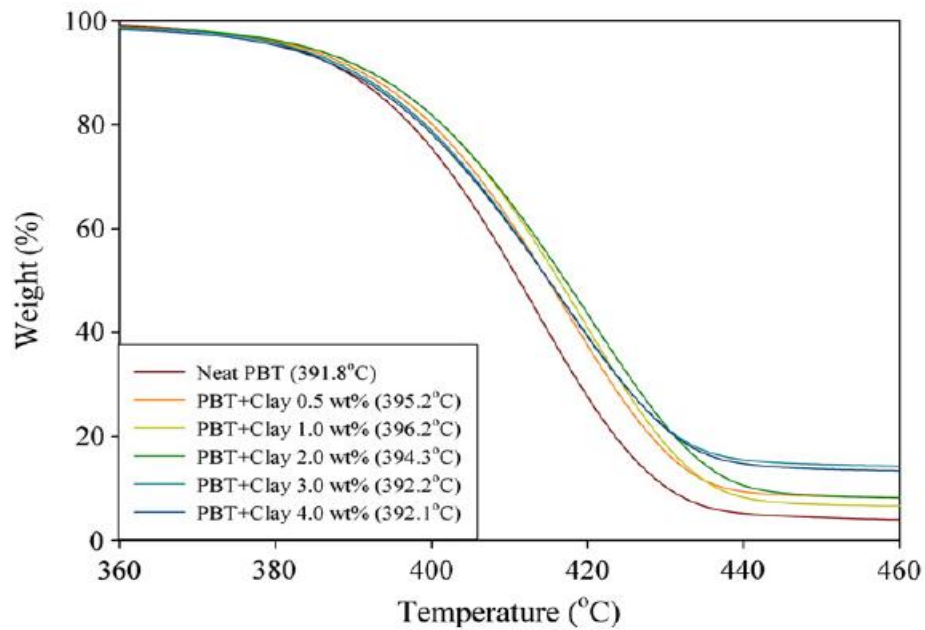
Figure 2.26. TGA curves of neat PBT and PBT/clay nanocomposites. (Hwang *et al.* 2010)
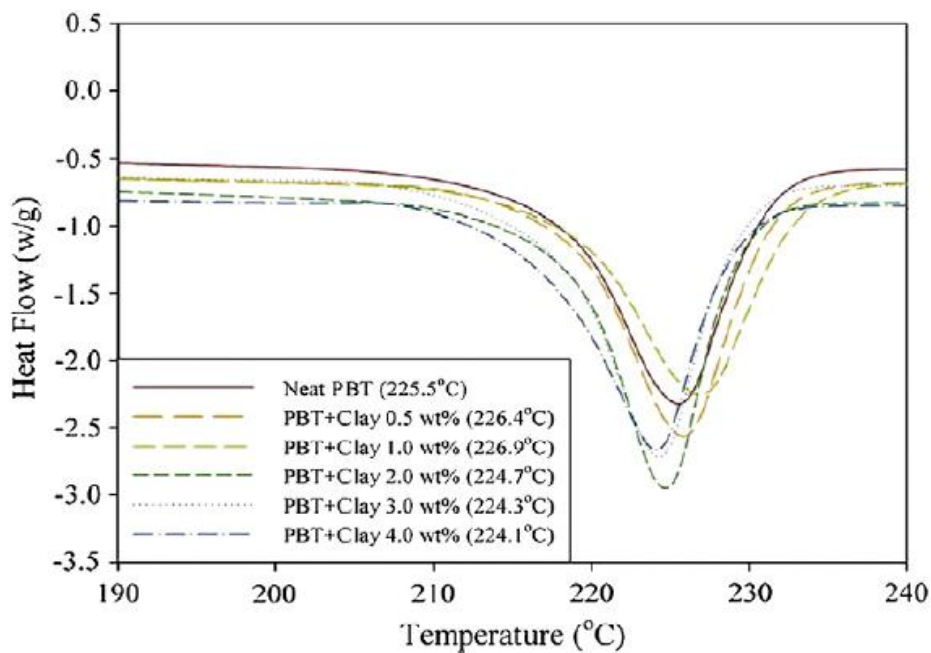
Figure 2.27. DSC curves of the melting temperature of neat PBT and PBT/clay nanocomposites. (Hwang *et al.* 2010)

Actually, despite the general improvement of thermal stability for nanocomposites, a number of studies reported decreases in the thermal stability for some cases of higher nanoclay loading. Paul *et al.* (2003) studied the thermal stability of Poly (L-lactide) (PLA) based nanocomposites. The authors reported that thermal stability increased with increased clay content, with the maximum thermal stability achieved by 5 wt% of nanoclay. However, a reduction in the thermal stability was observed for polymers filled with 10 wt% nanoclay.

This concurs with another study done by Valera-Zaragoza *et al.* (2006). They investigated the thermal and flammability properties of ethylene vinyl acetate (EVA) copolymer/organoclay nanocomposites. It was reported that thermal stability increased as clay contents increased up to 6 wt% of nanoclay loading, then thermal stability decreased when nanoclay load increased to more than 6 wt%. Figure 2.28 shows the weight loss versus temperature for EVA and EVA/Cloisite nanocomposites with 4, 6 and 8 wt% nanoclay.
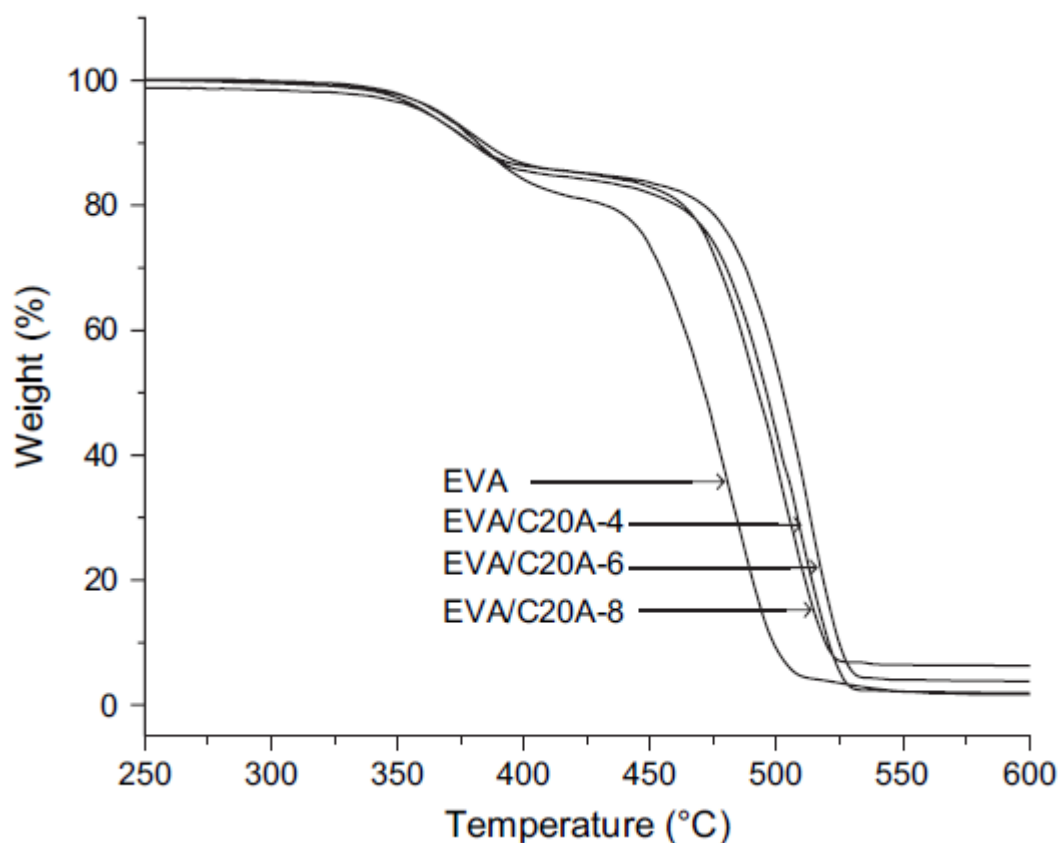
Figure 2.28. TGA curves of EVA and EVA/Cloisite nanocomposites with 4, 6 and 8 wt% nanoclay. (Valera-Zaragoza *et al.* 2006)

Another conforming conclusion was made by Araújo *et al.* (2009) in their study of Polyamide 66 (PA66)/clay nanocomposites. The results demonstrated that the addition of nanoclay improved

the thermal stability of nanocomposites over the neat PA66. The authors concluded that the thermal stability of the nanocomposites was influenced by the two opposing functions of the nanoclay in it. The first one is the barrier properties to the oxygen, which results in the improvement in the thermal stability. The other is the catalytic effect of the nanoclay in the degradation of the polymer, which decreases the resistance to degradation and resulting in reduction in thermal stability. At a low addition of nanoclay, the first effect is most likely to accrue. But when the load of clay increases, thermal stability of the nanocomposite decreases due to the increase in the dominance of the catalyzing effect.

Another thermal property of polymers is the glass transition temperature (T_g). The effect of clay addition on T_g of the system has been widely investigated by many researchers, results have shown a variety of behaviours, depending on different conditions. An increase in T_g has been observed by some of them, whilst others showed a reduction or no change.

Liu *et al.* (2005b) investigated the thermal properties of epoxy/clay nanocomposites made by either direct-mixing method (DMM) or a high pressure mixing method (HPMM). Nanocomposites synthesized by both methods showed to be slightly decreasing in T_g as the clay contents increased. However, samples made by HPMM showed higher T_g than those made by DMM. The reduction in T_g could be explained by the fact that clay can change the network of the epoxy system by catalyzing the homo-polymerization of the resin during the mixing stage.

Auad *et al.* (2007) studied the T_g of epoxy-phenolic clay nanocomposites. In general, it was found that T_g decreased with increasing nanoclay contents. This reduction in T_g was related to the effect of the cross-linking density on the interference between clay and matrix.

Ye *et al.* (2007) also used Epoxy/HNT (halloysite nanotubes) to measure T_g. They found that the addition of HNT decreased T_g in nanocomposites. However, the presence of HNT improved their thermal stability. Addition of 1.6 wt% of HNT increased the maximum thermal of the nanocomposites from about 393 ^{o}C to 416 ^{o}C. In similar study, Deng *et al.* (2008) investigated the T_g of epoxy filled HNT. Result showed that clay has no significant effect on the value of T_g.

Yasmin *et al.* (2006) studied the thermal behaviour of epoxy/clay nanocomposites. Nanocomposites with two types of nanoclay (Cloisite 30B & Nanomer I.28E) at different clay concentrations (1-10 wt %) were prepared by shear mixing. The results indicated that the T_g in nanocomposites decreased with increasing clay contents for both types of nanoclay as shown in Figure 2.29. The authors argued that the drop in T_g may be related to various of reasons such as clay aggregates, interphase regions, adhesion problems at the clay– matrix interface at elevated temperatures.
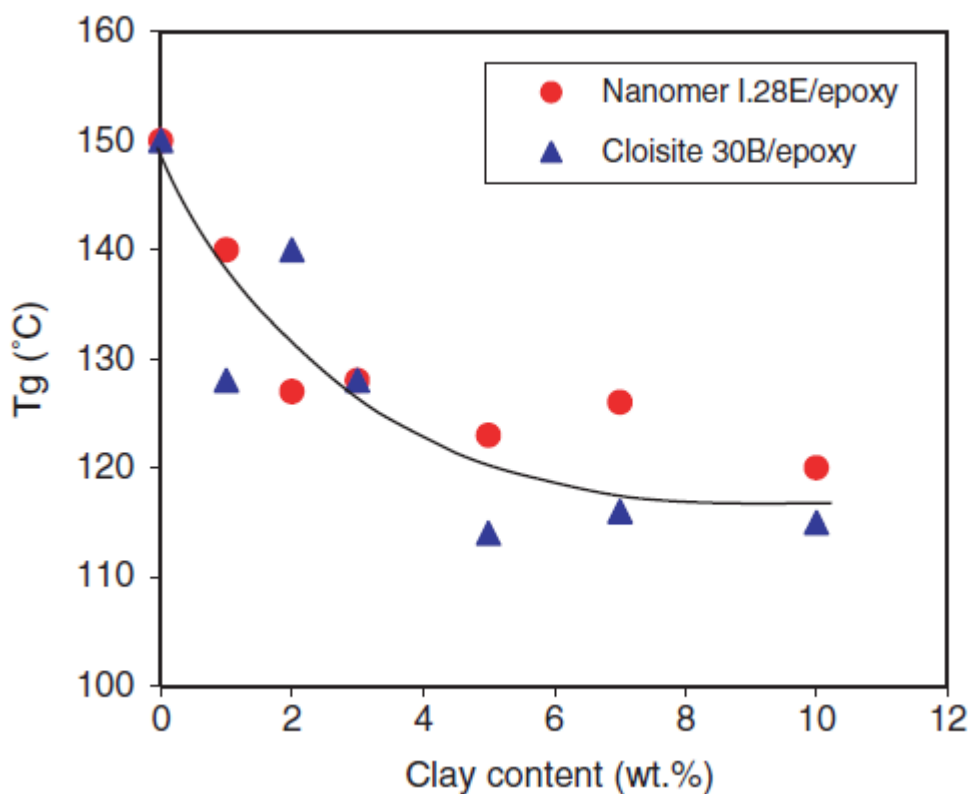
Figurue 2.29. T_g as a function of clay content. (Yasmin *et al.* 2006)

Zainuddin *et al*. (2010) investigated the thermal properties of nanoclay–epoxy nanocomposites. The results showed an increase in T_g with increase clay content as seen in Table 2.10. T_g increased from 99 to 115 ^{o}C for nanocomposites with addition of only 2 wt% clay. The authors elucidated their results as the incorporation of nanoclay into epoxy led to increasing in the cross-link density of the nanocomposites. This increase in cross-linking slowed down the segmental motion of the polymer chains which require higher temperatures to initiate segmental motion and resulted in increased T_g.

59

Table 2.10. Glass transition temperature (T_g) results of neat and 1–3 wt% epoxy nanocomposite. (Zainuddin *et al.* 2010)

Sample	Glass transition temperature, T_g (°C)	% Change over neat
neat	99 ± 3.2	-
1 wt.%	105 ± 4.7	+6.06
2 wt.%	115 ± 2.5	+16.16
3 wt.%	110 ± 4.1	+11.11

This explanation concurs with a previous study done by Yeh *et al.* (2006). They had reported an increase in both T_g and storage modulus for nanocomposites over neat epoxy as the clay concentration increased. Figure 2.30 shows glass transition temperature (T_g) epoxy resin and epoxy/clay nanocomposites. The incorporation of 7 wt% nanoclay into the epoxy matrix enhanced its T_g by about 35% from 73.19 °C to 96.77 °C.
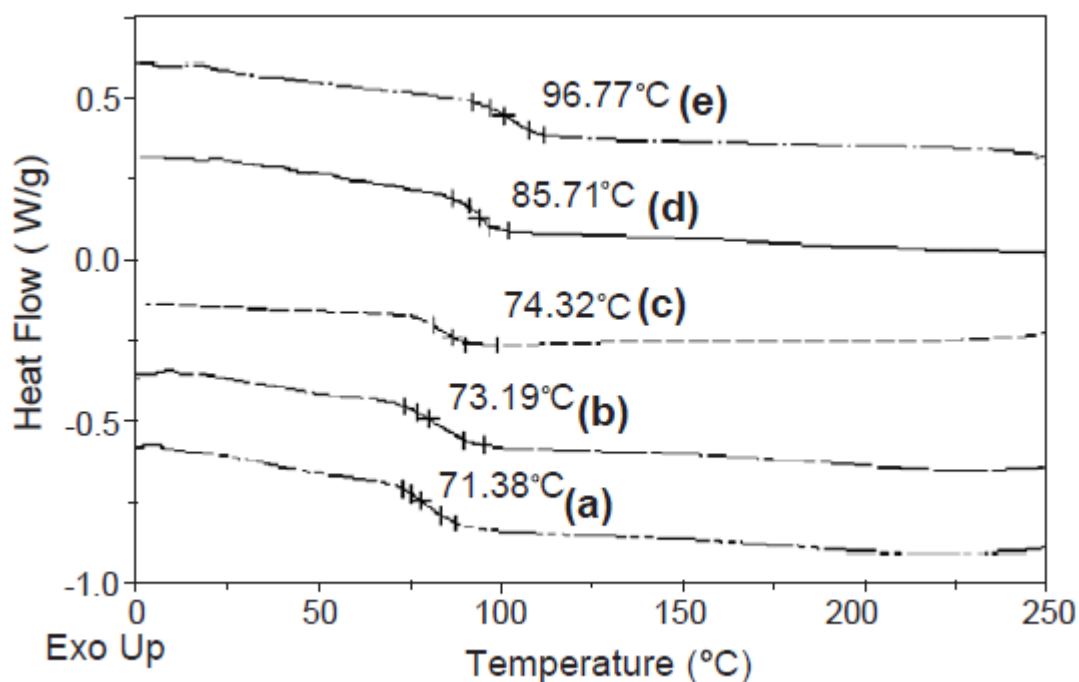
Figure 2.30. T_g of: (a) epoxy, (b) CLMA1, (c) CLMA3, (d) CLMA5, and (e) CLMA7. (Yeh *et al.* 2006)

Another highly interesting aspect revealed by polymer/clay nanocomposites is their excellent barrier properties. The integration of layered silicate usually increases the barrier properties of nanocomposites against oxygen, nitrogen, carbon dioxide, water vapour, gasoline and reduces the water uptake. This improvement of the barrier properties is attributed to the large aspect ratio of the nanoclay layers, which increases the tortuous path of the gas and water molecules that permeate into the material as they diffuse into the nanocomposite as shown in Figure 2.31.
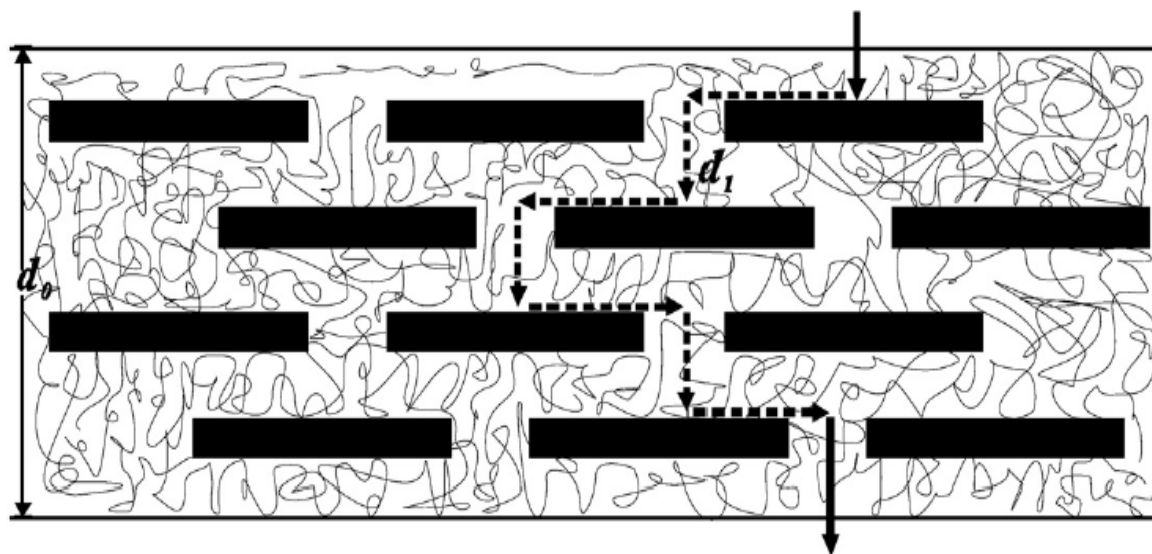
Figure 2.31. Gas barrier properties in polymer/clay nanocomposites showed as torturous zigzag diffusion path. (Zhang *et al*. 2010)

It was reported by the Toyota researchers in 1990 that the addition of nanoclay reduced the rate of water absorption of their polyamide 6-clay hybrid by about 40% over pure polymer (Liu *et al.* 2008). Later on, they were followed by Messersmith and Giannelis in 1995 who observed a remarkable decrease of water permeability reach up to 80% with about 5 wt% of clay into poly (ε-caprolactone) matrix (Messersmith and Giannelis 1995; Liu *et al.* 2008). After that, many researchers have been carried out the water absorption and barrier properties of polymer/clay nanocomposites.

Becker *et al.* (2004) studied the water uptake of high performance epoxy layered silicate nanocomposites. It was found that the addition of nanoclay reduced the maximum water uptake for all nanocomposites compared to pure epoxy systems. However, the diffusion rate of water uptake was observed to be unaffected by the incorporation of nanoclay.

Liu *et al.* (2005a) investigated the water absorption of epoxy/clay nanocomposites. The results revealed significant reductions in both diffusivity and maximum water uptake for nanocomposites over neat epoxy. Water uptake and diffusivity decreased gradually with increasing nanoclay content as shown in Table 2.11.

Table 2.11. Maximum water uptakes (M_∞) and diffusion coefficients (D) of nanocomposites as function of nanoclay loading at 23 ^{o}C. (Liu *et al.* 2005a)

Clay loading (phr)	M_∞ (%)	D X 10^{-8} (mm^2/s)
0	7.76	8.80
3	7.50	8.74
6	7.26	8.33
9	7.07	7.90
12	6.92	7.51
15	6.69	7.34

Alexandre *et al.* (2009) studied the water barrier properties of polyamide 12/C30B nanocomposite. Their study demonstrated that water permeability and the diffusivity of nanocomposites decrease with increasing clay volume fraction up to 2.5% of clay content. However, with more increase in clay content barrier properties was reduced for both structure intercalated and exfoliated. In general, the exfoliated structure displayed better properties than the intercalated structure. The authors concluded that the water diffusion properties depend on a number of factors such as nanocomposite structures, polymer crystallinity, plasticization phenomenon, solubility and free volume variations.

Other studies have focused on nanocomposite barrier properties against gases and vapours. Ke and Yongping (2005) investigated the O_2 permeability of film made by PET/clay nanocomposites with different clay contents varying from 1 to 3 wt%. Figure 2.32, illustrates that the presence of clay dramatically reduced the permeability of O_2 for nanocomposites with maximum reduction reach of up to 50% at 3 wt% of nanoclay load over pure PET film.
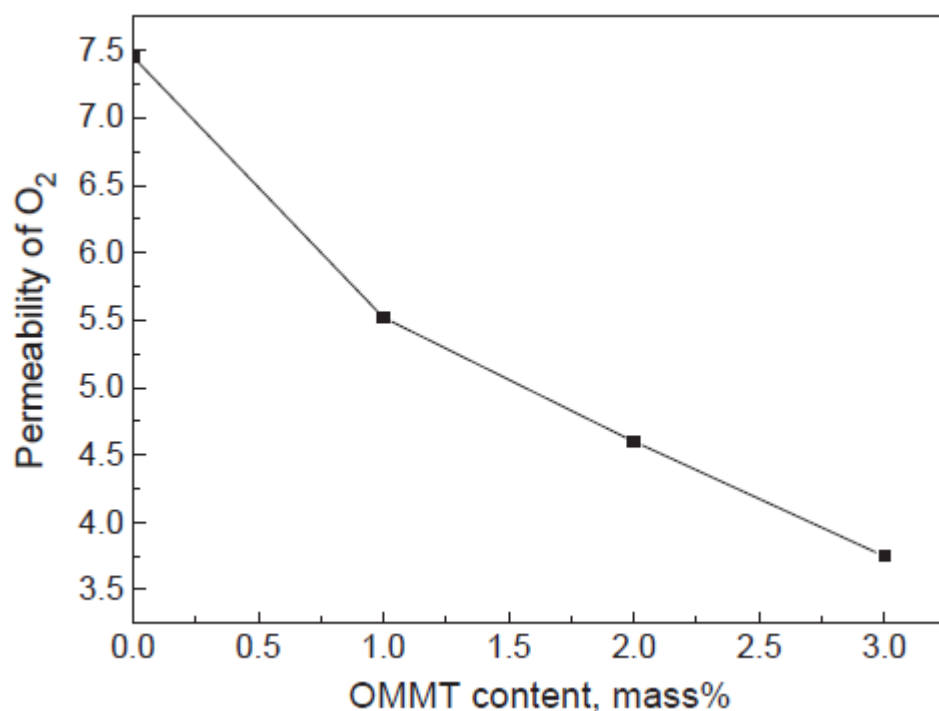
Figure 2.32. The permeability of O_2 for PET/OMMT nanocomposites. (Ke and Yongping 2005)

Ogasawara *et al.* (2006) measured the helium gas permeability of epoxy/MMT nanocomposites. The authors reported that the incorporation of nanoclay improved the barrier properties of epoxy by reducing the helium gas permeability. It was also found that the gas diffusivity decreased as the clay contents increased.

Reddy *et al.* (2007) studied the oxygen permeation properties of low density polyethylene (LDPE) nanocomposites prepared by melt intercalating method. Their results showed that oxygen permeation of LDPE system decreased after the addition of nanoclay. The authors reported that the exfoliation structure of clay dispersion was the reason for the good barrier properties. Such dispersion with high aspect ratio of clay layers can create more tortuous paths for the gas as it diffuses into the nanocomposite.

Zhang *et al.* (2010) investigated the gas permeability of a series of kaolin/natural rubber composites prepared by melt blending. It was found that the addition of nanoclay significantly decreased the nitrogen permeability with the increase in clay content as it can be seen in Figure 2.33. The authors explained that this improvement in barrier properties was due to two factors. Firstly, the high aspect ratio of the impenetrable nanoclay layers forced gas molecules to diffuse in a tortuous path. Secondly, the presence of the nanoclay increased the polymer crystallinity, which resulted in decrease of free volume for the penetrating gas molecules.
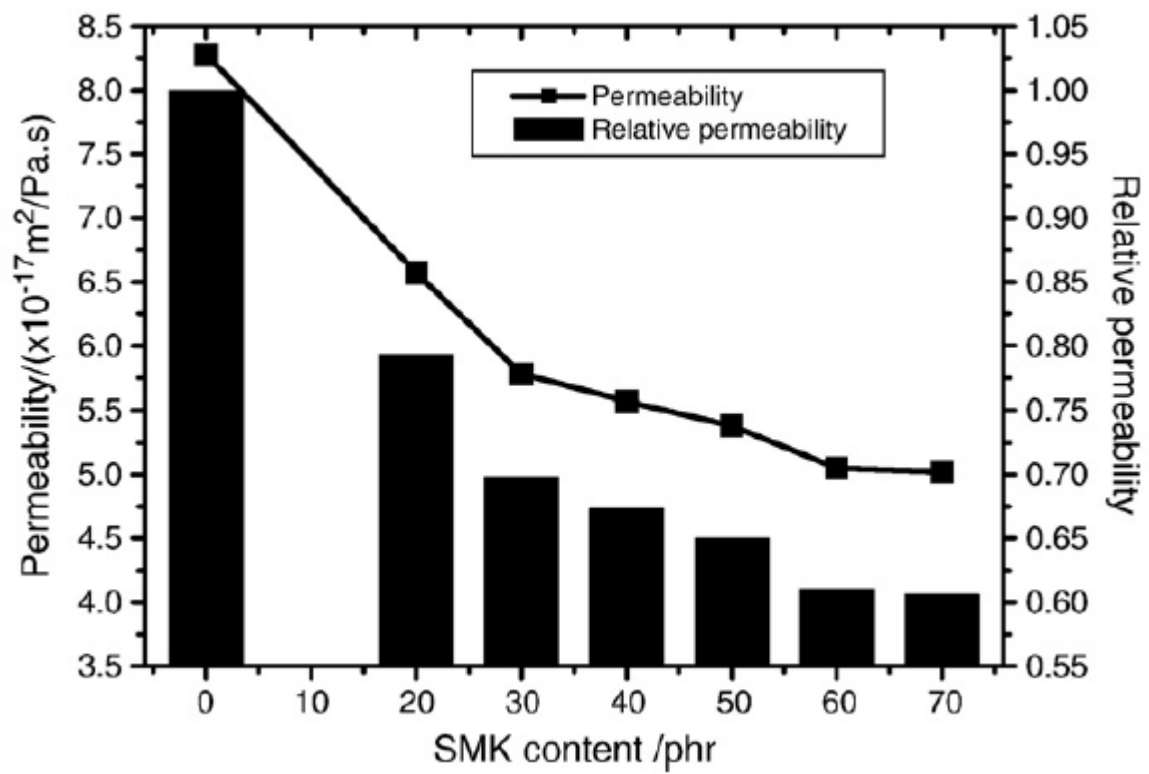
Figure 2.33. The nitrogen permeability as a function of clay content of kaolin/natural rubber composites. (Zhang *et al.* 2010)

2.5 Halloysite/Epoxy Nanocomposites

In enhancing the thermal and mechanical properties of polymers, Halloysite nanotubes (HNTs) as new types of additives have recently received much attention (Deng *et al.* 2009; Tang *et al.* 2011; Prashantha *et al.* 2011). These are a type of naturally occurring aluminosilicate clays, chemically similar to kaolinite with chemical composition ($Al_2Si_2O_5(OH)_4$-$2H_2O$). Halloysite is a 1:1 layered clay mineral, containing one alumina octahedron sheet and one silica tetrahedron sheet (Tang *et al.* 2011). HNTs have a structure of hollow nanotubular with a multi-layered wall structure similar to that of carbon nanotubes (CNTs) (Deng *et al.* 2009; Tang *et al.* 2011; Prashantha *et al.* 2011). The length of HNTs range from 500 nm to1.6 μm and the thickness is smaller than 100 nm (Ye *et al.* 2007; Hedicke-Höchstötter *et al.* 2009). The resemblance of HTNs to CNTs in aspect ratio resulting from their unique crystal structure, lowered cost of HNTs as compared to CNTs, ability of HTNs to disperse easily in a polymer matrix and the fact that halloysites are rigid materials have resulted to halloysite nanotubes being considered as ideal materials in polymer nanocomposites preparation (Ye *et al.* 2007; Deng *et al.* 2009; Prashantha *et al.* 2011).

The use of HNTs in reinforcing epoxy matrices is still new in the field of polymer nanocomposites. Previous researchers have found that the mechanical performance of epoxy resins materials including toughness, modulus and strength were increased through the addition of a small amount of halloysite particles without necessarily sacrificing other properties such as thermal stability and glass transition temperature (T_g). Ye *et al.* (2007) investigated the mechanical and thermal properties of HNTs/epoxy nanocomposites. It was reported an improvement in impact strength of halloysite–epoxy nanocomposites without sacrificing strength and thermal properties. Figure 2.34 shows the mechanical properties of epoxy nanocomposites reinforced with different load of HNTs. Impact strength gradually increased with maximum enhancement 400% at 2.3 wt% HNT load. Authors stated that massive micro-cracking, particle (breaking, bridging and pull-out) and crack deflection were responsible for the significant enhancement in impact toughness as seen in Figure 2.34. Flexural strength and modulus were slightly increased due the addition of halloysite tubes (Figure 2.34).
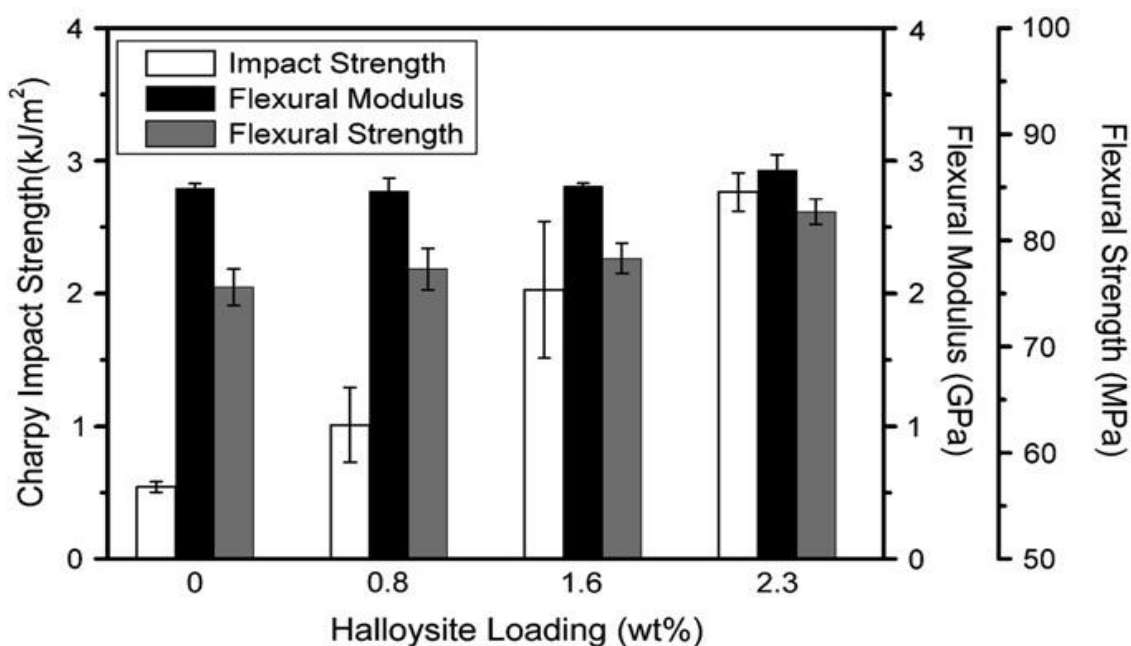
Figure 2.34. Mechanical properties of epoxy/HNT nanocomposites as a function on HNTs loading. (Ye *et al*. 2007)

It was also found that the incorporation of HNTs in epoxy matrix increased the thermal stability by increasing the maximum thermal decomposition temperature and char yield at 700 °C of nanocomposites (Figure 2.35).
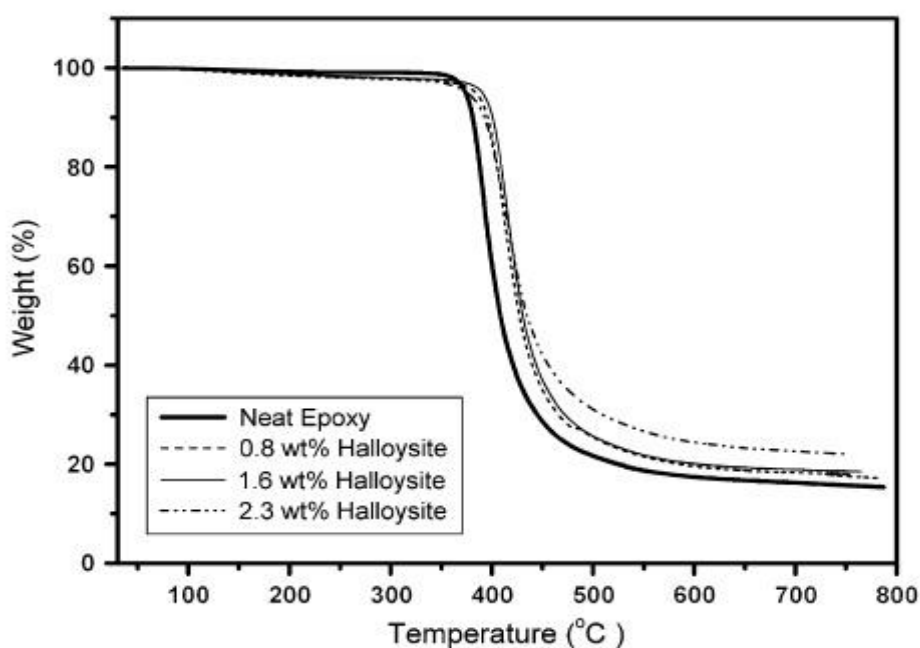
Figure 2.35. TGA curve for neat epoxy and its nanocomposites. (Ye *et al*. 2007)

Deng *et al.* (2008) reported a great increase in impact and fracture toughness without a reduction in strength and thermal properties of HNT-epoxy composites. Results showed that fracture toughness and impact toughness increased as HNTs content increased (Figure 2.36). Maximum enhancement in fracture toughness (50%) and impact toughness (127%) were achieved at 10 wt% HNTs load.
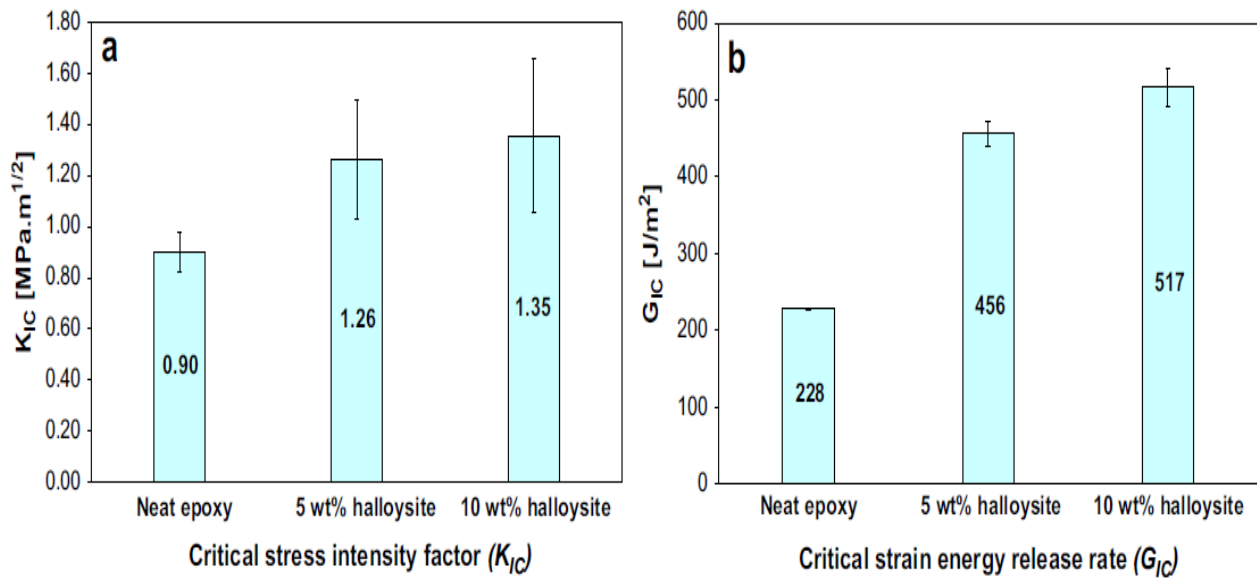
Figure 2.36. HNT effect on both (a) fracture toughness and (b) impact toughness. (Deng *et al.* 2008)

Figure 2.37 shows typical stress/strain curves of tensile test for epoxy and its nanocomposites. The presence of HNTs obviously increased tensile strength for epoxy filled with HNTs compared to unfilled composites.
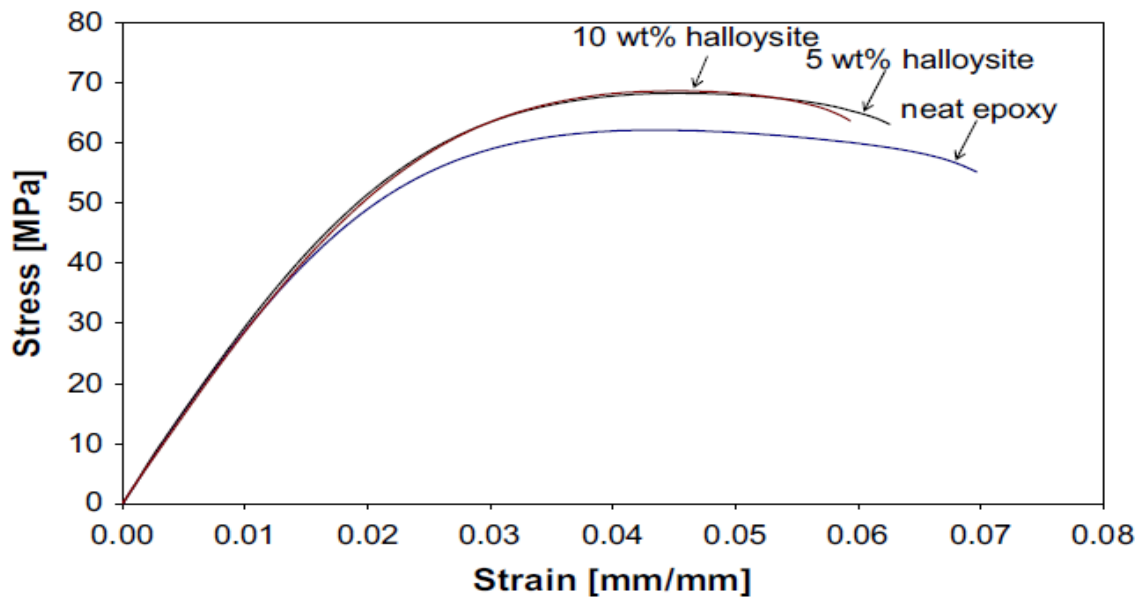
Figure 2.37. Stress/strain curve of tensile test for neat epoxy and its nanocomposites. (Deng *et al.* 2008)

Later on, Deng and co-workers (2009) reported an enhancement in facture toughness of halloysite tube–epoxy nanocomposites without sacrificing thermal properties after improving HNTs particles dispersion into epoxy matrix though chemical treatments and ball mill homogenization.

Tang *et al.* (2011) studied the mechanical properties of treated halloysite reinforced epoxy nanocomposites. Intercalated structure was achieved due to the treatment by phenylphosphonic acid (PPA). It was reported that the fracture toughness of epoxy significantly increased by 78.3% due to the presence of 10 wt% of intercalated HNTs. This enhancement as authors claimed was due to the facture mechanism such as fibre (breakage, debonding and pullout), crack deflection, crack bridging and plastic deformation. It was also found that tensile strength, tensile modulus and glass transition temperatures (T_g) slightly increased after the addition of treated HNTs.

There have been other studies on using HNT as a modifier for other polymer matrixes. For example, Ismail *et al.* (2008) investigated the mechanical and thermal properties of halloysite

nanotubes filled ethylene propylene diene monomer (EPDM) nanocomposites. Results showed that tensile strength and modulus increased dramatically as HNT content increased. Thermal stability and flammability properties also increased as a result of HNTs addition. Authors reported that this enhancement in tensile and thermal properties was due to the well-dispersion of HNTs inside EPDM matrix and to the formation of zig-zag structure by HNTs interaction. Pasbakhsh *et al.* (2010) studied the tensile properties of a modified HNTs reinforced ethylene propylene diene monomer (EPDM) nanocomposites. γ-methacryloxypropyl trimethoxysilane (MPS) was used to treat HNTs and improve their dispersion inside EPDM matrix. It was reported that samples filled with modified HNTs displayed better tensile strength and modulus than those filled with unmodified HNTs. SEM and TEM micrographs revealed that the dispersion of modified HNTs was better than unmodified HNTs due to the treatment by MPS. Hedicke- Höchstötter *et al.* (2009) investigated the tensile properties of HNT/polyamide-6 nanocomposites prepared by melt extrusion and an adjacent injection moulding method. Tensile strength and modulus were found to increase due to the presence of HNTs. However, authors compared between polyamide-6 reinforced with HNTs and same matrix reinforced with organically modified montmorillonite. Results showed that samples filled with organoclay exhibited higher tensile strength and modulus than those filled with HNTs. Prashantha *et al.* (2011) studied the effect of unmodified HNTs and quaternary ammonium salt treated halloysite nanotubes (QM-HNTs) on the mechanical and thermal properties of HNT/polypropylene (PP) nanocomposites. Results indicated that tensile strength and modulus, flexural strength and modulus, impact strength and glass transition temperature (T_g) increased due the addition of HNTs. However, samples reinforced with modified HNTs showed better mechanical and thermal properties than those filled with unmodified HNTs. Authors explained that by the enhancement in matrix/particles interface and particles dispersion in the matrix due to the quaternary ammonium salt treatment. Figure 2.38 shows the impact strength as a function of HNT content of PP/HNT and PP/QM-HNT nanocomposites.
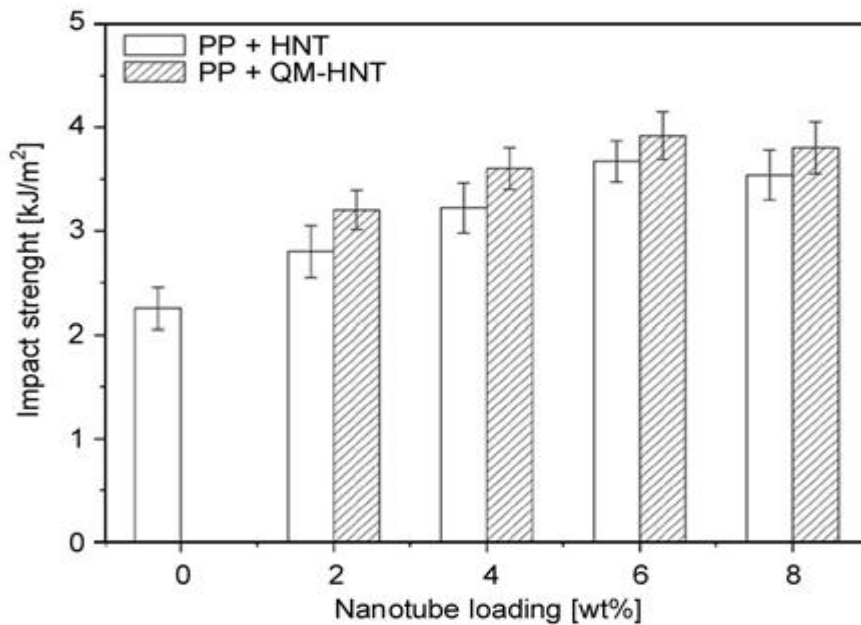
Figure 2.38. Impact strength as a function of HNT content of PP/HNT and PP/QM-HNT nanocomposites. (Prashantha *et al.* 2011)

2.6 Silicon Carbide/Epoxy Nanocomposites

Silicon carbide particles are very attractive ceramic material that can be used as filler in different polymer matrices due to the unique properties including high thermal conductivity, low thermal expansion coupled with high strength, high hardness and high elastic modulus (Satapathy *et al.* 2009). Silicon carbide (SiC) is rigid crystalline material that compound of silicon and carbon and has been used in grinding abrasive products including wheels for over a period of 100 years. Currently, the material has been developed to a point that it has very good mechanical properties as a high-quality grade ceramic used in numerous high-performance applications (Satapathy *et al.* 2009). Therefore, ceramic filled polymer composites have been the subject of extensive research in the last two decades (Rodgers *et al.* 2005; Wetzel *et al.* 2006; Zhao *et al.* 2008; Liao *et al.* 2011). Rodgers *et al.* (2005) investigated SC-15 epoxy based nanocomposites reinforced with three different loading (0.5, 1 and 1.5 wt%) of β-SiC nano-particles, which were prepared by high intensity ultrasonic liquid processor. Results showed that SiC dispersion was homogenous into epoxy system. In general, the presence of SiC particles into epoxy increased thermal and mechanical properties. The addition of only 1 wt% of SiC displayed better mechanical and thermal properties over neat epoxy and nanocomposites reinforced with 0.5 and

70

1.5 wt%. Tables (2.12 and 2.13) show thermal and mechanical properties of neat epoxy and epoxy/SiC nanocomposites. For example, the insertion of 1 wt% SiC increased T_g and flexural strength by 16% and 21.4%, respectively.

Table 2.12. Thermal properties of neat epoxy and epoxy/β-SiC nanocomposites. (Rodgers *et al.* 2005)

Material	DSC glass transition temperature (T_g) (°C)	TGA decomposition temperature (°C)
SC-15 epoxy, neat	73	356
+0.5 wt% SiC	80	378
+1.0 wt% SiC	85	385
+1.5 wt% SiC	65	358

Table 2.13. Flexural properties of neat epoxy and epoxy/β-SiC nanocomposites. (Rodgers *et al.* 2005)

Material	Flexural modulus (GPa)	Gain/loss in modulus (%)	Flexural strength (MPa)	Gain/loss in strength (%)
SC-15 epoxy, neat	2.45 ± 0.09		91.87 ± 5.13	
+0.5 wt% SiC	3.26 ± 0.21	33.06	111.73 ± 9.35	21.62
+1.0 wt% SiC	3.33 ± 0.21	35.92	111.53 ± 6.97	21.40
+1.5 wt% SiC	3.32 ± 0.10	35.51	95.86 ± 4.01	4.34

Wetzel *et al.* (2006) studied the mechanical properties of epoxy nanocomposites reinforced with either aluminium oxide (Al_2O_3) or titanium dioxide (TiO_2) nano-particles. Figure 2.39 shows the effect of nano-particles on flexural modulus and flexural strength of epoxy nanocomposites. It can be seen that both flexural modulus and strength increased as nano-fillers content increased.

Authors reported that fracture toughness increased significantly as nano-filler content increased as seen in Figure 2.40. Interestingly, the addition of Al_2O_3 particles showed better mechanical properties than TiO_2. Authors concluded that several toughness mechanisms were responsible for the toughness enhancements.
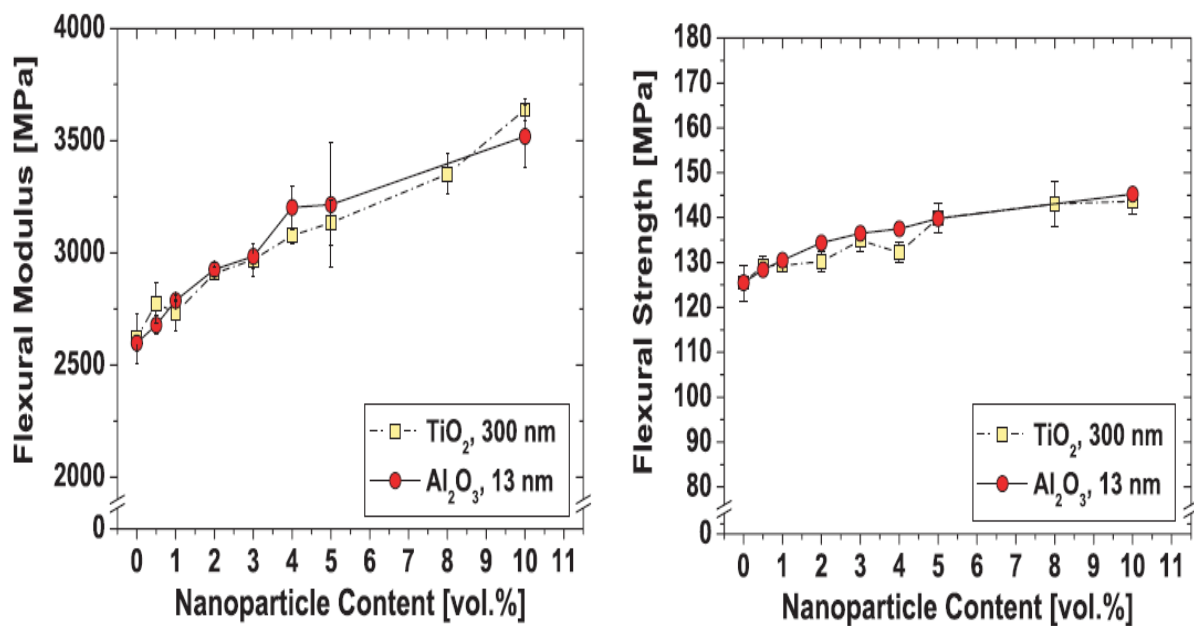
Figure 2.39. The effect of nano-particles content on (a) flexural modulus and (b) flexural strength. (Wetzel *et al.* 2006)
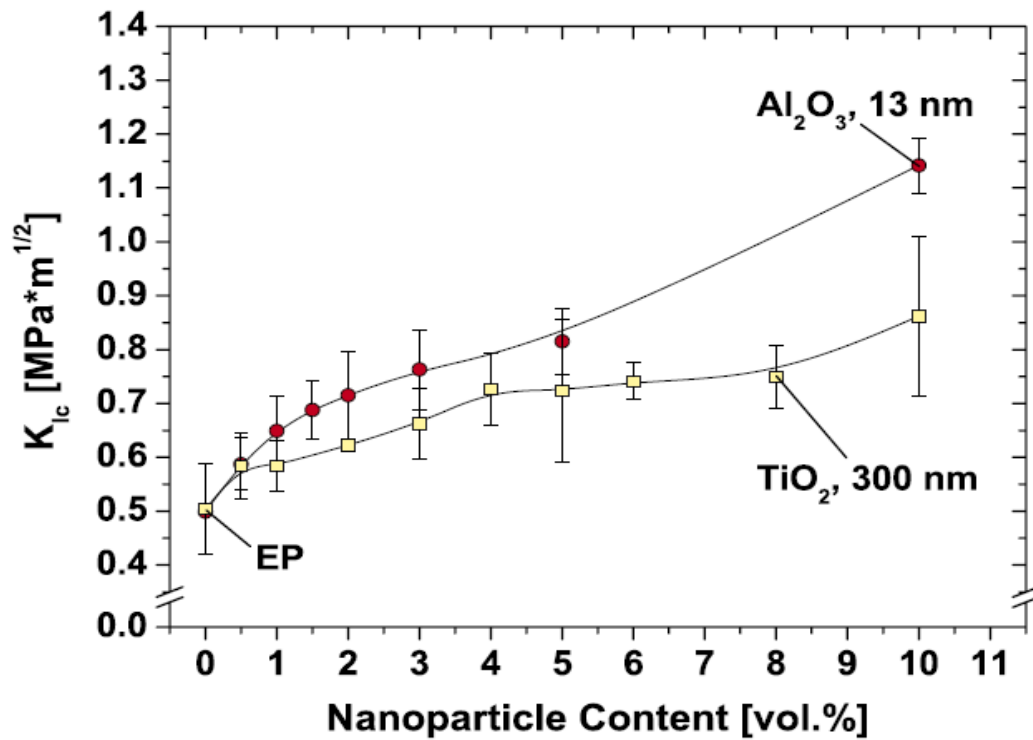
Figure 2.40. Fracture toughness of epoxy nanocomposites as a function of nano-particles content. (Wetzel *et al.* 2006)

Zhao *et al.* (2008) on the other hand used nano alumina particles to toughen epoxy resin. However, no improvement was reported in fracture toughness due to the addition of nano alumina. Chen *et al.* (2008) investigated the mechanical properties of silica-epoxy nanocomposites. It was reported that the addition of only 10 wt% nano-silica increased fracture toughness and tensile modulus by 30% and 25% respectively. Chatterjee and Islam (2008) carried out the mechanical and thermal properties of TiO_2/epoxy nanocomposites prepared by ultrasonic mixing process. Authors reported homogenous dispersion for nano-particles into the epoxy matrix with enhancement in thermal stability, glass transition temperature, tensile and flexural modulus due to the presence of nano-silica particles. However, no improvement was reported in tensile and flexural strength. Ma *et al.* (2008) investigated the effect of silica nano-particles on the mechanical property of two types of epoxy systems. It was found that the presence of nano-silica increased Young's modulus, tensile strength, fracture toughness and critical energy release rate for both epoxy systems. Figure 2.41 shows that facture toughness and critical energy release for both epoxy systems increases as silica load increases.
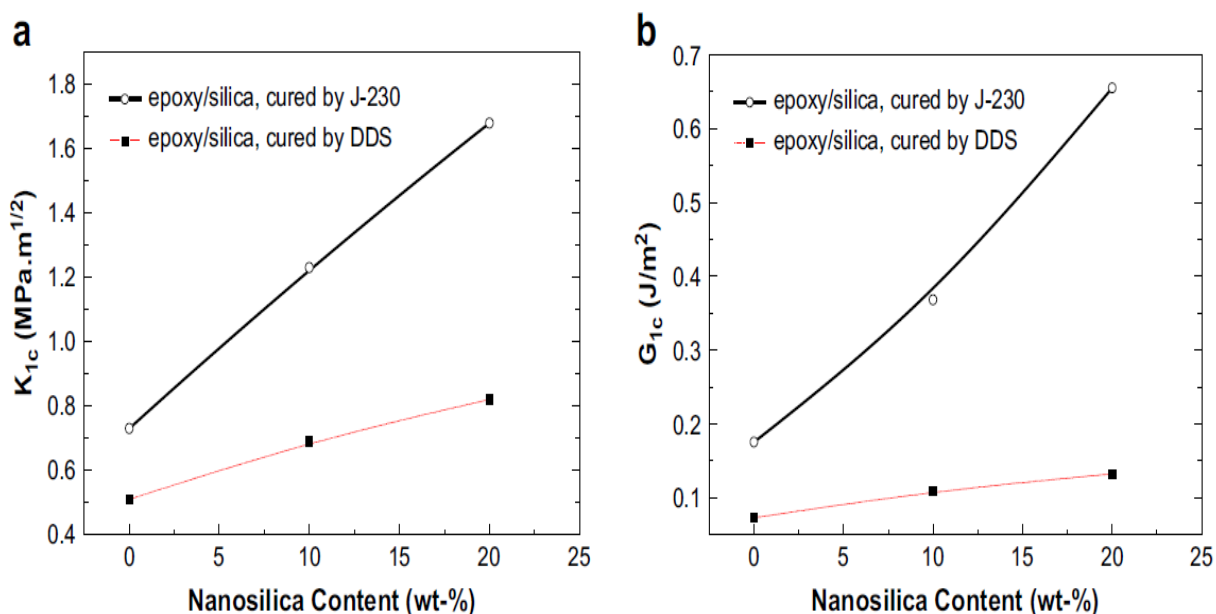
Figure 2.41. (a) Fracture toughness and (b) critical energy release rate, for two epoxy systems reinforced with nano-silica. (Ma *et al.* 2008)

Liao *et al.* (2011) studied the mechanical properties of maleated high density polyethylene (mPE) reinforced with SiC nano-particles. Injection moulding method was used to prepare nanocomposites with four different SiC loading (2, 4, 6 and 8) wt%. Results showed that Young's modulus and yield strength increased for nanocomposites as SiC content increased. However, the addition of SiC particles decreased impact strength of mPE nanocomposites when compared to unfilled mPE. Authors reported that the absence of particle cavitation and matrix fibrillation was the reason of the reduction in impact strength of mPE/SiC nanocomposites.

2.7 Fibre-Reinforced Polymer Nanocomposites

The use of nanocomposites filled with nano-particles (clays, silica, carbon nanotubes, silicon carbide, etc.) as a matrix for fibre-reinforced composites has been recently carried out by number of researchers (Bozkurt *et al.* 2007; Xu and Hoa 2008; Auad *et al.* 2007; Khan, Iqbal, *et al.* 2011). Previously published research on the use of nanoclay matrix for fibre composites showed that the addition of nanoclay enhances the mechanical properties of fibre reinforced epoxy composites (Bozkurt *et al.* 2007; Zulfli and Shyang 2010; Xu and Hoa 2008; Faruk and Matuana 2008; Mohan and Kanny 2011). For example, Bozkurt *et al.* (2007) investigated the effect of nanoclay dispersion on the mechanical properties of non-crimp glass fibre reinforced epoxy nanocomposites. It was found that flexural properties increased with the addition of unmodified clay (MMT) and modified clay (OMMT), up to 6 wt% of clay loading due the enhancement in

the interface between the glass fibre and epoxy matrix. Figure 2.42 shows flexural strength and flexural modulus as a function of clay content. It is can be seen that samples filled with OMMT displayed better flexural strength and modulus than those filled with unmodified clay.
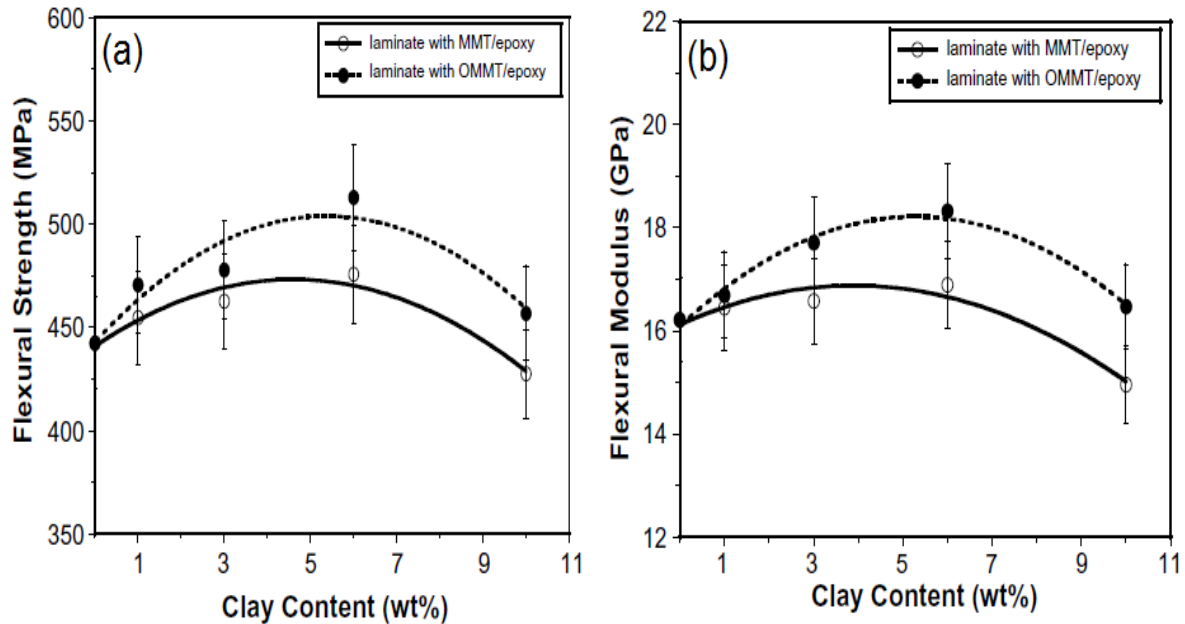
Figure 2.42. Flexural properties of non-crimp glass fibre reinforced clay/epoxy nanocomposites: (a) flexural strength, (b) flexural modulus. (Bozkurt *et al*. 2007)

In a similar study, Zulfli and Shyang (2010) reported an improvement in flexural strength and modulus of glass fibre reinforced epoxy/clay nanocomposites due to the addition of organo-treated nanoclay. The interface between the glass fibre and epoxy matrix was increased due to the presence of nanoclay.

Xu and Hoa (2008) investigated the mechanical properties of carbon fibre reinforced epoxy/clay nanocomposites. It was observed an increase in fracture toughness and flexural strength after the addition of a small content of nanoclay. Flexural strength result is shown in Figure 2.43.
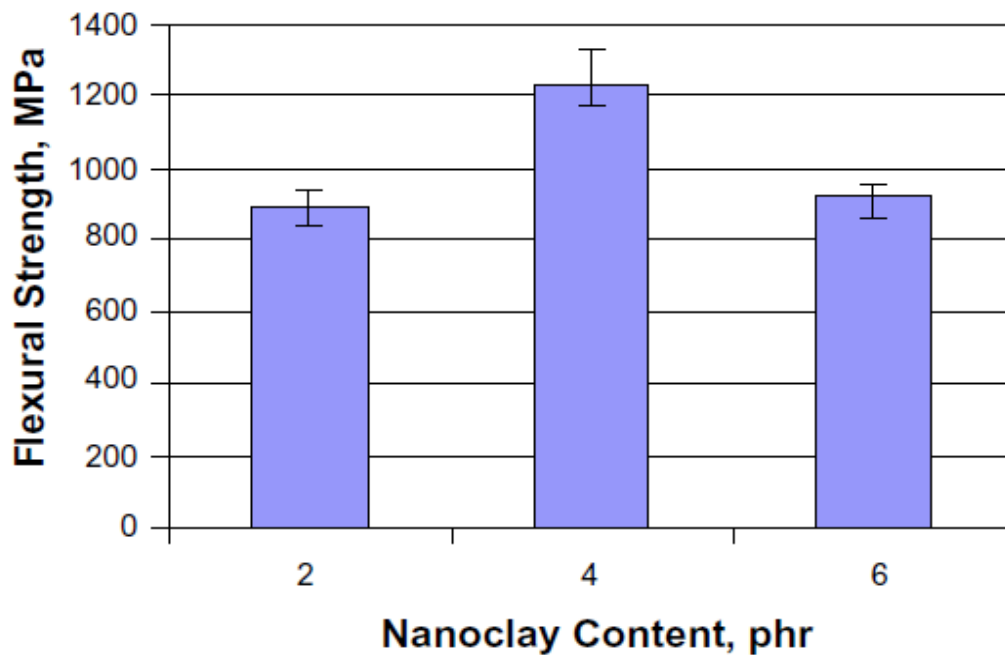
Figure 2.43. Flexural strength as a function of nanoclay content. (Xu and Hoa 2008)

An interesting study on wood/clay/epoxy nanocomposites was obtained by Faruk and Matuana (2008). They investigated the effect of five different types of nanoclay on the mechanical properties of wood/epoxy composites. Two different methods (melt blending process and direct dry blending process) were used to fabricate wood/epoxy nanocomposites. Melt blending process involved using the clay reinforced epoxy as a matrix for wood/epoxy nanocomposites while direct dry blending process involved adding the nanoclay directly into the wood/epoxy composites. Results are summarized in Table 2.14 and Table 2.15. Table 2.14 shows the effect of nanoclay types on the mechanical properties of clay/epoxy nanocomposites made by melt blending method. It can be seen that the addition of nanoclay increased flexural properties and tensile properties of epoxy based nanocomposites compared to unfilled epoxy composites. The addition of Cloisite 10A displayed better mechanical properties than other types of clay. This was attributed to the better intercalation of Cloisite 10A among other nanoclays.

Table 2.14. The effect of nanoclay types on mechanical properties of epoxy/clay nanocomposites. (Faruk and Matuana 2008)

Types of nanoclay in HDPE matrix	Flexural properties		Tensile properties	
	Strength (MPa)	Modulus (MPa)	Strength (MPa)	Modulus (MPa)
None (control)	25.3 ± 1.4	667 ± 61	24.8 ± 0.3	1050 ± 16
Cloisite 10A	31.7 ± 1.8	947 ± 76	27.6 ± 1.1	1353 ± 50
Cloisite 15A	24.7 ± 0.8	693 ± 40	25.0 ± 0.5	1333 ± 36
Cloisite 20A	26.4 ± 0.5	757 ± 35	25.1 ± 0.3	1334 ± 24
Cloisite 25A	26.8 ± 0.6	759 ± 21	25.1 ± 0.1	1341 ± 23
Cloisite 30B	25.7 ± 0.3	744 ± 19	25.3 ± 0.2	1335 ± 10

Table 2.15 shows the effect of mixing methods on the flexural properties of wood/Cloisite 10A/epoxy nanocomposites. As it can be seen, the addition of nanoclay by melt blending method increased flexural strength and modulus compared to unfilled wood/epoxy composites. However, using direct dry blending method led to reduction in flexural strength. Authors recommended using clay/epoxy as a matrix to wood/polymer nanocomposites to achieve better mechanical properties for wood/clay/polymer nanocomposites.

Table 2.15. The effect of blending method on flexural properties of wood/Cloisite 10A/epoxy nanocomposites. (Faruk and Matuana 2008)

Blending process	Flexural properties	
	Strength (MPa)	Modulus (MPa)
Control (no nanoclay)	28.9 ± 1.4	1919.7 ± 112
Direct dry blending (direct mix)	27.1 ± 1.4	2233.8 ± 144
Melt blending (HDPE/nanoclay as matrix)	33.5 ± 0.4	2726.9 ± 196

Mohan and Kanny (2011) investigated the water absorption behaviour of sisal fibre reinforced epoxy/clay nanocomposites. Results indicated that the presence of nanoclay improved the water barrier properties by reducing water mass uptake of sisal fibre/epoxy nanocomposites as seen in Figure 2.44. Water mass uptake decreased as clay content increased with maximum reduction occurred at 5 wt% nanoclay. Composites filled with 5 wt% nanoclay showed better barrier properties than those filled with 5 wt% microclay.
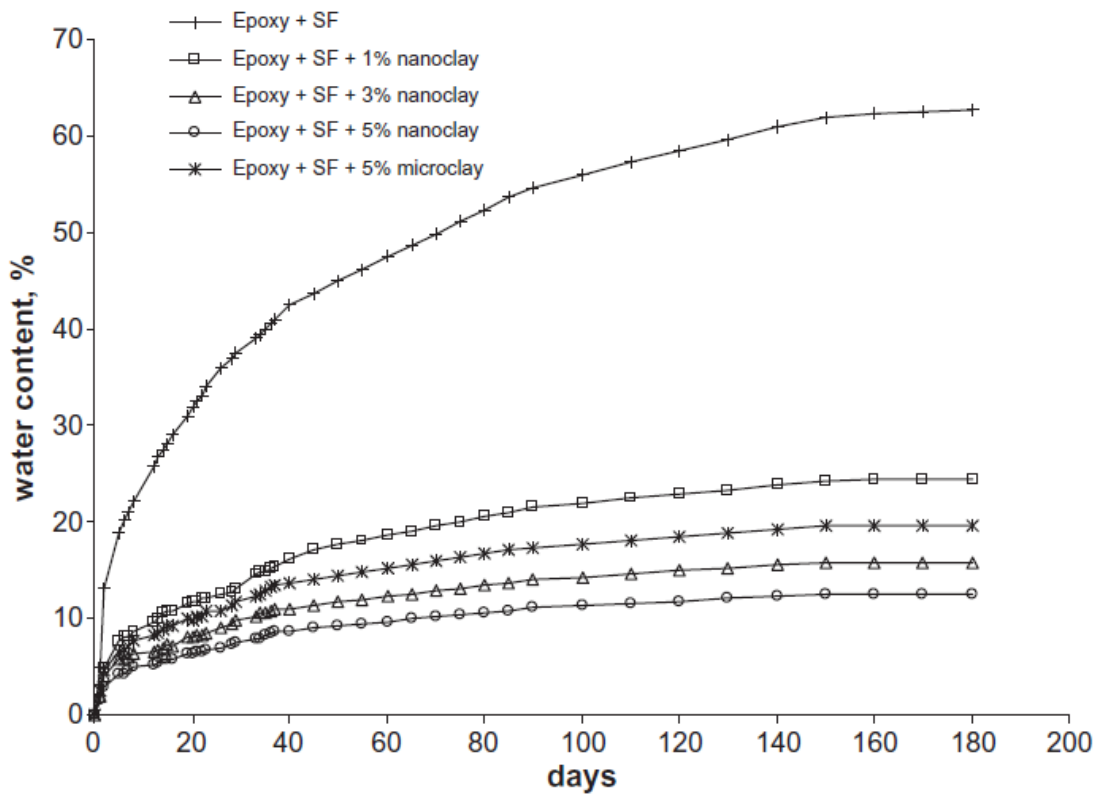
Figure 2.44. Water uptake of sisal/epoxy composites and sisal/epoxy nanocomposites. (Mohan and Kanny 2011)

Ye *et al.* (2011) studied the effect of halloysite nanotubes (HNTs) on the mechanical and thermal properties of epoxy/carbon fibre (CF) composites. It was reported that the addition of HNTs generally increased flexural strength, flexural modulus, impact strength and glass transmission temperature (T_g) of CF/epoxy nanocomposites compared to unfilled CF/epoxy composites. Adding only 2 wt% of HNTs increased impact strength by 25% compared to unfilled CF/epoxy composites. Figure 2.45 shows the impact strength of pure epoxy, HNT/epoxy nanocomposite, CF/epoxy composites and HNT/CF/epoxy composites. It can be seen that the combination of HNT/CF/epoxy displayed the best impact properties among other composites. This enhancement in impact strength was attributed to the toughness mechanisms due to the addition of HNTs as rigid particles as well as due to the presence of carbon fibres.
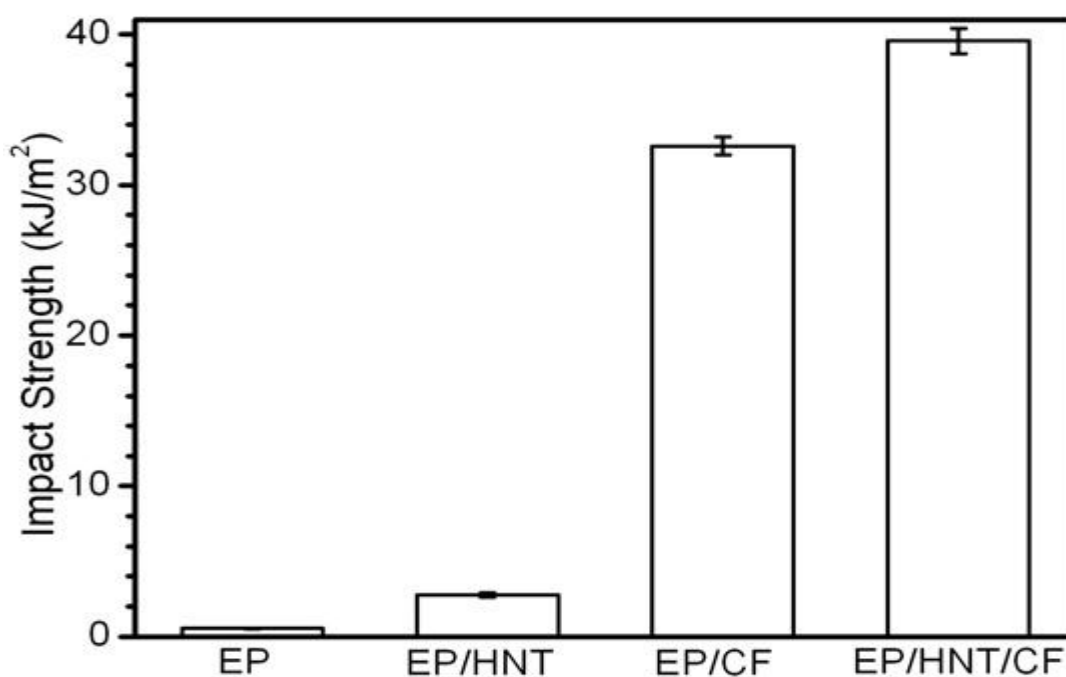
Figure 2.45. Impact strength of neat epoxy, HNT/epoxy, CF/epoxy and HNT/CF/epoxy composites. (Ye *et al.* 2011)

Satapathy *et al.* (2009) added nano-silicon carbide (SiC) to jute fibre reinforced epoxy composites and investigated the physical and mechanical properties of the resulted composites. In their studied, they prepared two different types of composites. The first type was about epoxy reinforced with three different loading of jute fibre (20, 30 and 40) wt%. The second type was about epoxy/40 wt% jute fibre composites filled with either 10 wt% SiC or 20 wt% SiC. Results showed that volume fraction of voids increased slightly due to the presence of jute fibre. However, voids significantly increased in composites after the addition of SiC. Tensile and flexural strength of unfilled composites increased as jute fibre content increased. However, the addition of SiC into composites led to a reduction in both tensile and flexural strength as seen in Figure 2.46. Authors claimed that the incorporation of SiC particles could reduce the stress transfer at the matrix/fibres interface resulted in low tensile strength.
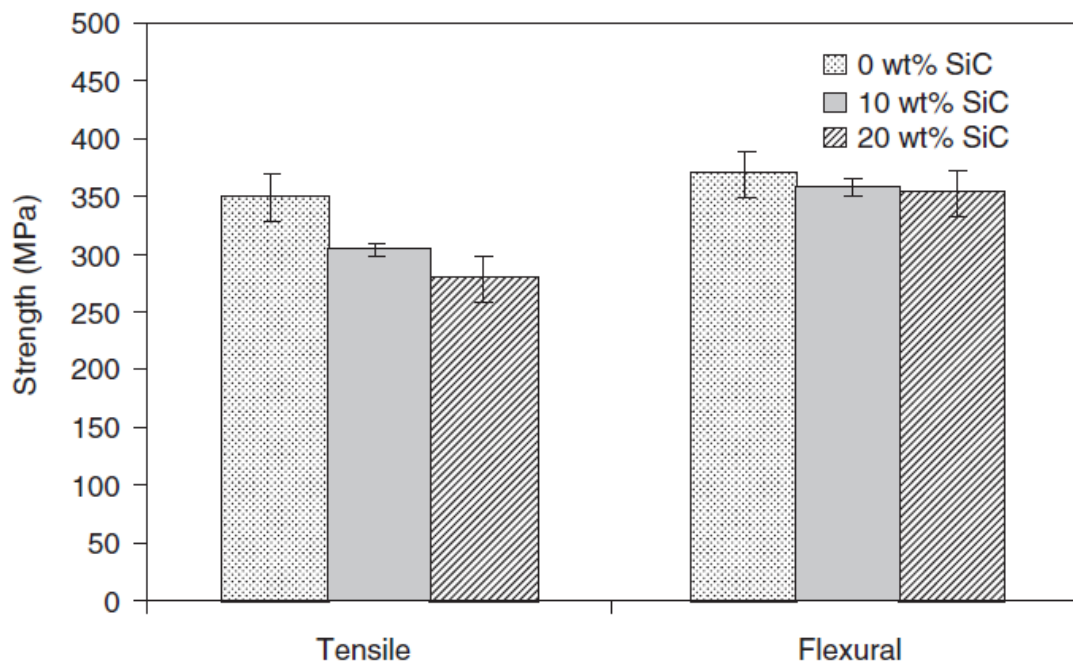
Figure 2.46. Tensile and flexural strength of jute fibre/epoxy composites as a function of SiC content. (Satapathy *et al.* 2009)

2.8 Effect of fibre character (dispersion, volume fraction, orientation and fibre-matrix interfacial adhesion) on mechanical properties of cellulose fibre reinforced polymer composites.

Cellulose fibres in this project can be considered as short fibres. There are several factors that influence the mechanical properties of short fibre reinforced polymer composites, such as, fibre dispersion, fibre aspect ratio, fibre orientation, fibre-matrix adhesion and fibre volume fraction. (Rowell *et al*. 1997; Li *et al*. 2000).

Fibre dispersion

One of the major factors that influence the mechanical properties of cellulose fibre reinforced polymer composites is fibre dispersion. Good dispersion of fibres in polymer matrix usually enhances the strength of composites (Bachtiar *et al*. 2008). However, poor dispersion of fibre normally results in creating an inhomogeneous mixture of resin-rich areas and fibre-rich areas which cause weakness to the resulted composites (Taib 1998). Poor dispersion of fibre normally leads to an increase in matrix-rich regions, which means that the matrix is not restrained by enough fibres. In this case, there is not sufficient fibre to carry the transferred load from the matrix. Therefore, composites exhibit highly localized strains at low stresses, which lead to low mechanical properties. Moreover, poor dispersion of the fibres leads to fibre agglomeration which acts as stress concentrators, resulting in crack initiation during loading (Taib 1998; Rowell *et al*. 1997).

Fibre-matrix adhesion

The strength of adhesion between fibre and matrix is a critical factor that influences the mechanical properties of cellulose fibre/polymer composites. For example, tensile or flexural strength of these types of composites is strongly depended on the interfacial adhesion between fibres and the matrix (Ku *et al*. 2011). Good interfacial bonding results in enhanced composites strength properties, since stress can be effectively transferred between the fibre and the matrix. Therefore, several chemical and physical treatments are required to improve the adhesion bonding between fibres and matrix (Ku *et al*. 2011). Several chemical treatments have been reported by various researchers (Ku *et al*. 2011; Kabir *et al*. 2011; Faruk *et al*. 2012). However, an enhancement in fibre-matrix interfacial bonding will normally lead to low fracture toughness due to the reduction in energy dissipation processes such as interfacial debonding, fibre pull-out and crack-bridging.

Volume fraction

Fibre loading or fibre volume fraction is an important factor that influences the mechanical properties of short fibre/polymer composites. Mechanical properties (i.e. strength, modulus, and toughness) are generally increased as fibre loading increase by virtue of the rule-of-mixtures. For instance, Hughes *et al.* (2002) reported that fracture toughness of hemp and jute fibre reinforced polyester composites increased as fibre volume fraction increased. Normally the strength of fibre reinforced polymer composites increases as the fibre content increases. A maximum strength is reached at a fibre volume fraction called the optimum or maximum fibre volume fraction. Any further increase in fibre content beyond the optimum fibre fraction can lead to a reduction in strength. This reduction in strength beyond the maximum fibre fraction is attributed to the lack of interfacial adhesion between the fibre and the matrix as a result of the increase in fibre-fibre interactions (Al-kaabi *et al.* 2005). Rong *et al*. (2001) reported an overall enhancement in flexural strength and modulus of sisal/epoxy composites as the fibre content increased up to ~75 vol%. Al-kaabi *et al*. (2005) reported that the ultimate flexural strength for date palm fibre-polyester composites was obtained at 9 wt% of fibres. Adding more fibres caused a reduction in strength. Ruoyuan *et al*. (2010) reported that the maximum flexural strength and modulus of silk fibre reinforced PBS composites occurred at a fibre content 40 wt%. Further increase in fibre content led to reduction in both strength and modulus. They attributed the reduction in flexural properties to insufficient filling of PBS matrix into the fibres. Table 2.16 shows the influence of composite architectures on failure strength and mode at different situations based on the rule-of-mixtures (Mitchell 2004).

Table 2.16. Failure strength and failure mode for different relative strains to failure of fibre and matrix and different volume fractions.

		$V_f < V_f'$	$V_f > V_f'$	Reference
$\varepsilon_f^* < \varepsilon_m^*$	Strength	$\sigma_1^* = (1 - V_f)\sigma_m^*$	$\sigma_1^* = V_f\sigma_f^* + (1 - V_f)\sigma_m'$	(Mitchell 2004)
	Failure Mode	Fibre fracture	Fibre fracture followed by matrix facture	
		$V_f < V_f'$	$V_f > V_f'$	
$\varepsilon_f^* > \varepsilon_m^*$	Strength	$\sigma_1^* = V_f\sigma_f' + (1 - V_f)\sigma_m^*$	$\sigma_1^* = V_f\sigma_f^*$	(Mitchell 2004)
	Failure Mode	Matrix facture	Multiple matrix fracture	

σ_1^* : Composite failure stress, σ_f^*: fibre failure stress, σ_m^*: Matrix failure stress, σ_f': the stress carried by fibre at matrix failure strain , σ_m': the stress carried by matrix at fibre failure strain.

If the failure strain of fibre that is smaller than the matrix ($\varepsilon_f^* < \varepsilon_m^*$); the fibre will start to fail before the matrix (Callister 2007). Here, two scenarios are possible depending on the fibre volume fraction. If the fibre volume fraction is smaller than its critical value ($V_f < V_f'$), the matrix is able to carry the applied load after fibre fracture and the composite fails when the matrix fails (Bowen *et al*. 2006, Mitchell 2004). If the fibre volume fraction is greater than its critical value ($V_f > V_f'$), the composite will fail at the failure strain of the fibre, since there is insufficient matrix to maintain the additional load which is transferred into the matrix from the fibres (Bowen *et al*. 2006, Mitchell 2004).

If the failure strain of the fibre is greater than that of the matrix ($\varepsilon_f^* > \varepsilon_m^*$); the failure of the matrix occurs prior to the failure of the fibres. In this case of ($V_f < V_f'$), the matrix failure represents the total failure of the composite. However, if the fibre volume fraction is greater than the critical value, multiple resin crackings can occur and the strength decreases due to insufficient matrix material. Figure 2.47 shows the relationship between tensile strength and fibre volume fraction for short fibre-reinforced composites.
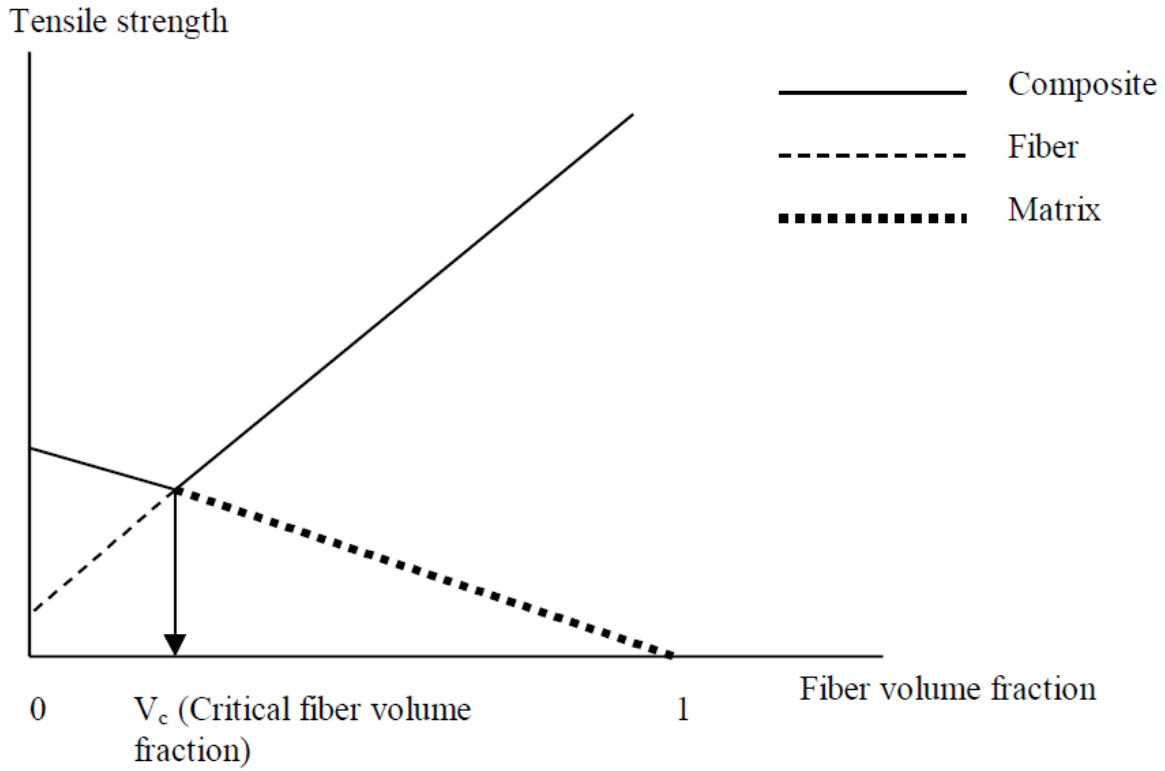
Figure 2.47. Typical relationship between tensile strength and fibre volume fraction for short fibre-reinforced composites. (Taib 1998)

Aspect ratio

The aspect ratio (length to width) of fibres is an essential parameter that influences the mechanical properties of fibre reinforced polymer composites (Faruk *et al*. 2012). Mechanical properties are normally enhanced as the aspect ratio of fibres increases (Faruk *et al*. 2012). However, the enhancement in mechanical properties is strongly affected by the critical aspect ratio, at which the maximum stress is achieved for a given load (Taib 1998, Kardos 1985). The fibre aspect ratio needs to be above its critical value in order to attain enhancement in the performance of composites. This will ensure sufficient stress transfer before the composite failures. The critical value of fibre aspect ratio (I_c/d) is variable, since it depends on fibre diameter (*d*) fibre ultimate strength σ_f^* and fibre-matrix bonding strength or interfacial shear stress (τ_c) according to the following equation (Callister 2007):

$$\frac{I_c}{d} = \frac{\sigma_f^*}{2\tau_c} \qquad\qquad 2.2$$

When a tensile stress equal to fibre strength (σ_f^*) is applied to the fibre reinforced composites, three scenarios are possible (Figure 2.48). If fibre length equals the critical length, the maximum fibre load is achieved only at the axial centre of the fibre (Figure 2.48a). Therefore, for maximum reinforcement, the fibre length should be above its critical value (Figure 2.48b). However, at fibre length lower than its critical value, insufficient stress will be transferred and reinforcement by the fibres will be ineffective (Figure 2.48c).
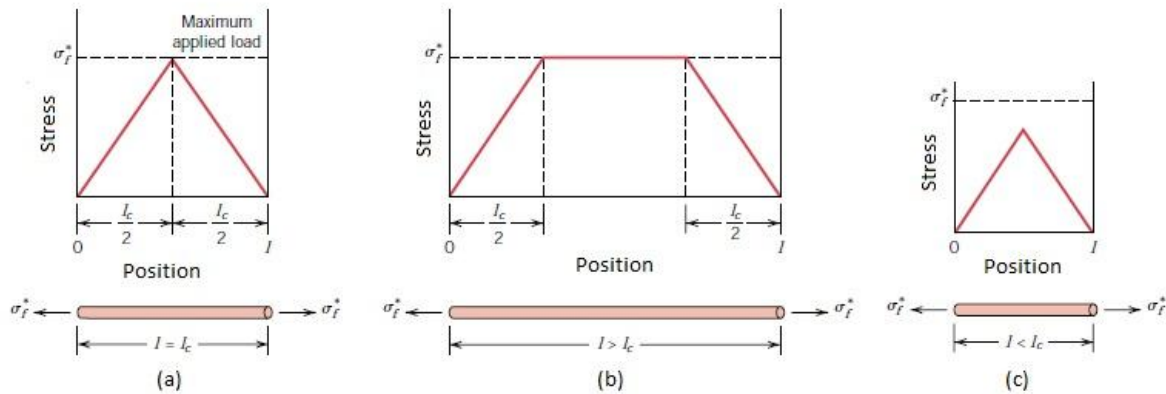
Figure 2.48. Stress–position profiles when fibre length (I) is: (a) equal to the critical length I_c, (b) greater than the critical length, and (c) less than the critical length for a fibre-reinforced composite that is subjected to a tensile stress equal to the fibre tensile strength (σ_f^*). (Callister 2007)

Fibre orientation

The mechanical properties of short fibre/polymer composites are also strongly affected by fibre orientation angle. Short fibres are generally randomly oriented. Therefore, the quality of transferring the stress along fibres is strongly dependent on the orientation of each individual fibre with respect to the loading axis (White and De 1996). Well-oriented fibres in composites lead to high mechanical performance. Thus, controlling fibre orientation during fabrication can be considered the most important factor that enhances the use of short fibres in composites (Kardos 1985). De Rosa *et al.* (2010) reported that short fibre composites exhibited lower mechanical properties than long fibre composites. The authors explained that in the case of short fibre composites, the stress was not uniform along the fibre, which resulted in the lack of stress transmission between the matrix and fibre causing reduction in mechanical properties. With respect to the fibre orientation, three cases of fibre distribution and orientation are shown in Figure 2.49.
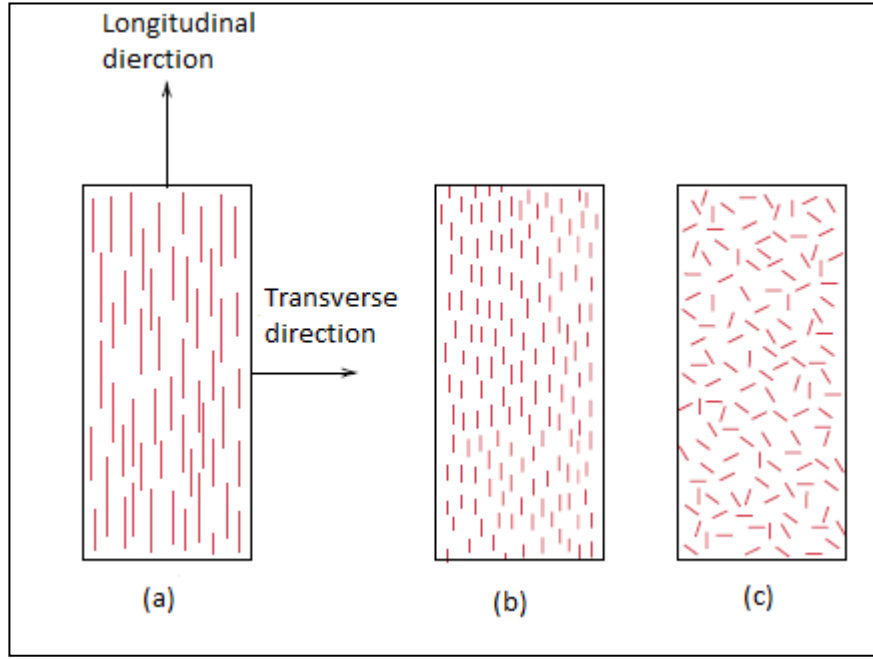
Figure 2.49. Schematic representations of (*a*) continuous and aligned, (*b*) discontinuous and aligned, and (*c*) discontinuous and randomly oriented fibre reinforced composites. (Callister 2007)

Under longitudinal loading and based on the rule-of-mixtures, the elastic modulus of the composite reinforced with continuous fibres is given by:

$$E_{cl} = E_m(1 - V_f) + E_f V_f \qquad\qquad 2.3$$

But in the case of transverse loading, the elastic modulus is (Callister 2007),

$$E_{ct} = \frac{E_m E_f}{E_f(1 - V_f) + E_m V_f} \qquad\qquad 2.4$$

For discontinuous and randomly orientated fibre composites, the fibres are randomly oriented and short. In this case, the elastic modulus can be expressed as follows (Callister 2007),

$$E_{cd} = k E_f V_f + E_m V_m \qquad\qquad 2.5$$

Where, k is a fibre efficiency parameter that depends on V_f and the ratio E_f/E_m. Table 2.17 shows effect of short fibre orientation on the reinforcement efficiency of fibre-reinforced composites under different directions of load application.

Table 2.17. Reinforcement efficiency of fibre-reinforced composites for several fibre orientations and at various directions of stress application. (Taken from Callister 2007)

Fibre orientation	Stress direction	Reinforcement efficiency
All fibres parallel	Parallel to fibres	1
	Perpendicular to fibres	0
Fibres randomly and uniformly distributed within a specific plane	Any direction in the plane of the fibres	3/8
Fibres randomly and uniformly distributed within three dimensions in space	Any direction	1/5

It can be seen from Table 2.17 that tensile strength is depended on fibre orientation and load direction. If the fibres are oriented parallel along with the stress direction, maximum reinforcement can be achieved. However, if the direction of the applied load is perpendicular to the fibre orientation, no reinforcement is attained. In the case of randomly oriented fibres, the reinforcement efficiency is moderate and varies between 0 and 1 depending on the orientation angle and stress direction.

2.9 Effect of nano-filler character (size, shape, loading and filler-matrix interfacial adhesion) on mechanical properties of filler reinforced polymer nanocomposites.

Mechanical properties of nanofiller reinforced polymer nanocomposites are mostly governed by filler size, shape, loading, dispersion and filler-matrix interface adhesion (Fu *et al*. 2008). These factors have a significant effect on mechanical properties (i.e. strength, modulus and facture toughness) of filler/polymer nanocomposites. In this section, different studies on the influence of such factors on mechanical properties of nano-filler reinforced polymer composites have been reported.

Effect of filler size

Reynaud *et al*. (2001) studied the effect of nano-silica size and loading on mechanical properties of polyamide 6 (PA6). Three different filler sizes (12, 25 and 50 nm) were used to fabricate PA 6/ silica nanocomposites. Results indicated that smaller particle size showed better strength than bigger particle size at the fixed filler content. In a similar study, Singh *et al*. (2002) investigated the effect of filler size and filler volume fraction on the facture toughness of polyester-aluminium composites. Fillers average diameter varied between 20 μm, 3.5 μm and 100 nm. Results showed that fracture toughness increased as filler size decreased at volume faction 2.3%. The increase in fracture toughness was contributed to crack front trapping as the primary toughening mechanism. The effects of particle size and volume fraction on fracture toughness of silica filled epoxy composites were also investigated by Adachi *et al*. (2008). Spherical silica particles with diameters varied from 240 nm to 1.56 μm and volume fraction ranged from 0 to 0.35 were used in that study. Results showed that fracture toughness significantly increased as filler size decreased from micro to nano-size. However, facture toughness was found to increase as filler volume fraction increased. These results imply that filler size has an effect on both strength and toughness of filler reinforced polymer nanocomposites. They stated that crack-trapping, crack-pinning and particle bridging were the main toughness mechanisms. Johnsen *et al*. (2007) investigated the toughening mechanisms of epoxy reinforced with nano-silica via a sol–gel technique. They reported that debonding followed by plastic void growth were the dominant dissipation mechanisms. In another study, Dittanet and Pearson (2012) investigated the size effect of nano-silica on toughening mechanisms in nano-silica filled epoxy. Toughness of silica filled epoxy nanocomposites was found to increase by 160% compared to unfilled epoxy. Particle debonding, matrix void growth, and matrix shear banding were reported as main toughness mechanisms. However, they found no significant increase in toughness as filler size increased from 23 to 170 nm. Similarly, Liang and Pearson reported in 2010 that there was no

obvious effect of the variation of nano-filler size on the toughness of hybrid epoxy-silica-rubber nanocomposites. In fact, the effect of nano-filler size on the toughness mechanism is still not completely understood yet (Dittanet and Pearson 2012).

Effect of filler shape

Yudin *et al*. (2008) studied the effect of nano-filler shape and loading on mechanical properties of polyimide nanocomposites. Three different nano-fillers with different shapes were used in that study (i.e., Cloisite Na$^+$ nanoclay platelets, Silicate nanotubes (SNT) and Zirconium dioxide (ZrO$_2$) with spherical shape). Results showed that nanocomposites filled with 10 wt% nanoclay platelets displayed the highest tensile strength and modulus among other fillers. For all types of nanocomposites, tensile strength was found to decrease as filler content increased. However, tensile modulus increased as the filler content increased. Knauert *et al*. (2007) investigated the effect of nano-filler shape on tensile strength of polymer based nanocomposites via molecular dynamics simulations. Three different models of nano-filler were used in the study (i.e., Icosahedral, tube and sheet-like). Results indicated that nanocomposites modified with sheet-like fillers exhibited better tensile strength than other types of nano-fillers. Similarly, Lim *et al*. (2010) investigated the effect of filler shape and size on mechanical properties of epoxy-alumina nanocomposites. Platelets and rod-shape alumina particles with size ranging from 10-40 nm were used in that study. Results showed that tensile strength and Young's modulus were influenced significantly by filler shape and content. The fracture toughness of neat epoxy increased by 54 and 32% due to the addition of 5 wt% of 10 nm platelet shaped filler and 12 nm rod-shaped filler, respectively. The SEM image of nanocomposites filled with platelet-shape filler showed number of toughness mechanism such as particle debonding, plastic deformation, particle pull-out and plastic void growth as seen in Figure 2.50a. The presence of these toughness mechanisms implied that the plastic shear yielding was the toughening mechanism in this type of nanocomposites. In contrast, nanocomposites filled with rod-shaped filler showed smoother facture surface with higher particle aggregates compared to samples with platelet-shaped fillers (Figure 2.50b). The presence of tail marks on the fracture surface of samples with rod-shaped filler indicated the presence of crack pinning process.
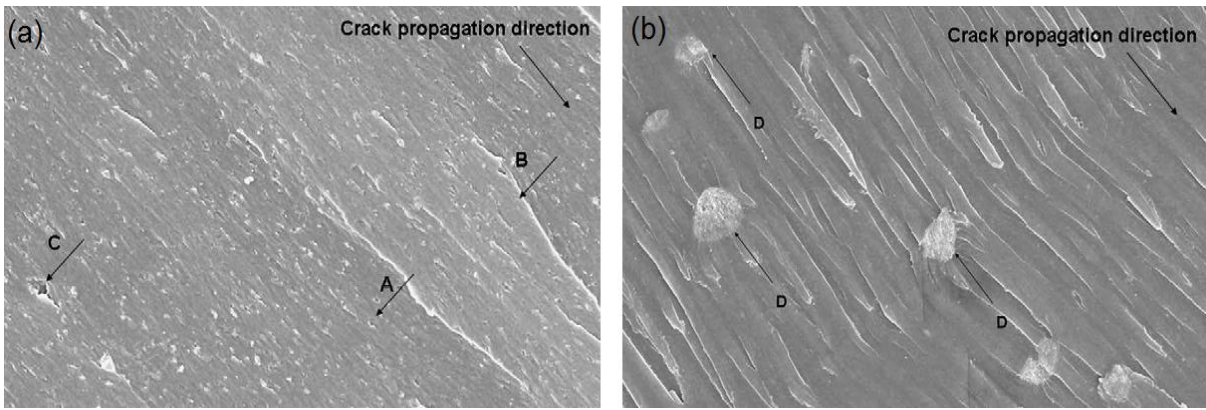
Figure 2.50. Fracture surfaces of: (a) epoxy-alumina nanocomposites with 10 nm alumina platelet shaped particles and (b) epoxy-alumina nanocomposites with 12 nm alumina rod shaped particles. [Legend: A= particle pull-out and B= plastic deformation, C= plastic void growth and D= crack pinning]. (Lim *et al*. 2010)

Effect of filler content

The effect of filler content on mechanical properties of halloysite nanotube (HNT)/epoxy nanocomposites was investigated by Ye *et al*. (2007). In that study, HNTs were introduced into epoxy matrix with three different loadings (i.e. 0.8, 1.6 and 2.3 wt%). Flexural strength and modulus showed slight increase as the HNT content increased while the impact strength was found to increase significantly with an increase in the filler content. They stated that massive micro-cracking, particle bridging and crack deflection were responsible for the significant enhancement in impact toughness as seen in Figure 2.51.
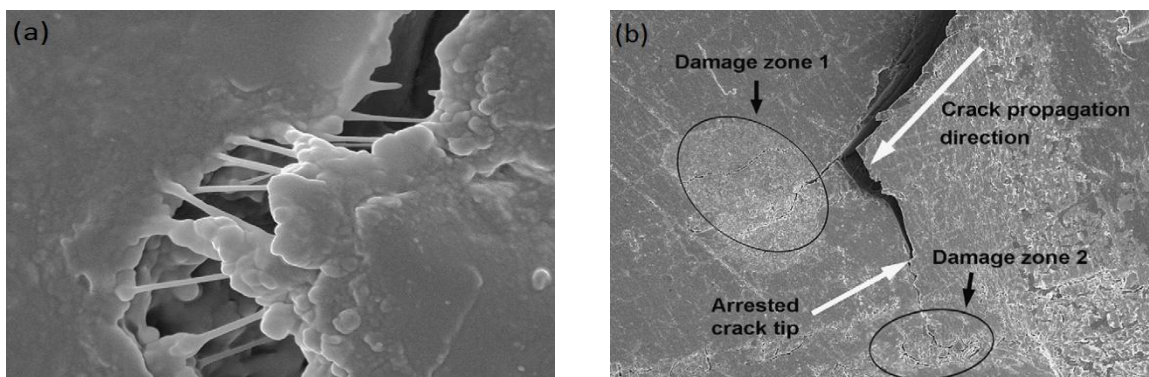
Figure 2.51. SEM images of fracture surface of HNT/epoxy nanocomposites showing: (a) crack-bridging by nanotubes, (b) crack propagation and damage zones. (Ye *et al*. 2007)

Effect of filler/ matrix interfacial adhesion

Ou *et al*. (1998) used untreated and aminobutyric acid treated silica nanoparticles to investigate the effect of particle/matrix interfacial adhesion on the mechanical properties of nylon 6/silica nanocomposites prepared via in-situ polymerization. Composites filled with treated silica showed significant increase in tensile strength and impact strength compared to composites filled with untreated silica. Ha *et al.* (2010) investigated the influence of chemical treatment on enhancing fracture toughness of clay-filled epoxy nanocomposites. They reported an increase in fracture toughness by 82% for nanocomposites with silane-treated clay over untreated clay/epoxy nanocomposites. This improvement in fracture toughness was due to the excellent dispersion of the treated clay into epoxy matrix and enhancement in interfacial adhesive strength between resin and clay layers. Prashantha *et al.* (2011) studied the effect of unmodified HNTs and quaternary ammonium salt treated halloysite nanotubes (QM-HNTs) on mechanical properties of HNT/polypropylene (PP) nanocomposites. Results showed that tensile strength, tensile modulus, flexural strength, flexural modulus and impact strength increased due to the addition of both types of HNTs. However, samples reinforced with modified HNTs showed better mechanical properties than those filled with unmodified HNTs. They concluded that enhanced filler/matrix interfacial bonding and filler dispersion led to better mechanical properties.

3. PUBLICATIONS FORMING PART OF THESIS

Alamri, H., and I. M. Low. 2012. Mechanical properties and water absorption behaviour of recycled cellulose fibre reinforced epoxy composites. *Polymer Testing* 31(5): 620-628.

Alamri, H., I. M. Low, and Z. Alothman. 2012. Mechanical, thermal and microstructural characteristics of cellulose fibre reinforced epoxy/organoclay nanocomposites. *Composites Part B: Engineering* 43: 2762-2771.

Alamri, H., and I. M. Low. 2012. Microstructural, mechanical, and thermal characteristics of recycled cellulose fibre-halloysite-epoxy hybrid nanocomposites. *Polymer Composites* 33(4): 589-600.

Alamri, H., and I. M. Low. 2012. Characterization of epoxy hybrid composites filled with cellulose fibres and nano-SiC. *Journal of Applied Polymer Science* 126: 221-231.

Alamri, H., and I. M. Low. 2012. Effect of water absorption on the mechanical properties of nano-filler reinforced epoxy nanocomposites. *Materials and Design* 42: 214-222.

Alamri, H., and I. M. Low. 2012. Effect of water absorption on the mechanical properties of n-SiC filled recycled cellulose fibre reinforced epoxy eco-nanocomposites. *Polymer Testing* 31(6): 810-818.

Alamri, H., and I. M. Low. 2013. Effect of water absorption on the mechanical properties of nanoclay filled recycled cellulose fibre reinforced epoxy hybrid nanocomposites. *Composites Part A: Applied Science and Manufacturing* 44: 23-31.

3.1 Mechanical Properties and Water Absorption Behaviour of Recycled Cellulose Fibre Reinforced Epoxy Composites.

Alamri, H., and I. M. Low. 2012. Mechanical properties and water absorption behaviour of recycled cellulose fibre reinforced epoxy composites. *Polymer Testing* 31(5): 620-628.

POLYMER
TESTING
200th Issue
Editor
ROGER BROWN
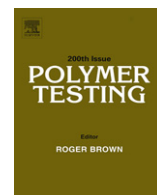
Material properties

Mechanical properties and water absorption behaviour of recycled cellulose fibre reinforced epoxy composites

H. Alamri, I.M. Low*

Department of Imaging & Applied Physics, Curtin University, GPO Box U1987, Perth, WA 6845, Australia

ARTICLE INFO

ABSTRACT

Recycled cellulose fibre (RCF) reinforced epoxy composites were fabricated with fibre loadings of 19, 28, 40 and 46 wt%. Results showed that flexural strength, flexural modulus, fracture toughness and impact strength increased as the fibre content increased. The ultimate mechanical properties were achieved with a fibre content of 46 wt%. The effect of water absorption on mechanical and physical properties of RCF/epoxy composites was investigated. The values of maximum water uptake and diffusion coefficient were found to increase with an increase in fibre content. Flexural strength, modulus and fracture toughness decreased as a result of moisture absorption. However, the impact strength was found to increase slightly after water absorption. XRD, FTIR and SEM studies were carried out to evaluate the composition and microstructure of RCF and RCF/epoxy composites.

Crown Copyright © 2012 Published by Elsevier Ltd. All rights reserved.

1. Introduction

In recent years, the use of cellulose fibre in polymer composite as a reinforcement has become popular in several engineering applications [1–3]. Due to the low cost, low density, good mechanical properties and recyclability of different cellulose fibres such as hemp, flax, sisal, jute and kenaf, it is possible to use them as alternatives to synthetic fibres (glass or carbon) in composite applications [4,5]. Furthermore, cellulose fibres are environmentally friendly, non-toxic and renewable materials. Therefore, manufacturing industries, especially packaging, building construction, automotive and furniture, have been encouraged to use plant fibres in their applications instead of the harmful and non-renewable reinforcing materials [6,7].

Recycled cellulose fibres (RCFs) obtained from cellulosic waste products such as cardboard and printed paper as well as recycled newspaper and magazine have many advantages compared to natural cellulose fibres. For example,

their availability in abundant volume throughout the world, low cost and being very friendly to the environment [5]. Thus, RCF based polymer composites can be classified as desirable performing composites owing to their environmental and economic advantages [3,8]. Composites reinforced with RCFs represent a new class of materials that have the potential of replacing wood and other plant composites in the future. This new class of materials could be utilized in housing and manufacturing of automotive components and furniture [3,8].

Several investigations have been carried out on various types of cellulose fibre such as kenaf, hemp, flax, bamboo, jute and wood to study the effect of these fibres on the mechanical and physical properties of composites materials. For instance, Shih [2] studied the mechanical properties of waste water bamboo husk fibre/epoxy composites. Chemically treated water bamboo husk and untreated powder obtained from water bamboo husks were used to reinforced epoxy matrix composites. It was found that the addition of treated fibre and untreated powder improved the mechanical properties of composites. Similarly, Liu and Hughes [9] investigated the fracture toughness of epoxy matrix reinforced with woven flax fibre. Their results showed that the fracture toughness of the composites was

* Corresponding author.
  E-mail address: j.low@curtin.edu.au (I.M. Low).

94

increased by 2–4 times due to the presence of flax fibre compared to pure epoxy samples. They concluded that this significant improvement in facture toughness was related to the fibre volume fraction. Maleque et al. [10] reported an increase in flexural strength and impact strength by 38 and 40%, respectively when banana woven fabric was added to the epoxy matrix. In another study, Low et al. [11] reported a significant increase in flexural strength, modulus, facture toughness, impact strength and impact toughness of recycled cellulose fibre reinforced epoxy composites.

Despite the enormous advantages presented by cellulose fibres, their utilization as reinforcement in polymer composites has been limited by their susceptibility to moisture absorption. This makes them susceptible to swelling, resulting in formation of micro-cracks and voids at the fibre-matrix interface region. This in turn reduces the dimensional stability and mechanical properties of composites [8,12,13]. The hydrophilic nature of cellulose fibres is facilitated by hydroxyl groups which are present in the structure of cellulose that makes them attract and bind with water molecules via hydrogen bonds [14–16].

This study will investigate the mechanical properties and water absorption behaviour of RCF/epoxy composites as a function of fibre content. Most of the studies involving plant or cellulose fibre reinforced polymer composites have mainly focused on mixing the fibres into the resins using mechanical blending or stirring [9]. These fabrication methods have limited the scope of geometry optimization and packing arrangement which often results in use of large volumes of fibres that consequently result in fibre damage, air bubble generation or fibre agglomeration [1,9]. In this study, thin layers of RCFs measuring about 2 μm will be used to construct multi-layered epoxy composites reinforced by cellulose fibre. This approach is aimed at production of composites with uniform fibre dispersion in the matrix, controlled microstructure and increased fibre volume fractions resulting from improved fibre packing.

In this paper, RCF reinforced epoxy composites with different fibre contents (19, 28, 40 and 46) wt% have been successfully fabricated. The effect of fibre content on the mechanical properties has been investigated in terms of flexural strength, flexural modulus, fracture toughness and impact strength. The effect of water absorption on the mechanical properties of composites has also been studied as a function of fibre content. X-ray diffraction, Fourier transforms infrared spectroscopy (FTIR) and scanning electron microscopy (SEM) have been used to investigate the morphology, micro-structure and failure mechanisms of RCF/epoxy composites.

2. Materials and methods

2.1. Materials and samples preparation

Recycled cellulose fibre (RCF) paper was used as reinforcement for the fabrication of epoxy-matrix composites. The RCF paper with grade 200 GSM and 200 μm thickness (fibres diameter between 5 μm to 10 μm and several micrometres in length) was supplied by Fuji Xerox Australia Pty. Limited, Belmont WA, Australia. General purpose low viscosity epoxy resin (FR-251) and epoxy hardener (FR-251) procured from Fibreglass & Resin Sales Pty Ltd, WA, Perth, Australia was used as a matrix. Composite samples were prepared by initially pre-drying the paper sheets for 60 min at 70 °C, and then fully immersing them into the epoxy system until they became entirely wetted by the resin. After that, the epoxy-soaked RCF sheets were carefully laid down in a closed silicone mould under 8.2 kPa compressive pressure and left for 24 h to cure at room temperature. RCF/epoxy composites were fabricated with different weight percentages of fibres (19, 28, 40 and 46%) to investigate the effect of fibre weight percentage on the physical and mechanical properties.

2.2. Characterization

X-ray diffraction (XRD) was performed on a D8 Advance Diffractometer (Bruker-AXS) with copper radiation. The Cu Kα (λ = 1.5406 Å) was operated at 40 kV and 30 mA. The 2θ range was selected within 4–30° using a scanning rate of 0.5°/min with step size of 0.02°. A knife edge collimator was fitted to reduce air scatter.

An FTIR spectrum of RCF was performed on a Perkin Elmer Spectrum 100 FTIR spectrometer in the range of 4000-500 cm^{-1} at room temperature. The spectrum was the average of 10 scans at a resolution of 2 cm^{-1} and corrected for the background.

Scanning electron microscopy imaging was obtained using a Zeiss Evo 40XVP. The SEM investigation was carried out in detail on the fractured surfaces of the RCF/epoxy composites. Specimens were coated with a thin layer of gold before observation by SEM to avoid charging.

2.3. Physical and mechanical measurements

Water uptake was carried out by immersing samples with dimensions 10 mm × 10 mm × 3.5 mm in a water bath at room temperature. Three specimens from each formulation were used and the weight gain of the samples was measured periodically over 234 days. All specimens were first dried using a tissue to remove any excess water, followed by weighing using a digital scale (AA-200, Denver Instrument Company, USA).

Five rectangular specimens of each composition with dimensions 60 mm × 10 mm × 6 mm were cut from the fully cured samples for three-point bend and Charpy impact tests. Three-point bend tests were performed on A LLOYD Material Testing Machines – Twin Column Bench Mounted (5–50 kN) with a span of 40 mm and displacement rate of 1.0 mm/min to determine flexural strength, flexural modulus and fracture toughness. Charpy impact tests were performed on un-notched samples using A Zwick Charpy impact machine with a 1.0 J pendulum hammer.

Flexural strength (σ_F) and flexural modulus (E_F) were computed using the following equations:

$$\sigma_F = \frac{3}{2}\frac{p_m S}{WD^2} \tag{1}$$

$$E_F = \frac{S^3}{4WD^3}\left(\frac{\Delta P}{\Delta X}\right) \tag{2}$$

where P_m is the maximum load at crack extension, S is the span of the sample, D is the specimen thickness and W is the specimen width. $\Delta P/\Delta X$ is the initial slope of the load–displacement curve. The impact strength was calculated using the following formula:

$$\sigma_I = \frac{E}{A} \tag{3}$$

where E is the impact energy to break a sample with a ligament of area A.

Single-edge notch bending (SENB) specimens were used to evaluate the fracture toughness. The ratio of notch length to width (a/w) was about (0.4). A sharp pre-crack was initiated in the notched specimens by tapping a sharp razor blade. The fracture toughness was calculated using the following equation as reported by Low et al. [1]:

$$K_{IC} = \frac{p_m S}{WD^{2/3}}f\left(\frac{a}{w}\right) \tag{4}$$

where a is the crack length, and $f(a/w)$ is the polynomial geometrical correction factor give as

simple calculation of the crystallinity index by using the following equation [19,22,23].

$$CrI = \frac{(I_{002} - I_{am})}{I_{002}} \times 100 \tag{6}$$

where I_{002} is the maximum intensity of the 002 crystalline peak and I_{am} is the minimum intensity of the amorphous material between 101 and 002 peaks as shown in Fig. 1.

The crystallinity index of RCF was found to be about 81.8%. A number of studies used the same method to measure the crystallinity index of variety of cellulose fibres. For example, Rong et al. [4] found that the cellulose crystallinity of untreated sisal fibre was 62.8%. Tserki et al. [18] reported that the crystallinity of flax, hemp and wood fibres were 86.1, 79.9, 65.1%, respectively. El-Sakhawy & Hassan [19] found that the crystallinity index of bleached bagasse, rice straw and cotton stalks fibres after treated by HCl acid were 76.0, 78.0, and 77.0%, respectively. Mwaikambo et al. [22] found that the crystallinity index of hemp, sisal, jute and kapok fibres were 87.9, 70.9, 71.4 and 45.8%, respectively. Janoobi et al. [17] reported that the crystallinity index of kenaf fibre was about 41%.

$$f\left(\frac{a}{W}\right) = \frac{3(a/W)^{1/2}\left[1.99 - (a/W)(1 - (a/W)) \times (2.15 - 3.93a/W + 2.7a^2/W^2)\right]}{2(1 + 2a/W)(1 - a/W)^{2/3}} \tag{5}$$

3. Results and discussion

3.1. X-ray diffraction analysis of RCF

The X-ray diffraction patterns of RCF are given in Fig. 1 showing a typical crystal lattice of native cellulose (cellulose I) [17–20]. The main patterns of cellulose fibre are seen at $2\theta = 15.5$, 16.5 and 22.8° corresponding to (101), (10$\bar{1}$) and (002) planes, respectively [20–22]. The peak (002) is the major crystalline peak of cellulose I. The fibre crystallinity index (CrI) of RCF was determined by using the Segal empirical method [17–19]. This method offers a quick and

3.2. FTIR analysis of RCF and RCF/epoxy composite

FTIR spectra of both RCF and RCF/epoxy composite are shown in Fig. 2. The FTIR spectra show a broad peak in the region between 3340 and 3275 cm^{-1} corresponding to the hydroxyl (OH) stretching vibration of free and hydrogen bonded –OH groups [24,25]. The peak at around 2902 cm^{-1} in the spectra of the RFC is probably associated with the (CH) stretching of cellulose fibre [26–28]. The absorbance peaks observed at around 1654 cm^{-1} are due to the (OH)

Fig. 1. X-ray diffraction patterns of RCF.
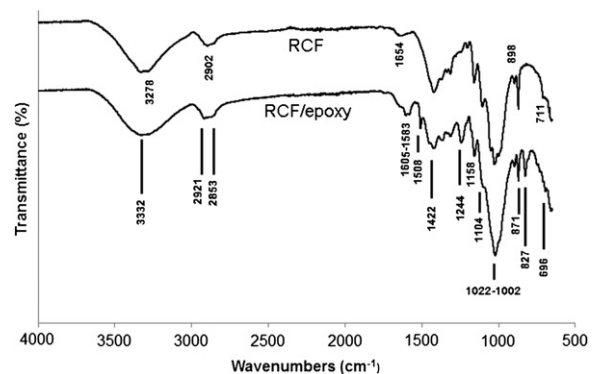
Fig. 2. FTIR spectra of RCF and RCF/epoxy composites.

bending vibration of absorbed water [18,24,25]. The peaks at 1422 and 1368 cm^{-1} can be attributed to CH_2 and CH_3 bending vibration of cellulose fibres, respectively [24]. The absorption peaks around 1000–1100 cm^{-1} may correspond to C–O stretching of cellulose fibre [29]. However, the presence of epoxy in the composites can be recognized by a number of peaks. The composites spectra show peaks at 2921 and 2853 cm^{-1}, which may belong to the asymmetric and symmetric CH_2 and CH_3 of epoxy resin [30]. The peaks at 1605, 1583 and 1508 cm^{-1} correspond to the benzene ring of epoxy or C=C stretching of aromatic ring [31]. The peaks appear at 1244 and 918 cm^{-1} are attributed to the C–O stretching of epoxide ring vibration [30–32]. Finally, the absorption band at 827 cm^{-1} could be assigned to the 1,4-substitution of aromatic ring for epoxy resin [33,34].

3.3. Effect of fibre content on water absorption behaviour

The amount of water uptake in the composites was determined using the following equation:

$$M_t(\%) = \left(\frac{W_t - W_o}{W_o}\right) \times 100 \tag{7}$$

where, W_t is the weight of the sample at time t and W_o is the initial weight of the sample.

Fig. 3 illustrates the effect of fibre content on the water absorption behaviour of the RCF/epoxy composites. It can be seen that water absorption increases with an increase in time of immersion for all samples. The water uptake rate is linear and very rapid in the beginning of the exposure, after which it slows down and reaches the saturation level [12,14]. It can be observed that water absorption increases as fibre content increases. This result is expected due the hydrophilic nature of cellulose fibres [14]. Moreover, cellulose fibres have a central hollow region (i.e. the lumen) which allows much water to be absorbed via the capillary effect [14]. Thus, as fibre loading increases in the composites, more interfacial area exists leading to an increase in water absorption. A similar study on moisture behaviour of plant fibre/polymer composites was done by Dhakal et al. [12]. Unsaturated polyester was reinforced with 2, 3, 4 and 5 layers of hemp fibre. It was found that moisture absorption increased as fibre content increased. Because of the hydrophilic nature of cellulose fibres, composites reinforced with cellulose fibres always tend to absorb more water than other types of composites. Rashdi et al. [35] also indicated in their study on kenaf fibre reinforced unsaturated polyester composites that, as fibre loading increased, moisture absorption also increased by virtue of the higher cellulose content.

The water absorption behaviour in the samples can be considered as Fickian. Therefore, for short immersion times the following formula has been used [36,37]:

$$\frac{M_t}{M_\infty} = 4\left(\frac{Dt}{\pi h^2}\right)^{1/2} \tag{8}$$

The maximum water absorptions and the diffusion coefficient values of RCF reinforced epoxy composites series are listed in Table 1. It can be seen that the addition of cellulose fibre increases the rate of water diffusion. Diffusivity increases slightly as fibre content increases from 0 to 40%. However, at 46% RCF loading, the diffusivity significantly increases by 52.7% compared to neat epoxy. This can be attributed to the increases in fibre content [12]. Furthermore, exposure to moisture causes the fibres to swell, resulting in formation of microcracks and voids at the fibre-matrix interface region. This in turn leads to increase in water diffusion via these microcracks and voids [12].

3.4. Effect of fibre content on the mechanical properties

3.4.1. Flexural stress-strain behaviour

Fig. 4 presents the stress-strain curves of selected RCF/epoxy specimens loaded with 19 and 46 wt% RCF. It can be seen that RCF filled composites generally display non-catastrophic fracture behaviour. Composites filled with low RCF loading show linear behaviour at very low strain (0.003%), followed by a knee in the curve. After that, a reduction in the modulus occurs and the composite fails at low stress. In contrast, composites filled with higher RCF loading show linear behaviour at higher strain (0.013%), followed by a slight reduction in slope until the composite fails at higher stress. This means that composites filled with higher RCF loading display higher flexural strength and modulus than composites filled with lower RCF loading. Moreover, the areas under the two curves give an indication that composites filled with higher RCF loading have higher toughness than those filled with lower RCF loading.

Two failure modes probably occur in the composites materials under three-point bending. One, termed the flexural failure mode, exists at the upper and lower surfaces of the specimen. This type of failure occurs when the specimen fails abruptly in a linear manner. The other type
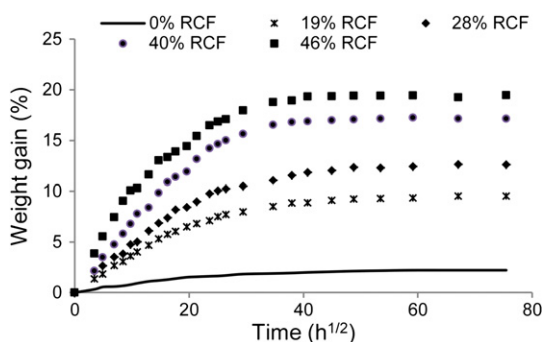
Fig. 3. Water absorption curves of RCF/epoxy composites.

Table 1
Maximum water uptake and diffusion coefficient (D) of RCF/epoxy composites.

Samples	RCF content (wt%)	M_∞ (%)	$D \times 10^{-07}$ (mm^2/sec)
Epoxy	0	2.21	9.17
RCF/epoxy	19	9.52	9.53
RCF/epoxy	28	12.59	9.30
RCF/epoxy	40	17.14	10.20
RCF/epoxy	46	19.46	14.00
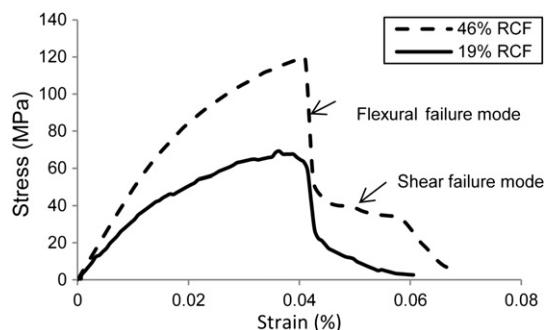
Fig. 4. Typical stress-strain curves of RCF/epoxy composites filled with 19 and 46 wt% RCF.

Fig. 6. Effect of fibre content on the flexural modulus of dry and wet RCF/epoxy composites.

of failure is termed shear failure mode and occurs at the neutral axis of the specimen as a result of interlaminar stress [4,38]. This failure occurs when the specimen fails in a less abrupt manner and the slope of the curve decreases gradually to zero [4,38]. However, according to the stress-strain curves, the failure mode of the RCF reinforced epoxy composites consists of both flexural and shears failure modes [38]. The composites first fail in the flexural mode, followed by the shear failure mode. This means that the failure first occurs in the top and bottom RCF layers, then the interlaminar failure takes place at the neutral axis of the composites.

3.4.2. Flexural strength and modulus

The effect of fibre content on flexural strength of dry RCF reinforced epoxy composites is plotted in Fig. 5 (dark bars). In dry conditions, flexural strength is found to increase as fibre content increases. Flexural strength of neat epoxy increases by 23.6, 63.5, 99.4 and 137.1% after the addition of 19, 28, 40 and 46 wt% RCF, respectively. This enhancement in RCF/epoxy flexural strength is due to the ability of cellulose fibre to resist the bending force [3]. The lower flexural strength at lower RCF content may be attributed to the lower loads transferred from the matrix to the fibres, thus resulting in lower load carried by the fibres [39]. However, the significant increase in flexural strength at higher RCF content is due to the increase in stress transferred to the fibre as a result of the increased bonding at the fibre-matrix interface [39]. Le Guen & Newman [40]

investigated the flexural properties of pulped leaf fibre reinforced epoxy composites where they reported an increase in both flexural strength and modulus as the fibre volume fraction increased.

The effect of moisture absorption on flexural strength is shown in Fig. 5 (light bars). It can be seen that flexural strength for all samples decreases due to the water absorption. Comparing to dry samples, the reductions in flexural strength of samples loaded with 19, 28, 40 and 46 wt% RCF are 10.4, 23.1, 26.9 and 34.9%, respectively. This means that in wet conditions flexural strength decreases progressively as fibre content increases due to the increase in moisture content [41]. The reduction in flexural strength of wet composites is mainly due to the reduction in bonding at the fibre-matrix interface, which results in lower stress transferred from the matrix to the fibres [12]. Similar results were reported by Dhakal et al. [12] and Athijayamani et al. [41].

The flexural modulus versus fibre weight percentage for RCF/epoxy composites in dry and wet conditions is shown in Fig. 6. In the case of dry composites, flexural modulus shows a similar trend to flexural strength. As fibre content increases, flexural modulus increases. The addition of 19 wt% of RCF increases flexural modulus by 262.1% compared to neat epoxy, while flexural modulus increased by 536.8% at 46 wt% of RCF. Significant increases in flexural modulus of plant fibre reinforced polymer composites were also reported by Rong et al. [4], Dhakal et al. [12], and Le Guen & Newman [40]. The influence of water absorption on flexural

Fig. 5. Effect of fibre content on the flexural strength of dry and wet RCF/epoxy composites.
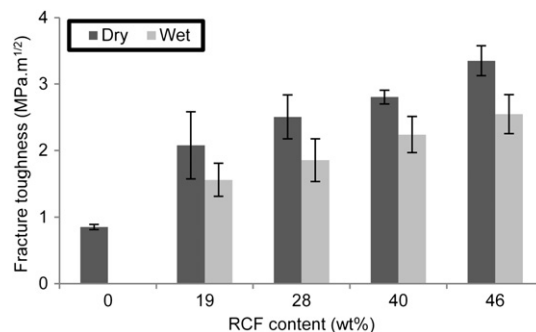
Fig. 7. Effect of fibre content on the fracture toughness of dry and wet RCF/epoxy composites.
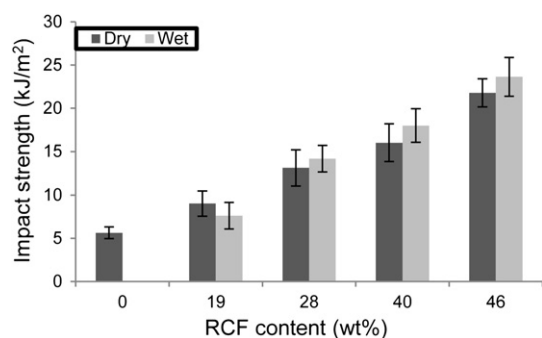
Fig. 8. Effect of fibre content on the impact strength of dry and wet RCF/epoxy composites.

modulus of RCF/epoxy composites is seen in Fig. 6 where flexural modulus decreases as a result of water absorption, and this reduction is most pronounced for composites with high cellulose fibre content.

3.4.3. Fracture toughness

The effect of cellulose fibre content on facture toughness of dry RCF/epoxy is presented in Fig. 7 (dark bars). It can be seen that the addition of recycled cellulose fibre gradually increases the fracture toughness of RCF/epoxy composites compared to neat epoxy. Cellulose fibres play a significant role in enhancing facture toughness of polymer matrices through several energy absorbing events such as fibre pull-out, fibre fracture and fibre-bridging [7,11]. The fracture toughness of epoxy reinforced with 46% wt% RCF increases

by a maximum of 294.1% compared to neat epoxy. This significant enhancement in facture toughness at higher RCF content is due to extensive fibre pull-outs, fibre fracture and fibre-bridging, as can be seen in the SEM images shown later. Hughes et al. [42] reported that facture toughness of hemp and jute fibre reinforced polyester composites increased as fibre volume fraction increased. In the present study, the values of fracture toughness of epoxy reinforced with 0, 19, 28, 40 and 46 wt% cellulose fibres are 0.85, 2.08, 2.51, 2.80 and 3.35 MPa$\cdot$m$^{1/2}$, respectively.

The effect of water absorption on fracture toughness of RCF/epoxy composites is shown in Fig. 7 (light bars). Generally, there is a reduction in fracture toughness due to moisture absorption. However, there is still a modest increase in fracture toughness as fibre content increases. Composites with higher fibre content in both dry and wet conditions display higher fracture toughness due to an increase in fibre pull-outs, fibre debonding and fibre-bridging, which in turn increase the resistance to crack propagation.

3.4.4. Impact strength

Impact strength is an essential property that gives an indication of the overall material toughness. Impact strength of fibre reinforced polymer is governed by the matrix-fibre interfacial bonding, and properties of matrix and fibres. When the composites undergo a sudden force, the impact energy is dissipated by the combination of fibre pull outs, fibre fracture and matrix deformation [43]. Normally in fibre reinforced polymer composites, impact strength increases as fibre content increases due to the increase in fibre pull out and fibre breakage [44].
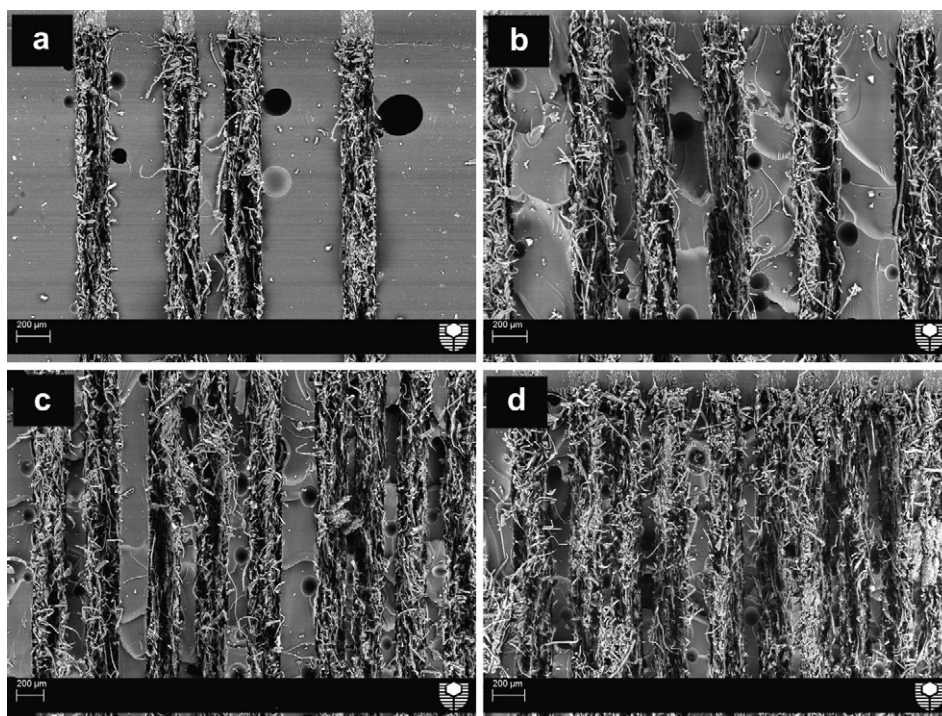
Fig. 9. SEM images of fracture surface of RCF/epoxy composites with fibre content (a) 19 wt%, (b) 28 wt%, (c) 40 wt% and (d) 46 wt%.

99
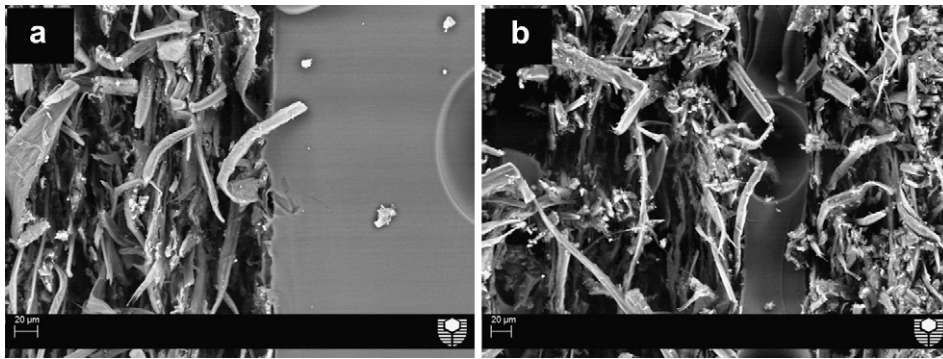
Fig. 10. High magnification SEM images of surface fracture of RCF/epoxy composites loaded with (a) 28 wt% RCF and (b) 46 wt% RCF.

The effect of fibre weight fraction for dry and wet RCF/epoxy composites is illustrated in Fig. 8. It can be observed that impact strength significantly increases as RCF content increases for both dry and wet composites. The presence of RCF layers in epoxy matrix increases the ability of these composites to absorb impact energy In dry conditions, the addition of RCF with contents of 19, 28, 40 and 46 wt% increases impact strength compared to neat epoxy by 59.9, 132.8, 184.0 and 286.3%, respectively. Similarly, Wambua et al. [43] reported that impact strength of kenaf reinforced polypropylene composites increased as fibre weight fraction increased. Impact strength increased slightly as kenaf fibre content increased from 30 to 40 wt% then increased dramatically as kenaf fibre content increased from 40 to 50 wt%. However, Bledzki and Faruk [45] reported a decrease in impact strength of wood fibre/polypropylene composites as fibre content increased from 40 to 60 wt%.

In wet conditions, it can be seen that impact strength generally increases as a result of water absorption for two weeks. This phenomenon was also observed by Karmaker [46] and Low et al. [11]. Karmaker [46] reported an increase in unnotched impact strength of jute fibre/polypropylene composites after immersing in water for 14 days. Similarly, Low et al. [11] reported an enhancement in unnotched impact strength of cellulose fibre reinforced epoxy composites after soaking in sea water for two weeks.

3.5. SEM observation on facture surface

The SEM micrographs in Fig. 9 show the typical fracture surfaces of RCF reinforced epoxy composites loaded with fibre contents of 19, 28, 40 and 46 wt%. Generally, fibre-pullouts, fibre-debonding, fibre breakage and matrix fracture can be observed after the fracture test for all composites. Such toughness mechanisms can lead to increase in fracture properties of samples reinforced with RCF sheets [3]. The effect of fibre content on the fracture surface is clearly seen in Fig. 9(a–d). Composites filled with lower fibre content (19 and 28) wt% show an increase in matrix rich regions compared to composites filled with higher fiber content. An increase in matrix-rich regions means that the matrix is not restrained by enough fibres [47]. In this case, there is not sufficient fibre to carry the

transferred load from the matrix. Therefore, composites exhibit highly localized strains at low stresses, which lead to low mechanical properties [47].

However, Fig. 9(c,d) display fracture surface with higher fibre-rich regions of composites filled with 40 and 46 wt% RCF. An increase in fibre-rich regions means that the matrix is sufficiently restrained with fibres and the stress is more evenly distributed leading to increase in composite stiffness [47]. In this case, the stress is effectively transferred from the matrix to the fibres resulting in an increase in
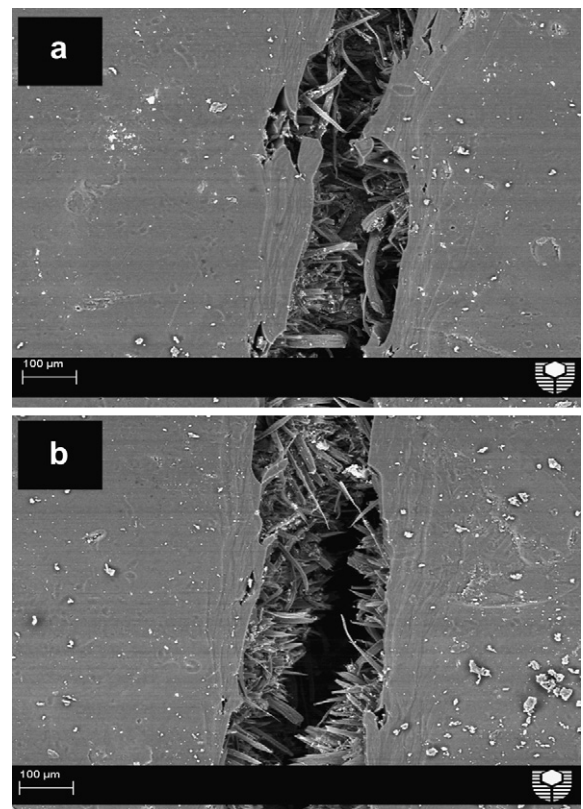
Fig. 11. SEM images of crack propagation in RCF/epoxy composites loaded with 46 wt% fibre.

mechanical properties. Moreover, an increase in energy dissipation due to the increase in fibre-fracture, fibre-debonding, fibre-pullout, fibre-bridging and matrix deformation is observed for composites loaded with higher fibre content, as shown in Fig. 9(c–d). This confirms the increase in fracture toughness for these composites.

Fig. 10(a,b) shows the high magnification images of the fracture surface of RCF/epoxy composites loaded with 28 and 46 wt% fibres. It can be observed that composites loaded with higher fibre content show better fibre-matrix interfacial bonding than those loaded with lower fibre content. Fibre debonding and gaps between fibres and matrix are more prevalent in composites with lower fibre content. This finding is an agreement with the result obtained by Pothan et al. [48].

Fig. 11(a,b) shows the crack propagation in RCF/epoxy composites with 46 wt% fibre. Extensive fibre fracture, fibre bridging and matrix fracture can be clearly observed. Such fracture mechanisms lead to enhance the mechanical properties in the composites.

4. Conclusions

The effect of fibre content on the morphology, structure, mechanical and physical properties of RCF reinforced epoxy composites has been investigated. The XRD results indicated that the RCF fibres are cellulose I type with crystallinity index about 81.8%. The mechanical properties (flexural strength, flexural modulus, fracture toughness and impact toughness) were found to increase as the fibre content increased. The stress-strain curves showed that the failure mode of the RCF reinforced epoxy composites consisted of both flexural and shear failure modes. SEM results showed an increase in energy dissipation events for composites filled with higher fibre content compared to their lower fibre content counterparts. Composites loaded with higher fibre content have better fibre-matrix interfacial bonding than those loaded with lower fibre content.

The effect of water absorption on the mechanical properties of RCF reinforced epoxy composites was investigated and compared to dry composites. Water absorption was observed to increase with increasing fibre content. Exposure to moisture for two weeks caused a reduction in flexural strength, flexural modulus and fracture toughness due to the degradation of bonding at the fibre–matrix interfaces. However, impact strength was found to increase slightly after water absorption. The effect of water absorption on mechanical properties was more pronounced at high fibre content than at low fibre content.

References

[1] I.M. Low, M. McGrath, D. Lawrence, P. Schmidt, J. Lane, B.A. Latella, Mechanical and fracture properties of cellulose fibre reinforced epoxy laminates, Composites: Part A 38 (2007) 963–974.

[2] Y.F. Shih, Mechanical and thermal properties of waste water bamboo husk fibre reinforced epoxy composites, Materials Science and Engineering A 445–446 (2007) 289–295.

[3] H. Alamri, I.M. Low, Microstructural, mechanical and thermal characteristics of recycled cellulose fiber- halloysite-epoxy hybrid nanocomposites, Polymer Composites 33 (4) (2012) 589–600.

[4] M.Z. Rong, M.Q. Zhang, Y. Lui, G. Yang, H.M. Zeng, The effect of fibre treatment on the mechanical properties of unidirectional sisal-reinforced epoxy composites, Composites Science and Technology 61 (2001) 1437–1447.

[5] H. Alamri, I.M. Low, Mechanical, thermal and microstructural characteristics of cellulose fibre reinforced epoxy/organoclay nanocomposites, Composites Part B: Engineering, in press.

[6] D. Bachtiar, S.M. Sapuan, M.M. Hamdan, The effect of alkaline treatment on tensile properties of sugar palm fibre reinforced epoxy composites, Materials and Design 29 (2008) 1285–1290.

[7] H. Alamri, I.M. Low, Characterization of epoxy hybrid composites filled with cellulose fibres and nano-SiC, Journal of Applied Polymer Science (2012), doi:10.1002/app.36815.

[8] B. Wang, S. Panigrahi, L. Tabil, W. Crerar, Pre-treatment of flax fibers for use in rotationally molded biocomposites, Journal of Reinforced Plastics and Composites 26 (5) (2007) 447–463.

[9] Q. Liu, M. Hughes, The fracture behaviour and toughness of woven flax fibre reinforced epoxy composites, Composites: Part A 39 (2008) 1644–1652.

[10] M.A. Maleque, F.Y. Belal, S.M. Sapuan, Mechanical properties study of pseudo-stem banana fibre reinforced epoxy composite, The Arabian Journal for Science and Engineering 32 (2b) (2007) 359–364.

[11] I.M. Low, J. Somers, H.S. Kho, I.J. Davies, B.A. Latella, Fabrication and properties of recycled cellulose fibre-reinforced epoxy composites, Composite Interfaces 16 (2009) 659–669.

[12] H.N. Dhakal, Z.Y. Zhang, M.O.W. Richardson, Effect of water absorption on the mechanical properties of hemp fibre reinforced unsaturated polyester composites, Composites Science and Technology 67 (2007) 1674–1683.

[13] Z. Leman, S.M. Sapuan, A.M. Saifol, M.A. Maleque, M.M. Ahmad, Moisture absorption behaviour of sugar palm fibre reinforced epoxy composites, Materials and Design 29 (2008) 1666–1670.

[14] H.J. Kim, D.W. Seo, Effect of water absorption fatigue on mechanical properties of sisal textile-reinforced composites, International Journal of Fatigue 28 (2006) 1307–1314.

[15] A.N. Fraga, E. Frullloni, O. de la Osa, J.M. Kenny, A. Vázquez, Relationship between water absorption and dielectric behaviour of natural fibre composite materials, Polymer Testing 25 (2) (2006) 181–187.

[16] T. Doan, H. Brodowsky, E. Mader, Jute fibre/polypropylene composites II. Thermal, hydrothermal and dynamic mechanical behaviour, Composites Science and Technology 67 (2007) 2707–2714.

[17] M. Jonoobi, J. Harun, P. Tahir, L. Zaini, S. SaifluAzry, M. Makinejad, Characteristics of nanofibers extracted from kenaf core, Bio-Resources 5 (4) (2010) 2556–2566.

[18] V. Tserki, N.E. Zafeiropoulos, F. Simon, C. Panayiotou, A study of the effect of acetylation and propionylation surface treatments on natural fibres, Composites: Part A 36 (2005) 1110–1118.

[19] M. El-Sakhawy, M.L. Hassan, Physical and mechanical properties of microcrystalline cellulose prepared from agricultural residues, Carbohydrate Polymers 67 (2007) 1–10.

[20] D.M. Georget, P. Cairns, A.C. Smith, K.W. Waldron, Crystallinity of lyophilised carrot cell wall components, International Journal of Biological Macromolecules 26 (1999) 325–331.

[21] S. Park, J.O. Baker, M.E. Himmel, P.A. Parilla, D.K. Johnson, Cellulose crystallinity index: measurement techniques and their impact on interpreting cellulose performance, Biotechnology for Biofuels 3 (2010) 10.

[22] L.Y. Mwaikambo, M.P. Ansell, Chemical modification of hemp, sisal, jute, and kapok fibres by alkalization, Journal of Applied Polymer Science 84 (2002) 2222–2234.

[23] M.B. Roncero, A.L. Torres, J.F. Colom, T. Vidal, The effect of xylanase on lignocellulosic components during the bleaching of wood pulps, Bioresource Technology 96 (2005) 21–30.

[24] T. Karbowiak, E. Ferret, F. Debeaufort, A. Voilley, P. Cayot, Investigation of water transfer across thin layer biopolymer films by infrared spectroscopy, Journal of Membrane Science 370 (2011) 82–90.

[25] A. Lasagabaster, M.J. Abad, L. Barral, A. Ares, R. Bouza, Application of FTIR spectroscopy to determine transport properties and water–

polymer interactions in polypropylene (PP)/poly(ethylene-co-vinyl alcohol) (EVOH) blend films: effect of poly(ethylene-co-vinyl alcohol) content and water activity, Polymer 50 (2009) 2981–2989.

[26] N. Sgriccia, M.C. Hawley, M. Misra, Characterization of natural fiber surfaces and natural fiber composites, Composites: Part A 39 (2008) 1632–1637.

[27] S.Y. Oh, D.I. Yoo, Y. Shin, G. Seo, FTIR analysis of cellulose treated with sodium hydroxide and carbon dioxide, Carbohydrate Research 340 (2005) 417–428.

[28] A.K. Bledzki, A.A. Mamun, J. Volk, Barley husk and coconut shell reinforced polypropylene composites: the effect of fibre physical, chemical and surface properties, Composites Science and Technology 70 (2010) 840–846.

[29] B.K. Deka, T.K. Maji, Study on the properties of nanocomposite based on high density polyethylene, polypropylene, polyvinyl chloride and wood, Composites: Part A 42 (2011) 686–693.

[30] D.K. Shukla, S.V. Kasisomayajula, V. Parameswaran, Epoxy composites using functionalized alumina platelets as reinforcements, Composites Science and Technology 68 (2008) 3055–3063.

[31] C.K. Chozhan, M. Alagar, R.J. Sharmila, P. Gnanasundaram, Thermo mechanical behaviour of unsaturated polyester toughened epoxy–clay hybrid nanocomposites, Journal of Polymer Research 14 (2007) 319–328.

[32] R. Rajasekaran, C. Karikalchozhan, M. Alagar, Synthesis, characterization and properties of organoclaymodified polysulfone/epoxy interpenetrating polymer network nanocomposites, Chinese Journal of Polymer Science 26 (6) (2008) 669–678.

[33] R. Khan, P. Khare, B.P. Baruah, A.K. Hazarika, N.C. Dey, Spectroscopic, kinetic studies of polyaniline-flyash composite, Advances in Chemical Engineering and Science 1 (2011) 37–44.

[34] G. Nikolic, S. Zlatkovic, M. Cakic, S. Cakic, C. Lacnjevac, Z. Rajic, Fast Fourier transform IR characterization of epoxy GY systems cross-linked with aliphatic and cycloaliphatic EH polyamine adducts, Sensors 10 (2010) 684–696.

[35] A.A. Rashdi, S.M. Sapuan, M.M. Ahmad, A. Khalina, Water absorption and tensile properties of soil buried kenaf fibre reinforced unsaturated polyester composites (KFRUPC), Journal of Food, Agriculture & Environment 7 (3&4) (2009) 908–911.

[36] T.P. Mohan, K. Kanny, Water barrier properties of nanoclay filled sisal fibre reinforced epoxy composites, Composites Part A: Applied Science and Manufacturing 42 (4) (2011) 385–393.

[37] C.R. Reddy, A.P. Sardashti, L.C. Simon, Preparation and characterization of polypropylene–wheat straw–clay composites, Composites Science and Technology 70 (2010) 1674–1680.

[38] S. Egusa, Anisotropy of radiation-induced degradation in mechanical properties of fabric-reinforced polymer-matrix composites, Journal of Materials Science 25 (3) (1990) 1863–1871.

[39] R. Ghosh, A.R. Krishna, G. Reena, B.L. Raju, Effect of fibre volume fraction on the tensile strength of Banana fibre reinforced vinyl ester resin composites, International Journal of Advanced Engineering Sciences and Technologies 4 (1) (2011) 89–91.

[40] M.J. Le Guen, R.H. Newman, Pulped phormium tenax leaf fibres as reinforcement for epoxy composites, Composites: Part A 38 (2007) 2109–2115.

[41] A. Athijayamani, M. Thiruchitrambalam, U. Natarajan, B. Pazhanivel, Effect of moisture absorption on the mechanical properties of randomly oriented natural fibers/polyester hybrid composite, Materials Science and Engineering A 517 (2009) 344–353.

[42] M. Hughes, C.A. Hill, J.R. Hague, The fracture toughness of bast fibre reinforced polyester composites. Part 1. Evaluation and analysis, Journal of Materials Science 37 (2002) 4669–4676.

[43] P. Wambua, J. Ivens, I. Verpoest, Natural fibres: can they replace glass in fibre reinforced plastics? Composites Science and Technology 63 (2003) 1259–1264.

[44] S. Mishra, A.K. Mohanty, L.T. Drzal, M. Misra, S. Parija, Studies on mechanical performance of biofibre/glass reinforced polyester hybrid composites, Composites Science and Technology 63 (2003) 1377–1385.

[45] A.K. Bledzki, O. Faruk, Creep and impact properties of wood fibre–polypropylene composites: influence of temperature and moisture content, Composites Science and Technology 64 (2004) 693–700.

[46] C. Karmaker, Effect of water absorption on dimensional stability and impact energy of jute fibre reinforced polypropylene, Journal of Materials Science Letters 16 (1997) 462–464.

[47] P.V. Joseph, K. Joseph, S. Thomas, Effect of processing variables on the mechanical properties of sisal-fibre-reinforced polypropylene composites, Composites Science and Technology 59 (1999) 1625–1640.

[48] L.A. Pothan, Z. Oommen, S. Thomas, Dynamic mechanical analysis of banana fibre reinforced polyester composites, Composites Science and Technology 63 (2003) 283–293.

3.2 Mechanical, Thermal and Microstructural Characteristics of Cellulose Fibre Reinforced Epoxy/Organoclay Nanocomposites.

Alamri, H., I. M. Low, and Z. Alothman. 2012. Mechanical, thermal and microstructural characteristics of cellulose fibre reinforced epoxy/organoclay nanocomposites. *Composites Part B: Engineering* 43: 2762-2771.

Mechanical, thermal and microstructural characteristics of cellulose fibre reinforced epoxy/organoclay nanocomposites

H. Alamri [a], I.M. Low [a,*], Z. Alothman [b]

[a] Department of Imaging & Applied Physics, Curtin University of Technology, GPO Box U1987, Perth, WA 6845, Australia
[b] Chemistry Department, College of Science, King Saud University, Riyadh, Saudi Arabia

ABSTRACT

Epoxy nanocomposites reinforced with recycled cellulose fibres (RCFs) and organoclay platelets (30B) have been fabricated and investigated in terms of WAXS, TEM, mechanical properties and TGA. Results indicated that mechanical properties generally increased as a result of the addition of nanoclay into the epoxy matrix. The presence of RCF significantly enhanced flexural strength, fracture toughness, impact strength and impact toughness of the composites. However, the inclusion of 1 wt.% clay into RCF/epoxy composites considerably increased the impact strength and toughness. The presence of either nanoclay or RCF accelerated the thermal degradation of neat epoxy, but at high temperature, thermal stability was enhanced with increased char residue over neat resin. The failure micromechanisms and energy dissipative processes in these nanocomposites were discussed in terms of microstructural observations.

Crown Copyright © 2012 Published by Elsevier Ltd. All rights reserved.

1. Introduction

The unique properties of epoxy resin such as heat resistance, excellent chemical, low shrinkage, high modulus and relatively high strength has rendered it one of the most important matrices used in fibre reinforced polymer. In manufacturing, it is widely used in applications such as aerospace structures, electronics, coatings and adhesives [1,2]. However, cured epoxy systems show low impact strength, poor resistance to propagation and crack initiation and low fracture toughness [1,2]. The brittleness and high cost of epoxy resins are major drawbacks to its industrial use [3].

Recently, the use of natural cellulose fibres such as flax, hemp, sisal, kenaf, banana and jute, as reinforcements in the polymeric matrices has gained a great attention in engineering applications due to their desirable properties, which include low density, low cost, renewability and recyclability as well as excellent mechanical characteristics such as flexibility, high toughness, specific strength and high specific modulus [4–7]. Moreover, manufacturing industries and in particular the packaging, construction and automotive industries have been pressurised by consumers as well as new environmental legislations to search and utilise new renewable materials in substituting the convectional, non-renewable reinforcing materials which include carbon, glass or aramid fibres [5]. Natural fibres are considered as green composites (environmentally friendly) which make them a suitable substitute for traditional fibre

(i.e. glass, carbon and aramid fibre) reinforced petroleum-based composites [6,7]. However, plant–fibre reinforced polymeric composites also have negative aspects such as incompatibility with some polymeric matrices, poor wettability and their high moisture absorption [5,8].

Recycled cellulose fibres (RCFs) can be obtained from cellulosic products such as cardboard, printed paper, recycled newspaper and other types of waste papers. In composites, RCFs are very attractive reinforcement materials due to their availability in large quantities, flexibility, renewability and their low cost which attracts their use as structural components in future housing industry such as load bearing roof systems, sub-flooring and framing components. These composites could also be used in doors, windows, furniture and automotive industry [7,9,10]. There is significant amount of literature on the effects of additional cellulose fibres on physical and thermal properties of the polymer systems [3,8,11–16].

Additionally, nano-clay reinforced polymer nanocomposites have received much attention due to their excellent characteristics which include improved physical (dielectric, optical, permeability and shrinkage) thermal (flammability, decomposition, coefficient of thermal expansion and thermal stability) and mechanical (toughness, strength and modulus) properties [17–19]. The demonstration of vast improvement in mechanical and physical properties on nylon-6/clay nanocomposites during the pioneering work of researchers at Toyota has since attracted more researchers to study the effect of nano-clay addition in the enhancement of thermal, physical and mechanical properties of other polymer matrices [20–28].

---

* Corresponding author.
  E-mail address: j.low@curtin.edu.au (I.M. Low).

Hitherto, the work on polymer/clay nanocomposites has mainly focussed on the synthesis and their mechanical, thermal and physical properties. However, there has not been much work done on the use of nanoclay-based matrix in the synthesis of fibre reinforced polymer composites. Previously published research [29–32] on the use of nanoclay matrix for fibre composites showed that the addition of nanoclay enhances the mechanical properties of fibre reinforced epoxy composites. Bozkurt et al. [29] investigated the effect of nanoclay dispersion on the mechanical properties of non-crimp glass fibre reinforced epoxy nanocomposites. It was found that flexural properties increased with the addition of clay due the enhancement in the interface between the glass fibre and epoxy matrix. In similar study, Zulfli and Shyang [30] reported an improvement in flexural strength and modulus of glass fibre reinforced epoxy/clay nanocomposites due to the addition of organo-treated nanoclay. The interface between the glass fibre and epoxy matrix was increased in the presence of nanoclay. Xu and Hoa [31] investigated the mechanical properties of carbon fibre reinforced epoxy/clay nanocomposites and observed an increase in fracture toughness and flexural strength after addition of a small content of nanoclay. Similar improvements in mechanical properties were obtained by Faruk and Matuana [32] where they used five different types of nanoclay as reinforcement for wood/epoxy composites.

In this paper, the focus is on generating different modes of toughening and strengthening and describing an alternative approach in designing eco-nanocomposites in which microstructural elements are tailored with the use of recycled cellulose fibres (RCFs) and nanoclay dispersions. The main trust of this work was the production of an outer epoxy layer dispersed with nanoclay for wear resistance hardness, barrier properties, heat resistance and thermal stability, and an underlayer of RCF reinforced epoxy/clay for damage tolerance. Here, epoxy eco-nanocomposites reinforced with recycled cellulose fibre (RCF) and nano-clay platelets (Cloisite 30B) have been fabricated and investigated. The nano- and microstructure of the nanocomposites have been investigated by wide angle X-ray scattering (WAXS), transmission electron microscopy (TEM) and scanning electron microscopy (SEM). The influences of RCF/nanoclay dispersions on flexural strength, fracture toughness, impact strength, impact toughness and thermal stability have been investigated and discussed. The failure micromechanisms and energy-dissipative processes in the nanocomposites have been evaluated and discussed in terms of the microstructural observations.

2. Experimental procedures

2.1. Materials

Recycled cellulose fibre (RCF) paper and organoclay platelets (Cloisite 30B) were used as reinforcements for the fabrication of epoxy–matrix composites. The RCF paper with grade 200GSM and 200 μm thickness was supplied by Fuji Xerox Australia Pty. Limited, Belmont WA, Australia. Organoclay platelets (Cloisite 30B) were provided by Southern Clay Products, United States based company. The specifications and physical properties of Cloisite 30B are outlined in Table 1 [33].

2.2. Sample fabrication

2.2.1. Nanocomposites

The nanoclay/epoxy nanocomposites were prepared by mixing the epoxy resin with three different wt.% (1%, 3% and 5%) of nanoclay (Cloiste 30B) using a high speed mechanical mixer for 10 min. After that, a hardener was added to the mixture and then stirred slowly to minimise the formation of air bubbles within the sample.

Table 1
Physical properties of the nanoclay (Cloisite 30B).

Physical properties of Cloisite 30B	
Colour	Off white
Density (g/cm^3)	1.98
d-spacing (0 0 1) (nm)	1.85
Aspect ratio	200–1000
Surface area (m^2/g)	750
Mean particle size (μm)	6

The final mixture was poured into silicon moulds and left for 24 h at room temperature for curing purpose. Pure epoxy sample was also made as a control.

2.2.2. RCF reinforced nanocomposites

Here, the epoxy system and the nanocomposites dispersed with organoclay were used as the matrix material. RCF sheets were first dried for 60 min at 70 °C. After that, RCFs sheets were fully-soaked into a mixture of epoxy/30B organoclay until they became entirely wetted by the mixture, before they were laid down in a closed silicone mould under 8.2 kPa compressive pressure and left 24 h for curing at room temperature. The same processing procedure was used to prepare RCF/epoxy ecocomposites without the addition of nanoclay. The amount of RCF in the final products was about 52 wt.%. All the samples made are summarised in Table 2.

2.3. Wide angle X-ray scattering (WAXS)

Wide-angle X-ray scattering measurement was carried out at the SAXS/WAXS beamline of the Australian Synchrotron in Melbourne, Australia. A beam energy of 20 keV (wavelength of 0.62 Å) was used in the 2θ range of = 0.29–30.00°.

2.4. Transmission electron microscopy (TEM)

Ultra-thin sections ($\sim$80 nm) of samples were prepared using an ultramicrotome (Leica microsystem) and were recovered on a copper grid. Transmission electron microscopy imaging was done using a Titan Cryotwin (FEI Company) operating at 300 kV equipped with a 4 × 4 k CCD camera (Gatan). TEM was carried out at King Abdullah University of Science and Technology (KAUST), Saudi Arabia.

2.5. Scanning electron microscopy (SEM)

Scanning electron microscope (Zeiss Evo 40XVP) was used to investigate the microstructures and the fracture surfaces of composites. Samples were coated with a thin layer of gold to prevent charging before the observation by SEM.

2.6. Thermogravimetric analysis (TGA)

The thermal stability of samples was studied by thermogravimetry analysis (TGA) and differential thermogravimetry (DTG). A Mettler Toledo TGA/DSC star system analyser was used for all these measurements. Samples with – $\sim$10 mg were placed in a platinum can and tests were carried out in nitrogen atmosphere with a heating rate of 10.0 °C/min from 35.0 °C to 800.0 °C.

2.7. Measurements of mechanical properties

2.7.1. Three-point bend test

Rectangular bars with dimensions 60 mm × 10 mm × 6 mm were cut for three-point bend tests to measure flexural strength, flexural modulus and fracture toughness. The three-point bend

Table 2
Compositions of synthesized 30B/epoxy and RCF-epoxy/30B nanocomposites.

30B/epoxy samples	Organoclay (wt.%)	RCF/organoclay/epoxy samples	Organoclay (wt.%)
Pure epoxy (PE)	0	PE/RCF	0
PE/30B1	1%	PE/RCF/30B1	1%
PE/30B3	3%	PE/RCF/30B3	3%
PE/30B5	5%	PE/RCF/30B5	5%

tests were performed using a LLOYD Material Testing Machines – Twin Column Bench Mounted (5–50 kN). The support span used was 40 mm with a displacement rate of 1.0 mm/min. Five specimens of each composition were tested to evaluate the mechanical tests. The flexural strength was evaluated using the following equation:

$$\sigma_F = \frac{3}{2}\frac{p_m S}{WD^2} \tag{1}$$

where P_m is the maximum load at crack extension, S is the span of the sample, D is the specimen thickness and W is the specimen width. Values of the flexural modulus were computed using the initial slope of the load–displacement curve, $\Delta P/\Delta X$, using the following formula:

$$E_F = \frac{S^3}{4WD^3}\left(\frac{\Delta P}{\Delta X}\right) \tag{2}$$

In order to determine the fracture toughness, a sharp razor blade was used to initiate a sharp crack in the samples. The ratio of crack length to width (a/w) was about (0.4). The fracture toughness was calculated using the following equation [6]:

$$K_{IC} = \frac{p_m S}{WD^{2/3}}f\left(\frac{a}{w}\right) \tag{3}$$

where a is the crack length, and $f(a/w)$ is the polynomial geometrical correction factor give as

$$f\left(\frac{a}{W}\right) = \frac{3(a/W)^{1/2}[1.99 - (a/W)(1 - a/W) \times (2.15 - 3.93a/W + 2.7a^2/W^2)]}{2(1 + 2a/W)(1 - a/W)^{2/3}} \tag{4}$$

2.7.2. Charpy impact test

Similar rectangular bars were cut for Zwick Charpy impact testing to evaluate the impact strength and impact toughness. A pendulum hammer with 1.0 J was used during the test to break the samples. Un-notched sampled were used to compute the impact strength using the following formula:

$$\sigma_I = \frac{E}{A} \tag{5}$$

where E is the impact energy to break a sample with a ligament of area A.

Samples of various notch lengths were used to determine the impact toughness of composites. In order to measure the impact toughness, the value of the critical strain energy release rate (G_{IC}) was evaluated as the slope of the fracture energy (U) versus the energy calibration factor (ϕ) as shown in the following equation [6]:

$$U = G_{IC}BD\phi + U_o \tag{6}$$

where U_o is the kinetic energy, D is the specimen width and B is the specimen thickness

3. Results and discussion

3.1. Nanostructural characterisation

3.1.1. Wide angle X-ray scattering (WAXS)

X-ray diffraction (XRD) is used to calculate the basal spacing (d-spacing) of nanoclay. WAXS patterns obtained for Cloisite (30B) organoclay, pure epoxy and epoxy/clay are shown in Fig. 1. It can be seen that epoxy has an amorphous structure without any diffraction peaks. In contrast, the organoclay exhibits a strong (0 0 1) peak at $2\theta = 1.92°$, which corresponds to a d-spacing or basal spacing of 1.85 nm. The diffraction patterns of all epoxy/clay nanocomposites exhibited similar plots with the (0 0 1) peak shifted to a lower angle compared to the nanoclay control powder, indicating an increase in the inter-layer distance between the clay platelets. The basal spacing of (0 0 1) is 3.4 nm at $2\theta = 1.03°$. This
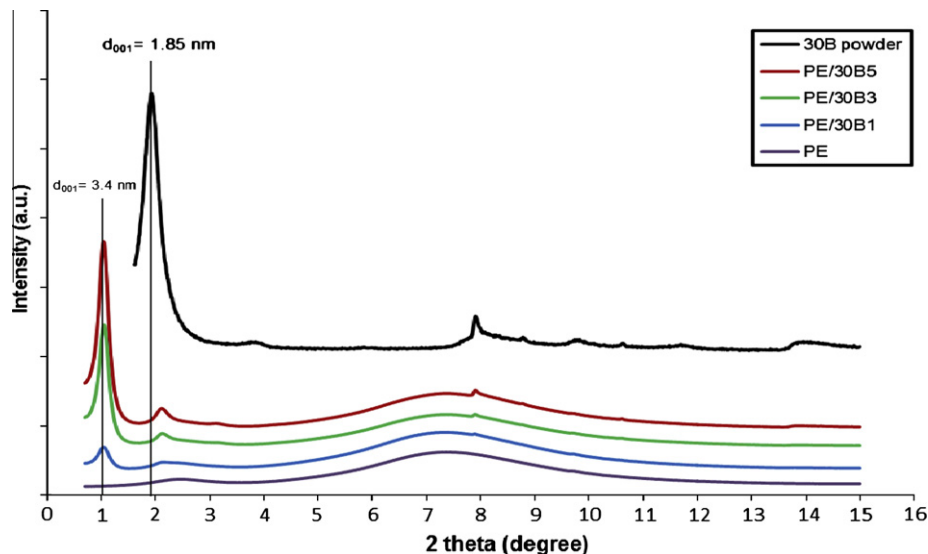
Fig. 1. XRD patterns of Cloisite 30B, pure epoxy and epoxy nanocomposites.

106

result indicates the intercalated structure of the fabricated nanocomposites.

3.1.2. Transmission electron microscopy (TEM)

TEM images for epoxy/clay nanocomposites loaded with 1–5 wt.% of Cloisite 30B nanoclay are shown in Figs. 2 and 3. The lower magnification images in Fig. 2a–c gives a general view of the nanoclay dispersion within the epoxy matrix. It can be seen that the nanoclay platelets are uniformly dispersed within the epoxy matrix. However, large agglomerations can be clearly observed at higher clay loading which implies that the degree of platelet dispersion decreases as the nanoclay concentration increases due to the increase in matrix viscosity. High magnification images in Fig. 3a–d shows the layer structure of clay platelets. It can be seen in Fig. 3d that epoxy was intercalated between the clay layers shifting them apart, which confirmed the intercalated structure of the resulted nanocomposites. The d-spacing of $(0\,0\,1)$ planes in nanoclay layers were 1.85 nm. However, as a result of intercalation with epoxy resin, the corresponding d-spacing increased to 2.93 nm. This observation relatively agrees with the X-ray diffraction results, which have indicated that the spacing between the clay layers in the nanocomposites was in the range of 3.4 nm.

3.2. Thermal properties

The thermal stability of samples was determined using thermogravimetric analysis (TGA). In this test, the thermal stability was studied in terms of the weight loss as a function of temperature in nitrogen atmosphere. The thermograms (TGA) of the epoxy/nanoclay and epoxy/nanoclay/RCF nanocomposites are shown in Fig. 4a and b respectively. The char yields at different temperatures are summarised in Table 3. It can be seen from TGA curves that epoxy and its nanocomposites exhibit two distinct stages of
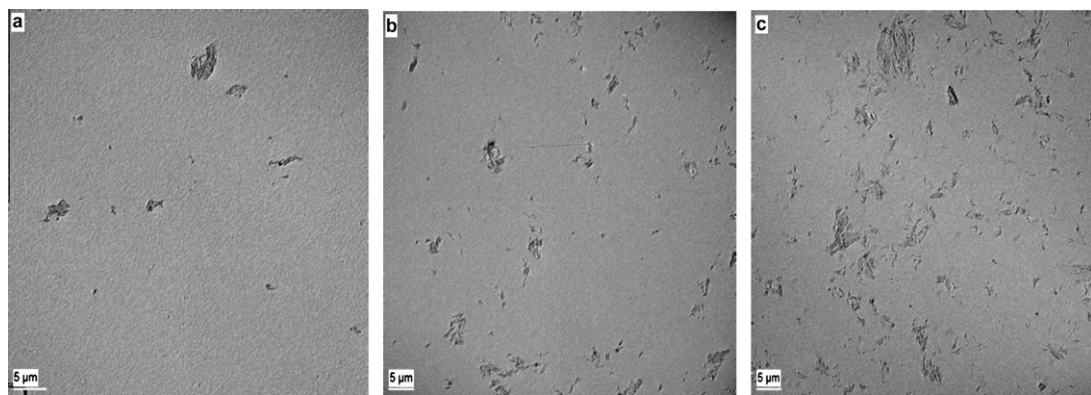
Fig. 2. TEM micrographs at low magnification of epoxy nanocomposites reinforced with different nanoclay concentration: (a) 1 wt.%, (b) 3 wt.% and (c) 5 wt.%.
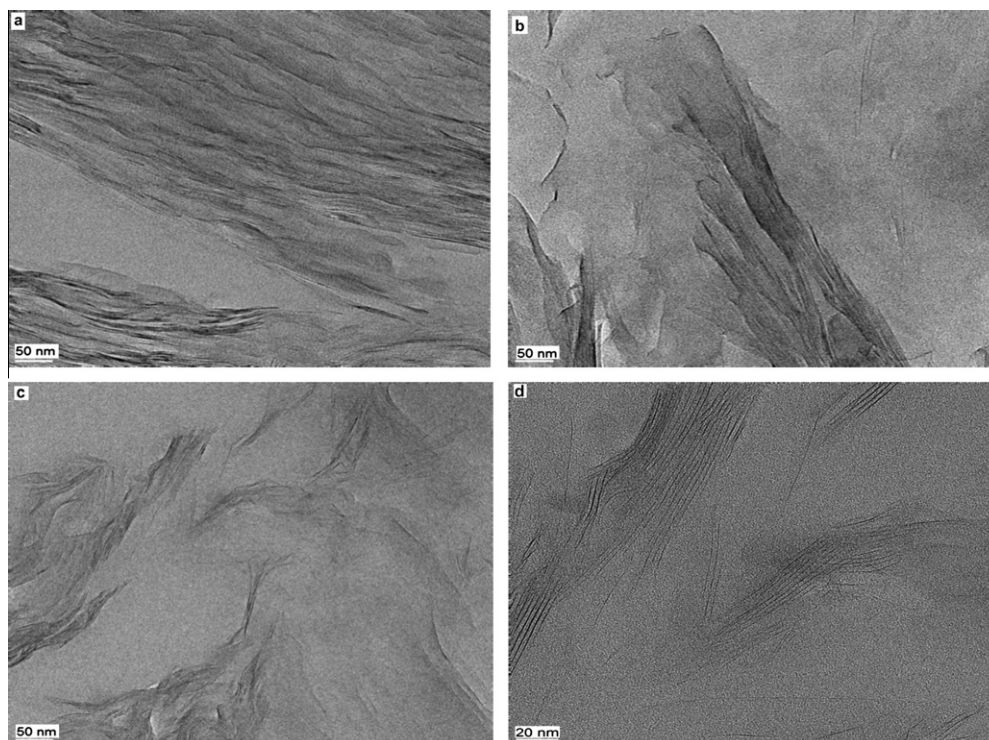
Fig. 3. TEM micrographs at high magnification of epoxy nancomposites reinforced with different nanoclay concentration: (a) 1 wt.%, (b) 3 wt.% and (c) 5 wt.%. (d) Basal spacing between the interlayers of clay/epoxy nanocomposites.

107
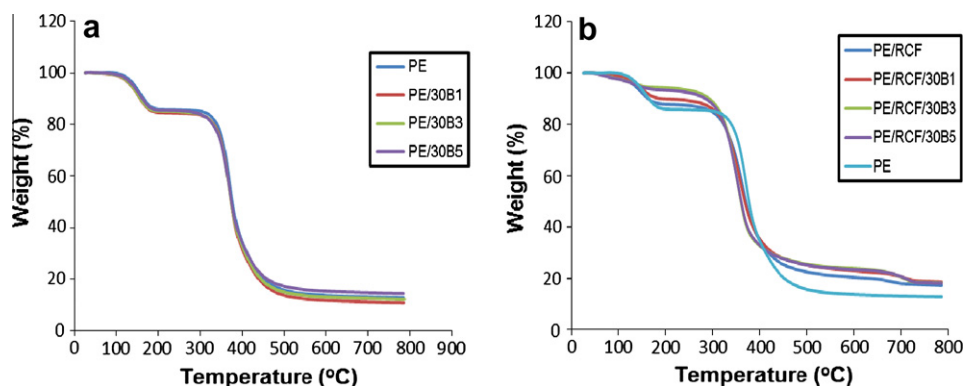
Fig. 4. TGA curves of epoxy and epoxy/clay nanocomposites, (a) without RCF and (b) with RCF.

decomposition. The first stage of decomposition may be related to the vaporisation of moisture in the composites. The second stage of decomposition may be related to degradation of epoxy and its additives. It also can be seen that the major degradation for all samples occurred in range of ~300–400 °C.

From the amounts of residue at low temperature from 100 to 300 °C, it can be seen that the presence of nanoclay slightly increased the rate of sample degradation compared to pure epoxy. But, the maximum decomposition temperature (T_{max}) of the composites remained unchanged after the addition of nanoclay. The maximum decomposition temperature of neat epoxy and epoxy filled with 1, 3 and 5 wt.% nanoclay were 367.3, 367.1, 367.5 and 367.4 °C respectively. However, at higher temperature, nanocomposite with 5 wt.% clay loading performed better in thermal stability than neat epoxy with higher char residue of 14.7 wt.% at 700 °C. It was reported in previous studies that the addition of nano-clay platelets would efficiently raise the char residue of polymers at high temperature [25,34–36].

The presence of RCF in epoxy system also accelerates the degradation at low temperature. But at temperature higher than 400 °C, the inclusion of RCF leads to an enhancement in thermal stability by increasing the char yield of epoxy at 700 °C from 13.1 wt.% to 18.0 wt.%. Shih [1] carried out the thermal stability of epoxy reinforced with waste water bamboo husk fibre and found that the char yield of epoxy at 700 °C increased by 13.5–52.8% due the addition of 10 wt.% of bamboo fibre. The increase in char yield is an indication of the potency of flame retardation of polymers. Thus, the addition of bamboo fibre enhanced the flame retardation of epoxy. Similar results were obtained by De Rosa and co-worker in year 2010 [8] where they found an improvement in thermal stability of untreated phormium tenax fibres/epoxy composites. The presence of plant fibre increased the maximum degradation temperature and the char yield of epoxy resin.

The addition of nanoclay to RCF/epoxy composites reduced the maximum decomposition temperature of the composites, which

means that the decomposition was accelerated when compared to neat epoxy. This reduction in thermal stability at low temperature is due to the Hofmann elimination reaction, where clay acts as a catalyser toward the degradation of the polymer matrix [36,37]. However, at 600 and 700 °C, the char residues of the RCF filled epoxy nanocomposites are significantly higher than that for pure epoxy and RCF reinforced epoxy composites. This means that at high temperature, the addition of nanoclay significantly enhances the thermal stability of epoxy/RCF composites. This enhancement on thermal properties is due to the presence of nanoclay, which acted as barriers and hindered the diffusion of volatile decomposition products out from the nanocomposites [35,36,38].

3.3. Mechanical properties

3.3.1. Flexural strength

In general, the incorporation of nanoclay platelets into epoxy matrix led to a modest enhancement in flexural strength for all nanocomposite samples as shown in Fig. 5a. The addition of 1% nanoclay resulted in the highest flexural strength of all nanocomposites samples. The flexural strength of epoxy/nanoclay composites containing 1 wt.% nanoclay was increased by 45.6% compared to neat epoxy. However, the addition of more clay caused a marked decrease in flexural strength. This can be due to the poor dispersion of the nanoclay in the epoxy resin at higher clay contents [26,31]. At high concentration of clay, nanoclay platelet poorly dispersed inside the matrix forming platelet agglomerations which act as stress concentrators which in turn cause reduction in flexural strength [26,28]. Zainuddin et al. [28] investigated the flexural properties of nanoclay–epoxy nanocomposites fabricated with 1–3 wt.% loading of montmorillonite. Results showed that flexural strength was increased as a maximum up to 8.7% for samples reinforced by only 2 wt.% of nanoclay over neat epoxy. Poor dispersion of nanoclay was thought to lead to poor mechanical properties. Moreover, it was observed in our study that the viscosity of the

Table 3
Thermal properties of epoxy, epoxy/RCF composites, epoxy/caly and epoxy/RCF/clay nanocomposites.

Sample	Char yield at different temperature (%)							T_{max} (°C)
	100 °C	200 °C	300 °C	400 °C	500 °C	600 °C	700 °C	
PE	99.86	86.10	85.24	35.26	15.69	13.69	13.08	367.29
PE/30B1	99.01	84.66	83.70	31.89	13.68	11.72	11.16	367.13
PE/30B3	99.13	85.13	83.94	33.02	14.92	13.05	12.49	367.47
PE/30B5	99.40	85.56	84.16	34.58	17.2	15.30	14.72	367.35
PE/RCF	98.65	87.88	85.01	34.58	22.49	20.37	17.96	359.62
PE/RCF/30B1	98.79	89.90	86.04	35.45	25.22	22.93	20.56	352.23
PE/RCF/30B3	97.70	94.29	89.12	32.63	25.51	23.85	20.46	350.97
PE/RCF/30B5	97.42	93.39	87.91	32.92	25.17	23.45	20.71	351.32
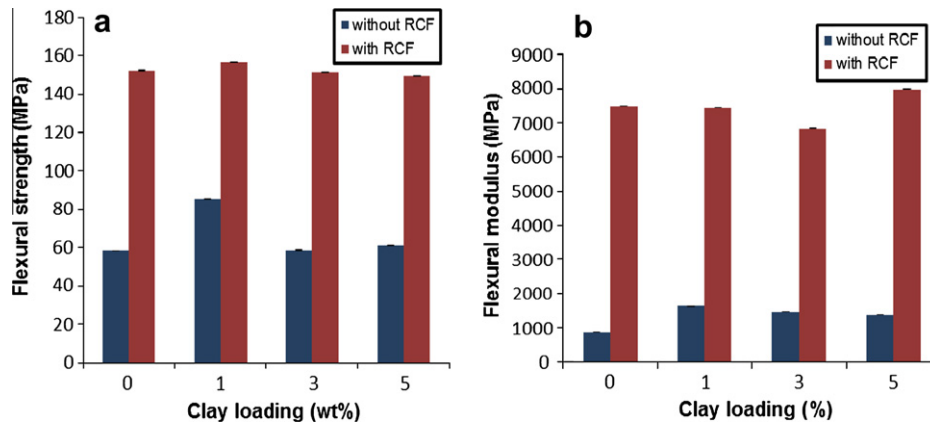
Fig. 5. (a) Flexural strength as a function of clay content for epoxy and its nanocomposites with and without RC; and (b) Flexural modulus as a function of clay content for epoxy and its nanocomposites with and without RCF.

matrix increased as clay content increased, which allowed small air-bubbles to be trapped in the resin during mixing process forming tiny voids in the sample. This in turn resulted in sample failure at relatively low stress. In contrast, with a lower loading of nanoclay, the potential of the formation of micro-voids is less, and the dispersion is more uniform which both lead to strength improvement [31].

The flexural strength of RCF reinforced epoxy/clay nanocomposites are also shown in Fig. 5a. It can be seen that the presence of the RCF sheets has significantly improved the flexural strength for all samples. The flexural strength of neat epoxy increased from 58.5 to 152.3 MPa after the addition of RCF sheets. This enhancement in flexural properties is clearly due the ability of recycled cellulose fibres to withstand bending force of the composites [39]. The inclusion of 1 wt.% nanoclay platelets to the RCF/epoxy composites was found to have positive effect on flexural strength.

However, adding more clay (i.e. 3 and 5 wt.%) led to a slight reduction in flexural strength. Previous studies have shown enhancement in strength properties of fibre based epoxy nanocomposites. Bozkurt et al. [29] studied the mechanical properties of non-crimp glass fibre reinforced layered clay/epoxy nanocomposites. They observed that flexural properties increased with the addition of clay due the enhancement in the interface between the glass fibre and epoxy matrix. In similar study, Zulfli and Shyang [30] reported an improvement in flexural strength and modulus for glass fibre reinforced epoxy/clay nanocomposites due to the addition of treated nanoclay. The presence of clay is believed to increase the interface between the glass fibre and epoxy matrix [30].

The flexural modulus can be used as an indicator of the stiffness of the materials in static bending condition [15]. Fig. 5b also shows the values of flexural modulus for all samples. The addition of 1 wt.% nanoclay in epoxy matrix has increased the flexural modulus by 87.6% over neat epoxy. In addition, the presence of RCF has a tremendous effect on flexural modulus for epoxy and its nanocomposites. Flexural modulus of epoxy was increased by about 760% after the addition of RCF sheet.

3.3.2. Fracture toughness

The influence of nanoclay on fracture toughness of epoxy/nanoclay composites is shown in Fig. 6. The fracture toughness of neat epoxy and epoxy/clay nanocomposites reinforced with 1, 3 and 5 wt.% nanoclay was 0.85, 1.11, 0.93 and 0.97 MPa $m^{1/2}$, respectively. Once again, it was observed that reinforcement with 1.0 wt.% of nanoclay could achieve better fracture properties with improvement reaching up to 30%. This enhancement in epoxy fracture toughness after adding nanloclay platelet is similar to

the work of Kim et al. [40] who reported that adding (0.5, 1.5 and 3 wt.%) nanoclay platelet to epoxy matrix increased fracture toughness by about 20, 46 and 50% respectively. However, Fig. 6 also shows that facture toughness of epoxy nanocomposites decreased slightly when more clay was added. It has been reported that poor dispersion of high content of nano-fillers leads to agglomeration which acts as a stress concentration that can initiate tiny cracks, which leads to crack propagation [33,41].

The influence of RCF sheets on fracture toughness is clearly shown in Fig. 6. As expected, samples reinforced with RCF sheets showed a significant increase in fracture toughness in all samples. For example, the addition of RCF in epoxy resin increased the fracture toughness by about 350%. This extraordinary enhancement is due to the unique properties of cellulose fibre in resisting fracture which resulted in increased energy dissipation from crack-deflection at the fibre–matrix interface, fibre-debonding, fibre-bridging, fibre pull-out and fibre-fracture [14]. This result is supported by the work of Lui and Huges [11] and Maleque and Belal [15] where they reported an enhancement in fracture toughness when cellulose fibres were added to epoxy matrix. The addition of nanoclay to the RCF/epoxy composites was found to have insignificant or negligible increase in fracture toughness. The fracture toughness for RCF/epoxy composite and RCF/epoxy nanocomposites reinforced with nanoclay loading 1, 3 and 5 wt.% was 3.8, 3.8, 3.9 and 3.9 MPa $m^{1/2}$, respectively. This result is in agreement with the work done by McGrath et al. [42]. They studied the mechanical properties of cellulose fibre/epoxy composites reinforced with kaolinite and micro-sized ZrO_2. It was found that fracture toughness increased with the addition of either kaolinite or ZrO_2 or both particles.
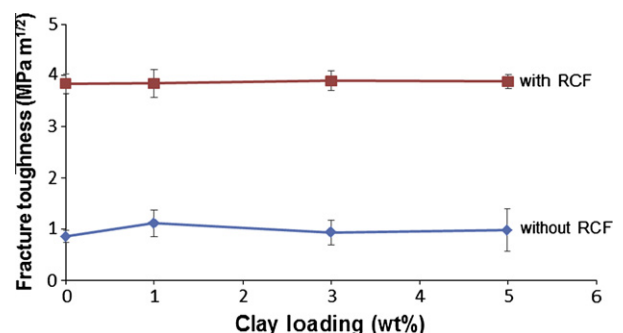
Fig. 6. Fracture toughness as a function of clay content for epoxy and its nanocomposites with and without RCF.
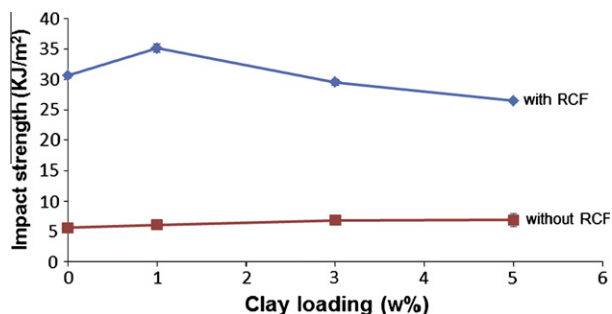
Fig. 7. Impact strength as a function of clay content for epoxy and its nanocomposites with and without RCF.
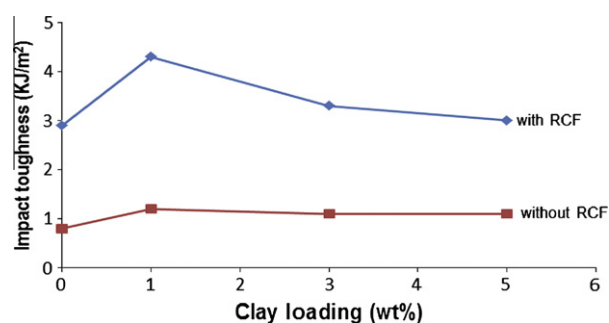
Fig. 8. Impact toughness as a function of clay content for epoxy and its nanocomposites with and without RCF.

3.3.3. Impact strength

Impact strength can be defined as the ability of the material to withstand impact loading. As shown in Fig. 7, the presence of nanoclay platelets slightly enhanced the impact strength for epoxy nanocomposites with maximum improvement reaching up to 22.45% at 5 wt.% nanoclay load. It can be seen that the impact strength of epoxy/clay nanocomposites increased as clay content increased. The impact strength of neat epoxy increased from 5.6 kJ/m^2 to 6.1, 6.9 and 6.9 kJ/m^2 after the addition of 1, 3 and 5 wt.% of clay respectively. Similarly, significant enhancement in impact strength was reported by Ye and co-workers [21]. Based on their observation, the addition of 2.3 wt.% halloysite nanotubes (HNTs) could increase the impact strength of neat epoxy 4 times without affecting the flexural properties and thermal stability.

The presence of RCF significantly improved impact strength by approximately 444% over pure epoxy from 5.6 kJ/m^2 to 30.7 kJ/m^2. This huge achievement is due to the fact that cellulose fibre has a better ability to absorb impact energy than unreinforced polymer. This result concurs with the work of Maleque and Belal [15] where they investigated the mechanical properties of pseudo-stem banana fibre–epoxy composites and found that the presence of banana woven fabric increased the impact strength over the neat epoxy by approximately 40%. However, the addition of nanoclay to RCF/ epoxy composites showed two different scenarios. At low clay content (1 wt.%), the impact strength of neat epoxy increased by 15% from 30.7 to 35.2 kJ/m^2. But as clay loading increased, the impact strength significantly decreased with 3.7% and 13.7% reduction at clay contents 3 and 5 wt.% respectively compared to neat epoxy. This reduction in impact strength at higher clay loading was due to the formation of clay agglomerates and voids as a result of increased system viscosity due to the presence of nanoclay which in turn reduced the fibre–matrix adhesion [26,43].
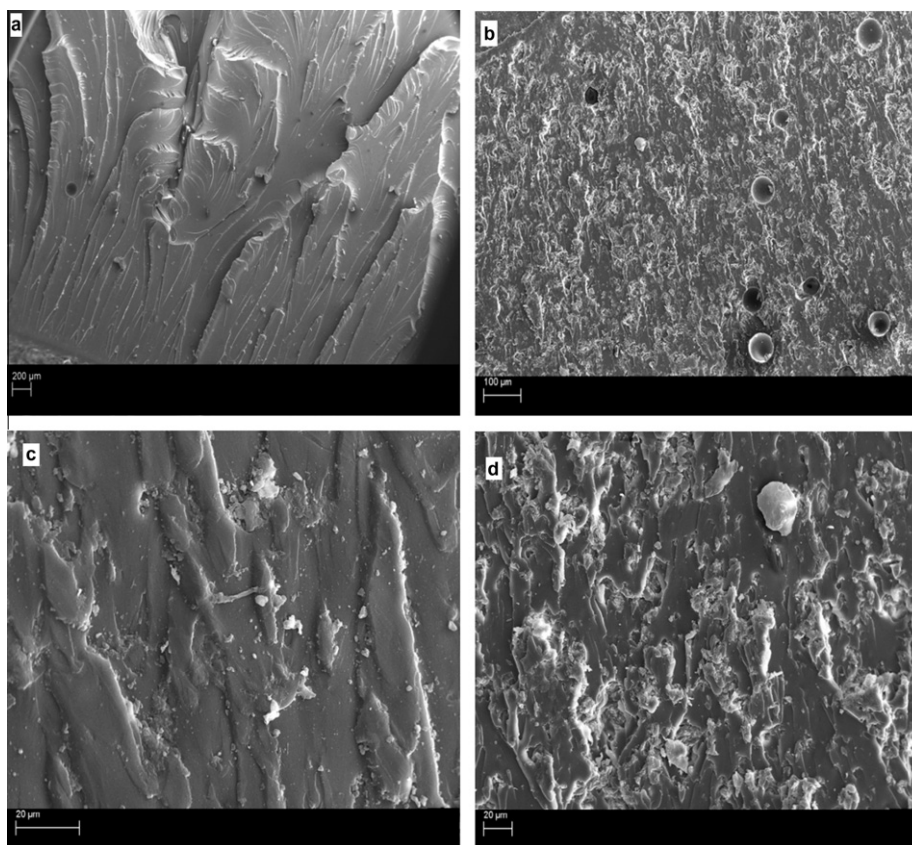
Fig. 9. Scanning electron micrographs after fracture toughness testing for: low magnification (a) PE; (b) PE/30B5 and high magnification; (c) EP/30B1 and (d) EP/30B5.

3.3.4. Impact toughness

The impact toughness in terms of energy release rate (G_{IC}) of epoxy/clay nanocomposites and RCF/epoxy/clay nanocomposites has been shown in Fig. 8. Several interesting characteristics are noteworthy. Firstly, the presence of RCF significantly enhanced the impact toughness of epoxy matrix. The impact toughness for pure epoxy and RCF reinforced epoxy are 0.8 and 2.9 kJ/m² respectively. This result indicates that recycled cellulose fibres improved the impact toughness of the pure epoxy material by approximately 262.5%. This extraordinary enhancement in toughness properties as discussed before is due to the fact that RCF displays a variety of fracture mechanisms in the crack path to resist crack propagation. These fracture mechanisms include fibre breakage, fibre pull-out, fibre-debonding and fibre-bridging which require high energy to be absorbed. This may explain why composites reinforced by RCF displayed higher toughness. Secondly, the addition of nanoclay in different concentration to the RCF/epoxy composites

increased the impact toughness by 48.3, 13.8 and 3.5% at clay loading 1, 3 and 5 wt.% respectively. Once again and similar to the impact strength behaviour, impact toughness displayed maximum value at 1 wt.% nanoclay load then dramatically decreased as clay contents increased.

Lastly, quite good improvements in impact toughness were observed for epoxy nanocomposites without RCF reinforcement. The incorporation of 1, 3 and 5 wt.% nanoclay increased impact toughness of neat epoxy by 50, 37.5 and 37.5% respectively. An increase in impact toughness of epoxy due to the addition of nano-filler was also reported by Ma et al. [44] where they found that the inclusion of silica nano-particles increased the toughness properties in terms of energy release rate (G_{IC}) of epoxy system by 81% at 20 wt.% silica load. In general, the enhancement in toughness properties as was observed by number of studies for polymers reinforced with nano-fillers was due to several toughness mechanisms for dissipating energy such as crack pinning, crack deflection, particle debond-
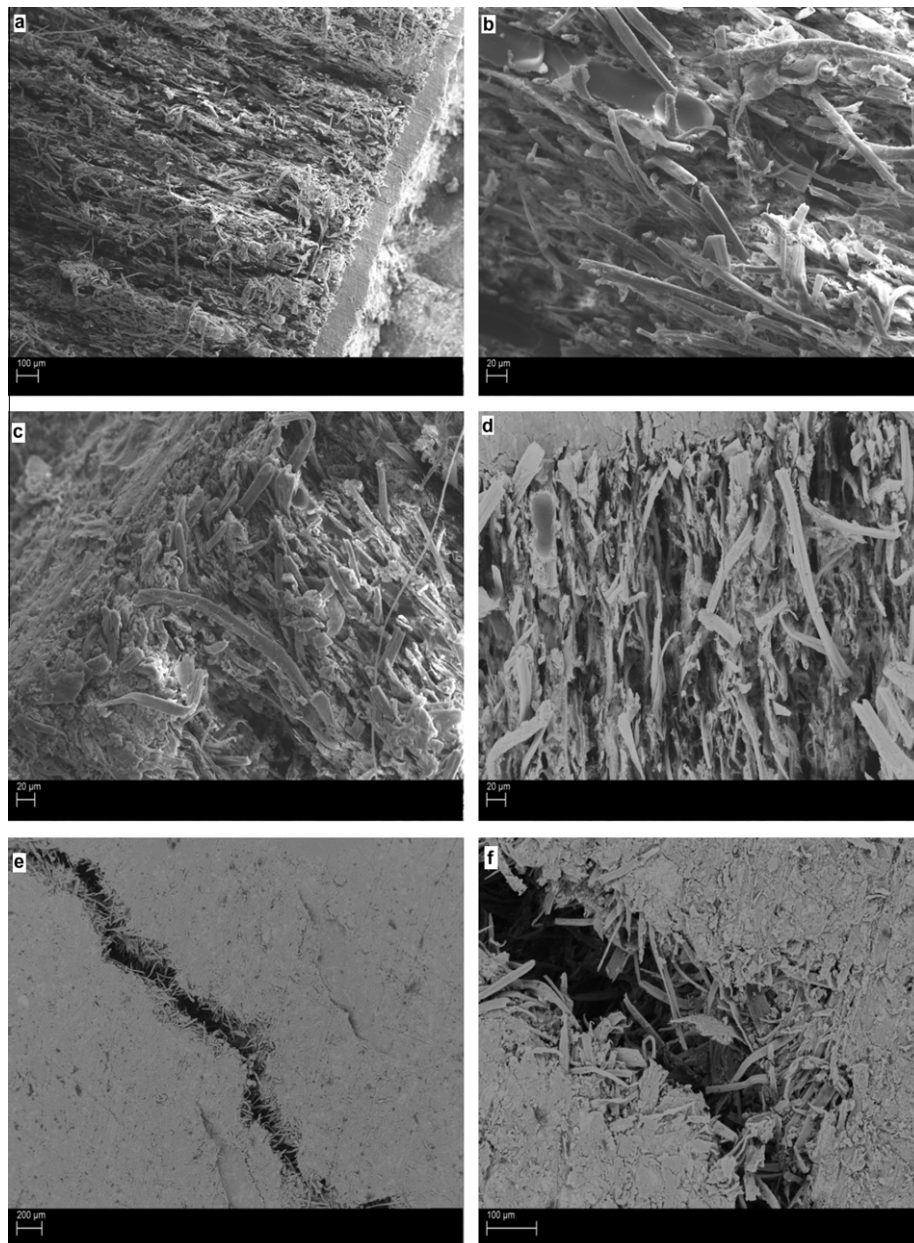
Fig. 10. SEM micrographs of facture surface: (a) PE/RCF low magnification, (b) PE/RCF high magnification, (c) PE/RCF/30B1, (d) PE/RCF/30B5, (e) crack propagation (low magnification) and (f) crack propagation (high magnification).

111

ing, plastic void growth, plastic deformation and particle pullout [44–48].

3.4. Failure micromechanisms and energy dissipative processes

The fracture surfaces of pure epoxy and epoxy nanocomposites reinforced with 1 and 5 wt.% nanoclay are shown in Fig. 9. It is clear that as a result of adding nanoparticles, epoxy/clay nanocomposites display a rougher fracture surface than that of neat resin. An increase in fracture surface roughness can be used as indicator to the presence of crack deflection mechanisms, which increase fracture toughness by increasing crack propagation length during deformation [45,47]. In the other hand, the fracture surface of pure epoxy was very smooth and featureless, which indicates typical brittle fracture behaviour with lack of significant toughness mechanisms [47]. Fig. 9c and d shows high magnification SEM micrograph of fracture surface for epoxy reinforced with 1 and 5 wt.% nanoclay platelet respectively. A variety of possible toughness mechanisms such as crack pinning, crack deflection, particle debonding, plastic void growth, plastic deformation and particle pullout can be observed. Such toughness mechanisms can lead to higher fracture toughness properties through resisting crack propagation [44–48].

Fig. 10 shows the SEM micrographs of the fracture surface for RCF/epoxy composite and RCF/epoxy nanocomposites reinforced with 1 and 5 wt.% clay after fracture toughness test. A variety of toughness mechanisms such as shear deformation, crack bridging, fibre pullout and fibre fracture and matrix fracture can be clearly observed which impart good fracture properties of samples reinforced by RCF. It can be seen from Fig. 10e and f that the sample of RCF mat composite didn't completely break in two pieces. This is due to the fact that fibres bridge the cracks and enhance the crack propagation resistance which led to improvement in fracture toughness. It also can be observed that the adhesion between the fibre and the matrix is quite good. These super toughness mechanisms of RCF were the major factor of increasing mechanical properties of samples reinforced with RCF when compared to samples without RCF.

4. Conclusions

Epoxy eco-composites and nano-composites reinforced with recycled cellulose fibres (RCFs) and organoclay have been fabricated and characterised. Intercalation and homogeneous dispersion of nanoclay platelet with some agglomerations was achieved by mixing the nanoclay with the epoxy resin. In the case of epoxy/nanoclay systems, good enhancements in flexural strength (45.6%), fracture toughness (30%), and impact toughness (50%) were achieved by the addition of 1 wt.% nanoclay. However, adding more clay showed no further increase in these properties due the increased viscosity, voids and poor dispersion with high clay contents. The presence of 5 wt.% nanoclay into epoxy increased the thermal stability in term of the char residue at high temperature. Thermal properties were found to increase as clay content increased.

In the case of the epoxy/RCF composites, it was found that the presence of RCF significantly increased flexural strength (160%), fracture toughness (350%), impact strength (444%) and impact toughness (263%) compared to pure epoxy. This remarkable enhancement is due the unique properties of cellulose fibre in withstanding bending force and resisting fracture force. For thermal stability, the addition of RCF to epoxy matrix was found to accelerate the composites degradation and decreased the temperature of maximum degradation. But, at higher temperature higher

than 400 °C, the presence of RCF led to an enhancement in thermal stability by increasing the char yield.

In the case of epoxy/RCF/clay nanocomposites, the inclusion of RCF into clay/epoxy nanocomposites significantly increased the mechanical properties compared to neat epoxy and its nanocomposites. On the other hand, the addition of nanoclay to RCF/epoxy composites was found to be insignificant for improvement of flexural strength and fracture toughness. For impact properties, the presence of 1% nanoclay considerably increased impact strength and impact toughness by 14.5% and 48.3% respectively over RCF/epoxy composites. The addition of nanoclay to RCF/epoxy composites was found to increase the thermal stability by increasing the char yield of composites at high temperatures. However, the rate of degradation increased after adding clay to RCF/epoxy composites.

References

[1] Shih YF. Mechanical and thermal properties of waste water bamboo husk fibre reinforced epoxy composites. Mater Sci Eng A 2007;445–446:289–95.
[2] Deng S, Zhang J, Ye L, Wu J. Toughening epoxies with halloysite nanotubes. Polymer 2008;49:5119–27.
[3] Ganan P, Garbizu S, Ponte R, Mondragon I. Surface modification of sisal fibres: effects on the mechanical and thermal properties of their epoxy composites. Polym Compos 2005;26(2):121–7.
[4] Nair S, Wang S, Hurley DC. Nanoscale characterization of natural fibre and their composites using contact-resonance force microscopy. Composites Part A 2010;41:624–31.
[5] Dhakal HN, Zhang ZY, Richardson MOW. Effect of water absorption on the mechanical properties of hemp fibre reinforced unsaturated polyester composites. Compos Sci Technol 2007;67:1674–83.
[6] Low IM, McGrath M, Lawrence D, Schmidt P, Lane J, Latella BA. Mechanical and fracture properties of cellulose fibre reinforced epoxy laminates. Composites Part A 2007;38:963–74.
[7] Marsh G. Next step for automotive materials. Mater Today 2003;6:36–43.
[8] De Rosa IM, Santulli C, Sarasini F. Mechanical and thermal characterization of epoxy composites reinforced with random and quasi-unidirectional untreated phormium tenax leaf fibres. Mater Des 2010;31:2397–405.
[9] Sanadi A, Young R, Rowell R. Recycled newspaper fibres as reinforcing fillers in thermoplastics: Part I – analysis of tensile and impact properties in polypropylene. J Reinforc Plast Compos 1994;13:54–67.
[10] Baroulaki I, Karakasi B, Pappa G, Tarantili P, Economides D, Magoulas K. Preparation and study of plastic compounds containing polyolefins and post used newspaper fibres. Composites: Part A 2006;37(10):1613–25.
[11] Lui Q, Hughes M. The fracture behaviour and toughness of woven flax fibre reinforced epoxy composites. Composites: Part A 2008;39:1644–52.
[12] Athijayamani A, Thiruchitrambalam M, Natarajan U, Pazhanivel B. Effect of moisture absorption on the mechanical properties of randomly oriented natural fibres/polyester hybrid composite. Mater Sci Eng A 2009;517:344–53.
[13] Harish S, Michael DP, Bensely A, Lal DM, Rajadurai A. Mechanical property evaluation of natural fibre coir composite. Mater Charact 2009;60:44–9.
[14] Low IM, Somers J, Kho HS, Davies IJ, Latella BA. Fabrication and properties of recycled cellulose fibre-reinforced epoxy composites. Compos Interface 2009;16:659–69.
[15] Maleque MA, Belal FY. Mechanical properties study of pseudo-stem banana fibre reinforced epoxy composite. Arab J Sci Eng 2007;32(2B):359–64.
[16] Rashdi AA, Sapuan SM, Ahmad MM, Khalina A. Water absorption and tensile properties of soil buried kenaf fibre reinforced unsaturated polyester composites (KFRUPC). J Food Agri Enviro 2009;7(3&4):908–11.
[17] Ma J, Xu J, Ren JH, Yu ZZ, Mai YW. A new approach to polymer/montmorillonite nanocomposites. Polymer 2003;44(16):4619–24.
[18] Lu C, Mai YW. Influence of aspect ratio on barrier properties of polymer-clay nanocomposites. Phys Rev Lett 2005;95:088303.
[19] Sinha SR, Okamoto M. Polymer/layered silicate nanocomposites: a review from preparation to processing. Prog Polym Sci 2003;28:1539–641.

[20] Usuki A, Kojima Y, Kawasumi M, Okada A, Fukushima Y, Kurauchi T, et al. Synthesis of nylon 6-clay hybrid. J Mater Res 1993;8:1179–84.

[21] Ye Y, Chen H, Wu J, Ye L. High impact strength epoxy nanocomposites with natural nanotubes. Polymer 2007;48:6426–33.

[22] Alexandre B, Langevin D, Médéric P, Aubry T, Couderc H, Nguyen QT, et al. Water barrier properties of polyamide 12/montmorillonite nanocomposite membranes: structure and volume fraction effects. J Membr Sci 2009;328:186–204.

[23] Araujo EM, Araujo KD, Paz RA, Gouveia TR, Barbosa R, Ito EN. Polyamide 66/ Brazilian clay nanocomposites. J Nanomater 2009;2009:23 [Article ID 136856].

[24] Ha SR, Rhee KY, Park SJ, Lee JH. Temperature effects on the fracture behaviour and tensile properties of silane-treated clay/epoxy nanocomposites. Compos Part B: Eng 2010;41:602–7.

[25] Hwang SS, Liu SP, Hsu PP, Yeh JM, Chang KC, Lai YZ. Effect of organoclay on the mechanical/thermal properties of microcellular injection molded PBT–clay nanocomposites. Int Commun Heat Mass Transfer 2010;37: 1036–43.

[26] Qi B, Zhang QX, Bannister M, Mai YW. Investigation of the mechanical properties of DGEBA-based epoxy resin with nanoclay additives. Compos Struct 2006;75:514–9.

[27] Kaynak C, Nakas GI, Lsitman NA. Mechanical properties, flammability and char morphology of epoxy resin/montmorillonite nanocomposites. Appl Clay Sci 2009;46:319–24.

[28] Zainuddin S, Hosura MV, Zhoua Y, Narteha AT, Kumarb A, Jeelani S. Experimental and numerical investigations on flexural and thermal properties of nanoclay–epoxy nanocomposites. Mater Sci Eng A 2010;527:7920–6.

[29] Bozkurt E, Kaya E, Tanoğlu M. Mechanical and thermal behaviour of non-crimp glass fibre reinforced layered clay/epoxy nanocomposites. Compos Sci Technol 2007;67:3394–403.

[30] Zulfli NHM, Shyang CW. Flexural and morphological properties of epoxy/glass fibre/silane-treated organo montmorillonite composites. J Phys Sci 2010;21:41–50.

[31] Xu Y, Hoa SV. Mechanical properties of carbon fibre reinforced epoxy/clay nanocomposites. Compos Sci Technol 2008;68:854–61.

[32] Faruk O, Matuana LM. Nanoclay reinforced HDPE as a matrix for wood-plastic composites. Compos Sci Technol 2008;68:2073–7.

[33] Yasmin A, Abot JL, Daniel IM. Processing of clay/epoxy nanocomposites by shear mixing. Scripta Materialia 2003;49:81–6.

[34] Chatterjee A, Islam MA. Fabrication and characterization of TiO$_2$–epoxy nanocomposite. Mater Sci Eng A 2008;487:574–85.

[35] Ismail H, Pasbakhsh P, Fauzi MN, Abu Bakar A. Morphological, thermal and tensile properties of halloysite nanotubes filled ethylene propylene diene monomer (EPDM) nanocomposites. Polym Test 2008;27:841–50.

[36] Madaleno L, Schjødt-Thomsen J, Pinto JC. Morphology, thermal and mechanical properties of PVC/MMT nanocomposites prepared by solution blending and solution blending + melt compounding. Compos Sci Technol 2010;70:804–14.

[37] Zhao C, Qin H, Gong F, Feng M, Zhang S, Yang M. Mechanical, thermal and flammability properties of polyethylene/clay nanocomposites. Polym Degrad Stab 2005;87:183–9.

[38] Yeh JM, Huang HY, Chena CL, Su WF, Yu YH. Siloxane-modified epoxy resin–clay nanocomposite coatings with advanced anticorrosive properties prepared by a solution dispersion approach. Surf Coat Technol 2006;200:2753–63.

[39] Satapathy A, Jha Ak, Mantry S, Singh SD, Patnaik A. Processing and characterization of jute-epoxy composites reinforced with SiC derived from rice husk. J Reinf Plast Compos 2010;29(18):2869–78.

[40] Kim BC, Park SW, Lee DG. Fracture toughness of the nano-particle reinforced epoxy composite. Compos Struct 2008;86:69–77.

[41] Deng S, Zhang J, Ye L. Halloysite–epoxy nanocomposites with improved particle dispersion through ball mill homogenisation and chemical treatments. Compos Sci Technol 2009;69:2497–505.

[42] McGrath M, Vilaiphand W, Vaihola S, Lopez A, Low IM, Latella BA. Synthesis and properties of clay-ZrO2-cellulose fibre-reinforced polymeric nano-hybrids. In: Atrens A, Boland JN, Clegg R, Griffiths JR, editors, Structural integrity and fracture international conference (SIF'04), Brisbane, Australia, 26–29 September; 2004. p. 265–270.

[43] Khan SU, Iqbal K, Munir A, Kim JK. Quasi-static and impact fracture behaviours of CFRPs with nanoclay-filled epoxy matrix. Composites: Part A 2010;42:253–64.

[44] Ma J, Mo MS, Du XS, Rosso P, Friedrich K, Kuan HC. Effect of inorganic nanoparticles on mechanical property, fracture toughness and toughening mechanism of two epoxy systems. Polymer 2008;49:3510–23.

[45] Zhao S, Schadler LS, Hillborg H, Auletta T. Improvements and mechanisms of fracture and fatigue properties of well-dispersed alumina/epoxy nanocomposites. Compos Sci Technol 2008;68:2976–82.

[46] Wetzel B, Rosso P, Haupert F, Friedrich K. Epoxy nanocomposites – fracture and toughening mechanisms. Eng Fract Mech 2006;73:2375–98.

[47] Tang Y, Deng S, Ye L, Yang C, Yuan Q, Zhang J, et al. Effects of unfolded and intercalated halloysites on mechanical properties of halloysite–epoxy nanocomposites. Composites: Part A 2011;42:345–54.

[48] Chen C, Justice RS, Schaefer DW, Baur JW. Highly dispersed nanosilica-epoxy resins with enhanced mechanical properties. Polymer 2008;49:3805–15.

3.3 Microstructural, Mechanical, and Thermal Characteristics of Recycled Cellulose Fibre-Halloysite-Epoxy Hybrid Nanocomposites.

Alamri, H., and I. M. Low. 2012. Microstructural, mechanical, and thermal characteristics of recycled cellulose fibre-halloysite-epoxy hybrid nanocomposites. *Polymer Composites* 33(4): 589-600.

Microstructural, Mechanical, and Thermal Characteristics of Recycled Cellulose Fiber-Halloysite-Epoxy Hybrid Nanocomposites

H. Alamri, I. M. Low

Department of Imaging and Applied Physics, Curtin University of Technology, Perth, Western Australia (WA) 6845, Australia

Epoxy hybrid-nanocomposites reinforced with recycled cellulose fibers (RCF) and halloysite nanotubes (HNTs) have been fabricated and investigated. The dispersion of HNTs was studied by synchrotron radiation diffraction (SRD) and transmission electron microscopy (TEM). The influences of RCF/HNTs dispersion on the mechanical properties and thermal properties of these composites have been characterized in terms of flexural strength, flexural modulus, fracture toughness, impact toughness, impact strength, and thermogravimetric analysis. The fracture surface morphology and toughness mechanisms were investigated by SEM. Results indicated that mechanical properties increased because of the addition of HNTs into the epoxy matrix. Flexural strength, flexural modulus, fracture toughness, and impact toughness increased by 20.8, 72.8, 56.5, and 25.0%, respectively, at 1 wt% HNTs load. The presence of RCF dramatically enhanced flexural strength, fracture toughness, impact strength, and impact toughness of the composites by 160%, 350%, 444%, and 263%, respectively. However, adding HNTs to RCF/epoxy showed only slight enhancements in flexural strength and fracture toughness. The inclusion of 5 wt% HNTs into RCF/epoxy ecocomposites increased the impact toughness by 27.6%. The presence of either HNTs or RCF accelerated the thermal degradation of neat epoxy. However, at high temperature, samples reinforced with RCF and HNTs displayed better thermal stability with increased char residue than neat resin. POLYM. COMPOS., 33:589–600, 2012. © 2012 Society of Plastics Engineers

INTRODUCTION

In the recent years, the use of natural cellulose fibers such as flax, hemp, sisal, kenaf, banana, and jute as reinforcements in the polymeric matrices has gained a great attention in engineering applications due to their tremendous properties that include low density, low cost, renewability, and recyclability, as well as excellent mechanical characteristics such as flexibility, high toughness, specific strength, and high-specific modulus. These advantages make natural fiber composites one of the high-performance composites in terms of economic and environmental advantages [1, 2]. For instance, recycled cellulose fibers (RCFs) obtained from cellulosic waste products such as cardboard, printed papers, and recycled newspapers among others are the best alternatives with respect to environmental friendliness when compared with conventional reinforcing fibers in composites [3]. RCF-reinforced composites are also of great importance when it comes to industrial areas where plants are used for technical purposes. For example, in the housing industry, RCF-based composites are a class of materials that have a good potential while considering the future use, whereby they can be used as structural components including framing components, subflooring, and as load-bearing roof systems [2, 4]. In addition, the composites can be used in the automotive industry, furniture, windows, and doors [2, 4]. However, the use of natural fiber-reinforced composites has been less attractive due to the poor resistance to moisture and their lack of good interfacial adhesion [5, 6]. A significant amount of work can be found in the literature on the effect of addition of cellulose fiber on the mechanical, thermal, and physical properties of polymer systems [6–13].

Polymer–clay nanocomposites have gained great attention due to their superior characteristics that include an improvement in physical (permeability, optical, dielectric, shrinkage), thermal (thermal stability, decomposition, flammability, coefficient of thermal expansion), and mechanical (modulus, strength, toughness) properties. There have been numerous studies on the effect of nanoclay in enhancing thermal, mechanical, and physical properties of polymer composites since the demonstration of improved mechanical and physical properties from pioneering studies done on nylon-6/clay nanocomposites at Toyota [14–22].

In enhancing the thermal and mechanical properties of polymers, halloysite nanotubes (HNTs) as new types of additives have recently received much attention [23–25]. These are a type of alumino-silicate clays with a structure

of hollow nanotubular with the chemical composition $(Al_2Si_2O_5(OH)_4\text{-}2H_2O)$ [23–25]. The resemblance of HNTs to CNTs (carbon nanotubes) in aspect ratio resulting from their unique crystal structure lowered cost of HNTs when compared with CNTs, ability of HNTs to disperse easily in a polymer matrix, and the fact that halloysites are rigid materials have resulted in HNTs being considered as ideal materials in polymer nanocomposites preparation [23, 25, 26].

Epoxy is considered one of the important matrices used for fiber-reinforced polymer due to its unique properties of relatively high strength, high modulus, low shrinkage, and excellent chemical and heat resistance [27, 28]. However, the high cost and brittleness of epoxy resins are the main drawbacks to its industrial use [13, 27, 28]. Previous researchers have found that the mechanical performance of epoxy resins including toughness, modulus, and strength was increased through the addition of a small amount of HNTs without necessarily sacrificing other properties such as thermal stability and glass transition temperature (T_g). Ye et al. [26] reported an improvement in impact strength of halloysite–epoxy nanocomposites without sacrificing thermal properties. Deng et al. [28] also reported a great increase in impact and fracture toughness without reduction in flexural strength and thermal properties of composites. Later on, Deng et al. [23] reported an enhancement in facture toughness of halloysite tube–epoxy nanocomposites without sacrificing thermal properties after improving HNTs particles dispersion into epoxy matrix through chemical treatments and ball mill homogenization.

Surprisingly, there is very little published work on nanocomposites use in fiber-reinforced composites as matrix despite the fact that most scientific work has recently focused on polymer nanocomposites and the study on their mechanical and physical properties.

In this work, hybrid nanocomposites of epoxy reinforced with HNTs and RCF have been fabricated. The influence of RFC/HNTs dispersion on the microstructure, mechanical, and thermal properties has been characterized and discussed in terms of synchrotron radiation diffraction (SRD), transmission electron microscopy (TEM), scanning electron microscopy (SEM), flexural strength and modulus, fracture toughness, impact strength, impact toughness, and thermogravimetric analysis (TGA).

MATERIALS AND FABRICATION

Materials

RCF paper and HNTs were used as reinforcements for the fabrication of epoxy-matrix composites. The RCF paper with grade 200 GSM and 200-μm thickness was supplied by Fuji Xerox Australia Pty., Belmont WA, Australia. HNTs (ultrafine grade) were provided by Imerys Tableware Asia, New Zealand. The brightness of HNTs is about

TABLE 1. Compositions of synthesized HNT/epoxy and RCF-epoxy/HNT hybrid nanocomposites.

HNT/epoxy samples	HNT (wt%)	RCF/HNT/epoxy samples	HNT (wt%)
Pure Epoxy (PE)	0	PE/RCF	0
PE/HNT1	1	PE/RCF/HNT1	1
PE/HNT3	3	PE/RCF/HNT3	3
PE/HNT5	5	PE/RCF/HNT5	5

98.9% as measured by a Minolta CR300 using D65 light source. The elemental compositions (wt %) are SiO_2, 50.4; Al_2O_3, 35.5; Fe_2O_3, 0.25; TiO_2, 0.05 [29]. Finally, general purpose low-viscosity epoxy resin (FR-251) and epoxy hardener (Isophorone-diamine) were supplied by Fibreglass & Resin Sales Pty, WA, Perth, Australia.

Sample Fabrication

Nanocomposites. The halloysite/epoxy nanocomposites were prepared by mixing the epoxy resin with three different weight percentages (1, 3, and 5%) of HNT using a high-speed mechanical mixer for 10 min. After that, a hardener (isophorone-diamine) was added to the mixture and then stirred slowly to minimize the formation of air bubbles within the sample. The final mixture was poured into silicon molds and left for 24 h at room temperature for curing purpose. Pure epoxy samples were made as controls.

RCF-Reinforced Nanocomposites. In this section, pure epoxy system and epoxy filled with HNTs were used as matrix materials for RCF/epoxy composites and RCF/HNT/epoxy nanocomposites. RCF sheets were first dried for 60 min at 70°C. After that, RCFs sheets were fully soaked into a mixture of epoxy/HNTs until they became entirely wetted by the mixture, before they were laid down in a closed silicone mold under 8.2 kPa compressive pressure and left 24 h for curing at room temperature. The same processing procedure was used to prepare RCF/epoxy ecocomposites without the addition of HNTs. The amount of RCF in the final products was about 52 wt%. All the samples made are summarized in Table 1.

Synchrotron Radiation Diffraction

Synchrotron radiation diffraction (SRD) measurement was carried out on the powder diffraction beamline at the Australian Synchrotron. The diffraction patterns of each sample were collected using a wavelength of 1.377 Å in the two-theta range of 2°–82°.

Transmission Electron Microscopy

Ultrathin sections (~80 nm) of samples were prepared using an ultramicrotome (Leica microsystem) and recovered on a copper grid. Transmission electron microscopy

116

(TEM) imaging was done using a Titan Cryotwin (FEI Company) operating at 300 kV equipped with a 4k × 4k CCD camera (Gatan). TEM was carried out at King Abdullah University of Science and Technology (KAUST), Saudi Arabia.

Scanning Electron Microscopy

Scanning electron microscope (Zeiss Evo 40XVP) was used to investigate the microstructures and the fracture surfaces of composites. Samples were coated with a thin layer of gold to prevent charging before the observation by SEM.

Thermogravimetric Analysis

The thermal stability of samples was studied by thermogravimetry analysis (TGA) and differential thermogravimetry. A Mettler Toledo TGA/DSC star system analyzer was used for all these measurements. Samples with ~10 mg were placed in a platinum can, and tests were carried out under nitrogen atmosphere with a heating rate of 10.0°C/min from 35 to 800°C.

Measurements of Mechanical Properties

Three-Point Bend Tests. Rectangular bars with dimensions 60 mm × 10 mm × 6 mm were cut for three-point bend tests to measure the flexural strength, flexural modulus, and fracture toughness. The three-point bend tests were performed using a LLOYD Material Testing Machines—Twin Column Bench Mounted (5–50 kN). The support span used was 40 mm with a displacement rate of 1.0 mm/min. Five specimens of each composition were tested to evaluate the mechanical tests. The flexural strength was evaluated using the following equation:

$$\sigma_F = \frac{3}{2} \frac{p_m S}{WD^2} \quad (1)$$

where P_m is the maximum load at crack extension, S is the span of the sample, D is the specimen thickness, and W is the specimen width. Values of the flexural modulus were computed using the initial slope of the load–displacement curve, $\Delta P / \Delta X$, using the following formula:

$$E_F = \frac{S^3}{4WD^3} \left(\frac{\Delta P}{\Delta X} \right) \quad (2)$$

To determine the fracture toughness, a sharp razor blade was used to initiate a sharp crack in the samples. The ratio of crack length to width (a/w) was about (0.4). The fracture toughness was calculated using the following equation [1]:

$$K_{IC} = \frac{p_m S}{WD^{2/3}} f \left(\frac{a}{w} \right) \quad (3)$$
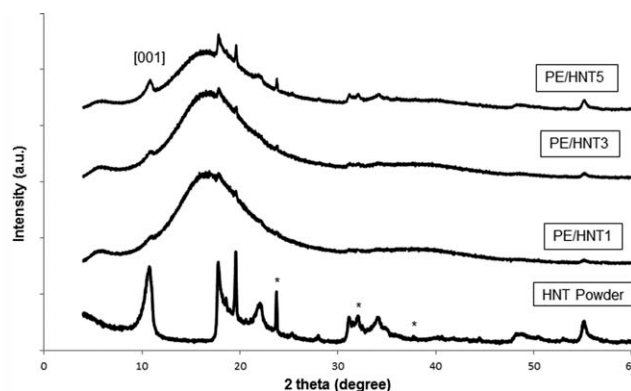
FIG. 1. Synchrotron radiation diffraction (SRD) patterns of HNTs powder and epoxy/HNTs nanocomposites. (Q: quartz).

where a is the crack length and $f(a/w)$ is the polynomial geometrical correction factor give as

$$f \left(\frac{a}{W} \right) = \frac{3(a/W)^{1/2}[1.99 - (a/W)(1 - a/W) \times (2.15 - 3.93a/W + 2.7a^2/W^2)]}{2(1 + 2a/W)(1 - a/W)^{2/3}} \quad (4)$$

Charpy Impact Test. Similar rectangular bars were cut for Zwick Charpy impact testing to evaluate the impact strength and impact toughness. A pendulum hammer with 1.0 J was used during the test to break the samples. Un-notched samples were used to compute the impact strength using the following formula:

$$\sigma_I = \frac{E}{A} \quad (5)$$

where E is the impact energy to break a sample with a ligament of area A.

Samples of various notch lengths were used to determine the impact toughness of composites. To measure the impact toughness, the value of the critical strain energy release rate (G_{IC}) was evaluated as the slope of the fracture energy (U) versus the energy calibration factor (ϕ) as shown in the following equation [1]:

$$U = G_{IC}WD\phi + U_o \quad (6)$$

where U_o is the kinetic energy, W is the specimen width, and D is the specimen thickness.

RESULTS AND DISCUSSION

Nanocomposites Characterization

Synchrotron radiation Powder Diffraction. The synchrotron radiation powder diffraction (SRD) patterns of HNT powder and PE/HNT nanocomposites are shown in Fig. 1. The HNTs show a sharp peak at 10.73°, which correspond to [001] basal spacing of 0.735 nm [24, 30]. In addition to halloysite, there are also small amounts of quartz in
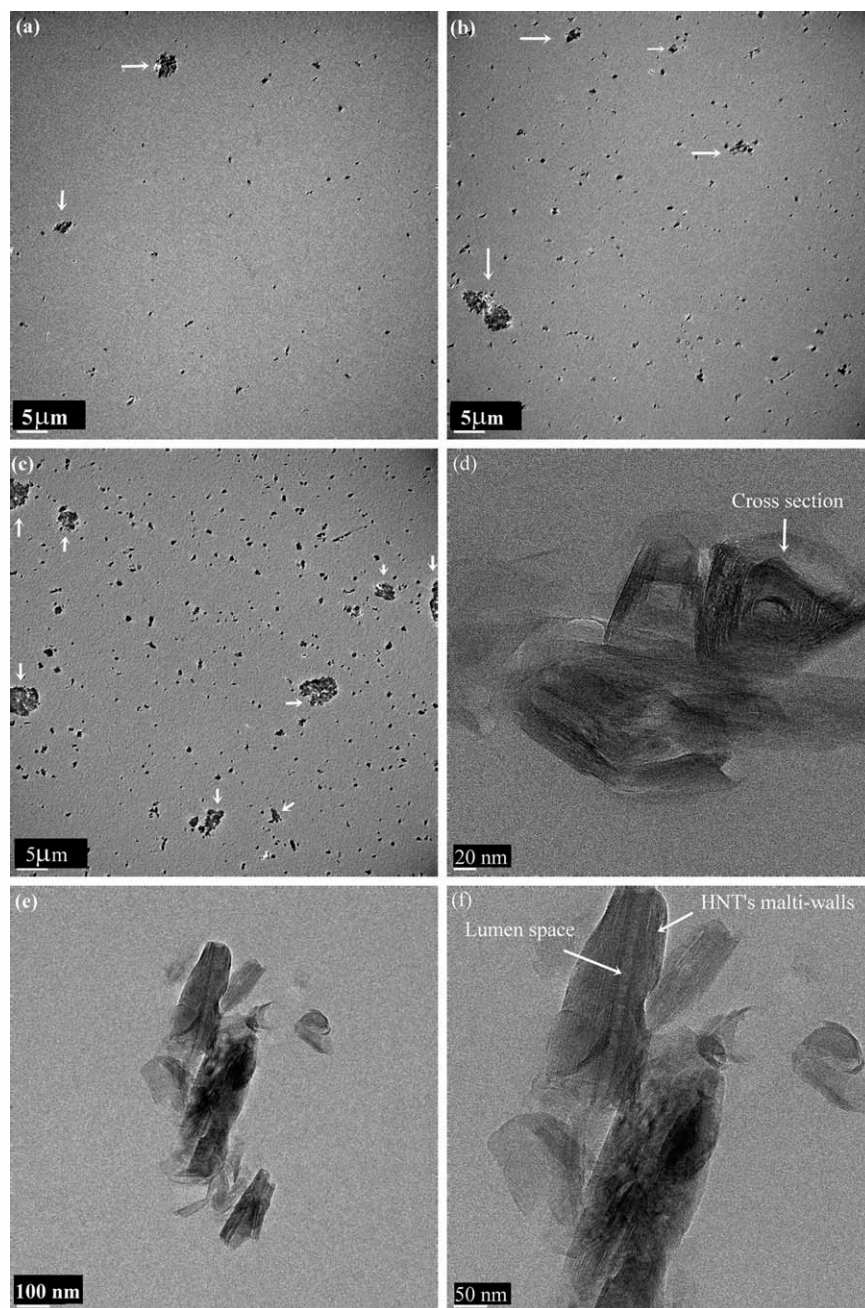
FIG. 2.   TEM micrographs of epoxy nanocomposites reinforced with different HNTs concentration: (a) 1 wt%, (b) 3 wt%, (c) 5 wt%, and (d, e and f) are high magnification TEM images of HNTs.

the powders as has been reported by Joussein et al. [31] and Deng et al. [28]. Epoxy/HNT nanocomposites patterns show no change in HNTs peaks positions. However, it can be seen that the height of the diffraction peaks of HNT increases as halloysite content increases in HNT/epoxy nanocomposites.

Transmission Electron Microscopy.   Transmission electron microscopy (TEM) images for epoxy/HNT materials loaded with 1, 3, and 5 wt% HNTs are shown in Fig. 2. The low-magnification images in Fig. 2a–c give a general view of the HNTs dispersion within the epoxy matrix. It

can be seen that the HNTs are uniformly dispersed within the epoxy matrix. However, bigger agglomerations of HNTs can be clearly observed at higher clay loading. This suggests the quality of HNT dispersion decreases as clay concentration increases due to the increase in matrix viscosity [23, 32]. At higher magnification images shown in Fig. 2d–f, it can be seen that HNTs have tubular shape similar to the multiwalled carbon nanotube with an average diameter of about 20–40 nm and length ranging from 500 nm to1.6 μm [25, 30].

Figure 2d shows the cross-section of the HNTs, while Fig. 2f shows the longitudinal section. This would indi-

118
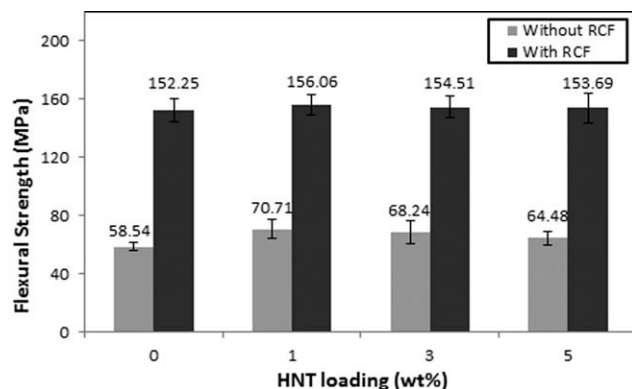
FIG. 3. Flexural strength as a function of HNTs content for epoxy and its nanocomposites reinforced with or without RCF.

cate that the dispersion of HNTs within the epoxy matrix is quite random. The dimension of the lumen structure of HNTs and their walls are clearly shown in Fig. 2e and f, which confirms the multiwall nanotubular structures of HNTs. Finally, it was reported that HNTs have two different interlayer surfaces; the inner walls contain alumina while the outer surfaces contain silica [23, 33].

Mechanical Properties of HNT/Epoxy Nanocomposites

The flexural strength, flexural modulus, impact strength, fracture toughness, and impact toughness of HNT/epoxy composites are shown in Figs. 3–7. In general, the incorporation of HNT into epoxy matrix enhances the mechanical properties for all nanocomposites samples. The enhancement in flexural strength is shown in Fig. 3 as a function of HNT content. The addition of 1 wt% HNTs has resulted in the highest flexural strength of all nanocomposites samples. Flexural strength of epoxy/HNT composites containing 1 wt% HNTs was increased by 20.8% compared to neat epoxy. This can be linked to the better dispersion of nanofillers at low-HNTs loading. However, adding more HNTs slightly decreases the flexural strength. This can be due to the presence of filler agglomerations and microvoids at higher HNTs con-

tents [20, 34]. At high concentration of HNTs, they are poorly dispersed within the matrix-forming agglomerations that act as stress concentrators, which in turn cause reduction in flexural strength [20, 22]. Agglomerations of HNTs can be clearly seen in Fig. 2a–c. Additionally, it was observed an increase in matrix viscosity due to the increase in HNTs content, which in turn allowed small air-bubbles to be trapped in the resin during the mixing process forming tiny voids in the sample. This in turn resulted in sample failure at relatively low stress. In contrast, with a lower loading of HNTs, the potential of microvoid formation is less, and the dispersion is more uniform that both lead to strength improvement [34]. Similar observations have been reported by Prashantha et al. [25] in their study of HNTs-filled polypropylene nanocomposites. It was found that the addition of HNTs resulted in a slight improvement in flexural strength of neat polymer. However, at higher HNTs loading (8 wt%), flexural strength decreased due the tendency of HNTs to agglomerate [25]. Figure 4 demonstrates the flexural modulus of HNT/epoxy nanocomposites as a function of HNTs loading. The introduction of HNTs into epoxy matrix significantly increases the flexural modulus for all epoxy nanocomposites samples. The addition of 1 wt% HNTs in epoxy matrix increases the flexural modulus by 72.8% over neat epoxy. This means that the presence of HNTs increases the stiffness of the matrix. This enhancement in modulus can be explained by the strong stiffening effect of the HNTs fillers, which themselves have a higher modulus than epoxy.

Impact strength can be defined as the ability of the material to withstand impact loading. As shown in Fig. 5, the presence of HNTs gradually increases the impact strength for epoxy nanocomposites with maximum enhancement reaching up to 23.4% at 5 wt% HNTs load. The impact strength of neat epoxy increases from 5.6 kJ/m^2 to 6.4 and 7.0 kJ/m^2 after the addition of 3 and 5 wt% of HNTs, respectively. At high-HNTs loading, HNT clusters may act as crack stoppers and increase the ability of the material to absorb energy by forming tortuous pathways for crack propagation which resulting the

FIG. 4. Flexural modulus as a function of HNTs content for epoxy and its nanocomposites reinforced with or without RCF.
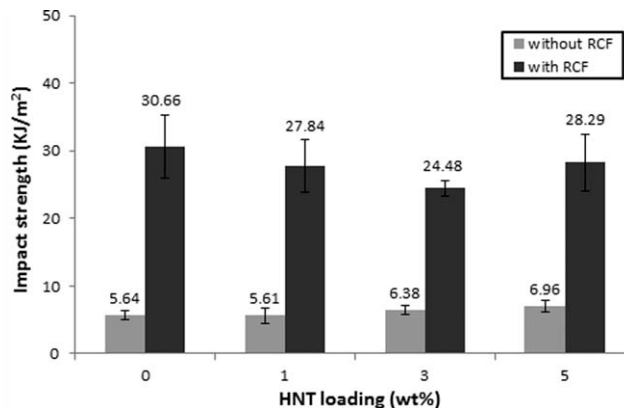
FIG. 5. Impact strength as a function of HNTs content for epoxy and its nanocomposites reinforced with or without RCF.
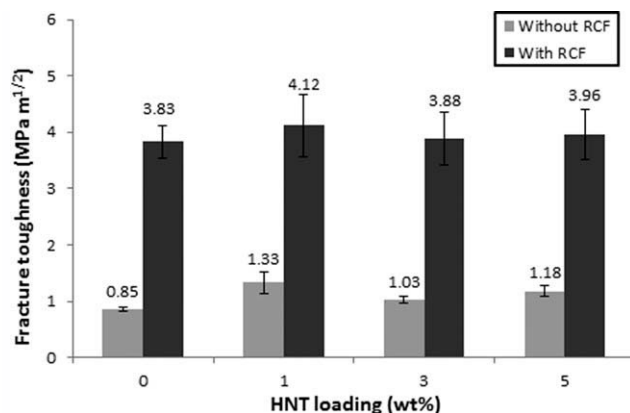
FIG. 6. Fracture toughness as a function of HNTs content for epoxy and its nanocomposites reinforced with or without RCF.

impact strength to increase [23]. Similarly, remarkable improvement in impact strength was reported by Ye et al. [26]. Based on their observation, the addition of 2.3 wt% HNTs could increase the impact strength of neat epoxy four times without affecting the flexural properties and thermal stability. The discrepancy in results between our work and that of Ye et al. [26] could be attributed to the geometry and condition of samples tested. In our study, the samples were not notched, whereas notched samples were used by Ye et al. [26].

The effect of HNTs on fracture toughness of epoxy/ HNT nanocomposites is shown in Fig. 6. The fracture toughness of neat epoxy and epoxy/HNT nanocomposites reinforced with 1, 3, and 5 wt% HNTs is 0.85, 1.33, 1.03, and 1.18 MPa.m$^{1/2}$, respectively. Fracture toughness increased by 56.5%, 21.2%, and 38.8% when 1, 3, and 5 wt% HNTs are added. This significant enhancement in fracture toughness is similar to the study of Deng et al. [23]. They reported a significant enhancement in facture toughness of HNT/epoxy nanocomposites compared to neat epoxy. In their study, fracture toughness increased by 38 and 47% when 5 and 10 wt% halloysite were added. This was due to the toughness mechanisms of halloysite tube such as particles pull-out and debonding. Once again, it was observed in our study that reinforcement with 1.0 wt% of halloysite tubes displayed superior fracture properties than those reinforced with higher contents of HNTs. It has been reported that nanoparticles easily tend to agglomerate at higher filler contents acting as stress concentration that can initiate tiny cracks, which leads to crack propagation [23, 35].

Figure 7 displays the impact toughness in terms of the energy release rate of epoxy/HNT nanocomposites. The addition of 1, 3, and 5 wt % HNTs significantly increases impact toughness of neat epoxy by 25.0, 50.0, and 62.5%, respectively. This remarkable enhancement in toughness properties for nanocomposites is due to several toughness mechanisms for dissipating energy such as crack pinning, crack deflection, particle debonding, plastic void growth, plastic deformation, and particle pull-out as was reported

by number of studies for polymers reinforced with nano-fillers [24, 36–39]. Ma et al. [36] reported an increase in impact toughness of epoxy system due to the addition of nanofiller. Authors found that the inclusion of silica nano-particles increased the toughness properties in terms of energy release rate (G_{1C}) of epoxy system by 81% at 20 wt% silica load.

Mechanical Properties of RCF-Reinforced HNT/Epoxy Nanocomposites

The flexural strength, flexural modulus, impact strength, fracture toughness, and impact toughness of RCF-reinforced HNT/epoxy nanocomposites are also plotted in Figs. 3–7. In general, the addition of RCF into epoxy matrix and HNT/epoxy nanocomposites significantly increases the mechanical properties compared to neat epoxy and its nanocomposites. This is due to the unique properties of cellulose fibers in enhancement polymer mechanical properties [10]. In detail, Fig. 3 displays the flexural strength of RCF/HNT/epoxy composites as a function of HNTs loading. First, it can be seen that the presence of RCF into epoxy matrix significantly increases the flexural strength of neat epoxy by 160.3% from 58.5 to 152.3 MPa. This significant enhancement in flexural properties is clearly due to the ability of RCFs in resisting bending force of the composites [40]. The addition of HNTs to the RCF/epoxy composites is found to have a positive effect on flexural strength when compared with unfilled RCF/epoxy composites. This slight improvement in flexural strength can be related to the enhanced RCF-matrix interface due to the presence of HNT tubes. However, flexural strength gradually decreases as HNTs content increases. This decline in flexural strength can be due to the lack in stress transferring between matrix and RCF as a result of increased matrix viscosity. Previous studies showed enhancement in strength properties of fiber-based epoxy nanocomposites. Ye et al. [41] investigated the mechanical properties of carbon fiber-reinforced epoxy/HNT composites. Flexural properties slightly increased due to the addition of HNT particles. In another
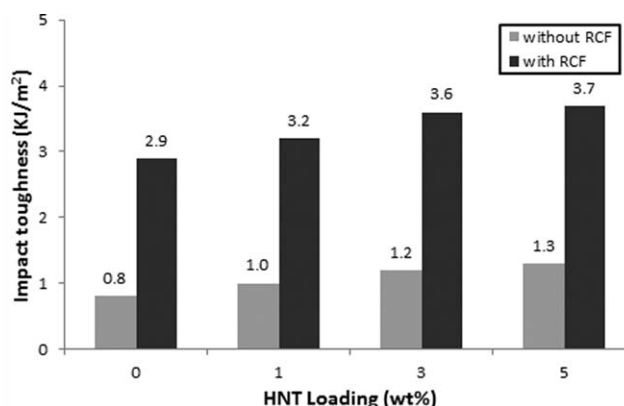
FIG. 7. Impact toughness as a function of HNTs content for epoxy and its nanocomposites reinforced with or without RCF.

120
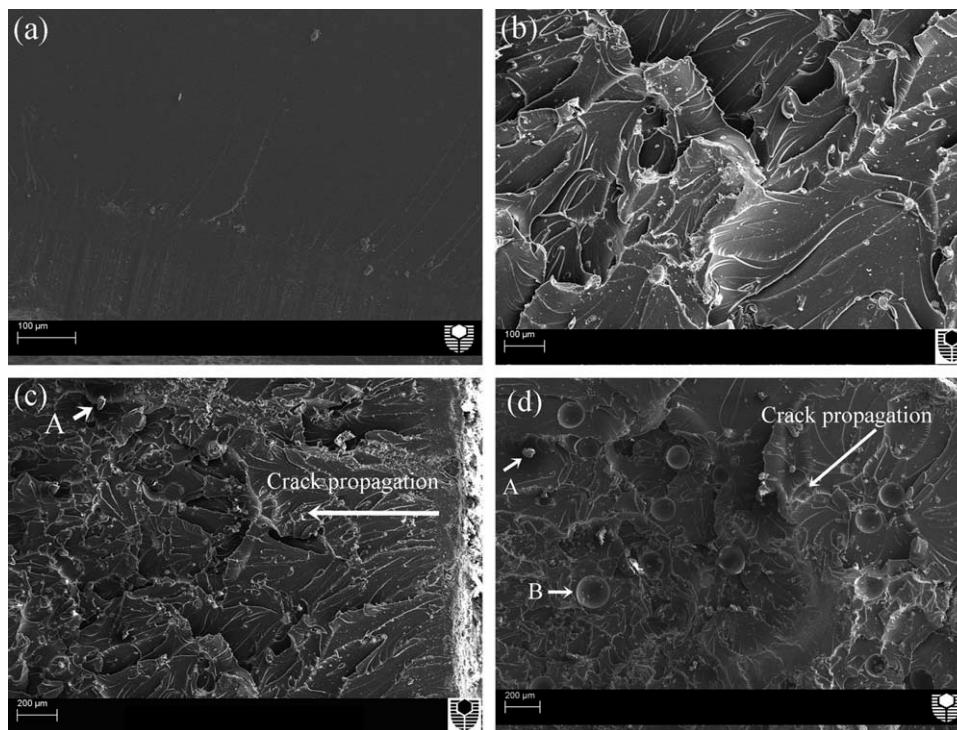
FIG. 8. Scanning electron micrographs after fracture toughness testing for: (a) PE; (b) PE/HNT1; (c) PE/HNT1 and (d) PE/HNT5. [Legend: A= HNTs clusters and B = voids].

study, Zulfli and Shyang [42] reported an improvement in flexural strength and modulus of glass fiber-reinforced epoxy/clay nanocomposites due to the addition of treated nanoclay. The presence of clay enhanced the interface between the glass fiber and epoxy matrix. The addition of RCF to epoxy system significantly increases flexural modulus by seven times as seen in Fig. 4. Adding HNTs to RCF/epoxy samples slightly enhances flexural modulus.

Figure 5 illustrates the impact strength of epoxy reinforced with RCF sheets and HNTs. The presence of RCF sheets significantly increases the impact strength of unfilled epoxy by $\sim$444% from 5.6 to 30.7 kJ/m^2. This enormous achievement is due to the fact that cellulose fiber has a better ability to absorb impact energy than unreinforced polymer. This result is in accordance with the work of Maleque and Belal [11], where they investigated the mechanical properties of pseudo-stem banana fiber-epoxy composites and found that the presence of banana woven fabric increased the impact strength over the neat epoxy by $\sim$40%. However, the incorporation of HNTs into RCF/epoxy composites slightly reduces the impact strength compared to unfilled RCF/epoxy composites Fig. 5. Samples reinforced with 5 wt% HNTs display better impact strength than those reinforced with 1 and 3 wt% HNTs. Impact strength of RCF/epoxy nanocomposites filled with 1, 3, and 5 wt% HNTs is 27.8, 24.5, and 28.3 kJ/m^2, respectively.

The effect of RCF sheets on fracture properties of unfilled epoxy composites and HNTs filled epoxy nanocomposites is plotted in Fig. 6. As can be seen from Fig. 6, the addition of RCF sheets remarkably increases the fracture toughness for all samples when compared with the same samples without RCF. For example, the addition of RCF in epoxy resin increases the fracture toughness by about 350% compared to neat epoxy. This incredible improvement is due to the unique properties of cellulose fiber in resisting fracture, which resulted in increased energy dissipation from crack-deflection at the fiber–matrix interface, fiber-debonding, fiber-bridging, fiber pull-out, and fiber-fracture [10]. This result is supported by the work of Lui and Huges [7]. They investigated the toughness and fracture behavior of epoxy matrix composites reinforced with woven flax fiber textiles. It was found that the fracture toughness of the composites was increased by two to four times due to the presence of woven flax fiber when compared with pure epoxy samples. In the case of RCF/epoxy nanocmposites, the addition of HNTs to the RCF/epoxy composites shows no significant differences in fracture toughness with a maximum increase (7.6%) at 1 wt% HNTs load. This reveals that fracture toughness in RCF/epoxy nanocmposites is mostly dominated by RCFs with slight effect of HNTs. Khan et al. [43] investigated the fracture properties of carbon fiber/clay-reinforced epoxy nanocomposites. Results showed that the incorporation of (1, 3, and 5) wt% nanoclay gradually increased the fracture toughness by (8, 19, and 23%), respectively. Authors concluded that several toughness mechanism such as formation of voids, crack front deflection, crack pining, and microcracking was responsible for toughness enhancement [43].
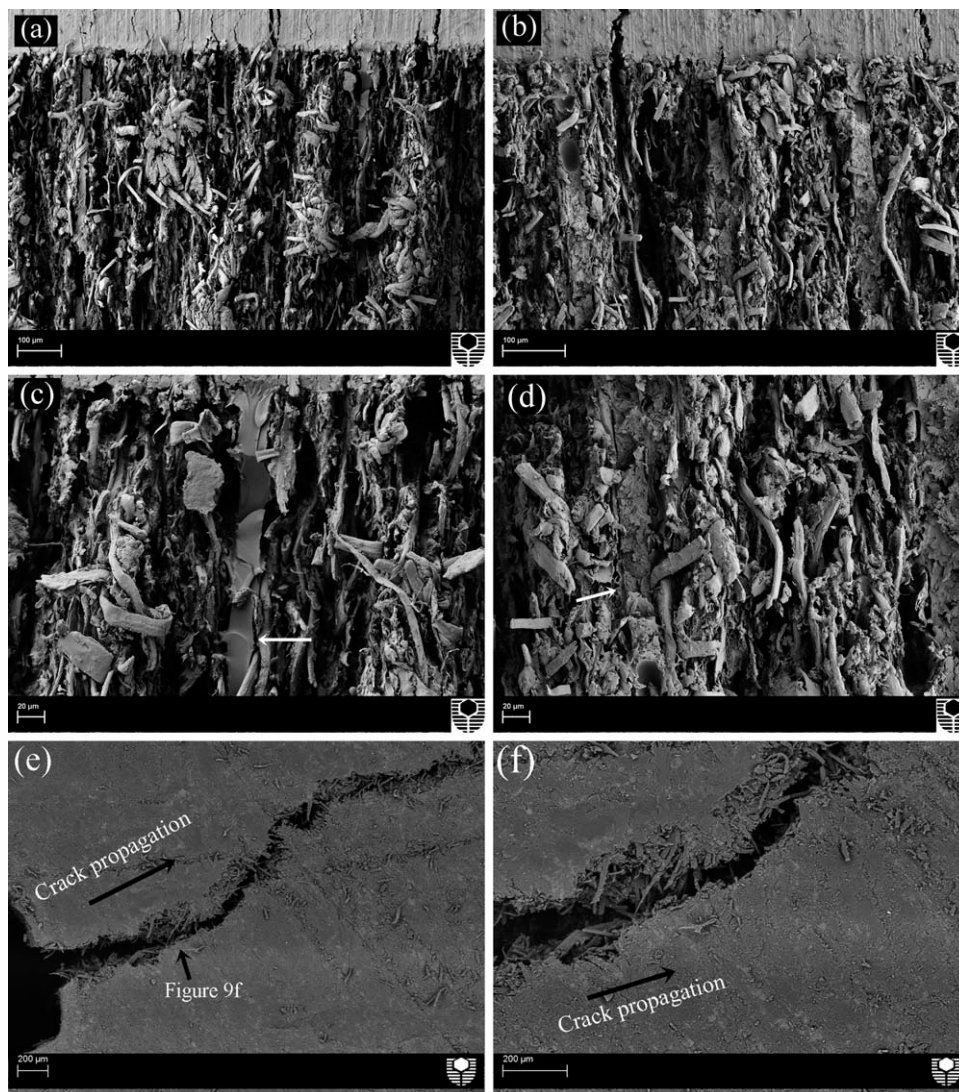
FIG. 9. Scanning electron micrographs after fracture toughness testing for (a) PE/RCF; (b) PE/RCF/HNT5; (c) PE/RCF (high magnification) and (d) PE/RCF/HNT5 (high magnification), (e) crack propagation and (f) crack propagation (high magnification). White arrow indicates the location of epoxy matrix.

The impact toughness in terms of the energy release rate of HNTs/epoxy nanocomposites reinforced with RCF sheets is plotted in Fig. 7 as a function of HNTs content. As expected, the influence of RCF sheets on the impact toughness of HNT/epoxy and unfilled epoxy matrices is remarkable. The impact toughness of pure epoxy increases from 0.8 to 2.9 KJ/m^2 due to the addition of RCF sheets. This result indicates that recycled cellulose fibers improve the impact toughness of the epoxy resin by ∼262.5%. This extraordinary enhancement in toughness properties as discussed before is due to the fact that RCF displays a variety of fracture mechanisms in the crack path to resist crack propagation. These fracture mechanisms include fiber breakage, fiber pull-out, fiber-debonding, and fiber-bridging, which require high energy to be absorbed. The incorporation of HNTs in different concentration to the RCF/epoxy composites gradually enhances the impact toughness by 10.3, 24.1, and 27.6% at HNTs content 1, 3, and 5 wt%, respectively. The extra improve-ment in impact toughness for RCF-based nanocomposites is due to the participating of HNTs in resisting the crack growth.

Fracture Surface and Toughness Mechanisms

Figure 8 shows the facture surfaces of pure epoxy and epoxy nanocomposites containing 1 and 5 wt% of HNTs. It can be seen from Fig. 8a that the fracture surface of pure epoxy is very smooth and featureless, which indi-cates typical brittle fracture behavior with lack of signifi-cant toughness mechanisms [24]. However, epoxy/HNT nanocomposites display a rougher fracture surface than that of neat resin as a result of the presence of nanopar-ticles Fig. 8c and d. An increase in fracture surface roughness can be used as indicator to the presence of crack deflection mechanisms, which increase fracture toughness by increasing crack propagation length during deformation [24, 37]. Figure 8b shows high-magnification

122
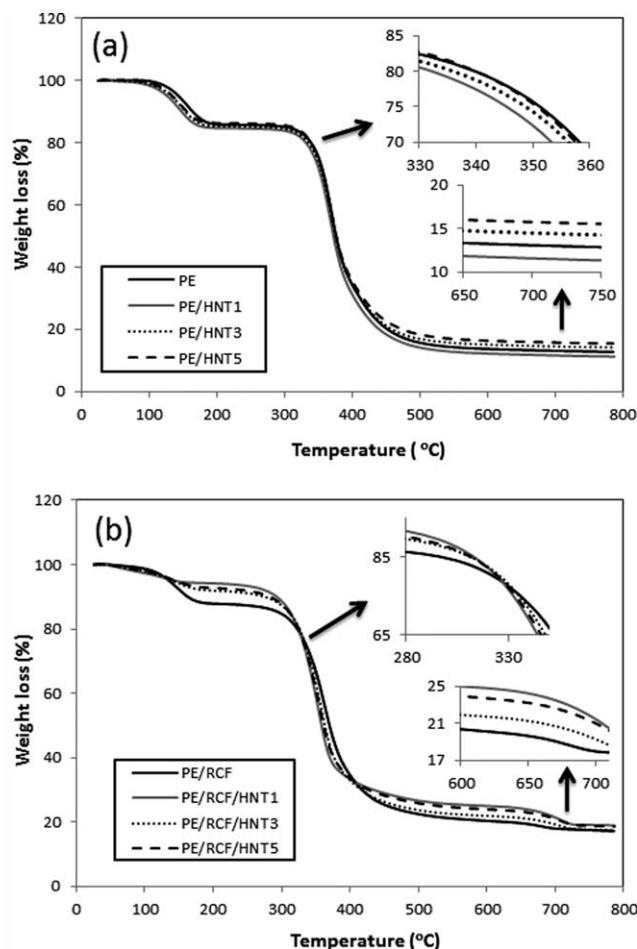
FIG. 10.   TGA curves of epoxy and epoxy/HNTs nanocomposites, (a) without RCF, (b) with RCF.

SEM micrograph of fracture surface for epoxy reinforced with 1% HNTs. A range of possible toughness mechanisms such as crack pinning, crack deflection, particle debonding, plastic void growth, plastic deformation, and particle pull-out can be observed. Such toughness mechanisms can lead to higher fracture toughness properties through resisting crack propagation [24, 36–39]. When compared between samples filled with 1 and 5 wt% HNT Fig. 8c and d, it can be seen that sample with high-HNTs loading has large particle agglomerations than those filled with lower HNTs loading as confirmed in TEM images Fig. 2a–c. These particles clusters act as a stress concentrator leading to low-facture toughness. Moreover, an increase in particles pull-out and voids formation is observed for samples with higher HNT loading. This can be attributed to the lack in HNTs-matrix interfacial adhesion. This observation confirms the result of fracture toughness test, which indicates that epoxy reinforced with 1 wt% HNT has the highest fracture toughness value compared to samples filled with either 3 or 5 wt% HNT.

Figure 9 illustrates the SEM micrograph of the fracture surface for RCF/epoxy composite and RCF/epoxy nanocomposites reinforced with 5 wt% HNTs after fracture toughness test. Figure 9a and b shows the low-magnifica-

tion images of RCF/epoxy sample and RCF/epoxy filled with 5 wt% HNT, while Fig. 9c and d shows the high-magnification images of same samples. A variety of toughness mechanisms such as shear deformation, crack bridging, fiber pull-out, and fiber fracture and matrix fracture can be clearly observed, which lead to good fracture properties of samples reinforced by RCF sheets. These SEM images confirm the enhancement in mechanical properties due the presence of RCF sheets. Moreover, a very close look at Fig. 9c and d (white arrows), it can be seen that HNT/epoxy matrix displays rougher fracture surface than unmodified epoxy matrix, which indicates the positive participation of HNT/epoxy matrix in the energy absorption during fracture test. This observation confirms the slight enhancement in fracture toughness for RCF/epoxy samples filled with HNTs compared to unfilled RCF/epoxy samples.

Figure 9e and f displays low- and high-magnification back-scattered SEM images of crack propagation in RCF/epoxy sample. It was observed that samples filled with RCF sheets did not completely break in two pieces. This is due to the fact that fibers bridge the cracks and enhance the crack propagation resistance, which led to the improvement in fracture toughness. The tortuous pathway for the crack propagations indicates the high-energy absorbance by the RCF sheets. It can also be observed that the adhesion between the fiber and the matrix is quite good. These super toughness mechanisms of RCF are the major factors of increasing mechanical properties of samples reinforced with RCF when compared with samples without RCF.

Thermal Stability and Properties

The thermal stability of the samples was determined using thermogravimetric analysis (TGA). In this test, the thermal stability was studied in terms of the weight loss as a function of temperature under nitrogen atmosphere. The thermograms (TGA) of the epoxy/HNT and epoxy/HNT/RCF nanocomposites are shown in Fig. 10a and b, respectively. The temperature at different weight loss (%), the maximum decomposition temperature (T_{max}), and the char yield at 700°C are all summarized in Table 2. In general, it can be seen from TGA curves that epoxy and its nanocomposites expose two similar distinct stages of decomposition. The first decomposition, which is in the region of 80–180°C, may be related to the vaporization of water in the composites. The second decomposition may be related to epoxy degradation and its additives. It can also be seen that the major degradation for all samples occurs in the range of ∼300–400°C.

In essence, it can be seen from Table 2 that the temperature at 10% weight loss ($T_{10\%}$) of neat epoxy decreases as a result of the presence of HNTs. The ($T_{10\%}$) of neat epoxy and epoxy filled with 1, 3, and 5 wt% HNTs are 165.0, 148.7, 154.7, and 156.5°C, respectively. However, as HNTs content increases, ($T_{10\%}$) increases,

TABLE 2. Thermal properties of epoxy, epoxy/RCF eco-composites, epoxy/HNT, and epoxy/RCF/HNT hybrid nanocomposites.

Sample	$T_{10\%}$ (°C)	$T_{20\%}$ (°C)	$T_{50\%}$ (°C)	$T_{80\%}$ (°C)	T_{max} (°C)	Char yield at 700°C (wt%)
PE	165.0	339.4	376.9	452.6	367.3	13.1
PE/HNT1	148.7	331.8	372.8	440.4	367.1	11.6
PE/HNT3	154.7	335.9	375.7	459.3	367.6	14.5
PE/HNT5	156.5	339.6	376.9	474.3	367.3	15.8
PE/RCF	162.9	322.8	370.3	629.3	359.6	18.0
PE/RCF/HNT1	292.9	324.2	358.5	714.9	351.5	21.6
PE/RCF/HNT3	275.0	326.1	363.4	686.8	351.2	19.3
PE/RCF/HNT5	282.8	324.8	361.7	712.8	351.2	21.0

which reveals that the addition of more halloysite decreases the moisture access to the sample. Then, epoxy and its nanocomposites remained stable without significant degradation from 200 to around 300°C just before the major degradation get started as seen in Fig. 10a. In this study, the temperature at 20% weight loss ($T_{20\%}$) is considered as the onset temperature of the major degradation. The presence of 1 and 3 wt% HNTs decreases the ($T_{20\%}$) for epoxy from 339.4 to 331.8 and 335.9°C, respectively, while the addition of 5 wt% HNT increases ($T_{20\%}$) slightly to 339.6°C. This indicates that thermal stability enhances as HNTs content increases for nanocomposites samples. However, the maximum decomposition temperatures (T_{max}) of the composites remain after the addition of HNTs. The maximum decomposition temperatures of neat epoxy and epoxy filled with 1, 3, and 5 wt% HNTs are 367.3, 367.1, 367.6, and 367.3°C, respectively. At high temperature (when samples lose 80% of their initial weight), epoxy reinforced with 3 and 5 wt% HNTs show better thermal stability than neat epoxy. ($T_{80\%}$) of neat epoxy (PE), PE/HNT1, PE/HNT3, and PE/HNT5 are 452.6, 440.4, 459.3, and 474.3°C, respectively. As a result of this enhancement in thermal stability at high temperature, the char residue at 700°C of neat epoxy increases from 13.0 to 14.5 and 15.8% after the addition of 3 and 5 wt% HNTs, respectively. It was reported in previous studies that the addition of nanoparticles would efficiently raise the char residue of polymers at high temperatures [19, 33, 44, 45].

The presence of RCF into epoxy system accelerates the degradation at low temperature (<400°C). The temperature at 20% weight loss of pure epoxy is significantly reduced from 339.4 to 322.8°C, and the maximum decomposition temperature (T_{max}) of epoxy is reduced from 367.3 to 359.6°C as a result of the inclusion of RCF sheets. However, at temperature higher than 400°C, the presence of RCF leads to an enhancement in thermal stability by increasing the char yield at 700°C of epoxy system from 13.1 to 18.0 wt%. Shih [27] carried out the thermal stability of epoxy reinforced with bamboo husk fiber and powder. It was found that the char yield of epoxy at 700°C increased by 13.5–52.8% due the addition of 10 wt% of bamboo fiber or powder. Author cited that

the increasing in char yield could be an indication of the potency of flame retardation of polymers. Thus, the addition of bamboo fiber or powder enhanced the flame retardation of epoxy. Similar results were obtained by De Rosa et al. [6]. They found an improvement in thermal stability of untreated phormium tenax fibers/epoxy composites. The presence of plant fiber increased the maximum degradation temperature and the char yield of epoxy resin.

The addition of HNTs to RCF/epoxy composites and its influence on thermal stability can be seen in Fig. 10b and Table 2. The presence of HNTs into RCF/epoxy nanocomposites increases the temperature at (10 and 20%) weight loss compared to unfilled RCF/epoxy composites. However, at the major degradation, unfilled RCF/epoxy shows better thermal stability that those samples filled with HNTs. The maximum decomposition temperature (T_{max}) of RCF/epoxy nanocomposites is decreased by 8°C compared to unfilled RCF/epoxy composite. This is due to the catalytic effect of HNT tubes on RCF/epoxy nanocomposites. This redaction in thermal stability is also confirmed by measuring the temperature at 50% weight loss ($T_{50\%}$). The addition of HNTs into RCF/epoxy composites reduces the ($T_{50\%}$) by 7–12°C compared to unfilled RCF/epoxy sample. However, at high temperatures (>400°C), the presence of HNTs increases the thermal stability of epoxy/RCF nanocomposites by increasing the char yield. The char yields at 700°C of epoxy/RCF composites reinforced with (0, 1, 3, and 5) wt% HNT are 18.0, 21.6, 19.3, and 21.0%, respectively. This enhancement on thermal properties is due to the presence of HNT nanotubes, which act as barriers and hinder the diffusion of volatile decomposition products out from the nanocomposites [33, 45, 46].

CONCLUSIONS

Epoxy ecocomposites and nanocomposites reinforced with RCFs and HNTs have been fabricated and characterized. Based on TEM, homogeneous dispersion of HNTs with some agglomerations was achieved by mixing the HNTs with the epoxy resin. Particles agglomeration increased as HNTs content increased.

In the case of epoxy/HNTs nanocomposites, the presence of only 1 wt% HNTs increased flexural strength (20.8%), flexural modulus (72.8%), fracture toughness (56.5%), and impact toughness (25.0%) over unmodified epoxy. However, adding more HNTs showed no further increase in flexural strength and fracture toughness properties due the increased viscosity, voids, and poor dispersion with high-clay contents. Impact strength and impact toughness were found to increase as HNTs loading increased. The fracture surface features of modified epoxies were found to be rougher than neat epoxy due to the presence of HNTs. The addition of 3 and 5 wt% HNTs into epoxy did not change the maximum decomposition temperatures (T_{max}). However, epoxies modified

124

with 3 and 5 wt% HNTs showed better thermal stability than unmodified epoxy at high temperatures.

In the case of the epoxy/RCF composites, it was found that the presence of RCF significantly increased flexural strength (160%), fracture toughness (350%), impact strength (444%), and impact toughness (263%) compared to pure epoxy. This remarkable enhancement is due the unique properties of cellulose fiber in withstanding bending force and resisting fracture force. For thermal stability, the addition of RCF to epoxy matrix was found to accelerate the composites degradation and decreased the temperature of maximum degradation. But, at higher temperature higher than 400°C, the presence of RCF led to an enhancement in thermal stability by increasing the char yield.

In the case of epoxy/RCF/HNTs econanocomposites, the insertion of HNTs to RCF/epoxy ecocomposites slightly increased flexural strength and fracture toughness over unfilled RCF/epoxy samples. Impact strength decreased after the addition of HNTs to RCF/epoxy samples. The presence of HNTs gradually increased impact toughness of RCF/epoxy system by 10.3, 24.1, and 27.6% at HNTs loading 1, 3, and 5 wt%, respectively. The addition of HNTs to RCF/epoxy ecocomposites was found to increase the thermal stability by increasing the char yield of composites at high temperatures. However, the rate of degradation increased after adding HNTs to RCF/epoxy composites.

ACKNOWLEDGMENTS

REFERENCES

1. I.M. Low, M. McGrath, D. Lawrence, P. Schmidt, J. Lane, and B.A. Latella, *Compos.: Part A*, **38**, 963 (2007).

2. G. Marsh, *Mater. Today*., **6**, 36 (2003).

3. A. Sanadi, R. Young, and R. Rowell, *J. Reinforc. Plast. Compos.*, **13**, 54 (1994).

4. I. Baroulaki, B. Karakasi, G. Pappa, P. Tarantili, D. Economides, and K. Magoulas, *Compos.: Part A*, **37**, 1613 (2006).

5. H.N. Dhakal, Z.Y. Zhang, and M.O.W. Richardson, *Compos. Sci. Technol.*, **67**, 1674 (2007).

6. I.M. De Rosa, C. Santulli, and F. Sarasini, *Mater. Design*, **31**, 2397 (2010).

7. Q. Lui and M. Hughes, *Compos.: Part A*, **39**, 1644 (2008).

8. A. Athijayamani, M. Thiruchitrambalam, U. Natarajan, and B. Pazhanivel, *Mater. Sci. Eng. A*, **517**, 344 (2009).

9. S. Harish, D.P. Michael, A. Bensely, D.M. Lal, and A. Rajadurai, *Mater. Character.*, **60**, 44 (2009).

10. I.M. Low, J. Somers, H.S. Kho, I.J. Davies, and B.A. Latella, *Compos. Interf.*, **16**, 659 (2009).

11. M.A. Maleque and F.Y. Belal, *Arab J. Sci. Eng.*, **32**, 359 (2007).

12. A.A. Rashdi, S.M. Sapuan, M.M. Ahmad, and A. Khalina, *J. Food. Agric. Enviro.*, **7**, 908 (2009).

13. P. Ganan, S. Garbizu, R. Ponte, and I. Mondragon, *Polym. Compos.*, **26**, 121 (2005).

14. A. Usuki, Y. Kojima, M. Kawasumi, A. Okada, Y. Fukushima, T. Kurauchi, and O. Kamigaito, *J. Mater. Res.*, **8**, 1179 (1993).

15. Y. Kojima, A. Usuki, M. Kawasami, A. Okada, Y. Fukushima, T. Karauchi, and O. Kamigaito, *J. Mater. Res.*, **8**, 1185 (1993).

16. B. Alexandre, D. Langevin, P. Médéric, T. Aubry, H. Couderc, Q.T. Nguyen, A. Saiter, and S. Marais, *J. Membr. Sci.*, **328**, 186 (2009).

17. E.M. Araujo, K.D. Araujo, R.A. Paz, T.R. Gouveia, R. Barbosa, and E.N. Ito, *J. Nanomater.*, 2009. Article ID 136856, 5 pages (2009).

18. S.R. Ha, K.Y. Rhee, S.J. Park, and J.H. Lee, *Compos., Part B: Eng.*, **41**, 602 (2010).

19. S.S. Hwang, S.P. Liu, P. P. Hsu, J. M. Yeh, K. C. Chang, and Y. Z. Lai, *Int. Commun. Heat. Mass. Transfer*, **37**, 1036 (2010).

20. B. Qi, Q.X. Zhang, M. Bannister, and Y.W. Mai, *Compos. Struct.*, **75**, 514 (2006).

21. C. Kaynak, G.I. Nakas, and N.A. Lsitman, *Appl. Clay Sci.*, **46**, 319 (2009).

22. S. Zainuddin, M.V. Hosura, Y. Zhoua, A.T. Narteha, A. Kumarb, and S. Jeelani, *Mater. Sci. Eng.*, **527**, 7920 (2010).

23. S. Deng, J. Zhang, and L. Ye, *Compos. Sci. Technol.*, **69**, 2497 (2009).

24. Y. Tang, S. Deng, L. Ye, C. Yang, Q. Yuan, J. Zhang, and C. Zhao, *Composites: Part A*, **42**, 345 (2011).

25. K. Prashantha, M.F. Lacrampe, and P. Krawczak, *Express Polym. Lett.*, **5**, 295 (2011).

26. Y. Ye, H. Chen, J. Wu, and L. Ye, *Polymer*, **48**, 6426 (2007).

27. Y.F. Shih, *Mater. Sci. Eng. A*, **445**, 289 (2007).

28. S. Deng, J. Zhang, L. Ye, and J. Wu, *Polymer*, **49**, 5119 (2008).

29. Technical Information of Imerys Tableware Asia Limited. Available from: http://www.nzcc.co.nz/technical1.htm (2011).

30. P. Pasbakhsh, H. Ismail, M.N.A. Fauzi, and A.A. Bakar, *Appl. Clay. Sci.*, **48**, 405 (2010).

31. E. Joussein, S. Petit, J. Churchman, B. Theng, D. Righi, and B. Delvaux, *Clay Miner.*, **40**, 383 (2005).

32. M. Lui, B. Guo, M. Du, X. Cai, and D. Jia, *Nanotechnology*, **18**, 455703 (2007).

33. H. Ismail, P. Pasbakhsh, M.N.A. Fauzi, and A.A. Bakar, *Polym. Test.*, **27**, 841 (2008).

34. Y. Xu and S.V. Hoa, *Compos. Sci. Technol.*, **68**, 854 (2008).

35. A. Yasmin, J.L. Abot, and I.M. Daniel, *Scripta Mater*, **49**, 81 (2003).

36. J. Ma, M.S. Mo, X.S. Du, and P. Rosso, *Polymer*, **49**, 3510 (2008).

37. S. Zhao, L.S. Schadler, H. Hillborg, and T. Auletta, *Compos. Sci. Technol.*, **68**, 2976 (2008).

38. B. Wetzel, P. Rosso, F. Haupert, and K. Friedrich, *Eng. Fract. Mech.*, **73**, 2375 (2006).

39. C. Chen, R.S. Justice, D.W. Schaefer, and J.W. Baur, *Polymer*, **49**, 3805 (2008).

40. A. Satapathy, A.k. Jha, S. Mantry, S.D. Singh, and A. Patnaik, *J. Reinf. Plast. Compos.*, **29**, 2869 (2010).

41. Y. Ye, H. Chen, J. Wu, and C.M. Chan, *Composites: Part B* **42**, 2145 (2011).

42. N.H.M. Zulfli and C.W. Shyang, *J. Phys. Sci.*, **21**, 41 (2010).

43. S.U. Khan, K. Iqbal, A. Munir, and J.-K. Kim, *Compos.: Part A*, **42**, 253 (2011).

44. A. Chatterjee and M.A. Islam, *Mater. Sci. Eng. A*, **487**, 574 (2008).

45. L. Madaleno, J. Schjødt-Thomsen, and J.C. Pinto, *Compos. Sci. Technol.*, **70**, 804 (2010).

46. C. Zhao, H. Qin, F. Gong, M. Feng, S. Zhang, and M. Yang, *Polym. Degrad. Stab.*, **87**, 183 (2005).

126

Alamri, H., and I. M. Low. 2012. Characterization of epoxy hybrid composites filled with cellulose fibres and nano-SiC. *Journal of Applied Polymer Science* 126: 221-231.

Characterization of Epoxy Hybrid Composites Filled with Cellulose Fibers and Nano-SiC

H. Alamri, I. M. Low

Department of Imaging and Applied Physics, Curtin University of Technology, GPO Box U1987, Perth, WA 6845, Australia

ABSTRACT: Three different approaches have been applied and investigated to enhance the thermal and mechanical properties of epoxy resin. Epoxy system reinforced with either recycled cellulose fibers (RCF) or nanosilicon carbide (n-SiC) particles as well as with both RCF and n-SiC has been fabricated and investigated. The effect of RCF/n-SiC dispersion on the mechanical and thermal properties of these composites has been characterized. The fracture surface morphology and toughness mechanisms were investigated by scanning electron microscopy. The dispersion of n-SiC particles into epoxy nanocomposites was studied by synchrotron radiation diffraction and transmission electron microscopy. Results indicated that mechanical properties increased as a result of the addition of n-SiC. The presence of RCF layers significantly increased the mechanical properties of RCF/epoxy composites when compared with neat epoxy and its nanocomposites. The influence of the addition of n-SiC to RCF/epoxy composites in mechanical properties was found to be positive in toughness properties. At high temperatures, thermal stability of neat epoxy increased due to the presence of either n-SiC particles or RCF layers. However, the presence of RCF accelerated the thermal degradation of neat epoxy as well as the addition of n-SiC to RCF/epoxy samples increased the rate of the major thermal degradation. © 2012 Wiley Periodicals, Inc. J Appl Polym Sci 126: E221–E231, 2012

Key words: recycled cellulose fibers; silicon carbide nanoparticles; nanocomposites; mechanical properties; thermal properties

INTRODUCTION

Epoxy is considered to be one of the important matrices used for fiber-reinforced polymer due to its unique properties of relatively high strength, high modulus, low shrinkage, and excellent chemical and heat resistance.[1,2] It has been widely used in manufacturing applications, such as adhesives, coatings, electronics, and aerospace structures. However, majority of cured epoxy systems show low impact strength, poor resistance to crack propagation and initiation, and low fracture toughness.[1,2] The high cost and brittleness of epoxy resins are the main draw backs to its industrial use.[3] Two different approaches have recently been reported in the literature to substantially enhance the properties and reduce the cost of the composite compared to that for the neat epoxy resin.

The first approach dealt with the use of natural cellulose fibers such as flax, hemp, sisal, kenaf, and jute, as reinforcements in the polymeric matrices for making low cost engineering materials. Cellulose fiber reinforced polymers have gained a great attention in engineering applications due to their tremen-

dous properties, which include low density, low cost, renewability and recyclability as well as excellent mechanical characteristics such as flexibility, high toughness, specific strength, and high specific modulus.[4-6] Moreover, there is much pressure on manufacturing industries especially packaging, construction and automotive industries to utilize new materials in substituting the nonrenewable reinforcing materials for instance glass fiber emerging from consumers and new environmental legislation due to increased sensitivity on environmental pollution.[4] Natural fibers have been preferred as they are considered to be environmental friendly (green composites), thus being utilized as a substitute to traditional fiber reinforced petroleum-based composites including aramid fibers, carbon, and glass fibers.[5,6] However, plant fiber reinforced polymeric composites have several drawbacks which include fiber high moisture absorption, incompatibility with some of the polymeric matrices, and poor wettability.[4,7] There is significant amount of work can be found in the literature on the effects of additional cellulose fibers on mechanical, physical, and thermal properties of the polymer systems.[3,7-13]

The second approach dealt with the use of nanosized inorganic particles as modifiers for brittle polymers. In recent years, polymer-clay nanocomposites (PCNs) have drawn much attention due to their excellent characteristics such as improvement in physical (shrinkage,

optical, dielectrics, and permeability), thermal (i.e. thermal expansion coefficient, flammability, decomposition, and thermal stability), and mechanical (i.e. toughness, strength, and modulus) properties.[14–16] Many researchers have studied nanoclay addition effect on thermal, mechanical, and physical properties of polymeric composites since the demonstration of vast improvements in mechanical and physical properties by the pioneering work of researchers on nylon-6/clay nanocomposites at Toyota.[17–25]

Silicon carbide particles are very attractive ceramic material that can be used as filler in different polymer matrices due to the unique properties including high thermal conductivity, low thermal expansion coupled with high strength, high hardness, and high elastic modulus.[26] Silicon carbide (SiC) is rigid crystalline material that compound of silicon and carbon that has been used in grinding abrasive products including wheels for over a period of 100 years.[26] Currently, the material has been developed to a point that it has very good mechanical properties as a high-quality grade ceramic used in numerous high-performance applications.[26] Therefore, ceramic-filled polymer composites have been the subject of extensive research in the last two decades.[27–32] Blackman et al.[27] and Johnsen et al.[28] both reported a significant improvement in fracture toughness for epoxy nanocomposites due to the addition of nanosilica. Zhao et al.[29] on the other hand used nanoalumina particles to toughen epoxy resin. However, no improvement was reported in fracture toughness due to the addition of nanoalumina. Chen et al.[30] reported an increment by 30% in fracture toughness of silica-epoxy nanocomposites compared to neat epoxy. Chatterjee et al.[31] carried out the mechanical and thermal properties of TiO_2/epoxy nanocomposites prepared by ultrasonic mixing process. Authors reported an enhancement in thermal stability, glass transition temperature, tensile and flexural modulus due to the presence of nanosilica particles. However, no improvement was reported in tensile and flexural strength. Ma et al.[32] investigated the effect of silica nanoparticles on the mechanical properties of two types of epoxy systems. It was found that the presence of nanosilica increased Young's modulus, tensile strength, fracture toughness, and impact toughness for both epoxy systems. An increase in nanosilica subsequently resulted to increased mechanical properties.

In this article, the focus is on generating different modes of toughening and strengthening by describing an alternative approach in designing eco-nanocomposites in which elements are tailored with fine dispersions of recycled cellulose fibers (RCF) and nanosilicon carbide (n-SiC). The main idea is to produce an outer epoxy layer dispersed with nanosized SiC for wear resistance and hardness, and with under layers RCF/SiC reinforced epoxy for damage tolerance and toughness. The effect of RCF/n-SiC disper-

TABLE I
Physical Properties of n-SiC Powder

Properties	Values
Color	Light grey
Particle size	<100 nm
Surface area	70–90 m^2/g
Bulk density	0.069 g/cm^3
Density	3.22 g/cm^3 at 25°C

sion on the microstructure, mechanical, and thermal properties have been characterized and discussed in terms of synchrotron radiation diffraction (SRD), transmission electron microscopy (TEM), scanning electron microscopy (SEM), flexural strength and modulus, fracture toughness, impact strength, impact toughness, and thermogravimetric analysis (TGA).

MATERIALS AND FABRICATION

Materials

RCF paper and nanosilicon carbide (n-SiC) particles were used as reinforcements for the fabrication of epoxy-matrix composites. The RCF paper with grade 200 GSM and 200 μm thickness was supplied by Fuji Xerox Australia, Belmont WA, Australia. n-SiC particles were provided by Sigma-Aldrich LLC, USA. The physical properties of n-SiC particles are outlined in Table I.[33] Finally, general purpose low viscosity epoxy resin (FR-251) and epoxy hardener were supplied by Fiberglass and Aesin Sales, WA, Perth, Australia.

Sample fabrication

Nanocomposites

The n-SiC/epoxy nanocomposites were prepared by mixing the epoxy resin with three different weight percentages (1, 3, and 5%) of n-SiC particles using high speed mechanical mixer for 10 min with a rotation speed of 1200 rpm. After that, a hardener was added to the mixture and then stirred slowly to minimise the formation of air bubbles within the sample. The final mixture was poured into silicon moulds and left for 24 h at room temperature for curing purpose. Pure epoxy (PE) sample was made as a control.

RCF reinforced nanocomposites

In this section, the epoxy system and the nanocomposites dispersed with n-SiC particles were used as the matrix material. RCF sheets were first dried for 60 min at 70°C. After that, RCFs sheets were fully-soaked into a mixture of epoxy/n-SiC until they became entirely wetted by the mixture, before they were laid down in a closed silicone mould under 8.2 kPa compressive pressure and left 24 h for curing at room temperature. The same processing procedure

TABLE II
**Compositions of Synthesized n-SiC/Epoxy and
RCF-Epoxy/n-SiC Nanocomposites**

n-SiC/epoxy samples	n-SiC (wt %)	RCF/SiC/epoxy samples	n-SiC (wt %)
Pure epoxy (PE)	0	PE/RCF	0
PE/SiC1	1	PE/RCF/ SiC1	1
PE/SiC3	3	PE/RCF/ SiC3	3
PE/SiC5	5	PE/RCF/ SiC5	5

was used to prepare RCF/epoxy ecocomposites without the addition of n-SiC. The amount of RCF in the final products was about 48 wt %. All the samples made are summarized in Table II.

Synchrotron radiation diffraction

SRD measurement was carried out on the powder diffraction beamline at the Australian Synchrotron. The diffraction patterns of each sample were collected using a beam of wavelength 1.377 Á in the two-theta range of 2–82°.

Transmission electron microscopy

Ultra-thin sections ($\sim$ 80 nm) of samples were prepared using an ultramicrotome (Leica microsystem) and were recovered on a copper grid. Transmission electron microscopy imaging was done using a Titan Cryotwin (FEI Company) operating at 300 kV equipped with a 4 k $\times$ 4 k CCD camera (Gatan). TEM was carried out at King Abdullah University of Science and Technology (KAUST), Saudi Arabia.

Scanning electron microscopy

Scanning electron microscope (Zeiss Evo 40XVP) was used to investigate the microstructures and the fracture surfaces of composites. Samples were coated with a thin layer of gold to prevent charging before the observation by SEM.

Thermogravimetric analysis

The thermal stability of samples was studied by TGA and differential thermogravimetry (DTG). A

Mettler Toledo TGA/DSC star system analyzer was used for all these measurements. Samples with $\sim$ 10 mg were placed in a platinum can and tests were carried out in nitrogen atmosphere with a heating rate of 10°C/min from 35 to 800°C.

Measurements of mechanical properties

Three-point bend tests

Rectangular bars with dimensions $60 \times 10 \times 6$ mm^3 were cut for three-point bend tests to measure flexural strength, flexural modulus, and fracture toughness. The three-point bend tests were performed using a LLOYD material testing machines—Twin Column Bench Mounted (5–50 kN). The support span used was 40 mm with a displacement rate of 1.0 mm/min. Five specimens of each composition were tested to evaluate the mechanical tests. The flexural strength was evaluated using the following equation:

$$\sigma_F = \frac{3}{2}\frac{p_m S}{WD^2} \tag{1}$$

where P_m is the maximum load at crack extension, S is the span of the sample, D is the specimen thickness, and W is the specimen width. Values of the flexural modulus were computed using the initial slope of the load–displacement curve, $\Delta P/\Delta X$, using the following formula:

$$E_F = \frac{S^3}{4WD^3}\left(\frac{\Delta P}{\Delta X}\right) \tag{2}$$

In order to determine the fracture toughness, a sharp razor blade was used to initiate a sharp crack in the samples. The ratio of crack length to width (a/w) was about (0.4). The fracture toughness was calculated using the following eq. (5):

$$K_{IC} = \frac{p_m S}{WD^{2/3}}\, f\left(\frac{a}{w}\right) \tag{3}$$

where a is the crack length and $f(a/w)$ is the polynomial geometrical correction factor given as:

$$f\left(\frac{a}{W}\right) = \frac{3(a/W)^{1/2}[1.99 - (a/W)(1 - a/W) \times (2.15 - 3.93a/W + 2.7a^2/W^2)]}{2(1 + 2a/W)(1 - a/W)^{2/3}} \tag{4}$$

Charpy impact test

Similar rectangular bars were cut for Zwick Charpy impact testing to evaluate the impact strength and impact toughness. A pendulum hammer with 1.0 J was used during the test to break the samples. Un-

notched samples were used to compute the impact strength using the following formula:

$$\sigma_I = \frac{E}{A} \tag{5}$$

130
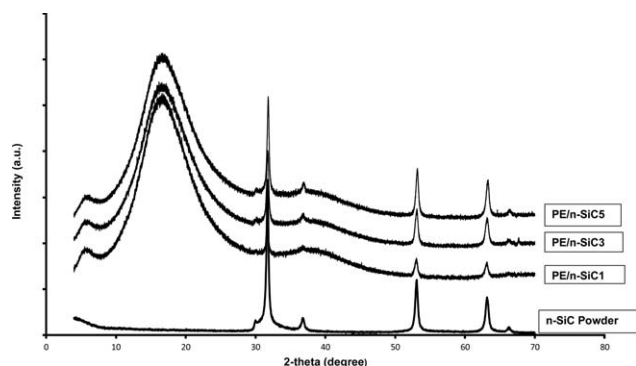
Figure 1 Synchrotron radiation diffraction patterns of n-SiC powder and epoxy/n-SiC nanocomposites.

where E is the impact energy to break a sample with a ligament of area A.

Samples of various notch lengths were used to determine the impact toughness of composites. In order to measure the impact toughness, the value of the critical strain energy release rate (G_{IC}) was evaluated as the slope of the fracture energy (U) versus the energy calibration factor (φ) as shown in the following equation:[5]

$$U = G_{IC}\, WD\phi + U_o \qquad (6)$$

where U_o is the kinetic energy, W is the specimen width, and D is the specimen thickness.

RESULTS AND DISCUSSION

Nanocomposites characterization

Synchrotron radiation diffraction

The SRD diffractograms for epoxy/n-SiC nanocomposites and n-SiC powder are shown in Figure 1. The n-SiC patterns show crystalline pattern structure with five sharp peaks in the range of $2\theta = 30$–$70°$. It also can be seen from Figure 1 that epoxy shows an amorphous structure without distinct repeating unit. The addition of n-SiC particles to epoxy matrix clearly increased the crystallinity of the epoxy/n-SiC composites due to the presence of sharp narrow diffraction peaks. It also can be seen that the highest of the diffraction peaks of n-SiC increased as nanofiller content increased in the epoxy/n-SiC composites.

Transmission electron microscopy

TEM images of the epoxy nanocomposite with different contents of n-SiC particles are shown in Figure 2. The lower magnification images in Figure 2(a–c) give a general observation of n-SiC particles dispersion into the epoxy matrix. It can be seen that the n-SiC particles are homogeneously dispersed inside the epoxy matrix except for some particle

agglomerations can be clearly seen at higher n-SiC loading. These agglomerations increase as n-SiC particle content increases. As it was observed during sample fabrication, the matrix viscosity significantly increased as nanoparticles concentration increased, which made particles dispersion rather poor and easily to aggregate in micro-size. At higher magnification images Figure 2(d–f), it can be seen that n-SiC particles have spherical shape with crystalline structure.

Mechanical properties

Flexural strength and modulus

Figures 3 and 4 illustrate the effect of n-SiC particles on the flexural strength and modulus of epoxy nanocomposites. Both flexural strength and modulus increase due the presence of n-SiC particles. In particular, flexural strength of epoxy increases by a maximum 21.5% with the addition of only 1% wt n-SiC. The enhancement in flexural strength may be ascribed to the good dispersion of n-SiC particles into the matrix, which increases matrix/n-SiC interaction surface providing good stress transferring from the matrix to the nanofillers resulting in an improve in sample strength properties. However, with further n-SiC loading (3 and 5%), flexural strength tends to decrease to values less than PE. The reason could be seen in Figure 2(a–c), at high concentration of n-SiC, n-SiC particles poorly dispersed inside the matrix forming particles agglomerations, which could weaken the adhesion strength between the matrix and the filler.[23,34] Besides, these agglomerations may act as stress concentrators, which in turn cause reduction in flexural strength.[23,25,34] Zainuddin et al.[25] investigated the flexural properties of epoxy/clay nanocomposites. Nanocomposites were fabricated with 1–3 wt % loading of montmorillonite layered silicate via magnetic stirring mixing for 5 h. Result showed that flexural strength was increased by a maximum up to 8.7% for samples reinforced with only 2 wt % of nanoclay compared to neat epoxy. Authors stated that poor dispersion of nanoclay led to poor mechanical properties.[25] Flexural modulus of epoxy nanocomposites are demonstrated in Figure 4. It can be seen that flexural modulus have similar trend to flexural strength values. The addition of (1, 3, and 5) wt % n-SiC significantly increase the modulus of epoxy system by 83, 59.2, and 58.9%, respectively. This expected result is due the fact that n-SiC particles have higher modulus than epoxy resin. Therefore, the presence of these rigid particles into the epoxy matrix increases the modulus of epoxy nanocomposites when compared with neat resin.[32]

The flexural strength of RCF reinforced n-SiC/epoxy nanocomposites are shown in Figure 3. It can be
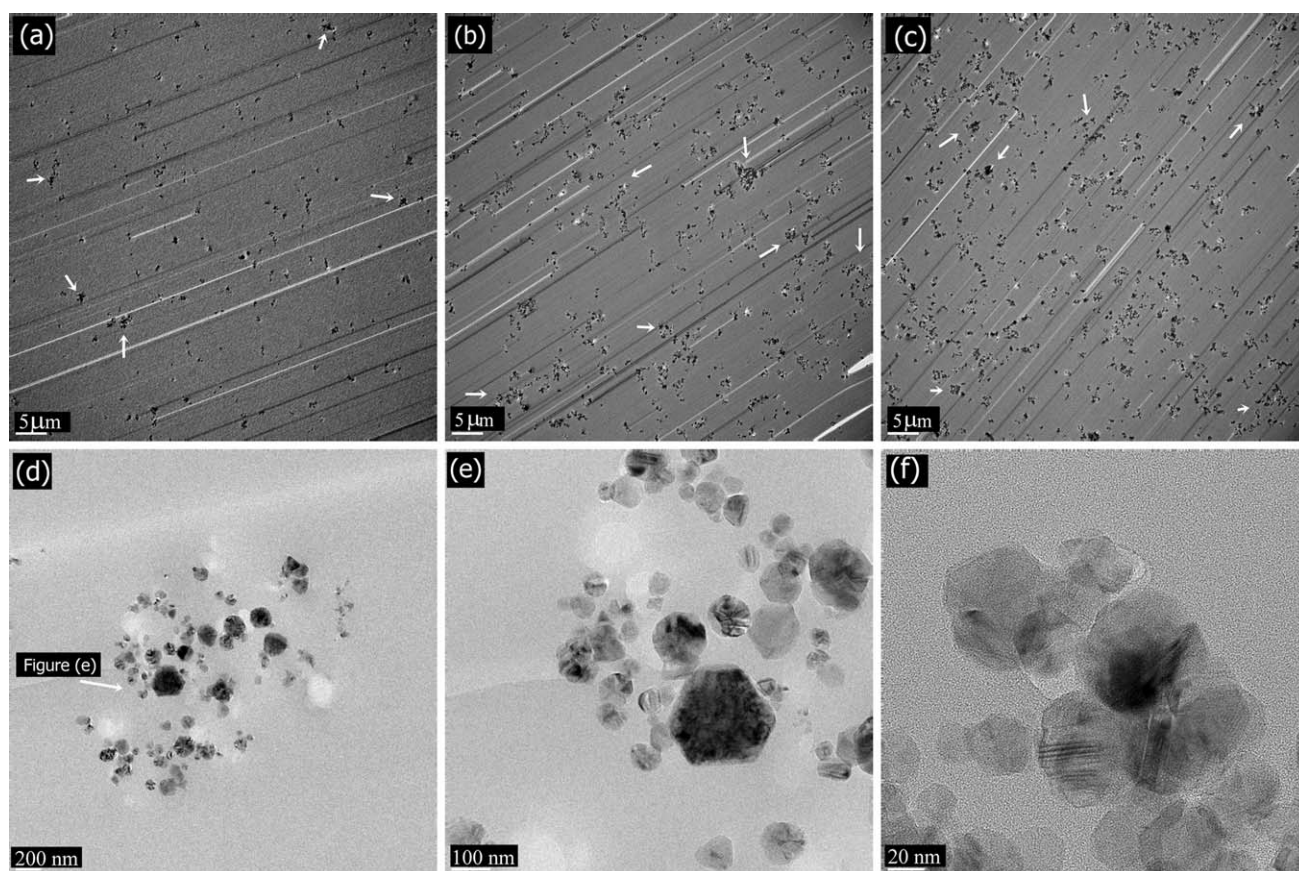
Figure 2 TEM micrographs of epoxy nanocomposites reinforced with different n-SiC concentration: (a) 1 wt %, (b) 3 wt %, (c) 5 wt %, and (d–f) are high magnification TEM images of n-SiC particles inside epoxy matrix. (The white arrows indicate n-SiC clusters).

seen that the presence of the RCF layers significantly improve the flexural strength for all kinds of samples. The flexural strength of the neat epoxy resin increase from 58.5 to 152.3 MPa after the addition of RCF layers with enhancement reaches up to 160%. This enhancement in flexural properties is due to the advantages of recycled cellulose fibers in resisting bending force of the composites.[26] In the case of RCF reinforced n-SiC/epoxy nanocomposites, the

insertion of 1 wt % n-SiC slightly increases the flexural strength of RCF/epoxy composites. However, adding more SiC (3 and 5 wt %) lead to an insignificant reduction in strength. These results are in agreement with those obtained by Satapathy et al.[26] in their study on the influence of SiC particles derived from rice husk on flexural strength of jute/epoxy composites. Flexural strength was found insignificantly decreased after adding 10 and 20 wt % of SiC particles.[26] The presence of RCF into epoxy
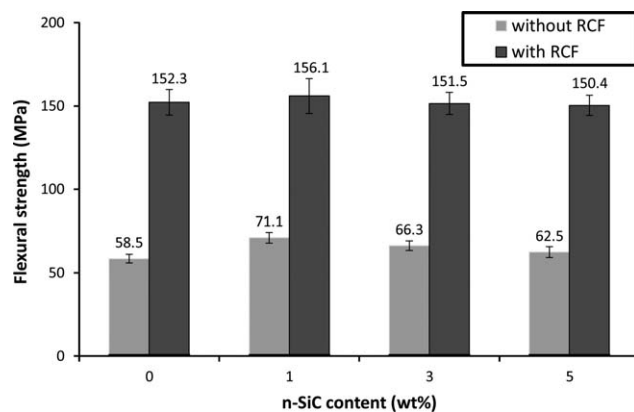
Figure 3 Flexural strength as a function of n-SiC content in unfilled composites and RCF-filled composites.
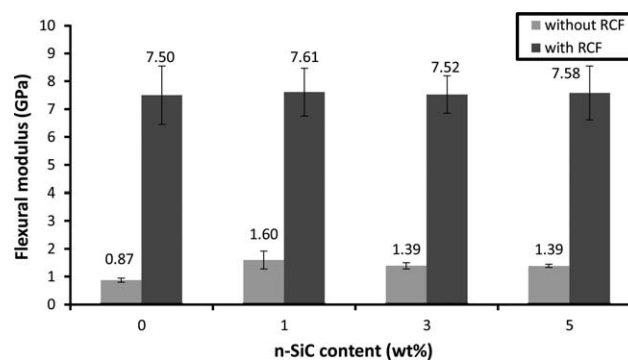
Figure 4 Flexural modulus as a function of n-SiC content in unfilled composites and RCF-filled composites.
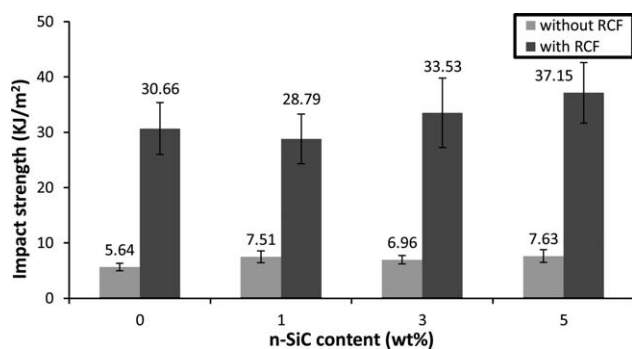
Figure 5 Impact strength as a function of n-SiC content in unfilled composites and RCF-filled composites.

matrix significantly increases the flexural modulus by about seven times compared to neat epoxy. Adding n-SiC particles to the RCF/epoxy slightly increases flexural modulus (Fig. 4).

Impact strength and toughness

The impact strength of epoxy nanocomposites and RCF reinforced epoxy nanocomposites are plotted in Figure 5. The presence of n-SiC particles increases the impact strength for epoxy nanocomposites with maximum improvement 35.5% at 5 wt % n-SiC load. The impact strength of neat epoxy increases from 5.6 to 7.5, 7.0, and 7.6 kJ/m^2 after the addition of 1, 3, and 5 wt % of n-SiC respectively. Similar significant enhancement in impact strength was reported by Lu et al.[35] They investigated the mechanical properties of hybrid epoxy/SiO$_2$ nanocomposites. It was found that impact strength for nanocomposites filled with 2 wt % SiO$_2$ increased by maximum 43.3% when compared with neat epoxy. However, adding more SiO$_2$ content (2.5 and 3) wt % caused impact strength to decrease due to the poor dispersion of SiO$_2$ particles at higher filler content. As illustrated in Figure 5, the presence of RCF significantly improves impact strength by ~ 444% over PE from 5.6 to 30.7 kJ/m^2. This great achievement is due to the fact that cellulose fiber has a better ability to absorb impact energy than unreinforced polymer. This result is in agreement with the work of Maleque and Belal.[12] They studied the mechanical properties of pseudo-stem banana fiber-epoxy composites and found that the presence of banana woven fabric increased the impact strength over the neat epoxy by ~ 40%. The effect of the addition of n-SiC on impact strength properties of RCF/epoxy nanocomposites is shown in Figure 5. It can be seen that impact strength of n-SiC filled RCF/epoxy nanocomposites increases as n-SiC loading increases. The impact strength of RCF/epoxy displays a maximum increase of 21% with only 5 wt % of n-SiC particles. It was observed an increase in n-SiC clusters into

epoxy nanocomposites due to the increase in n-SiC loading as seen in Figure 2(a–c). These clusters may act as crack stoppers and increase the ability of the material to absorb energy by forming tortuous pathways for crack propagation, which resulting the impact strength to increase.[36]

The impact toughness in terms of the energy release rate (G_{1C}) for n-SiC/epoxy nanocomposites is illustrated in Figure 6. It can be seen that impact toughness gradually increases as the n-SiC content increases yielding a maximum at 5 wt % n-SiC load. The addition of 1, 3, and 5 wt % n-SiC into epoxy matrix significantly enhance impact toughness by 25.0, 50.0, and 62.5% over neat epoxy, respectively. This remarkable enhancement in toughness properties for nanocomposites is due to several toughness mechanisms for dissipating energy such as, crack pinning, crack deflection, particle debonding, plastic void growth, plastic deformation, and particle pull-out as has been reported by number of studies for polymers reinforced with nanofillers.[29,30,32,37,38] Ma et al.[32] reported an increase in impact toughness of epoxy system due to the addition of nanofiller. Authors found that the inclusion of silica nanoparticles increased the toughness properties in terms of energy release rate (G_{1C}) of epoxy system by 81% at 20 wt % silica load. In the case of RCF/epoxy nanocomposites, the inclusion of RCF layers into epoxy resin remarkably enhances the impact toughness by about 262.5%. This extraordinary enhancement in toughness properties is due to the fact that RCF displays a variety of fracture mechanisms in the crack path to resist crack propagation.[11] These fracture mechanisms such as fiber breakage, fiber pullout, fiber debonding, and fiber bridging require high energy to be absorbed. The presence of n-SiC particles into RCF/epoxy increases impact toughness by 10.3, 24.1, and 27.6% at (1, 3, and 5) wt % n-SiC load, respectively. The extra improvement in impact toughness for RCF-based nanocomposites is due to the participating of n-SiC in resisting the crack growth.
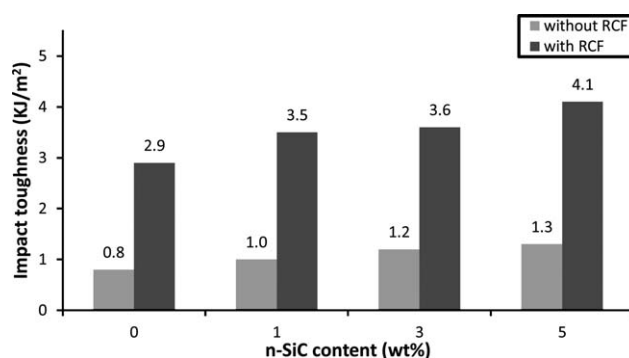
Figure 6 Impact toughness as a function of n-SiC content in unfilled composites and RCF-filled composites.

133
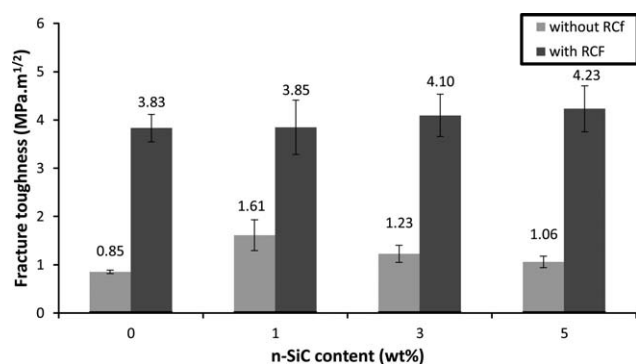
Figure 7 Fracture toughness as a function of n-SiC content in unfilled composites and RCF-filled composites.

Fracture toughness

The influence of n-SiC particles on fracture toughness of epoxy/n-SiC composites is shown in Figure 7. It can be seen that fracture toughness increases due to the presence of n-SiC particles. The addition of only 1 wt % n-SiC significantly increases facture toughness by a maximum 89.4% compared to neat

epoxy. However, fracture toughness tends to decline as n-SiC content increases to (3 and 5) wt %. This could be due the poor dispersion of n-SiC and forming particle agglomeration at higher filler content as can be seen in Figure 2(a–c).[36,39] This significant enhancement in fracture toughness is similar to the work of Chen et al.[30] They found that the addition of (1 and 5) wt % of nanosilica to epoxy matrix increased fracture toughness by about 30%. However, adding more silica (10 wt %) led to decreasing in toughness.

The effect of RCF layers on fracture toughness is clearly shown in Figure 7. As expected, samples reinforced with RCF layers shows a significant increase in fracture toughness in all samples. For example, the addition of RCF in epoxy resin increased fracture toughness by about 350%. This extraordinary enhancement, as can be seen later in Figure 9, is due to the unique properties of cellulose fiber in resisting fracture, which resulted in increased energy dissipation from crack-deflection at the fiber–matrix interface, fiber debonding, fiber
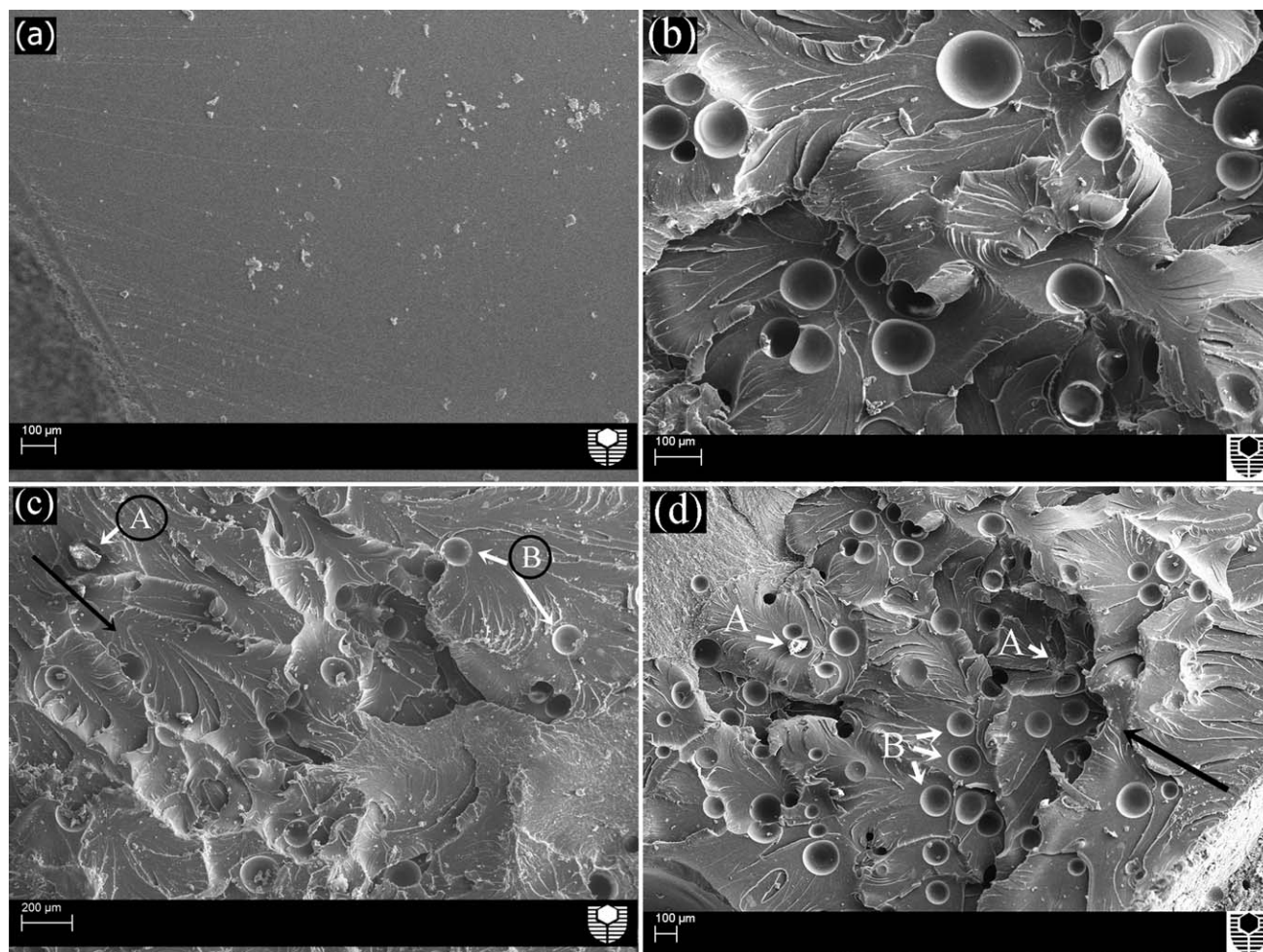
Figure 8 Scanning electron micrographs showing the fracture surfaces of: (a) PE, (b) PE/SiC5 (high magnification), (c) PE/SiC1, and (d) PE/SiC5. (Legend: (A) n-SiC clusters and (B) voids).

134
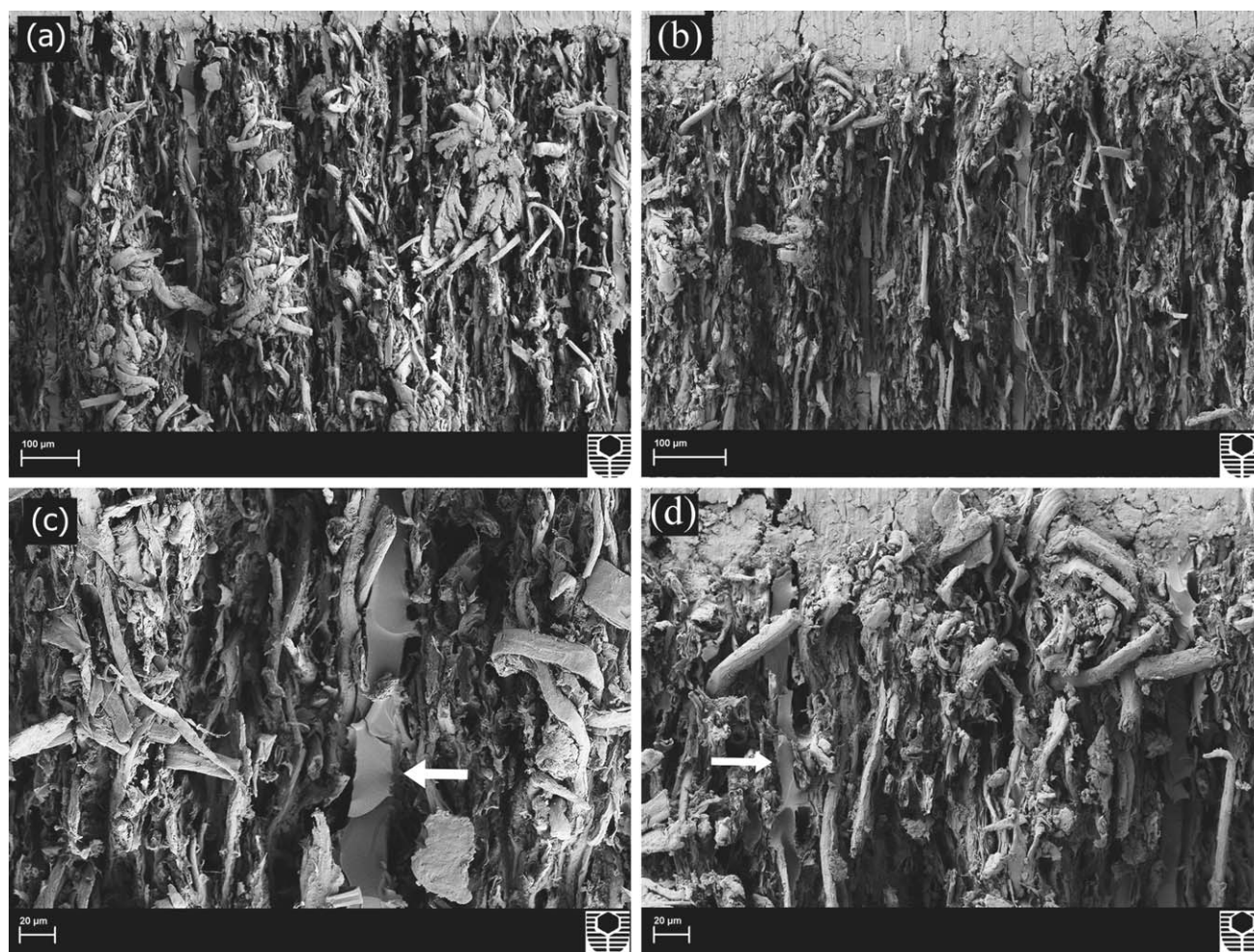
Figure 9 Scanning electron micrographs showing the fracture surfaces of: (a) PE/RCF, (b) PE/RCF/SiC1, (c) PE/RCF (high magnification), and (d) PE/RCF/SiC1 (high magnification). (The white arrow indicates the matrix).

bridging, fiber pullout, and fiber fracture.[11] This result is supported by the work of Lui and Huges[8] and Maleque and Belal.[12] They reported an enhancement in fracture toughness when cellulose fiber was added to epoxy matrix. In the case of epoxy eco-nanocomposites, the addition of n-SiC to the RCF/epoxy composites gradually increases the fracture toughness for all n-SiC filled RCF/epoxy samples. Fracture toughness of RCF/epoxy reinforced with 5 wt % n-SiC increases by maximum 10% over unfilled RCF/epoxy samples. This reveals that fracture toughness in RCF/epoxy eco-nanocomposites is mostly dominated by recycled cellulose fibers with slight effect of n-SiC particles.

Fracture surface and toughness mechanisms

The fracture surfaces of PE and epoxy nanocomposites reinforced with 1 and 5 wt % n-SiC particles are shown in Figure 8. It can be seen from Figure 8(a) that the fracture surface of PE is very smooth and featureless, which indicates typical brittle fracture behavior with lack of significant toughness mechanisms.[38] However, epoxy/n-SiC nanocomposites shows rougher fracture surfaces than that of neat resin as a result of the addition of nanofillers as can be seen in Figure 8(c,d). An increase in fracture surface roughness can be used as indicator to the presence of crack deflection mechanisms, which increase fracture toughness by increasing crack propagation length during deformation.[29,38] Figure 8(b) shows high magnification SEM micrograph of fracture surface for epoxy reinforced with 5 wt % n-SiC particles. A number of possible toughness mechanisms such as crack pinning, crack deflection, particle debonding, plastic void growth, plastic deformation, and particle pullout can be observed. Such toughness mechanisms can lead to higher fracture toughness properties through resisting crack propagation.[29,30,32,37,38] Moreover, particles agglomerations and voids in microscale are observed for epoxy/n-SiC nanocomposites. Samples with 5 wt % n-SiC shows increase in particle agglomerates and voids than samples filled with 1 wt % n-SiC. This result agrees with TEM results.

135
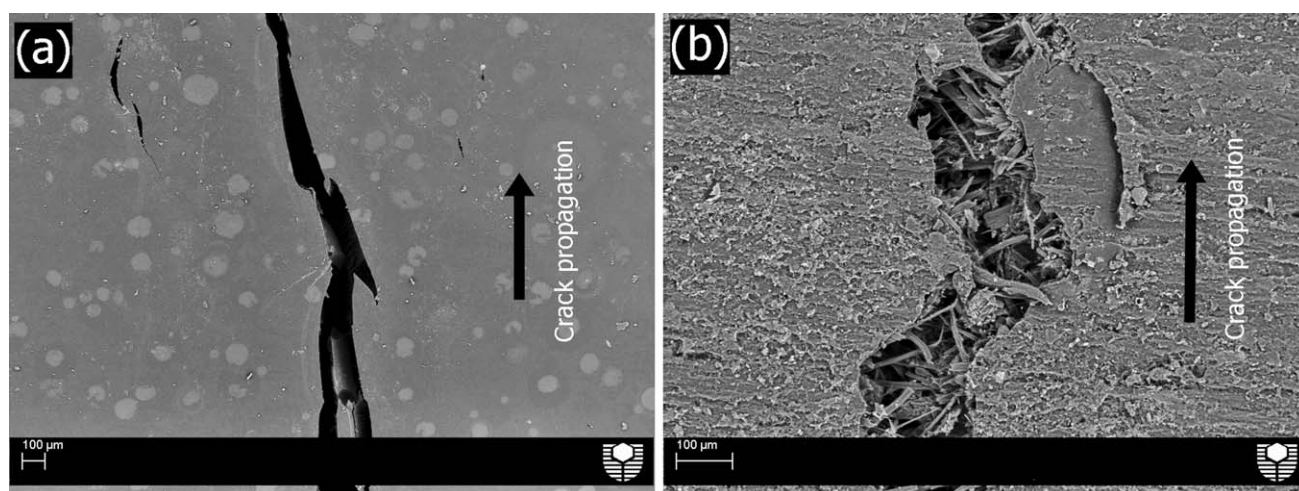
Figure 10 Scanning electron micrographs showing the crack propagation behavior in: (a) PE/SiC1 and (b) PE/RCF/SiC1.

Figure 9(a,b) illustrate low magnification image of RCF/epoxy sample and RCF/epoxy filled with 1 wt % n-SiC, while Figure 9(c,d) show high magnification image of same samples. A variety of toughness mechanisms such as, shear deformation, crack bridging, fiber pullout, and fiber fracture and matrix fracture can be clearly observed, which lead to good fracture properties of samples reinforced by RCF layers. Figure 10(a,b) display the back-scattered SEM images of crack propagation in epoxy/n-SiC and RCF/epoxy/n-SiC nanocomposites filled with 1% wt n-SiC. It is observed that samples reinforced with RCF layers did not completely break in two pieces. This is due to the fact that fibers bridge the cracks and enhance the crack propagation resistance, which lead to improvement in fracture toughness. The tortuous pathway for the crack propagations indicates the high energy absorbance by the RCF sheets. These super toughness mechanisms of RCF are the major factors of increasing mechanical properties of sam-

ples reinforced with RCF when compared with samples without RCF.

Thermal stability and properties

The thermal stability of the samples was determined using TGA. In this test, the thermal stability was studied in terms of the weight loss as a function of temperature in nitrogen atmosphere. The thermograms (TGA) and the derivatives thermograms (DTA) of neat epoxy, epoxy/RCF, epoxy/n-SiC, and epoxy/n-SiC/RCF nanocomposites filled with 5 wt % n-SiC are shown in Figures 11 and 12. The maximum decomposition temperature (T_{max}) and the char yields at different temperatures for all samples types are summarized in Table III.

In the case of epoxy resin and its nanocomposites, it can be seen from Table III that at low temperatures ($<400°C$) PE displays better thermal stability than those filled with n-SiC particles. This means that the presence of n-SiC accelerates the degradation of epoxy nanocomposites compared to epoxy
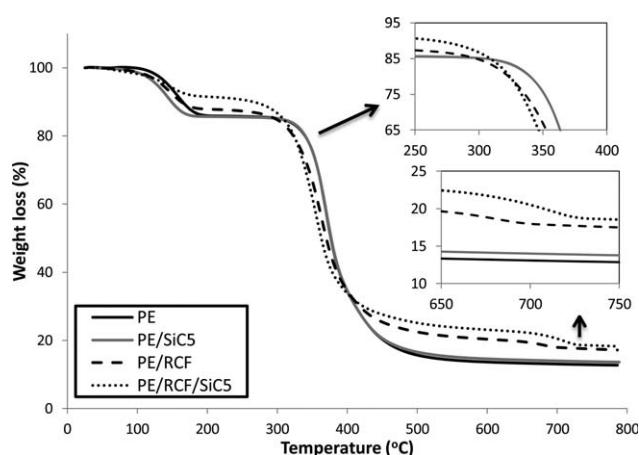
Figure 11 TGA curves of PE, PE/SiC5, PE/RCF, and PE/RCF/SiC5.
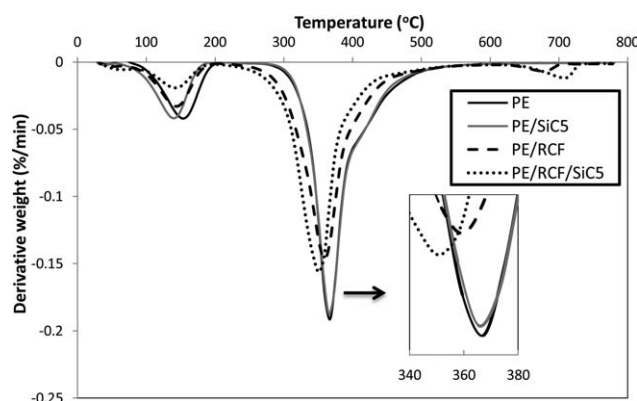
Figure 12 DTG curves of PE, PE/SiC5, PE/RCF, and PE/RCF/SiC5.

136

TABLE III
Thermal Properties of Epoxy, Epoxy/RCF Composites, Epoxy/n-SiC and Epoxy/RCF/n-SiC Nanocomposites

Sample	Char yield at different temperature (%)							T_{max} (°C)
	100°C	200°C	300°C	400°C	500°C	600°C	700°C	
PE	99.86	86.10	85.24	35.26	15.69	13.69	13.08	367.29
PE/SiC1	99.09	83.19	82.44	32.25	14.45	12.43	11.85	367.25
PE/SiC3	98.29	84.55	83.96	34.54	15.85	13.82	13.20	365.47
PE/SiC5	98.62	85.68	85.09	34.70	16.60	14.60	14.00	365.53
PE/RCF	98.65	87.88	85.01	34.58	22.49	20.37	17.96	359.62
PE/RCF/SiC1	97.34	94.30	88.48	33.72	26.90	25.15	21.66	351.43
PE/RCF/SiC3	97.96	92.74	87.65	33.83	25.84	23.92	20.87	351.37
PE/RCF/SiC5	98.22	91.51	86.65	33.84	25.15	23.14	20.50	350.87

resin. This observation has been reported as the Hofmann elimination reaction, where nanoparticles act as a catalyser toward the degradation of the polymer matrix.[40–42] The maximum decomposition temperature (T_{max}) of the nanocomposites slightly decreases by 2°C after the addition of (3 and 5) wt % n-SiC compared to PE. However, at high temperatures (>400°C), epoxy reinforced with 3 and 5 wt % n-SiC show better thermal stability than neat epoxy. The char residue at 700°C of neat epoxy increased from 13.1 to 13.2% and 14.0% after the addition of 3 and 5 wt % n-SiC, respectively. It was reported in previous studies that the addition of nanoparticles would efficiently raise the char residue of polymers at high temperature.[22,31,40,41]

The presence of RCF layers increases the amount of residue at temperatures range from 180 to 250°C. At the second decomposition where the major degradation occurs, the addition of RCF clearly decreases the maximum decomposition temperature (T_{max}) by 7.7°C compared to neat epoxy. Figure 12 shows that the peak of the maximum decomposition of RCF/epoxy composites shifted to lower temperature compared to neat epoxy, which indicates that the addition of RCF increases the rate of the sample major degradation. However, at high temperature (>400°C), where samples lose (>70%) of their initial weight, the presence of RCF leads to significant enhancement in thermal stability by increasing the char yield at 500, 600, and 700°C compared to epoxy system. The char yield at 700°C of neat epoxy increase from 13.1 to 18.0 wt % after the addition of RCF. Similar results were obtained by Shih[1] and De Rosa et al.[7] They reported an improvement in thermal stability of plant fiber/epoxy composites by increasing char yield at high temperatures. Shih[1] cited that the increasing in char yield is an indication of the potency of flame retardation of polymers. Thus, the addition of plant fiber enhanced the flame retardation of epoxy.

The addition of n-SiC to RCF/epoxy increases the thermal stability by increasing the amount of the residue at temperatures 200 and 300°C. However, at the region of major degradation, the unfilled RCF/epoxy shows better thermal stability than samples filled with n-SiC. The maximum decomposition temperature (T_{max}) of RCF/epoxy nanocomposites decreased by ~ 8°C compared to unfilled RCF/epoxy composite. Figure 12 shows that the peak of the major decomposition of RCF/epoxy filled with 5 wt % n-SiC moved to a lower temperature compared to unfilled RCF/epoxy composites. This is due to the catalytic effect of n-SiC particles on RCF/epoxy nanocomposites. But, at high temperatures (>400°C) n-SiC filled RCF/epoxy nanocomposites show better thermal stability than unfilled RCF/epoxy composite by increasing the char residues at temperatures 500, 600, and 700°C. This means that at high temperature, the addition of n-SiC particles significantly enhances the thermal stability of epoxy/RCF nanocomposites. This enhancement on thermal properties is due to the presence of n-SiC, which acted as barriers and hindered the diffusion of volatile decomposition products out from the nanocomposites.[40–43]

CONCLUSION

Epoxy ecocomposites and nanocomposites reinforced with recycled cellulose fibers (RCF) and n-SiC have been fabricated and characterized. The crystalline structure and the dispersion of the n-SiC particles into epoxy matrix were investigated by synchrotron radiation diffraction and TEM. The distribution of n-SiC particles was homogeneous with some particles agglomerations. In general, the inserting of n-SiC into epoxy matrix increased flexural strength, flexural modulus, impact strength, impact toughness and fracture toughness. The fracture surface features of modified epoxies were found to be rougher than neat epoxy due to the presence of n-SiC particles. The addition of n-SiC to epoxy matrix increased the thermal stability at high temperatures (above 400°C) when compared with neat epoxy.

The presence of RCF layers in the epoxy resin significantly increased all mechanical properties compared to neat epoxy and epoxy nanocomposites. This remarkable enhancement is due the unique

properties of cellulose fiber in withstanding bending force and resisting fracture force compared to brittle polymers. SEM micrographs showed a number of toughness mechanisms such as, shear deformation, crack bridging, fiber pullout and fiber fracture and matrix fracture. These super toughness mechanisms of RCF were the major factors of increasing mechanical properties of samples reinforced with RCF when compared with neat epoxy and its nanocomposites. The presence of RCF layers accelerated the major degradation for epoxy filled with RCF compared to neat epoxy. Maximum decomposition temperature decreased as a result to the addition of RCF layers.

The inclusion of n-SiC particles to the RCF/epoxy composites gradually increased fracture toughness and impact toughness compared to unfilled RCF/epoxy samples. Flexural strength increased after the addition of only 1 wt % n-SiC. However, adding more SiC caused decline in flexural strength due to the poor dispersion of n-SiC particles and formation of particle agglomerations at higher filler content. The addition of n-SiC to RCF/epoxy composites was found to increase the thermal stability by increasing the char yield of composites at high temperatures. However, the rate of degradation increased after adding n-SiC to RCF/epoxy composites by decreasing the maximum decomposition temperatures by about 8°C.

References

1. Shih, Y. F. Mater Sci Eng A 2007, 445, 289.
2. Deng, S.; Zhang, J.; Ye, L.; Wu, J. Polymer 2008, 49, 5119.
3. Ganan, P.; Garbizu, S.; Ponte, R.; Mondragon, I. Polym Compos 2005, 26, 121.
4. Dhakal, H. N.; Zhang, Z. Y.; Richardson, M. O. W. Compos Sci Technol 2007, 67, 1674.
5. Low, I. M.; McGrath, M.; Lawrence, D.; Schmidt, P.; Lane, J.; Latella, B. A. Compos A 2007, 38, 963.
6. Marsh, G. Mater Today 2003, 6, 36.
7. De Rosa, I. M.; Santulli, C.; Sarasini, F. Mater Design 2010, 31, 2397.
8. Lui, Q.; Hughes, M. Compos A 2008, 39, 1644.
9. Athijayamani, A.; Thiruchitrambalam, M.; Natarajan, U.; Pazhanivel, B. Mater Sci Eng A 2009, 517, 344.
10. Harish, S.; Michael, D. P.; Bensely, A.; Lal, D. M.; Rajadurai, A. Mater Character 2009, 60, 44.
11. Low, I. M.; Somers, J.; Kho, H. S.; Davies, I. J.; Latella, B. A. Compos Interface 2009, 16, 659.
12. Maleque, M. A.; Belal, F. Y. Arab J Sci Eng 2007, 32, 359.
13. Rashdi, A. A.; Sapuan, S. M.; Ahmad, M. M.; Khalina, A. J Food Agr Environ 2009, 7, 908.
14. Ma, J.; Xu, J.; Ren, J. H.; Yu, Z. Z.; Mai, Y. W. Polymer 2003, 44, 4619.
15. Lu, C.; Mai, Y. W. Phys Rev Lett 2005, 95, 088303.
16. Sinha, S. R.; Okamoto, M. Prog Polym Sci 2003, 28, 1539.
17. Usuki, A.; Kojima, Y.; Kawasumi, M.; Okada, A.; Fukushima, Y.; Kurauchi, T.; Kamigaito, O. J Mater Res 1993, 8, 1179.
18. Kojima, Y.; Usuki, A.; Kawasami, M.; Okada, A.; Fukushima, Y.; Karauchi, T.; Kamigaito, O. J Mater Res 1993, 8, 1185.
19. Alexandre, B.; Langevin, D.; Médéric, P.; Aubry, T.; Couderc, H.; Nguyen, Q. T.; Saiter, A.; Marais, S. J Membr Sci 2009, 328, 186.
20. Araujo, E. M.; Araujo, K. D.; Paz, R. A.; Gouveia, T. R.; Barbosa, R.; Ito, E. N. J Nanomaterials Vol. 2009, 2009, Article ID 136856, 5 pages.
21. Ha, S. R.; Rhee, K. Y.; Park, S. J.; Lee, J. H. Compos B 2010, 41, 602.
22. Hwang, S. S.; Liu, S. P.; Hsu, P. P.; Yeh, J. M.; Chang, K. C.; Lai, Y. Z. Int Commun Heat Mass Transfer 2010, 37, 1036.
23. Qi, B.; Zhang, Q. X.; Bannister, M.; Mai, Y. W. Compos Struct 2006, 75, 514.
24. Kaynak, C.; Nakas, G. I.; Lsitman, N. A. Appl Clay Sci 2009, 46, 319.
25. Zainuddin, S.; Hosura, M. V.; Zhoua, Y.; Narteha, A. T.; Kumarb, A.; Jeelani, S. Mater Sci Eng 2010, 527, 7920.
26. Satapathy, A.; Jha, A. k.; Mantry, S.; Singh, S. D.; Patnaik, A. J Reinforc Plast Compos 2010, 29, 2869.
27. Blackman, B. R. K.; Kinloch, A. J.; Sohn Lee, J., Talor, A. C.; Agarwal, R.; Schueneman, G. J Mater Sci 2007, 42, 7049.
28. Johnsen, B. B.; Kinloch, A. J.; Mohammed, R. D.; Taylor, A. C.; Sprenger, S. Polymer 2007, 48, 530.
29. Zhao, S.; Schadler, L. S.; Hillborg, H.; Auletta T. Compos Sci Technol 2008, 68, 2976.
30. Chen, C.; Justice, R. S.; Schaefer, D. W.; Baur, J. W. Polymer 2008, 49, 3805.
31. Chatterjee, A.; Islam, M. A. Mater Sci Eng A 2008, 487, 574.
32. Ma, J.; Mo, M. S.; Du, X. S.; Rosso, P.; Friedrich, K.; Kuan, H. C. Polymer 2008, 49, 3510.
33. Technical Information of Sigma-Aldrich. LLC. Available at http://www.sigmaaldrich.com/australia.html, 2011.
34. Xu, Y.; Hoa, S. V. Compos Sci Technol 2008, 68, 854.
35. Lu, S-R.; Jiang, Y-M.; Wei, C. J Mater Sci 2009, 44, 4047.
36. Deng, S.; Zhang, J.; Ye, L. Compos Sci Technol 2009, 69, 2497.
37. Wetzel, B.; Rosso, P.; Haupert, F.; Friedrich, K. Eng Fract Mech 2006, 73, 2375.
38. Tang, Y.; Deng, S.; Ye, L.; Yang, C.; Yuan, Q.; Zhang, J.; Zhao, C. Compos A 2011, 42, 345.
39. Yasmin, A.; Abot, J. L.; Daniel, I. M. Script Mater 2003, 49, 81.
40. Madaleno, L.; Schjødt-Thomsen, J.; Pinto, J. C. Compos Sci Technol 2010, 70, 804.
41. Ismail, H.; Pasbakhsh, P.; Fauzi, M. N. A.; Abu Bakar, A. Polym Test 2008, 27, 841.
42. Zhao, C.; Qin, H.; Gong, F.; Feng, M.; Zhang, S.; Yang, M. Polym Degrad Stab 2005, 87, 183.
43. Yeh, J. M.; Huang, H. Y.; Chena, C. L.; Su, W. F.; Yu, Y. H. Surf Coat Technol 2006, 200, 2753.

3.5 Effect of Water Absorption on the Mechanical Properties of Nano-Filler Reinforced Epoxy Nanocomposites.

Alamri, H., and I. M. Low. 2012. Effect of water absorption on the mechanical properties of nano-filler reinforced epoxy nanocomposites. *Materials and Design* 42: 214-222.

Effect of water absorption on the mechanical properties of nano-filler reinforced epoxy nanocomposites

H. Alamri, I.M. Low *

Department of Imaging & Applied Physics, Curtin University of Technology, GPO Box U1987, Perth, WA 6845, Australia

ABSTRACT

This study aimed to investigate the effect of water absorption on the mechanical properties of nano-filler reinforced epoxy nanocomposites as well as to study the influence of different types of nano-fillers such as nano-clay platelets, halloysite nanotubes (HNTs) and nano-silicon carbide (n-SiC) particles on the water absorption behaviour of epoxy based nanocomposites. Results indicated that the addition of nano-fillers into epoxy matrix was found to decrease both water uptake and diffusivity compared to unfilled epoxy. Flexural strength and modulus of epoxy based nanocomposites were found to decrease due to the water absorption. However, the addition of nano-fillers enhanced the flexural strength and modulus of nanocomposites compared to wet unfilled epoxy. Surprising, fracture toughness and impact strength of all types of nanocomposites were found to increase after exposing to water. The presence of nano-fillers increased both fracture toughness and impact strength of nanocomposites compared to wet neat epoxy.

© 2012 Published by Elsevier Ltd.

1. Introduction

Epoxy is characterized by unique properties such as relatively high strength and modulus, low shrinkage, and excellent chemical and heat resistance. It is an important matrix used for fibre-reinforced polymer. Due to its features, epoxy has been used in manufacturing applications such as adhesives, coatings, electronic and aerospace structures. Despite its use, cured epoxy systems indicated low impact strength, poor resistance to crack propagation and initiation and low fracture toughness [1,2]. A recent approach is advocated to try to enhance polymer properties via incorporation of inorganic nanoparticles or fillers in the nanometre scale into the polymer matrices [3].

Nanoparticles embedded in polymer matrix have attracted increasing interest because of the unique mechanical, optical, electrical and magnetic properties compared to neat polymers [3,4]. Polymer nanocomposite materials possess two phases consisting of inorganic particles of nanometre scale in the range between 1 and 100 nm that are dispersed in a matrix of polymeric material [5]. Due to nanometre size of these particles, nanoparticles demonstrate remarkable properties because of their comparative large surface area per unit volume. Such properties are the results of the phase interactions that take place between the polymer matrix and the nanoparticles at the interfaces since many essential chemical and physical interactions are governed by surfaces [5,6]. The

interest in polymer nanocomposites comes from the fact that the addition of nanosized fillers into a polymeric matrix would have a great effect on the properties of the matrix. In 1990, the Toyota research group carried out the first study on the polymer nanocomposites. These researchers synthesized polymer nano-composites based on nylon-6/montmorillonite clay via the in situ polymerization method. When 5 wt.% clay was added to nylon-6 polymer, the tensile modulus increased by 68% and the flexural modulus by 224% [6,7]. This research was the fore-runner of the global trend researches in polymer/layered silicate nanocomposites and polymer nanocomposites in general [8].

Kaynak et al. [9] investigated the flexural strength and fracture toughness of nanoclay (Na-montmorillonite) based epoxy nanocomposites. Results showed an improvement in flexural strength and fracture toughness with maximum value at 0.5% nanoclay loading. Manfredi et al. [10] found that flexural strength, flexural modulus and impact strength were increased by 20%, 29% and 23%, respectively, for composites made with the addition of 5 wt.% of nanoclay. Tang et al. [11] studied the mechanical properties of treated halloysite reinforced epoxy nanocomposites. It was reported that the fracture toughness of epoxy significantly increased by 78.3% due to the presence of 10 wt.% of intercalated HNTs. Wetzel et al. [12] reported an increase in flexural strength (up to 15%), flexural modulus (up to 40%) and fracture toughness (up to 120%) for epoxy nanocomposites reinforced with aluminium oxide (Al_2O_3).

In our previous works [1,13] we studied the mechanical and thermal properties of epoxy nanocomposites reinforced with

* Corresponding author. Tel.: +61 892667544; fax: +61 892662377.
  E-mail address: j.low@curtin.edu.au (I.M. Low).

organo-clay platelets (30B), halloysite nanotubes (HNTs) and nano-silicon carbide (n-SiC), respectively. Results showed that the addition of only 1 wt.% of intercalated nanoclay increased flexural strength (up to 45.6%), flexural modulus (up to 87.6%), fracture toughness (up to 30%), and impact toughness (up to 50%) compared to neat epoxy. Likewise, the addition of 1 wt.% HNT increased flexural strength (up to 20.8%), flexural modulus (up to 72.8%), fracture toughness (up to 56.5%), and impact toughness (up to 25.0%) over neat epoxy. Furthermore, the addition of 1 wt.% n-SiC increased flexural strength (up to 21.5%), flexural modulus (up to 83.0%), fracture toughness (up to 89.4%), and impact toughness (up to 25.0%) compared to pure epoxy.

In this study, the effect of long term water absorption on the mechanical properties of epoxy based nanocomposites reinforced with organoclay, HNT and n-SiC has been studied. The influence of different types of nano-filler on the barrier properties of epoxy based nanocomposites has been examined in terms of the weight gain curve of water absorption. The effect of nano-filler addition on enhancing epoxy matrix mechanical properties in wet condition has been investigated in terms of flexural strength, flexural modulus, facture toughness and impact strength. Transmitted electron microscopy (TEM), Fourier transforms infrared spectroscopy (FTIR) and scanning electron microscopy (SEM) have been used to investigate the morphology, micro-structure and failure mechanism of epoxy based nanocomposites.

2. Materials and methods

2.1. Materials

Organoclay platelets (Cloisite 30B), halloysite nanotubes (HNTs) and nano-silicon carbide (n-SiC) particles were used in this study as reinforcements for the fabrication of epoxy–matrix nanocomposites. The organoclay platelets (Cloisite 30B) were provided by Southern Clay Products, a United States based company. The halloysite nanotubes (HNTs) (ultrafine grade) were provided by Imerys Tableware Asia Limited, New Zealand. The brightness of HNTs is about 98.9% as measured by a Minolta CR300 using D65 light source. The nano-silicon carbide (n-SiC) particles were supplied by Sigma–Aldrich Co. LLC, United State. Finally, general purpose low viscosity epoxy resin (FR-251) and epoxy hardener (Isophorone-diamine) were supplied by Fibreglass & Resin Sales Pty. Ltd., WA, Perth, Australia. Table 1 represents the physical properties of Cloisite 30B and n-SiC particles and Table 2 shows the chemical composition and physical properties of HNT [13–15].

2.2. Sample fabrication

Nano-particles including nanolcay (30B), HNTs and n-SiC were first dried for 60 min at 70 °C before they were mixed individually with epoxy resin. Nanocomposites were prepared by mixing the epoxy resin with three different weight percentages (1%, 3% and 5%) of each type of nanoparticles using high speed mechanical mixer for 10 min with a rotation speed of 1200 rpm. After that, a hardener was added to the mixture and then stirred slowly to minimize

Table 1
Physical properties of (Cloisite 30B) and n-SiC particles.

Physical properties	Cloisite 30B	n-SiC
Colour	Off white	Light grey
Density(g/cm³)	1.98	3.22
Surface area(m²/g)	750	70–90
Particle size	2–13 μm	<100 nm
d-spacing(0 0 1)	1.85 nm	–

Table 2
Chemical composition and physical properties of HNTs.

SiO$_2$	50.4 wt.%
Al$_2$O$_3$	35.5 wt.%
Fe$_2$O$_3$	0.25 wt.%
TiO$_2$	0.05 wt.%
Colour	Bright white
Surface area	20 m^2/gm
Particle size	0.2–6.0 μm
d-spacing(0 0 1)	0.74 nm

the formation of air bubbles within the sample. The final mixture was poured into silicon moulds and left for 24 h at room temperature for curing. Pure epoxy sample was also made as a control.

2.3. Characterization

2.3.1. Transmission electron microscopy (TEM)
The transmission electron microscopy was performed on a Titan Cryotwin (FEI Company) equipped with a 4 k × 4 k CCD camera (Gatan) at an acceleration voltage of 300 kV. An ultramicrotome (Leica microsystem) was used to prepare cut ultra-thin sections (~80 nm) of samples before recovered on a copper grid.

2.3.2. Fourier transform infrared (FTIR) spectra
The Fourier transform infrared spectroscopy (FTIR) was performed on Perkin Elmer Spectrum 100 FTIR spectrometer in the transmission mode at room temperature. FT-IR spectra were recorded in the range (600–4000 cm^{-1}) at a resolution of 2 cm^{-1} with 10 scans. Background spectra were taken in the empty chamber before measurements to eliminate the influence of water moisture and CO$_2$ in air.

2.3.3. Scanning electron microscopy (SEM)
A scanning electron microscopy imaging was obtained using Zeiss Evo 40XVP to investigate the microstructures and the fracture surfaces of composites. The samples were mounted on aluminium stubs using carbon tape. The samples were then coated with a thin layer of gold to prevent charging before the observation by SEM.

2.3.4. Differential scanning calorimetry (DSC)
DSC analysis was performed on a Perkin Elmer (DSC 6000) in dry nitrogen atmosphere with heating rate of 10 °C/min. In this study, DSC was only conducted for neat epoxy in both dry and wet conditions to investigate the effect of water absorption on the glass transition temperature (T_g).

2.4. Physical and mechanical properties

2.4.1. Water absorption
Specimens with dimensions 10 mm × 10 mm × 3.5 mm were cut from the fabricated composites and placed in water bath at room temperature for about 130 days. At regular intervals, each sample was first removed from water and dried with a tissue before weighting using electronic balance. The percentage of the water content (M_t) was determined using the following equation:

$$M_t(\%) = \left(\frac{W_t - W_o}{W_o}\right) \times 100 \qquad (1)$$

where W_t is the weight of the sample at time t and W_o is the initial weight of the sample. Assuming that water absorption in the samples follows Fick's second law [16]. Thus, for one-dimensional diffusion during short immersion times the following formula can be used to calculate the diffusivity D_{eff} [16,17]:

$$\frac{M_t}{M_\infty} = 4\left(\frac{D_{eff}t}{\pi h^2}\right)^{1/2} \qquad (2)$$

where M_t is the water content at time t, M_∞ is the equilibrium water content, D_{eff} is the effective diffusion coefficient and h is the sample thickness. Therefore, the diffusivity D_{eff} can be determined from the initial slope of the water absorption versus the square root of time.

2.4.2. Mechanical properties

Five rectangular specimens of each composition with dimensions 60 mm × 10 mm × 6 mm were cut from the fully cured samples for three-point tests and Charpy impact tests to evaluate the mechanical properties.

Flexural strength, flexural modulus and facture toughness of the composites were determined using three-point bending test and performed on a LLOYD Material Testing Machines - Twin Column Bench Mounted (5–50 kN). A span of 40 mm was used during the test with a displacement rate of 1.0 mm/min. The flexural strength (σ_F) was evaluated using the following equation:

$$\sigma_F = \frac{3}{2}\frac{P_m S}{WD^2} \qquad (3)$$

where P_m is the maximum load at crack extension, S is the span of the sample, D is the specimen thickness and W is the specimen width. Values of the flexural modulus (E_F) were computed using the initial slope of the load–displacement curve, $\Delta P/\Delta X$, using the following formula:

$$E_F = \frac{S^3}{4WD^3}\left(\frac{\Delta P}{\Delta X}\right) \qquad (4)$$

Fracture toughness was evaluated using single edge notch bending (SENB) specimens. A notch was introduced at the central of the specimen bar using a diamond blade saw followed by introducing sharp pre-crack into the notch via tapping a sharp razor blade. The ratio of notch length to width (a/w) was about (0.4). Fracture toughness (K_{IC}) was calculated using the following equation according to [18].

$$K_{IC} = \frac{p_m S}{WD^{2/3}}f\left(\frac{a}{w}\right) \qquad (5)$$

where a is the crack length, and $f(a/w)$ is the polynomial geometrical correction factor give as

$$f\left(\frac{a}{W}\right) = \frac{3(a/W)^{1/2}[1.99 - (a/W)(1 - a/W) \times (2.15 - 3.93a/W + 2.7a^2/W^2)]}{2(1 + 2a/W)(1 - a/W)^{2/3}} \qquad (6)$$

Impact strength was measured using Zwick Charpy impact test with 1.0 J pendulum hammer. Un-notched impact strength in the units of kJ/m^2 was evaluated using the following formula:

$$\sigma_I = \frac{E}{A} \qquad (7)$$

where E is the impact energy to break a sample with a ligament of area A.

3. Results and discussion

3.1. TEM observation

Fig. 1a–c shows the dispersion for 5 wt.% of nanoclay, HNT and n-SiC within the epoxy matrix, respectively. It can be seen that the dispersion of these fillers was quite homogenous with some particle agglomerations that found to increase as filler content increased due to the increase in matrix viscosity. Fig. 1d–f shows high magnification TEM images for nanoclay (Cloisite 30B), HNT and n-SiC in the epoxy matrix. It can be seen in Fig. 1d that mixing the nanoclay platelet with epoxy resin resulted in intercalated

structure with d-spacing ranges from 2.3 nm to 4.3 nm compared to 1.8 nm of nanoclay platelet. Separated single layers of clay platelet can be also observed. Fig. 1e shows that HNT has hollow nanotubular structure with an average diameter of about 20–40 nm and length ranging from 500 nm to 1.6 μm. While Fig. 1f indicates that n-SiC particles are spherical in shape with diameter ranging from 40 nm to ⩾100 nm.

3.2. Effect of nano-filler on the water absorption of epoxy based nanocomposites

The water absorption curve of nanoclay/epoxy nanocomposites, HNT/epoxy nanocomposites and n-SiC/epoxy nanocomposites are illustrated in Fig. 2a–c, respectively. It can be seen that all nanocomposites exhibit typical water absorption behaviour of polymers that follow Fick's low [19,20]. In general, the presence of nano-fillers is found to decrease the water uptake of modified composites compared to neat epoxy. This phenomenon is due to the excellent barrier properties of these nano-fillers [19–21]. The presence of high aspect ratio nano-fillers can create a tortuous pathway for water molecules to diffuse into the composites [21].

In the case of nanoclay reinforced epoxy nanocomposites, the maximum water uptake decreases gradually with increasing clay contents [20]. The maximum water absorption of nanoclay filled epoxy nanocomposites decreases by 14.1, 17.9 and 24.8% after the addition of 1, 3 and 5 wt.% nanoclay, respectively, when compared to neat epoxy. Similarly, the presence of 1, 3 and 5 wt.% HNT decreases the water absorption by 10.3%, 18.8% and 20.1%, respectively. Interestingly, the nanocomposites filled with n-SiC show better barrier properties than other filled nanocomposites. The incorporation of 1, 3 and 5 wt.% n-SiC decreases water uptake by 21.8, 28.6 and 33.3%, respectively, as compared to neat epoxy. For all nanocomposites, water uptake decreases with increasing filler content. This can be attributed to the increase in the tortuosity effect with increasing filler content [20,21]. Several studies showed that the maximum water absorption of polymer system decreased due the presence of nano-filler [17,19–21]. Becker et al. [19] reported a reduction in maximum water uptake for different types of epoxy systems reinforced with layered silicate. Similarly, Zhao and Li [21] investigated the water absorption of Al$_2$O$_3$/epoxy nanocomposites. Results showed that the water uptake of epoxy decreased after the addition of Al$_2$O$_3$ nanoparticles.

Table 3 shows the maximum water uptake and the effective diffusion coefficient of neat epoxy and epoxy based nanocomposites filled with nanoclay, HNT and n-SiC. It can be seen that the diffusivity of nanocomposites generally decreases due to the addition of nano-fillers. Compared to neat epoxy, significant reduction in diffusivity (30.0%, 31.7% and 36.3%) were achieved with only 5 wt.% of nanoclay, HNT and n-SiC content, respectively. The reduction in the diffusivity may be attributed to the tortuosity of diffusion path created by the nano-filler addition [19]. Similar results were obtained by Kim et al. [16]. It was found that the addition of 5 wt.% nanoclay (I30P and Cloisite 20A) decreased the diffusivity of epoxy by 36% and 39%, respectively.

3.3. FTIR analysis of epoxy based nanocomposites

The FTIR spectra of epoxy and epoxy based nanocomposites filled with nanoclay, HNT and n-SiC in dry condition is investigated. Table 4 presents the main FTIR bands of epoxy and its nanocomposites. The FTIR spectra showed the broad band in the region 3317–3373 cm^{-1} corresponds to the stretching vibration of the hydroxyl groups (OH) of free and hydrogen bonded —OH groups [22]. The peak at 1647 cm^{-1} is assigned to the (OH) bending vibration [22,23]. The absorption peaks at 2869 and 2921 cm^{-1} are attributed to C—H symmetric and asymmetric stretching vibration

142
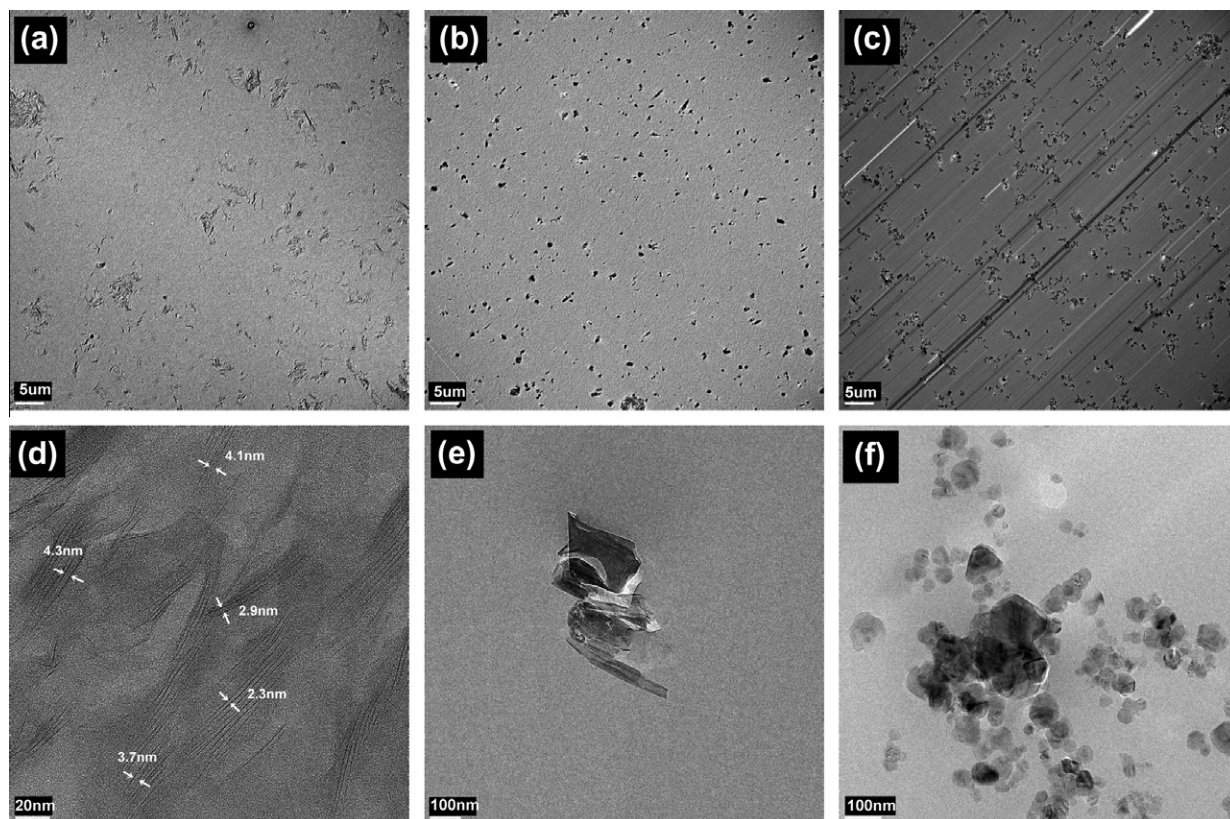
Fig. 1. TEM images of epoxy-based nanocomposites filled with nanoclay (a and d), HNT (b and e), and n-SiC (c and f).

[24]. The absorption peaks at 1607, 1582 and 1508 cm^{-1} are associated with characteristic adsorptions of the benzene ring of epoxy or C=C stretching of aromatic ring [25]. The absorption bands at 1362 and 1453 cm^{-1} can be attributed to CH$_3$ and CH$_2$ bending vibration, respectively [26]. The C—O stretching of epoxide ring vibration showed peaks at 1237 and 917 cm^{-1} [2]. The peak appeared at 826 cm^{-1} could be assigned to the 1,4-substitution of aromatic ring for epoxy resin [26]. There are number of peaks existed in the FTIR spectra due to the presence of nanoclay, HNT and n-SiC into epoxy system. For example, the peaks appeared at 3621 and 3695 cm^{-1} in the HNT/epoxy spectrum correspond to Al$_2$OH stretching of halloysite nanotube [27]. The absorption bands at 911 and 1031 cm^{-1} are attributed to Al—OH vibrations and Si—O stretching vibrations in the halloysite nanotube [24]. In the FTIR spectrum of n-SiC/epoxy nanocomposites, the peaks found at 911 and 1105 cm^{-1} may correspond to Si—C bonds and Si—O—C bonds between n-SiC and epoxy matrix, respectively [28]. The spectrum of nanoclay filled epoxy composite showed peak at 3631 cm^{-1}, which belongs to the (OH) stretching for Al—OH and Si—OH of nanoclay [25,29]. Otherwise, it can be seen that the intensity of some peaks in the nanoclay/epoxy composites changed due to the presence of nanoclay.

Fig. 3a–c shows the principle peak of the hydroxyl group (OH) for dry and wet nanoclay/epoxy nanocomposites, HNT/epoxy nanocomposites and n-SiC/epoxy nanocomposites, respectively. This peak represents the water indirectly and directly bonded to the hydroxyl group and can be used as an indicator to water content in the materials [22]. It can be seen in Fig. 3a–c that after water absorption the peak of interest is found to increase compared to dry composites for all composites. Furthermore, the effect of nano-filler addition on the water absorption of epoxy system was investigated by studying the hydroxyl group (OH) peak at the range of 3317–3373 cm^{-1}. Fig. 3d–f shows the effect of nanoclay, HNT and n-SiC in reducing water uptake in epoxy

based nanocomposites, respectively. In general, it can be observed that the peak of interest decreases as the filler content increases. This confirms that the addition of nano-filler decreases the amount of absorbed water. The reduction in water uptake is most pronounced for nanocomposites filled with n-SiC particles. This result is in agreement with the weight gain study of water absorption.

3.4. Effect of water absorption on the mechanical properties of epoxy based nanocomposites

The effect of water absorption on the mechanical properties of epoxy based nanocomposites was investigated after placing the specimens in water for 6 months period at room temperature and compared with the same nanocomposites in dry conditions. All mechanical tests were carried out at room temperature for wet samples. The data of the nanocomposites in dry condition have been demonstrated here only for the purpose of benchmarking. More details about the mechanical properties of epoxy based nanocomposites filled with nanoclay, HNT and n-SiC particles in dry condition can be found in [1,13], respectively.

3.4.1. Flexural strength and modulus

Table 5 summarizes the flexural strength and modulus of nano-filler reinforced epoxy nanocomposites in both dry and wet conditions. In general, it can be seen that water absorption has a negative influence on flexural strength and modulus of epoxy based nanocomposites. Flexural strength of unmodified epoxy and modified epoxy based nanocomposites decreases after subjecting to water compared to dry nanocomposites. This reduction in flexural strength can be attributed to the plasticization effect of water absorption in epoxy matrix. This can lead to reduction in the interfacial strength between the epoxy and reinforcing particles resulting in drop in flexural strength values [30]. For example,
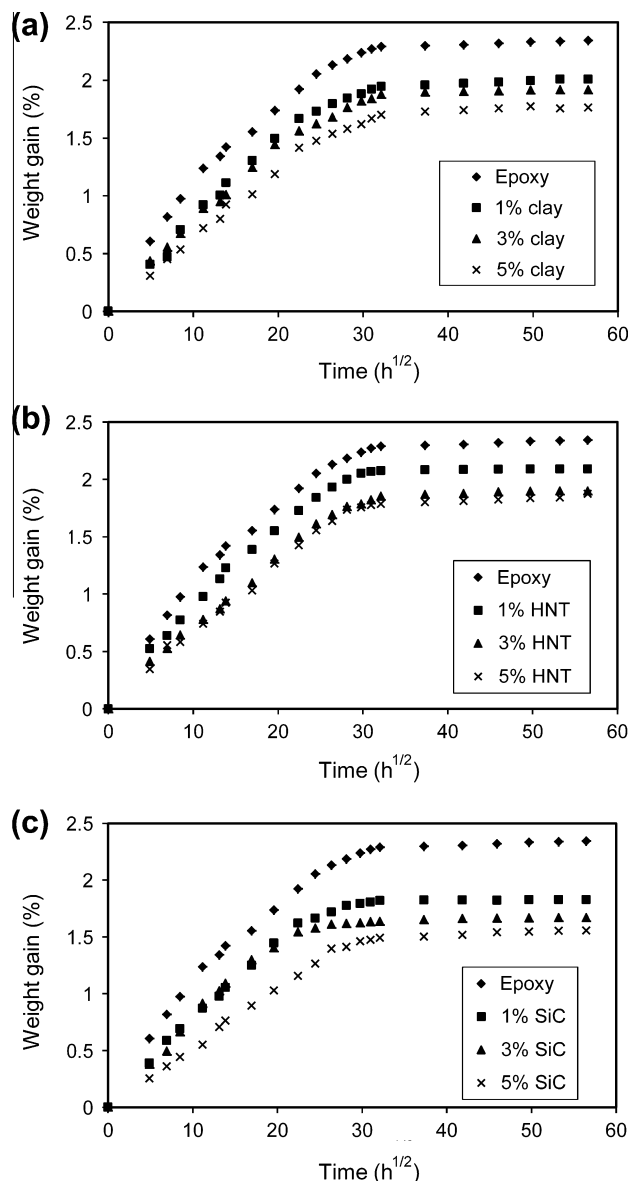
Fig. 2. Water absorption curves of epoxy-based nanocomposites filled with nanoclay (a), HNT (b), and n-SiC (c).

Table 3
Maximum water uptake and diffusion coefficient (D) of epoxy-based nanocomposites filled with nanoclay, HNT and n-SiC particles.

Sample	Maximum water uptake (%)	Diffusion coefficients (D) (10^{-7} mm²/s)
Epoxy	2.34	11.75
Epoxy/nanoclay (1%)	2.01	9.98
Epoxy/nanoclay (3%)	1.92	10.10
Epoxy/nanoclay (5%)	1.76	8.23
Epoxy/HNT (1%)	2.09	10.87
Epoxy/HNT (3%)	1.90	8.47
Epoxy/HNT (5%)	1.87	8.03
Epoxy/n-SiC (1%)	1.83	11.35
Epoxy/n-SiC (3%)	1.67	13.84
Epoxy/n-SiC (5%)	1.56	7.48

the flexural strength of water-absorbed epoxy decreases by 12.2% compared to epoxy in dry condition. In the case of nanoclay/epoxy nanocomposites, the flexural strengths of wet specimens filled with 1, 3 and 5 wt.% nanoclay decrease by 38.3, 10.3 and 13.4%, respectively, compared to nanoclay filled epoxy in dry condition. Similarly, for HNT/epoxy nanocomposites, the flexural strengths of wet specimens modified with 1, 3 and 5 wt.% HNT decrease by 21.1, 23.0 and 17.6%, respectively, compared to dry HNT filled epoxy. Furthermore, for n-SiC/epoxy nanocomposites, the flexural strengths of wet specimens filled with 1, 3 and 5 wt.% n-SiC decrease by 15.9, 14.8 and 12.0%, respectively, in comparison to n-SiC filled epoxy. A number of studies have reported reduction in flexural strength of epoxy based nanocomposites due to water absorption. For instance, Abacha et al. [31] reported a decrease in flexural strength and modulus of clay/epoxy nanocomposites due to the water absorption. Buehler and Seferis [32] also reported a drop in flexural strength values of carbon fibre/epoxy and glass fibre/epoxy composites as a result of moisture absorption.

The effect of nano-fillers on enhancing the flexural strength of wet epoxy matrix was investigated and compared to neat epoxy

in wet condition. Table 4 shows no significant change in flexural strength due to the presence of nanoclay. For example, the flexural strength increases by 2.2 and 3.0% after the addition of 1 and 5 wt.% nanoclay, respectively. For HNT/epoxy nanocomposites, maximum flexural strength (about 8.5% over neat epoxy) is obtained at 1 wt.% HNT loading. Similarly, the addition of 1 wt.% n-SiC increases flexural strength by 16.3% over unmodified wet epoxy. The increase in flexural strength of water-treated nanocomposites after the addition of nano-fillers can be attributed to the enhancement in the interfacial bonding between the filler and the matrix, thus increasing the surface area of matrix/filler interaction. As a result, this leads to good stress transfer from the matrix to the nano-fillers, thus resulting in improved flexural strength. In a similar study, Hossain et al. [33] investigated the effect of nanoclay on the flexural strength of carbon fibre reinforced epoxy composites after immersing in sea water for 30, 60 and 180 days. Their results showed that flexural strength increased due to the presence of nanoclay.

The effect of water absorption on the flexural modulus of nano-filler reinforced epoxy nanocomposites is presented in Table 4. At a glance, it can be argued that flexural modulus was not significantly influenced by water absorption for most of the nanocomposites. However, the decrease in flexural modulus is more expressed for nanocomposites filled with nanoclay than other nanocomposites. The reduction in flexural modulus can be attributed to the plasticization effect of water absorption on the epoxy matrix [21]. DSC analysis was conducted on neat epoxy before and after water treatment to evaluate the effect of water absorption on T_g. Fig. 4 showed that T_g significantly decreased from 53.1 to 47.5 due to the plasticization effect of absorbed water. Similar observation was obtained by Zhao and Li [21].

In the case of wet nanocomposites, it can be seen that the addition of nano-fillers increases the flexural modulus for all types of nanocomposites. The flexural modulus of epoxy modified with 1 wt.% of nanoclay, HNT and n-SiC increases by 80.7, 89.5 and 98.2%, respectively, as compared to wet unmodified epoxy. The enhancement in flexural modulus can be due to the presence of rigid fillers that have higher modulus than epoxy matrix [13]. Any further increase in fillers loading shows slight decrease in the modulus values. The reduction in flexural modulus due to the water absorption was also observed in several studies. Hossain and co-workers [33] observed a reduction in flexural modulus of carbon fibre/epoxy composites filled with nanoclay after immersing in water for 180 days. However, the addition of nanoclay increased flexural modulus of nanoclay filled composites in wet condition compared to unfilled composites. Buehler and Seferis [32] found that flexural modulus of carbon fibre/epoxy and glass fibre/epoxy composites decreased after water absorption.

144

Table 4
FTIR bands of epoxy and its nanocomposites.

Band	Peak location (cm^{-1})
OH stretching	3359
OH bending	1647
C—H symmetric and asymmetric stretching	2869 and 2921
C=C stretching of aromatic ring	1508, 1582 and 1607
CH$_3$ and CH$_2$ bending	1362 and 1453
C—O stretching of epoxide ring	917 and 1237
1,4-substitution of aromatic ring for epoxy resin	826
Al$_2$OH stretching of halloysite nanotube	3621 and 3695
Si—C bonds and Si—O—C bonds	911 and 1105
OH stretching for Al—OH and Si—OH of nanoclay	3631

3.4.2. Fracture toughness

Table 6 displays the fracture toughness of nano-filler/epoxy nanocomposites in both dry and wet conditions. Surprisingly, frac-

ture toughness for all types of nanocomposites is observed to increase due to exposing to a moist environment. This can be explained by increasing the ductility of the composites due to the plasticization effect of absorbed water, which tends to increase in fracture toughness [32]. Similarly, Wang et al. [34] observed an increase in fracture toughness of neat epoxy and exfoliated clay/ epoxy nanocomposites after subjecting to water for 30 days.

In details, fracture toughness of unmodified epoxy in wet condition increases by 48.9% compared to dry epoxy. In the case of nanoclay/epoxy nanocomposites, facture toughness of wet composites modified with 1, 3 and 5 wt.% nanoclay platelet increases by 29.3, 51.4 and 36.0%, respectively, compared to same nanocomposites in dry condition. Similarly, fracture toughness of wet HNT/ epoxy nanocomposites filled with 1, 3 and 5 wt.% HNT increases by 30.7, 57.4 and 11.1%, respectively, as compared to dry nanocomposites. Moreover, fracture toughness of n-SiC/epoxy nanocompos-
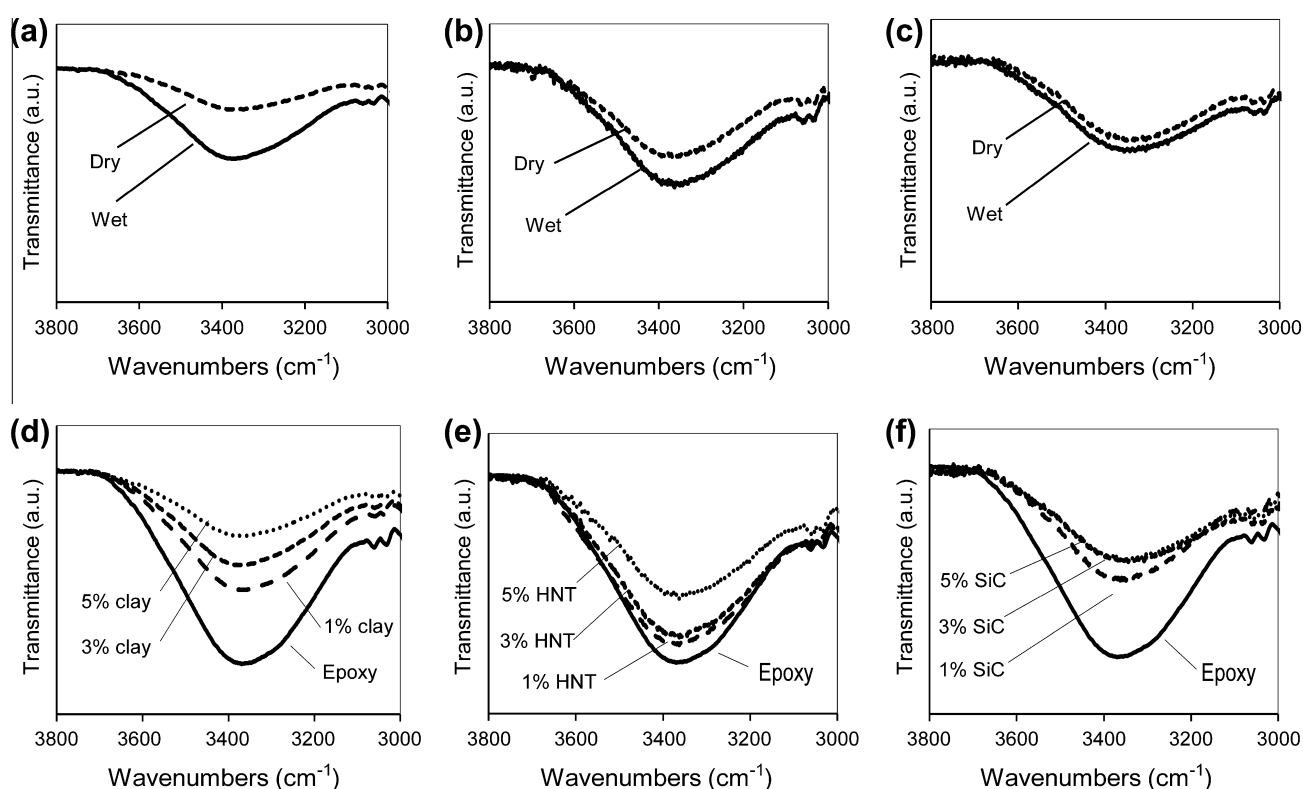
Fig. 3. FT-IR (3000–3800 cm^{-1}) of epoxy-based nanocomposites (a) dry and wet nanoclay/epoxy, (b) dry and wet HNT/epoxy, (c) dry and wet n-SiC/epoxy, (d) wet nanoclay/ epoxy series, (e) wet HNT/epoxy series, and (f) wet n-SiC/epoxy series.

Table 5
Flexural strength and modulus of epoxy and its nanocomposites before and after water treatment.

Samples	Before placing in water		After placing in water	
	Flexural strength (MPa)	Flexural modulus (GPa)	Flexural strength (MPa)	Flexural modulus (GPa)
Epoxy	58.5 ± 2.6	0.9 ± 0.1	51.4 ± 3.1	0.7 ± 0.2
+1% nanoclay	85.2 ± 2.5	1.6 ± 0.4	52.6 ± 4.3	1.3 ± 0.2
+3% nanoclay	58.7 ± 3.9	1.5 ± 0.1	52.7 ± 4.3	1.3 ± 0.2
+5% nanoclay	61.2 ± 3.5	1.4 ± 0.2	53.0 ± 3.9	1.3 ± 0.2
+1% HNT	70.7 ± 6.2	1.5 ± 0.2	55.8 ± 6.5	1.4 ± 0.2
+3% HNT	68.2 ± 8.1	1.3 ± 0.1	52.5 ± 4.9	1.3 ± 0.2
+5% HNT	64.5 ± 4.7	1.4 ± 0.2	53.1 ± 3.5	1.4 ± 0.2
+1% n-SiC	71.1 ± 3.2	1.6 ± 0.3	59.8 ± 4.3	1.4 ± 0.3
+3% n-SiC	66.3 ± 2.9	1.4 ± 0.2	56.5 ± 5.8	1.3 ± 0.3
+5% n-SiC	61.9 ± 3.2	1.4 ± 0.1	54.5 ± 3.4	1.4 ± 0.3

Table 6
Fracture toughness and impact strength of epoxy and its nanocomposites before and after water treatment.

Samples	Before placing in water		After placing in water	
	Fracture toughness (MPa m$^{1/2}$)	Impact strength (kJ/m^2)	Fracture toughness (MPa.m$^{1/2}$)	Impact strength (kJ/m^2)
Epoxy	0.9 ± 0.1	5.6 ± 0.7	1.3 ± 0.2	6.2 ± 1.4
+1% nanoclay	1.1 ± 0.1	6.1 ± 1.3	1.4 ± 0.3	7.4 ± 1.5
+3% nanoclay	0.9 ± 0.1	6.9 ± 1.4	1.4 ± 0.2	6.6 ± 1.5
+5% nanoclay	1.0 ± 0.2	7.8 ± 2.7	1.3 ± 0.3	7.3 ± 1.7
+1% HNT	1.3 ± 0.2	5.6 ± 1.1	1.7 ± 0.2	6.5 ± 1.8
+3% HNT	1.0 ± 0.1	6.4 ± 0.7	1.6 ± 0.5	6.3 ± 1.8
+5% HNT	1.2 ± 0.1	7.0 ± 0.9	1.3 ± 0.3	6.2 ± 1.5
+1% n-SiC	1.6 ± 0.3	7.5 ± 1.1	2.2 ± 0.3	9.1 ± 1.8
+3% n-SiC	1.2 ± 0.2	7.0 ± 0.8	2.1 ± 0.3	7.9 ± 2.2
+5% n-SiC	1.1 ± 0.1	7.6 ± 1.2	1.9 ± 0.3	8.2 ± 1.4
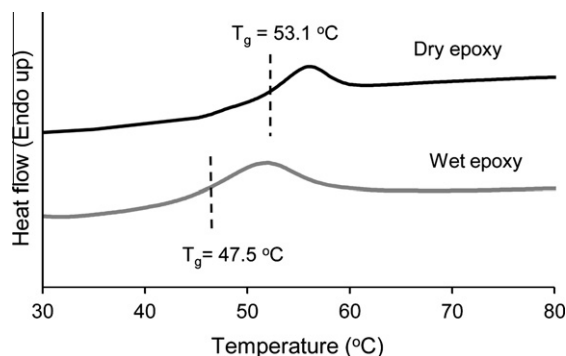
Fig. 4. The DSC curves of neat epoxy before and after water treatment.

ites reinforced with 1, 3 and 5 wt.% n-SiC increases by 34.1, 67.2 and 76.4%, respectively, when compared to dry nanocomposites.

The effect of nano-filler addition on the fracture toughness of wet epoxy based nanocomposites was studied. All types of nano-composites show similar fracture toughness trend. A maximum value achieved at 1 wt.% filler loading, followed by a decrease in fracture toughness value with further increase in filler content. Fracture toughness of composites filled with 1 wt.% of nanoclay, HNT and n-SiC increases by 10.6, 36.7 and 70.3%, respectively, compared to wet unfilled epoxy matrix. Nanocomposites reinforced with n-SiC particles show better fracture toughness than other nanocomposites. The enhancement in fracture toughness can be attributed to the increased resistance to crack propagation via number of possible toughness mechanisms such as crack pinning, crack deflection, particle-debonding, plastic void growth, plastic deformation and particle-pullout [13]. Similarly, Buehler and Seferis [32] reported an increase in fracture toughness of carbon fibre/epoxy composites after placement in water medium for 1200 h. Plasticization effect of water and increased fibre bridging were reported to be the reasons of the enhancement in fracture toughness.
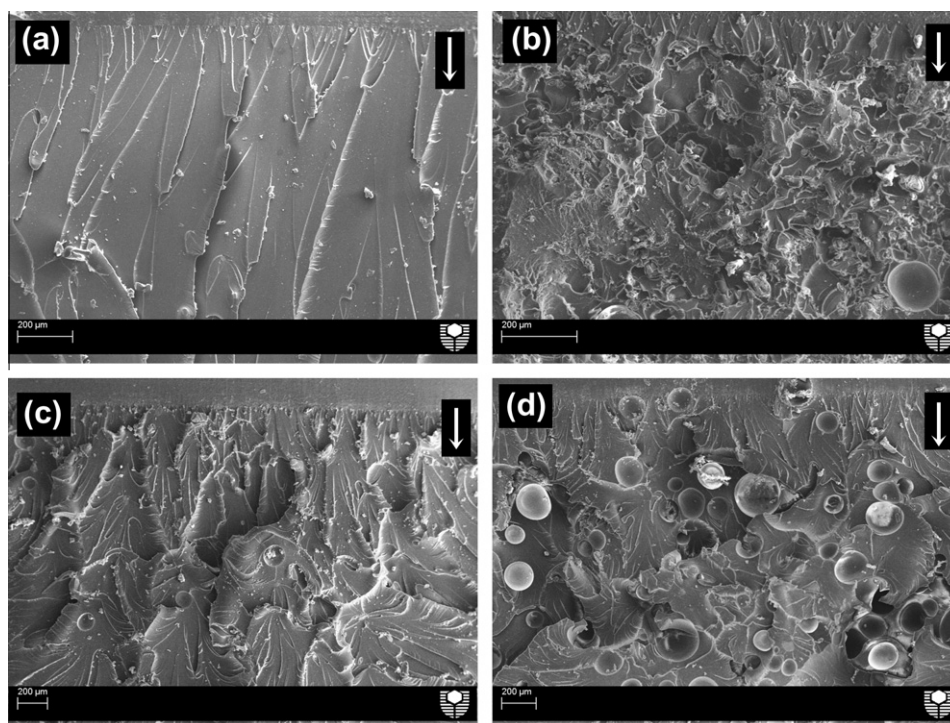
Fig. 5. SEM images showing the details of fracture surfaces for: (a) unfilled epoxy, (b) epoxy/nanoclay 5 wt.%, (c) epoxy/HNT 5 wt.%, and (d) epoxy/n-SiC 5 wt.%. [White arrow indicates the direction of crack propagation.]
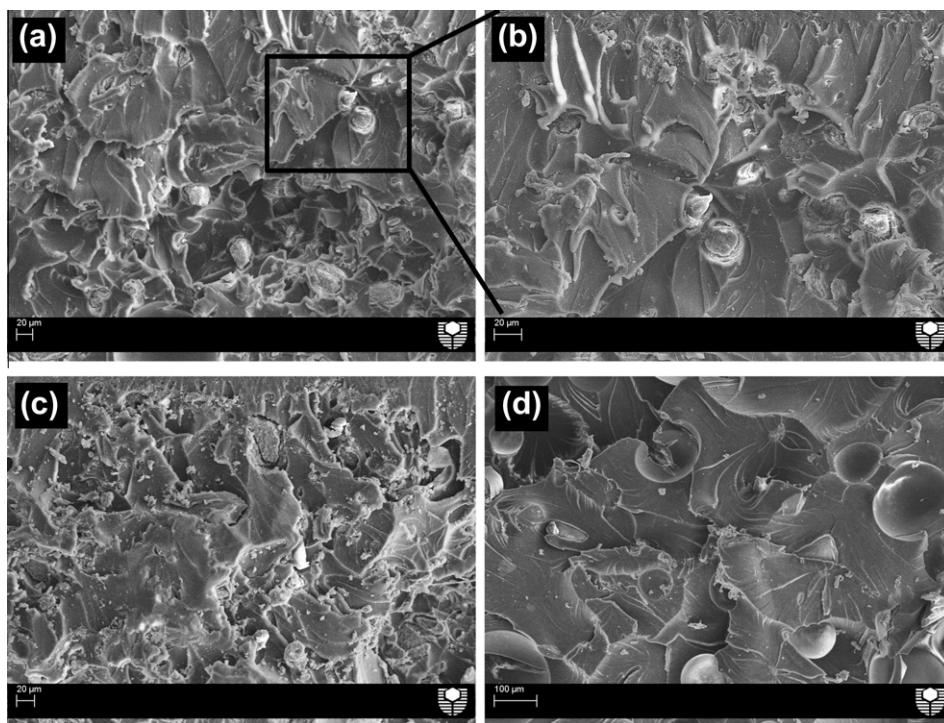
Fig. 6. SEM images showing the details of fracture surfaces e for epoxy-based nanocomposites filled with nanoclay (a and b), HNT (c), and n-SiC (d).

3.4.3. Impact strength

The effect of water absorption on the impact strength of nano-filler reinforced epoxy nanocomposites is presented in Table 6. It can be seen that nanocomposites filled with either nanoclay or HNT show no clear trend of the influence of water on impact strength. For nanocomposites filled with n-SiC, a significant increase in impact strength can be observed due to water absorption. In the case of wet condition, the impact strength of epoxy matrix increases due to the presence of nano-fillers. The increase in impact strength is more pronounced for nanocomposites modified with n-SiC particles. For all types of nanocomposites, reinforcing with 1 wt.% of nano-filler displays the highest value compared to other fillers content. Impact strength of nanocomposites reinforced with 1 wt.% of nanoclay, HNT and n-SiC increases by 20.0, 4.9 and 46.1%, respectively, compared to wet unfilled epoxy matrix. The increase in impact strength is due to the increase in the flexibility of the epoxy chains as a result of the plasticization action of the absorbed water [36]. Low and co-worker [37] reported an increase in impact strength for recycled cellulose fibre reinforced epoxy composites due to the plasticization effect of sea water.

3.5. SEM observation

The SEM micrographs of fracture surfaces of the water treated epoxy and epoxy based nanocomposites are shown in Figs. 5 and 6. Fig. 5a–d is low magnification images for unfilled epoxy and epoxy filled with nanoclay, HNT and n-SiC, respectively. All types of samples show different degree of surface roughness. The surface of neat epoxy displays lower roughness than nanocomposites as seen in Fig. 5a. River markings can be clearly observed for neat epoxy with quite smooth fracture surface indicating very fast and straight crack propagation [13]. However, it is evident that the presence of nano-fillers increases the roughness of the fracture surfaces. An increase in fracture surface roughness is an indicator of crack deflection mechanism, which increases the absorbed energy of fracture by increasing the crack length during deformation [13].

The formation of micro-voids are more pronounced in n-SiC nanocomposites. It was reported that the presence of micro-voids led to increase in fracture toughness [13]. This serves to explain why nanocomposites filled with n-SiC particles exhibited the highest fracture toughness among other nanocomposites.

Fig. 6a–d shows high magnification SEM images of epoxy nanocomposites filled with nanoclay, HNT and n-SiC. In general, several toughness mechanisms such as crack deflection, crack pinning, particle debonding, plastic void growth, plastic deformation and particle pullouts can be observed. Such toughness mechanisms can increase the energy dissipated by resisting crack propagation during deformation, which lead to an increase in fracture toughness values [13]. Close observation of Figs. 5 and 6 indicates that crack deflection and plastic deformation due to the presence of clay clusters are the dominant toughening mechanisms for nanocomposites filled with nanoclay [11]. For nanocomposites filled with HNT, crack deflection and crack pinning and bowing are the main toughening mechanisms [38]. In the case of nanocomposites filled with n-SiC, Figs. 5d and 6d show the existence of micro-voids, which reveals that the plastic deformation of the matrix around the voids and the crack deflection due to the presence of these voids are primary toughening mechanisms.

4. Conclusions

The effect of water absorption on the mechanical properties of nano-filler reinforced epoxy nanocomposites was studied. The influence of the nano-filler such as nanoclay platelet, HNT and n-SiC on enhancing the mechanical and barrier properties of epoxy based nanocomposites in wet condition was also investigated. Results indicated that the presence of nano-filler into epoxy matrix led to significant reduction in both water uptake and diffusion coefficients (D). This reduction was attributed to the tortuosity path created by the addition of the nano-fillers. Flexural strength and modulus of all types of nanocomposites decreased due to the plasticization effect of the water uptake compared to dry

147

nanocomposites. However, fracture toughness and impact strength were found to increase as a result to water absorption. Water treatment increased the mobility of the epoxy chain, which led to increase the ductility of the epoxy matrix resulting in enhancing the toughness of the composites.

The addition of nanoclay, HNT and n-SiC particles improved the mechanical properties of the nanocomposites after exposing to water compared to neat epoxy in same condition. The reinforcement with 1 wt.% nano-filler showed better mechanical properties than other filler content. The enhancement in barrier and mechanical properties of nanocomposites were more pronounced for nanocomposites filled with n-SiC than those filled with nanoclay platelet and halloysite nanotubes.

Acknowledgments

References

[1] Alamri H, Low IM. Mechanical and fracture properties of nano-filler-cellulose fibre-reinforced epoxy nanocomposites. In: Teh K, Davies I, Howard I, editors. Proceedings of the 6th Australasian congress on applied mechanics. Perth, WA: Engineers Australia; 2010. p. 1278–86.
[2] Mirmohseni A, Zavareh S. Preparation and characterization of an epoxy nanocomposite toughened by a combination of thermoplastic, layered and particulate nano-fillers. Mater Des 2010;31:2699–706.
[3] Shukla DK, Kasisomayajula SV, Parameswaran V. Epoxy composites using functionalized alumina platelets as reinforcements. Compos Sci Technol 2008;68:3055–63.
[4] Shokrieh MM, Kefayati AR, Chitsazzadeh M. Fabrication and mechanical properties of clay/epoxy nanocomposite and its polymer concrete. Mater Des 2012;40:443–52.
[5] Luo JJ, Daniel IM. Characterization and modelling of mechanical behaviour of polymer/clay nanocomposites. Compos Sci Technol 2003;63:1607–16.
[6] Pavlidou S, Papaspyrides CD. A review on polymer–layered silicate nanocomposites. Prog Polym Sci 2008;33(12):1119–98.
[7] Hussain F, Hojjati M, Okamoto M, Gorga RE. Review article: polymer-matrix nanocomposites, processing, manufacturing, and application: an overview. J Compos Mater 2006;40(17):1511–75.
[8] Gao F. Clay/polymer composites: the story. Mater Today 2004;7(11):50–5.
[9] Kaynak C, Nakas GI, Isitman NA. Mechanical properties, flammability and char morphology of epoxy resin/montmorillonite nanocomposites. Appl Clay Sci 2009;46(3):319–24.
[10] Manfredi LB, De Santis H, Vázquez A. Influence of the addition of montmorillonite to the matrix of unidirectional glass fibre/epoxy composites on their mechanical and water absorption properties. Compos Part A: Appl Sci Manuf 2008;39(11):1726–31.
[11] Tang Y, Deng S, Ye L, Yang C, Yuan Q, Zhang J. Effects of unfolded and intercalated halloysites on mechanical properties of halloysite–epoxy nanocomposites. Compos Part A: Appl Sci Manuf 2011;42(4):345–54.
[12] Wetzel B, Rosso P, Haupert F, Friedrich K. Epoxy nanocomposites – fracture and toughening mechanisms. Eng Fract Mech 2006;73(16):2375–98.
[13] Alamri H, Low IM. Microstructural, mechanical and thermal characteristics of recycled cellulose fiber-halloysite–epoxy hybrid nanocomposites. Polym Compos 2012;33:589–600.
[14] Technical Information of Sigma–Aldrich Co. LLC. Available from: <http://www.sigmaaldrich.com/australia.html>, 2011.
[15] Yasmin A, Abot JL, Daniel IM. Processing of clay/epoxy nanocomposites by shear mixing. Sci Mater 2003;49:81–6.
[16] Kim JK, Hu C, Woo R, Sham ML. Moisture barrier characteristics of organoclay–epoxy nanocomposites. Compos Sci Technol 2005;65:805–13.
[17] Mohan TP, Kanny K. Water barrier properties of nanoclay filled sisal fibre reinforced epoxy composites. Compos Part A: Appl Sci Manuf 2011;42(4):385–93.
[18] Low IM, McGrath M, Lawrence D, Schmidt P, Lane J, Latella BA. Mechanical and fracture properties of cellulose fibre reinforced epoxy laminates. Compos Part A 2007;38:963–74.
[19] Becker O, Varley RJ, Simon GP. Thermal stability and water uptake of high performance epoxy layered silicate nanocomposites. Euro Polym J 2004;40:187–95.
[20] Liu W, Hoa SV, Pugh M. Fracture toughness and water uptake of high-performance epoxy/nanoclay nanocomposites. Compos Sci Technol 2005;65:2364–73.
[21] Zhao H, Li RKY. Effect of water absorption on the mechanical and dielectric properties of nano-alumina filled epoxy nanocomposites. Compos: Part A 2008;39:602–11.
[22] Lasagabaster A, Abad MJ, Barral L, Ares A, Bouza R. Application of FTIR spectroscopy to determine transport properties and water–polymer interactions in polypropylene (PP)/poly(ethylene-co-vinyl alcohol) (EVOH) blend films: Effect of poly(ethylene-co-vinyl alcohol) content and water activity. Polymer 2009;50:2981–9.
[23] Tserki V, Zafeiropoulos NE, Simon F, Panayiotou C. A study of the effect of acetylation and propionylation surface treatments on natural fibres. Compos: Part A 2005;36:1110–8.
[24] Pasbakhsh P, Ismail H, Fauzi M, Abu Bakar A. EPDM/modified halloysite nanocomposites. Appl Clay Sci 2010;48:405–13.
[25] Chozhan CK, Alagar M, Sharmila RJ, Gnanasundaram P. Thermo mechanical behaviour of unsaturated polyester toughened epoxy–clay hybrid nanocomposites. J Polym Res 2007;14:319–28.
[26] Nikolic G, Zlatkovic S, Cakic M, Cakic S, Lacnjevac C, Rajic Z. Fast Fourier transform IR characterization of epoxy GY systems crosslinked with aliphatic and cycloaliphatic EH polyamine adducts. Sensors 2010;10:684–96.
[27] Liu M, Guo B, Du M, Cai X, Jia D. Properties of halloysite nanotube–epoxy resin hybrids and the interfacial reactions in the systems. Nanotechnol 2007;18:455703.
[28] Zhou T, Wang X, Mingyuan G, Liu X. Study of the thermal conduction mechanism of nano-SiC/ DGEBA/EMI-2,4 composites. Polymer 2008;49:4666–72.
[29] Ramadan AR, Esawi AM, Gawad AA. Effect of ball milling on the structure of Na+-montmorillonite and organo-montmorillonite (cloisite 30B). Appl Clay Sci 2010;47:196–202.
[30] Lee JH, Rhee KY, Lee JH. Effects of moisture absorption and surface modification using 3-aminopropyltriethoxysilane on the tensile and fracture characteristics of MWCNT/epoxy nanocomposites. Appl Surf Sci 2010;256:7658–67.
[31] Abacha N, Kubouchi M, Tsuda K, Sakai T. Performance of epoxy-nanocomposite under corrosive environment. Exp Polym Lett 2007;1(6):364–9.
[32] Buehler FU, Seferis JC. Effect of reinforcement and solvent content on moisture absorption in epoxy composite materials. Compos: Part A 2000;31:741–8.
[33] Hossain MK, Imran KA, Hosur MV, Jeelani S. Degradation of mechanical properties of conventional and nanophased carbon–epoxy composites in seawater. J Eng Mater Technol 2011;133(4):41004.
[34] Wang L, Wang K, Chen L, He C, Zhang Y. Hydrothermal effects on the thermomechanical properties of high performance epoxy/clay nanocomposites. Polym Eng Sci 2006;46(2):215–21.
[36] Sombatsompop N, Chaochanchaikul K. Effect of moisture content on mechanical properties, thermal and structural stability and extrudate texture of poly(vinyl chloride)/wood sawdust composites. Polym Int 2004;53:1210–8.
[37] Low IM, Somers J, Kho HS, Davies IJ, Latella BA. Fabrication and properties of recycled cellulose fibre-reinforced epoxy composites. Compos Inter 2009;16:659–69.
[38] Sánchez-Soto M, Pagés P, Lacorte T, Briceño K, Carrasco F. Curing FTIR study and mechanical characterization of glass bead filled trifunctional epoxy composites. Compo Sci Technol 2007;67:1974–85.

Alamri, H., and I. M. Low. 2012. Effect of water absorption on the mechanical properties of n-SiC filled recycled cellulose fibre reinforced epoxy eco-nanocomposites. *Polymer Testing* 31(6): 810-818.

POLYMER
TESTING

200th Issue

Editor
ROGER BROWN
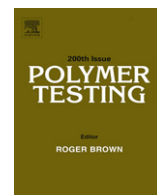
Material properties

Effect of water absorption on the mechanical properties of n-SiC filled recycled cellulose fibre reinforced epoxy eco-nanocomposites

H. Alamri, I.M. Low*

Department of Imaging & Applied Physics, Curtin University, GPO Box U1987, Perth, WA 6845, Australia

ABSTRACT

The effect of the addition of n-SiC particles on water absorption of n-SiC reinforced RCF/epoxy eco-nanocomposites was studied. Results indicated that water uptake decreased as n-SiC content increased. This was also shown by FTIR observation. The effect of water absorption on the mechanical properties of n-SiC filled RCF/epoxy eco-nanocomposites was investigated as a function of n-SiC content. Due to water absorption, flexural strength, flexural modulus and fracture toughness of n-SiC filled RCF/epoxy eco-nanocomposites significantly decreased compared to dry composites. The effect of n-SiC on these mechanical properties was found to be positive. Flexural strength, flexural modulus and fracture toughness increased by 14.4, 7.5 and 6.1%, respectively, compared to unfilled RCF/epoxy composites after the addition of 5 wt% n-SiC. SEM results showed clean pull out of cellulose fibres as a result of degradation in fibre-matrix interfacial bonding by water absorption. The addition of n-SiC was found to enhance the interfacial adhesion between fibre and matrix.

© 2012 Published by Elsevier Ltd.

1. Introduction

The use of natural fibres such as bamboo, wood, kenaf, cotton, coconut husk, oil palm, jute and hemp as fillers in polymer composites for making eco-friendly and low cost engineering materials has gained much interest in recent years. In the environment conscious present times, natural fibre dispersed polymer composites are being given a lot of research attention, not only because they are pose no harm to the environment but also because of they can be easily reproduced as replacements for the non-renewable reinforcing materials such as glass, carbon and Kevlar fibre. More stringent environmental safety regulations and consumer demands in the automotive, construction, and packaging industries have made research on natural fibre composites more significant [1–3]. Natural fibre

composites offer exceptional mechanical properties, low density, low cost and good chemical resistance. The more conventional glass and other reinforcing materials can be replaced or substituted by natural fibres such as hemp, jute, wood, and even waste cellulose products in the automotive, construction and packaging industries due to their desirable qualities such as stiffness, impact resistance, flexibility and modulus [2–5]. Also, their ready availability in large quantities, their biodegradability and renewable nature are much appreciated in these industries. Additional properties such as low density, low cost, less equipment abrasion, less irritation of skin and respiration, damping of vibrations and recovery of more energy have made these composites very welcome in various industries as good alternatives to the traditional synthetic fibre composites [3,5].

However, one of the major drawbacks that have limited the use of plant fibres as reinforcement in polymer composites is their susceptibility to moisture absorption which, in turn, can lead to swelling of the fibre, forming voids and micro-cracks at the fibre-matrix interface region,

---

* Corresponding author.
  E-mail address: j.low@curtin.edu.au (I.M. Low).

150

resulting in reduction of mechanical properties and dimensional stability of composites [6,7]. Cellulose fibres are hydrophilic in nature and they tend to absorb or attract water, the amount depending on the environmental conditions. The chemical reason for this is due the presence of hydroxyl groups in the cellulose structure which attracts water molecules and binds them through hydrogen bonding [8–11].

Several studies have reported an enhancement in fibre-matrix interfacial bonding and fibre resistance to moisture as well as composites mechanical properties via various chemical treatments [7,12–14]. In this study, a novel approach will be used to improve the resistance of cellulose fibre reinforced polymer composites to water absorption and to enhance the mechanical properties of these composites in extreme wet conditions by introducing a second phase that has good resistance to water diffusion, such as nano-silicon carbide (n-SiC) particles. It was reported that the incorporation of small amount of nano-filler such as nanoclay led to increase in the barrier properties of nanocomposites against oxygen, nitrogen, carbon dioxide, water vapour, gasoline and reduces the water uptake [15–17]. This improvement in the barrier properties is attributed to the large aspect ratio of the nanoclay layers, which increases the tortuous path of the gas and water molecules that permeate through the material.

In this work, nano-silicon carbide (n-SiC) will be used as nano-filler to enhance the moisture barrier and mechanical properties of RCF/epoxy composites in extreme wet conditions. This study is a part of a large project on enhancing the mechanical, thermal and barrier properties of n-SiC/RCF reinforced epoxy eco-nanocomposites. In our earlier work, we studied the mechanical and thermal properties of hybrid RCF/n-SiC reinforced epoxy eco-nanocomposites [18]. Results indicated that the addition of n-SiC particles to RCF/epoxy composites led to an increase in flexural modulus, impact strength, fracture toughness and impact toughness compared to unfilled RCF/epoxy composites. Flexural strength increased after the addition of only 1 wt% n-SiC. However, increased addition of SiC resulted to a decline in flexural strength. In comparison to unfilled RCF/epoxy composites, the addition of 5 wt% n-SiC displayed optimum increase in fracture toughness (by 10.4%), impact strength (by 21.2%) and impact toughness (by 41.4%). The addition of n-SiC to RCF/epoxy composites was found to increase the thermal stability by increasing the char yield of composites at high temperatures. However, the rate of degradation increased after adding n-SiC to RCF/epoxy composites by decreasing the maximum decomposition temperatures by about 8 °C compared to unfilled RCF/epoxy composites [18].

In this study, the effect of water absorption for six months on the mechanical properties of n-SiC filled RCF/epoxy eco-nanocomposites has been studied in terms of flexural strength, flexural modulus, fracture toughness and impact strength. The role of n-SiC addition on enhancing mechanical and moisture barrier properties of RCF/epoxy eco-nanocomposites has been investigated. Fourier transforms infrared spectroscopy (FTIR) has been used to observe the change in the (OH) stretching vibration and (OH) bending vibration of n-SiC filled RCF/epoxy composites due to the water absorption. Scanning electron microscopy (SEM) has been used to observe the effect of water absorption on the fibre strength and fibre-matrix interfacial bonding.

2. Materials and methods

2.1. Materials and samples preparation

Recycled cellulose-fibre (RCF) paper and nano-silicon carbide (n-SiC) particles were used as reinforcements for the fabrication of n-SiC/RCF/epoxy nano-ecocomposites. General purpose low viscosity epoxy resin (FR-251) was used as a matrix. For fabrication, n-SiC particles were pre-dried at 50 °C for 30 min, then a mixture of n-SiC and epoxy was prepared by mixing the epoxy resin with three different weight percentages (1, 3 and 5%) of n-SiC particles using a high speed mechanical mixer for 10 min at a rotation speed of 1200 rpm. After that, a hardener (Isophorone-diamine) was added to the mixture and stirred slowly to minimise the formation of air bubbles within the sample. The RCF sheets were first heated at 70 °C for 60 min in order to get rid of the absorbed moisture. Then, RCF sheets were fully-soaked in the mixture of n-SiC/epoxy until they became entirely wetted then laid down in a closed silicone mould under 8.2 kPa compressive pressure and left for 24 h to cure at room temperature. The amount of RCF in the final products was about 48 wt%. More details about materials and fabrication are available in [18].

2.2. Microstructure characterization

Transmission electron microscopy was performed on a Titan Cryotwin (FEI Company) equipped with a 4 k × 4 k CCD camera (Gatan) at an acceleration voltage of 300 kV. Ultra-thin sections (~80 nm) of samples were prepared using an ultra-microtome (Leica microsystem) and were recovered on a copper grid. TEM was carried out at King Abdullah University of Science and Technology (KAUST), Saudi Arabia.

FTIR spectra of n-SiC filled RCF/epoxy eco-nanocomposites in both dry and wet conditions was performed on a Perkin Elmer Spectrum 100 FTIR spectrometer in the region of 4000-600 cm^{-1} at room temperature. Each spectrum was the average of 10 scans at a resolution of 2 cm^{-1} and corrected for the background.

Scanning electron microscopy imaging was obtained using a Zeiss Evo 40XVP. The SEM investigation was carried out in detail on the fracture surfaces of n-SiC filled RCF/epoxy eco-nanocomposites. Specimens were coated with a thin layer of gold before observation by SEM to avoid charging.

2.3. Physical and mechanical characterizations

Water absorption test was carried out by immersing samples with dimensions 10 mm × 10 mm × 3.5 mm in a water bath at room temperature for about 133 days. The weight gain of the samples was measured periodically using a digital scale (AA-200, Denver Instrument Company, USA). Each sample was first removed from the water and dried with a tissue before weighting, and then immersed again in the water bath for the next measurement. Three

specimens from each formulation were used for water absorption measurements.

Five rectangular specimens of each composition with dimensions 60 mm × 10 mm × 6 mm were cut from the fully cured samples for three-point bend and Charpy impact tests. Flexural strength, flexural modulus and fracture toughness of the composites were determined using three-point bending test performed on a Twin Column Bench Mounted Lloyd Material Testing Machine – (5-50 kN). A span of 40 mm was used during the test with a displacement rate of 1.0 mm/min. Fracture toughness was evaluated using single edge notch bending (SENB) specimens [18].

Flexural strength (σ_F) and flexural modulus (E_F) were computed using the following equations:

$$\sigma_F = \frac{3}{2}\frac{p_m S}{WD^2} \tag{1}$$

$$E_F = \frac{S^3}{4WD^3}\left(\frac{\Delta P}{\Delta X}\right) \tag{2}$$

where P_m is the maximum load at crack extension, S is the span of the sample, D is the specimen thickness and W is the specimen width. $\Delta P/\Delta X$ is the initial slope of the load–displacement curve.

Fracture toughness (K_{IC}) was calculated using the following equation according to [19].

$$K_{IC} = \frac{p_m S}{WD^{2/3}}f\left(\frac{a}{w}\right) \tag{3}$$

where a is the crack length, and $f(a/w)$ is the polynomial geometrical correction factor give as

Impact strength was measured using a Zwick Charpy impact tester with 1.0 J pendulum hammer. Un-notched

found to increase with increasing filler content. As mentioned in our previous work [18], the increase in matrix viscosity due to the increase in filler content was the reason behind the presence of particles agglomeration in composites. More details can be found in [18].

3.2. Water absorption behaviour

The amount of absorbed water in the composites M_t was determined using the following equation:

$$M_t(\%) = \left(\frac{W_t - W_o}{W_o}\right) \times 100 \tag{6}$$

where, W_t is the weight of the sample at time t and W_o is the initial weight of the sample.

The effect of the addition of n-SiC particles on the water absorption behaviour of the RCF/epoxy eco-nanocomposites is plotted in Fig. 2. It can be observed that all composites display identical curves. This implies that the addition of n-SiC has no effect on the basic mechanism of water diffusion in RCF/epoxy composites. A similar observation was reported by Zhao and Li [20] for water absorption of nano-Al$_2$O$_3$ filled epoxy nanocomposites. For all composites, water uptake continuously increases with increasing time of immersion. However, water absorption is found to decrease gradually due to the presence of n-SiC. It was reported that the presence of high aspect ratio nano-filler in polymer matrix enhances the barrier properties of the materials by creating tortuous pathways for water molecules to diffuse into the composites, which leads to a reduction in absorbed water [20,21]. Maximum water uptake of RCF/epoxy composites filled with 5 wt% n-SiC decreases by 47.5% compared to unfilled RCF/epoxy composites. Similarly, Mohan and Kanny [15] reported a dramatic decrease in water mass uptake of nanoclay filled sisal fibre/epoxy composites.

The water absorption behaviour in the composites can

$$f\left(\frac{a}{W}\right) = \frac{3(a/W)^{1/2}\left[1.99 - (a/W)(1 - a/W) \times (2.15 - 3.93a/W + 2.7a^2/W^2)\right]}{2(1 + 2a/W)(1 - a/W)^{2/3}} \tag{4}$$

impact strength was evaluated using the following formula:

$$\sigma_I = \frac{E}{A} \tag{5}$$

where E is the impact energy to break a sample with a ligament of area A.

3. Results and discussion

3.1. TEM observations

Fig. 1a and b shows the dispersion of 1 and 5 wt% n-SiC inside the epoxy matrix. The TEM results indicate that the dispersion of n-SiC particles in the epoxy matrix was fairly homogenous with some particle agglomerations that were

be studied as Fickian behaviour. Therefore, the following formula has been used for short immersion times [15,22]:

$$\frac{M_t}{M_\infty} = 4\left(\frac{Dt}{\pi h^2}\right)^{1/2} \tag{7}$$

where, M_t is the moisture content at time t, M_∞ is the equilibrium moisture content, D is the diffusion coefficient and h is the sample thickness. Therefore, the diffusivity D can be determined from the initial slope of the moisture absorption versus the square root of time:

$$D = \frac{\pi}{16}\left(\frac{M_t/M_\infty}{\sqrt{t}/h}\right)^2 \tag{8}$$

152
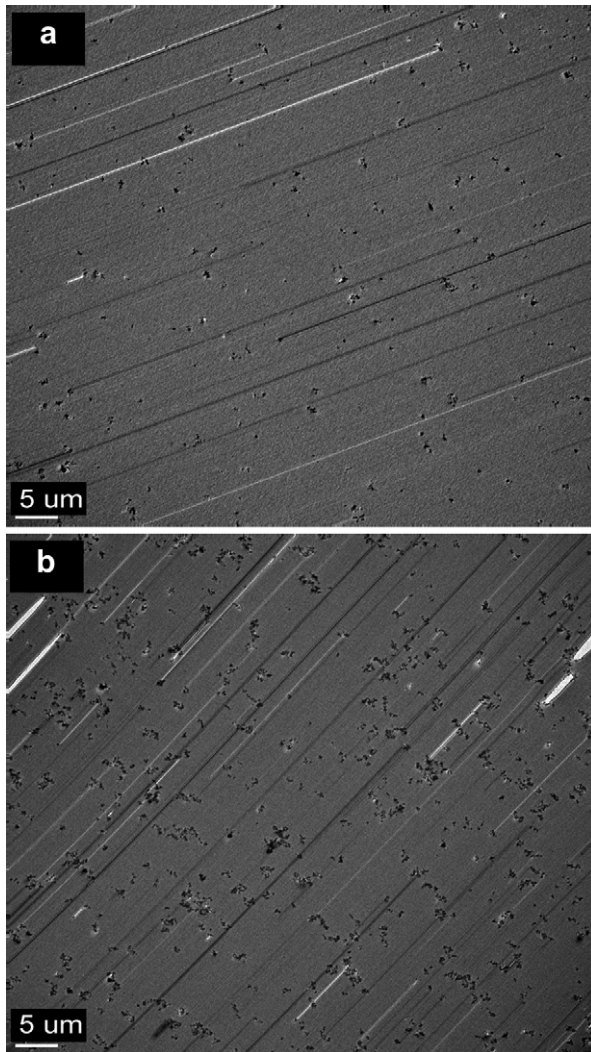
Fig. 1. TEM images of epoxy-based nanocomposites filled with (a) 1 wt% n-SiC and (b) 5 wt% n-SiC.

Table 1
Maximum water uptake and diffusion coefficient (D) of n-SiC filled RCF/epoxy eco-nanocomposite.

Samples	$M\infty$ (%)	$D \times 10^{-06}$ (mm²/sec)
RCF/epoxy	23.28	4.26
1% n-SiC/RCF/epoxy	17.51	6.06
3% n-SiC/RCF/epoxy	16.14	5.28
5% n-SiC/RCF/epoxy	12.23	4.19

The maximum water absorption and diffusion coefficient of RCF/epoxy composites filled with (0, 1, 3 and 5 wt%) n-SiC are presented in Table 1. It can be observed that the diffusivity increases after the addition of 1 wt% n-SiC, and then
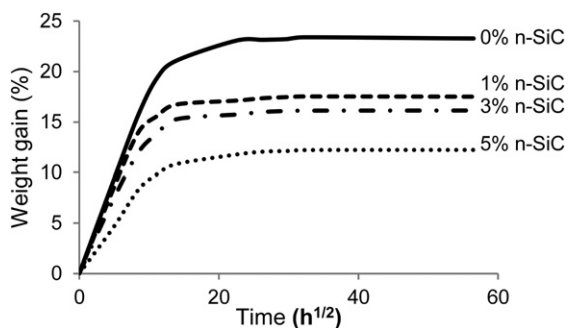
Fig. 2. Water absorption curves of n-SiC filled RCF/epoxy eco-nanocomposites.

decreases as filler content increases. For example, the diffusivity of 5 wt% n-SiC filled composites decreased by 30.9% compared to 1 wt% n-SiC filled composites. This significant reduction in diffusion coefficients may be attributed to increase in the tortuosity of diffusion path created by higher n-SiC content [21].

3.3. FTIR observation

The effect of the moisture absorption on the (OH) stretching vibration and (OH) bending vibration of dry and wet n-SiC filled RCF/epoxy eco-nanocomposites was investigated by FTIR. Fig. 3a displays the FTIR spectra of 3 wt% n-SiC filled RCF/epoxy composites in dry and wet conditions. The FTIR spectra show a broad peak in the region between 3335 and 3280 cm^{-1} which relates to the stretching vibration of the hydroxyl groups (OH) of both un-associated water (higher frequency peak) and strongly bound water (lower frequency peak) [23,24]. Other sign of water absorption can be seen in the peak at 1642 cm^{-1}, which belongs to in-plane (OH) bending vibration. The effect of water absorption on these peaks is clearly seen in the FTIR spectra in Fig. 3a. It can be observed that the peaks of (OH) stretching and bending vibration at 3335 and 1642 cm^{-1}, respectively, increase significantly due to the water absorption. This remarkable increase is expected due to the presence of RCF in the composites, since cellulose fibre is hydrophilic in nature and tends to absorb a large amount of water in wet conditions [22].

Fig. 3b displays the fundamental OH stretching vibration and OH bending vibration of wet RCF/epoxy composites filled with 1, 3 and 5 wt% n-SiC. It can be seen that the intensity of the fundamental OH peak gradually decreases with increasing n-SiC content. Maximum reduction is observed for composites filled with 5 wt% n-SiC. This reduction in water absorption is attributed to the enhancement in composites barrier properties due to the presence of nano-filler. Moreover, the absorption peak of OH stretching vibration for 5 wt% filled RCF/epoxy composites is moved to higher wave number centred at 3400 cm^{-1}. This indicates an increase in free OH groups, where water molecules are indirectly bonded to the hydroxyl groups through another water molecule [25]. A similar observation was reported for bamboo husk fibre treated by silane coupling agents [25].

3.4. Effect of water absorption on the mechanical properties of n-SiC filled RCF/epoxy eco-nanocomposites

The effect of water absorption on the mechanical properties of RCF/epoxy composites filled with n-SiC
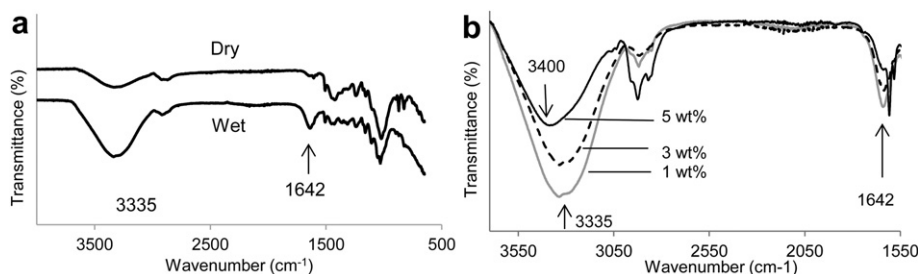
Fig. 3. FTIR spectra of (a) 3 wt% n-SiC filled RCF/epoxy eco-nanocomposites in dry and wet conditions and (b) n-SiC filled RCF/epoxy eco-nanocomposites in wet condition.

particles was investigated after water treatment for 6 months at room temperature and compared with the same composites in dry conditions. The data for the composites in dry conditions are reported here only for the purpose of benchmarking. More details about the mechanical and thermal properties of n-SiC filled RCF/epoxy eco-nanocomposites in dry conditions can be found in [18].

3.4.1. Stress-strain behaviour

Fig. 4 illustrates the typical flexural stress-strain curves for unfilled RCF/epoxy and 5 wt% n-SiC filled RCF/epoxy composites before and after placing in water. It can be seen that the addition of n-SiC particles decreases the maximum stress of RCF/epoxy composites in dry conditions. However, the presence of n-SiC leads to increase in maximum stress after water treatment. It also can be seen that flexural properties for both types of composites severely decrease due to the water absorption. The significant drop in maximum stress after water treatment can be attributed to the fibre damage and degradation in fibre-matrix interfacial bonding due to the absorbed water [10]. Maximum bending strain of the composites is found to increase significantly due to water absorption. Water molecules act as a plasticizer agent in fibre reinforced composites leading to an increase in materials ductility, which results in increase in maximum strain [6,10,20].

3.4.2. Flexural strength

Fig. 5 illustrates the effect of water absorption on the flexural strength of n-SiC filled RCF/epoxy eco-nanocomposites. It can be clearly seen that flexural
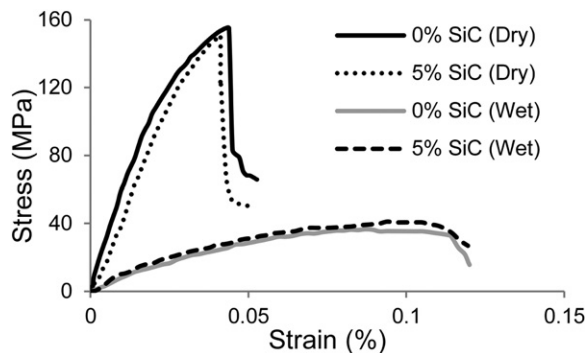
Fig. 4. Typical stress-strain curves of RCF/epoxy composites filled with 0 and 5 wt% n-SiC in dry and wet conditions.

strength significantly dropped due to the water absorption for all composites. In comparison to dry composites, flexural strength of composites filled with 1 and 5 wt% n-SiC decreased by 77.4 and 73.3%, respectively, after immersing in water for six months. This significant reduction in flexural strength is attributed to severe damage to the bonding at the fibre-matrix interface due to the water absorption, which leads to reduction in stress transfer between matrix and fibre, thus resulting in low flexural strength [6,22]. Similar reduction in flexural strength due to water absorption was observed by Athijayamani et al. [26] where they reported a reduction in flexural strength ranged from 5.7% to 21.7% for polyester matrix reinforced with different loading (10, 20 and 30 wt%) and length (50, 100 and 150 mm) of roselle and sisal fibres. In a previous study [22], we investigated the effect of water absorption for two weeks on the flexural strength of RCF/epoxy composites as a function of fibre content. Results indicated that flexural strength decreased as fibre content increased due to the water absorption [22].

The effect of n-SiC on enhancing flexural strength of RCF/epoxy composites in wet conditions was investigated and shown in Fig. 5 (dark bars). It can be observed that the presence of n-SiC particles leads to a slight enhancement in flexural strength. In particular, composites filled with 3 and 5 wt% n-SiC display an increase in flexural strength by 16.4 and 14.4% over unfilled RCF/epoxy composites. This enhancement in flexural strength is attributed to the presence of the nano-particles increasing the interfacial bonding between the fibre and matrix. Also, the addition of n-SiC reduces the effect of water absorption on the mechanical properties of the composites by increasing the water absorption resistance. Interestingly, in dry conditions, the flexural strength was found to decrease with n-SiC content [18]. However, in wet conditions, it is found to increase as n-SiC content increases.

3.4.3. Flexural modulus

Fig. 6 displays the flexural modulus of n-SiC filled RCF/epoxy eco-nanocomposites as a function of n-SiC content in dry and wet conditions. It can be seen that all wet composites display very low flexural modulus when compared to the same composites in dry conditions. Flexural modulus of RCF/epoxy composites filled with 0, 1, 3 and 5 wt% n-SiC significantly decrease by 82.7, 81.7, 81.4 and 81.5%, respectively, compared to dry composites. This drop in modulus values could be attributed to the increase in ductility due to plasticization by absorbed water, as
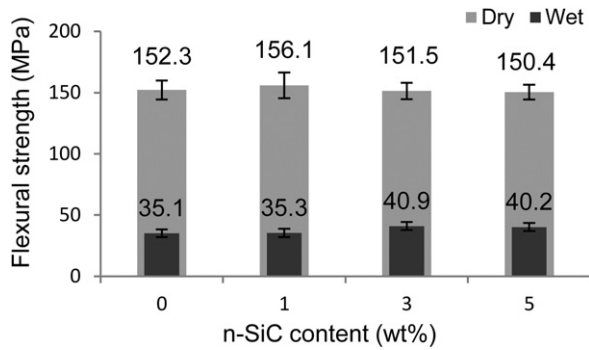
Fig. 5. Flexural strength of n-SiC filled RCF/epoxy eco-nanocomposites in dry and wet conditions.

Fig. 7. Fracture toughness of n-SiC filled RCF/epoxy eco-nanocomposites in dry and wet conditions.

reported by Zhao and Li [20] and Dhakal et al. [6]. In our previous work [22], we reported a reduction in flexural strength of RCF/epoxy composites reinforced with 46 wt% RCF by 17.1 after immersing in water for 2 weeks compared to dry composites.

The effect of n-SiC on the flexural modulus of wet n-SiC filled RCF/epoxy eco-nanocomposites is displayed in Fig. 6 (dark bars). It can be seen that the addition of n-SiC has a positive influence on the flexural modulus. This result is expected due to the fact that the presence of rigid nano-particle in the matrix can reduce the ductility of the matrix by restricting the mobility of polymer chains under loading, resulting in enhancement in n-SiC filled composites modulus [15]. The enhancement in flexural modulus of n-SiC filled composites can be considered insignificant when compared to unfilled composites. For instance, the addition of 5 wt% n-SiC increases flexural modulus by a maximum of 7.5% over unfilled composites.

3.4.4. Fracture toughness

The effect of water absorption on the fracture toughness of n-SiC filled RCF/epoxy eco-nanocomposites is plotted in Fig. 7 as a function of n-SiC content and compared to the same composites in dry conditions. It can be seen that fracture toughness of all types of composites considerably decreases compared to dry composites. The percentage reduction in fracture toughness of unfilled RCF/epoxy and
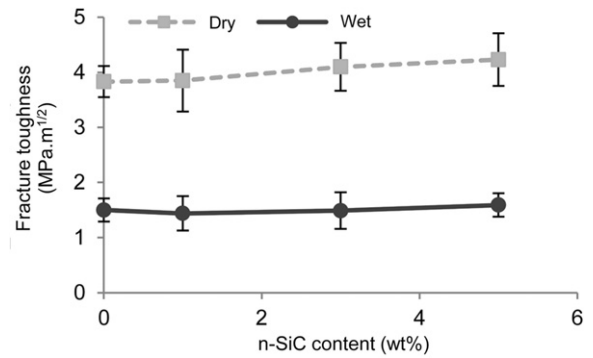
5 wt% n-SiC filled RCF/epoxy composites is 62.1 and 62.4%, respectively, compared to the same composites in dry conditions. The reason behind this significant drop in fracture toughness is due to the severe damage in fibre structure and interfacial bonding between fibre and matrix resulting from absorbed water. Water absorption causes swelling of fibres, which could create micro-cracks in the sample and eventually lead to failure [6,26]. Moreover, water molecules can diffuse into the fibre-matrix interfaces through these micro-cracks, which results in debonding and weakening at the fibre-matrix interface [10,15,26]. Kim and Seo [10] reported a decrease in fracture toughness of sisal fibre/epoxy composites as a function of increasing water treatment. Likewise, in our previous study we reported a decrease in fracture toughness of water treated RCF/epoxy composites with increasing fibre content [22].

The effect of n-SiC on the fracture toughness of RCF/ composites in wet conditions is shown in Fig. 7. In general, it can be observed that fracture toughness of n-SiC filled composites increases gradually as filler content increases. At low filler content (i.e. 1 wt%) fracture toughness decreases by about 4% compared to unfilled RCF/epoxy composites. However, the addition of 5 wt% n-SiC increases fracture toughness by 6.1% compared to unfilled composites. This enhancement in fracture toughness can be attributed to the increased resistance to crack propagation via a number of possible toughness mechanisms such as crack pinning, crack deflection, particle-debonding, plastic void growth, plastic deformation and particle-pullout [18].

3.4.5. Impact strength

Fig. 8 illustrates the effect of n-SiC particles on the impact strength of RCF/epoxy composites under wet conditions. It can be seen that due to the water absorption, unfilled and 1 wt% n-SiC filled RCF/epoxy composites unexpectedly display better impact strength than same composites in dry conditions. Compared to dry composites, it was observed that all composites exhibited partial fracture during Charpy tests. This non-brittle fracture implies an increase in the ductility of the matrix. Sombatsompop and Chaochanchaikul [27] observed an increase in impact strength of PVC/wood sawdust composites due to water absorption. They reported that the absorption of water led to the formation of hydrogen bonding between water molecules and fibres resulted in

Fig. 6. Flexural modulus of n-SiC filled RCF/epoxy eco-nanocomposites in dry and wet conditions.
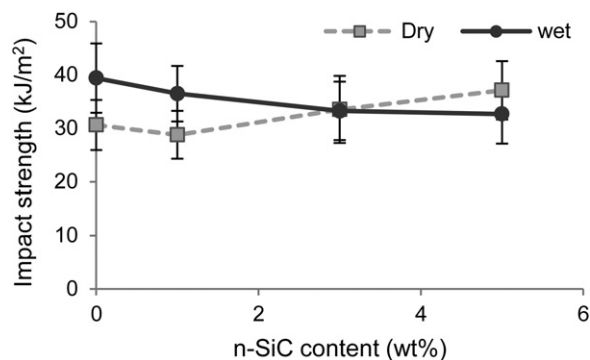
Fig. 8. Impact strength of n-SiC filled RCF/epoxy eco-nanocomposites in dry and wet conditions.

reduction in the dipole–dipole interaction between fibre and matrix molecules, which in turn increased the flexibility of matrix chain resulting in increase in impact strength. Moreover, water absorption can cause fibre swelling, which in turn increases fibre resistance to impact energy [6]. In our previous work [22], we reported an increase in impact

strength of cellulose fibre/epoxy composites as fibre content increased after water treatment for two weeks. Similarly, Karmaker [28] observed an enhancement in impact strength of jute fibre reinforced polypropylene composites after immersing in water for two weeks.

The addition of n-SiC is found to reduce the impact strength of n-SiC filled composites compared to unfilled composites. This result indicates that the ability of n-SiC filled composites to absorb impact energy decreases with increasing nano-filler content. In wet conditions, the impact strength of 5 wt% n-SiC filled epoxy composites decreases by 17% compared to unfilled RCF/epoxy composites. This reduction in impact strength could be attributed to decrease in polymer chain mobility due to the presence of nano-filler [15]. It is interesting to observe that the effect of n-SiC on the impact properties of n-SiC filled RCF/epoxy composites in wet conditions is completely different from the dry condition as can be seen in Fig. 8.

3.5. SEM observation

The SEM images in Fig. 9 (a & b) show the fracture surfaces of dry and wet 5 wt% n-SiC filled RCF/epoxy eco-
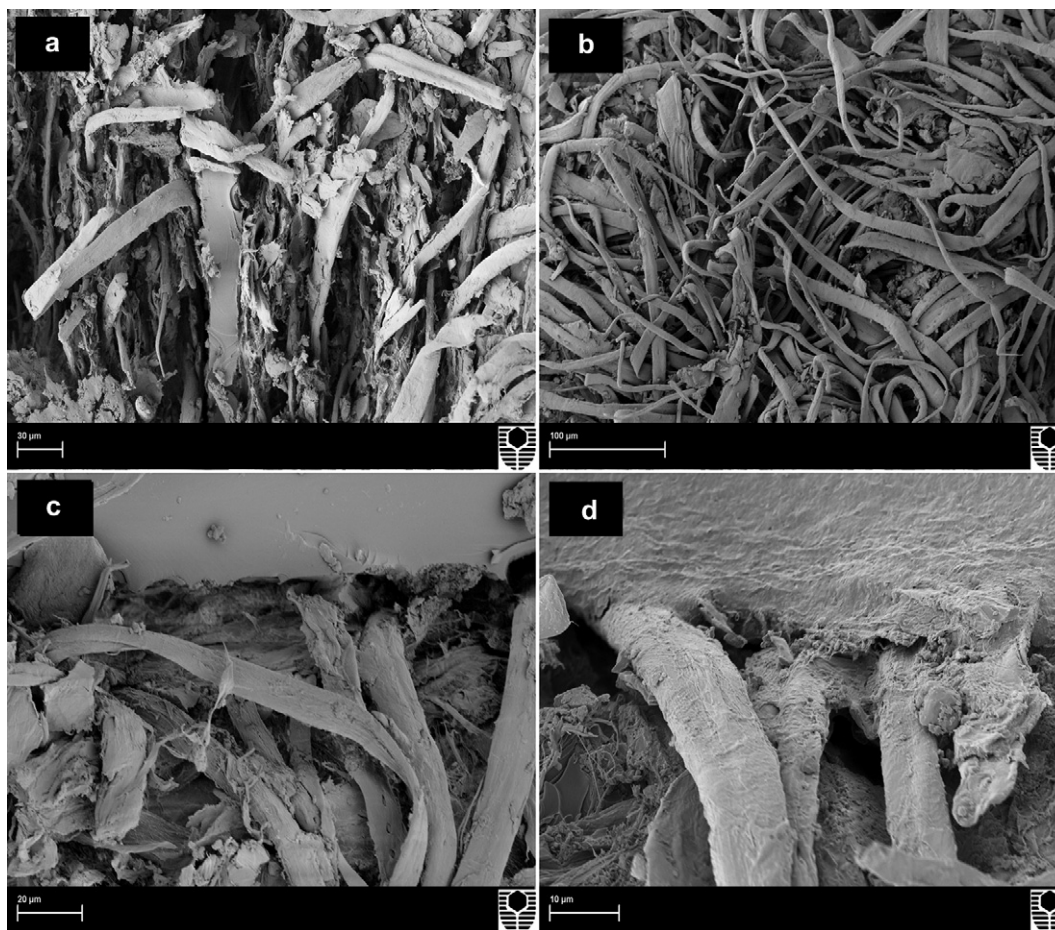
Fig. 9. SEM images showing the details of fracture surface for (a) 5 wt% n-SiC filled RCF/epoxy in dry condition, (b) 5 wt% n-SiC filled RCF/epoxy in wet condition, (c) RCF/epoxy in wet condition, and (d) 5 wt% n-SiC filled RCF/epoxy in wet condition.

nanocomposites, respectively. It can be seen that dry specimen displays rougher fracture surface with clear features, while the wet specimen displays smoother fracture with damaged and overlapped fibres. This means that water absorption reduces the strength of the fibres in wet composites and could eventually lead to failure. Moreover, fibre fracture can be easily seen in dry specimens while it is difficult to see in wet composites. However, the presence of unbroken fibres in wet composites after fracture reveals that fibres were easily pulled out from the matrix, which implies lack of adhesion between fibre and matrix.

Fig. 9 (c & d) displays SEM images of unfilled RCF/epoxy composite and 5 wt% n-SiC filled RCF/epoxy eco-nanocomposite after water treatment. It is can be seen that water absorption severely degraded the interfacial adhesion between the fibres and the matrix by substituting the strong covalent bonds with weaker hydrogen bonds [10]. As a result, fibre debonding (characterized by the appearance of gap between fibre and matrix) is clear evidence of weak fibre-matrix interfacial adhesion in the structure of wet composites. However, the presence of n-SiC particles leads to enhancement in the interfacial bonding between the fibre and matrix, as can be seen in Fig. 5d. Therefore, the presence of nano-filler plays an important role in improving the adhesion between fibre and matrix and hence enhances the mechanical properties of the composites.

4. Conclusions

The effect of water absorption on the mechanical properties of n-SiC filled RCF/epoxy eco-nanocomposites was studied. The influence of n-SiC particles on enhancing the mechanical and barrier properties of RCF/epoxy composites in wet conditions was investigated. Results indicated that maximum water uptake of n-SiC filled RCF/epoxy eco-nanocomposites decreased with increasing n-SiC content due to enhancement in composite barrier properties. Maximum reduction in water uptake and diffusivity occurred at 5 wt% n-SiC loading. The role of n-SiC addition in enhancing composites barrier properties was also evidenced by FTIR observation.

Exposure to water for six months was found to severely reduce flexural strength, flexural modulus and fracture toughness of unfilled and n-SiC filled RCF/epoxy composites. For example, significant drop in flexural strength by 73.3%, flexural modulus by 81.5% and fracture toughness by 62.41% for composites filled with 5 wt% n-SiC compared to the same composites in dry condition. These reductions are attributed to the degradation of bonding at the fibre–matrix interfaces and to the damage in the fibre strength and structure.

The effect of n-SiC on enhancing the mechanical properties of RCF/epoxy composites in wet conditions was investigated. In general, the edition of n-SiC was found to increase the flexural strength, modulus and fracture toughness of RCF/epoxy composites in wet conditions. The introduction of only 5 wt% n-SiC increased flexural strength by 14.4%, flexural modulus by 7.5%, and fracture toughness by 6.1% over unfilled RCF/epoxy composites. The increase in these mechanical properties is due to the ability of n-SiC to enhance the fibre-matrix interfacial boding and resist crack propagation. On the other hand, the presence of n-SiC particles was found to decrease the impact properties. SEM results showed clean pull out of cellulose fibres as a result degradation in fibre-matrix interfacial bonding by water absorption. The presence of nano-filler was found to enhance the adhesion between the fibre and the matrix.

References

[1] M.H. Moeini, S.H. Heidary, I. Amiri, A. Payami, Wood–polyvinyl chloride composite for insulation of electrical wires: fabrication and investigation of properties, Journal of Reinforced Plastics and Composites 29 (2009) 899–908.
[2] D. Bachtiar, S.M. Sapuan, M.M. Hamdan, The effect of alkaline treatment on tensile properties of sugar palm fibre reinforced epoxy composites, Materials and Design 29 (2008) 1285–1290.
[3] P. Wambua, J. Ivens, I. Verpoest, Natural fibres: can they replace glass in fibre reinforced plastics? Composites Science and Technology 63 (2003) 1259–1264.
[4] I.M. De Rosa, C. Santulli, F. Sarasini, Mechanical and thermal characterization of epoxy composites reinforced with random and quasi-unidirectional untreated Phormium tenax leaf fibres, Materials and Design 31 (2010) 2397–2405.
[5] S.S. Nair, S. Wang, D.C. Hurley, Nanoscale characterization of natural fibers and their composites using contact-resonance force microscopy, Composites Part A 41 (2010) 624–631.
[6] H.N. Dhakal, Z.Y. Zhang, M.O.W. Richardson, Effect of water absorption on the mechanical properties of hemp fibre reinforced unsaturated polyester composites, Composites Science and Technology 67 (2007) 1674–1683.
[7] B. Wang, S. Panigrahi, L. Tabil, W. Crerar, Pre-treatment of flax fibers for use in rotationally molded biocomposites, Journal of Reinforced Plastics and Composites 26 (5) (2007) 447–463.
[8] S.O. Han, L.T. Drzal, Water absorption effects on hydrophilic polymer matrix of carboxyl functionalized glucose resin and epoxy resin, European Polymer Journal 39 (9) (2003) 1791–1799.
[9] A.N. Fraga, E. Frullloni, O. de la Osa, J.M. Kenny, A. Vázquez, Relationship between water absorption and dielectric behaviour of natural fibre composite materials, Polymer Testing 25 (2) (2006) 181–187.
[10] H.J. Kim, D.W. Seo, Effect of water absorption fatigue on mechanical properties of sisal textile-reinforced composites, International Journal of Fatigue 28 (2006) 1307–1314.
[11] T. Doan, H. Brodowsky, E. Mader, Jute fibre/polypropylene composites II. Thermal, hydrothermal and dynamic mechanical behaviour, Composites Science and Technology 67 (2007) 2707–2714.
[12] M.A. Shenoy, D.J. D'Melo, Effect of water on mechanical properties of unsaturated polyester-acetylated hydroxypropyl Guar Gum composites, Journal of Reinforced Plastics and Composites 28 (2009) 2561–2576.
[13] M. Hughes, J. Carpenter, C. Hill, Deformation and fracture behaviour of flax fibre reinforced thermosetting polymer matrix composites, Journal of Materials Science 42 (2007) 2499–2511.
[14] H. Wang, K.C. Sheng, T. Lan, M. Adl, X.Q. Qian, S.M. Zhu, Role of surface treatment on water absorption of poly(vinyl chloride) composites reinforced by Phyllostachys pubescens particles, Composites Science and Technology 70 (2010) 847–853.
[15] T.P. Mohan, K. Kanny, Water barrier properties of nanoclay filled sisal fibre reinforced epoxy composites, Composites Part A: Applied Science and Manufacturing 42 (4) (2011) 385–393.
[16] B. Alexandre, D. Langevin, P. Médéric, T. Aubry, H. Couderc, Q.T. Nguyen, A. Saiter, S. Marais, Water barrier properties of polyamide 12/montmorillonite nanocomposite membranes: structure and volume fraction effects, Journal of Membrane Science 328 (1–2) (2009) 186–204.
[17] Y. Zhang, Q. Liu, Q. Zhang, Y. Lu, Gas barrier properties of natural rubber/kaolin composites prepared by melt blending, Applied Clay Science 50 (2) (2010) 255–259.

[18] H. Alamri, I.M. Low, Characterization of epoxy hybrid composites filled with cellulose fibres and nano-SiC, Journal of Applied Polymer Science (2012). http://dx.doi.org/10.1002/app.36815.

[19] I.M. Low, M. McGrath, D. Lawrence, P. Schmidt, J. Lane, B.A. Latella, Mechanical and fracture properties of cellulose fibre reinforced epoxy laminates, Composites: Part A 38 (2007) 963–974.

[20] H. Zhao, R.K.Y. Li, Effect of water absorption on the mechanical and dielectric properties of nano-alumina filled epoxy nanocomposites, Composites: Part A 39 (2008) 602–611.

[21] W. Liu, S.V. Hoa, M. Pugh, Fracture toughness and water uptake of high performance epoxy/nanoclay nanocomposites, Composites Science and Technology 65 (2005) 2364–2373.

[22] H. Alamri, I.M. Low, Mechanical properties and water absorption behaviour of recycled cellulose fibre reinforced epoxy composites, Polymer Testing 31 (5) (2012) 620–628.

[23] T. Karbowiak, E. Ferret, F. Debeaufort, A. Voilley, P. Cayot, Investigation of water transfer across thin layer biopolymer films by infrared spectroscopy, Journal of Membrane Science 370 (2011) 82–90.

[24] A. Lasagabaster, M.J. Abad, L. Barral, A. Ares, R. Bouza, Application of FTIR spectroscopy to determine transport properties and water–polymer interactions in polypropylene (PP)/poly(ethylene-co-vinyl alcohol) (EVOH) blend films: effect of poly(ethylene-co-vinyl alcohol) content and water activity, Polymer 50 (2009) 2981–2989.

[25] Y.F. Shih, Mechanical and thermal properties of waste water bamboo husk fibre reinforced epoxy composites, Materials Science and Engineering A 445–446 (2007) 289–295.

[26] A. Athijayamani, M. Thiruchitrambalam, U. Natarajan, B. Pazhanivel, Effect of moisture absorption on the mechanical properties of randomly oriented natural fibers/polyester hybrid composite, Materials Science and Engineering A 517 (2009) 344–353.

[27] N. Sombatsompop, K. Chaochanchaikul, Effect of moisture content on mechanical properties, thermal and structural stability and extrudate texture of poly(vinyl chloride)/wood sawdust composites, Polymer International 53 (2004) 1210–1218.

[28] C. Karmaker, Effect of water absorption on dimensional stability and impact energy of jute fibre reinforced polypropylene, Journal of Materials Science Letters 16 (1997) 462–464.

3.7 Effect of Water Absorption on the Mechanical Properties of Nanoclay Filled Recycled Cellulose Fibre Reinforced Epoxy Hybrid Nanocomposites.

Alamri, H., and I. M. Low. 2013. Effect of water absorption on the mechanical properties of nanoclay filled recycled cellulose fibre reinforced epoxy hybrid nanocomposites. *Composites Part A: Applied Science and Manufacturing* 44: 23-31.

.

Effect of water absorption on the mechanical properties of nanoclay filled recycled cellulose fibre reinforced epoxy hybrid nanocomposites

H. Alamri, I.M. Low *

Department of Imaging and Applied Physics, Curtin University of Technology, GPO Box U1987, Perth, WA 6845, Australia

A B S T R A C T

Recycled cellulose fibre (RCF) reinforced epoxy/clay nanocomposites were successfully synthesized with different weight percentages (0%, 1%, 3% and 5%) of organoclay platelets (30B). The objective of this study was to investigate the effect of water absorption on the physical and mechanical properties of the RCF reinforced epoxy/clay nanocomposites. TEM images indicated a well-intercalated structure of nanoclay/epoxy matrix with some exfoliated regions. Water absorption was found to decrease as the clay content increased. The flexural strength, flexural modulus and fracture toughness significantly decreased as a result of water absorption. However, the properties of impact strength and impact toughness were found to increase after exposing to water. The addition of nanoclay slightly minimized the effect of moisture on the mechanical properties. SEM images showed that water absorption severely damaged the cellulose fibres and the bonding at fibres–matrix interfaces in wet composites.

Crown Copyright © 2012 Published by Elsevier Ltd. All rights reserved.

1. Introduction

Plant fibres reinforced polymer composites are gaining a great attention in different applications due to their desirable properties, which include low density, low cost, renewability and recyclability as well as good mechanical properties [1–3]. Moreover, due to the increased sensitivity on environmental pollution, manufacturing industries especially packaging, construction and automotive industries have been pressurized by consumers and new environmental legislations to search and utilize new renewable materials in substituting the convectional and non-renewable reinforcing materials, such as glass fibres [1]. Plant fibres have been preferred as they are considered to be environmental friendly (green composites) thus being utilized as a substitute to traditional fibre reinforced petroleum-based composites including aramid fibre, carbon and glass fibres [2,3].

For instance, recycled cellulose fibres (RCFs) obtained from cellulosic waste products such as cardboard, printed paper and recycled newspapers among others are the best alternatives with regard to environmental friendliness as compared to plant reinforcing fibres in composites [4]. RCF reinforced composites are also of great importance when it comes to industrial areas where plants are utilized for technical purposes. RCFs are very attractive reinforcement materials due to their availability in large quantities, flexibility, renewability and their low cost which attracts their use as structural components in future housing industry such as load bearing roof systems, sub-flooring and framing components. These composites could also be used in doors, windows, furniture and automotive industries [3–5].

However, cellulose fibres are hydrophilic in nature and hence have poor resistance for water absorption. High moisture absorption is one of the major drawbacks of cellulose fibre, which restricts the use of cellulose fibre reinforced polymer composites in many outdoors applications. Water absorption can lead to swelling of the fibre forming voids and micro-cracks at the fibre–matrix interface region, which result in a reduction of mechanical properties and dimensional stability of composites [1,6]. Different Physical and chemical treatments have been used in several studies in order to reduce hydrophilic nature of cellulose fibre and hence improve fibres resistance to moisture absorption [7,8].

In recent years, polymer–clay nanocomposites (PCNs) have drawn much attention due to their excellent characteristics such as improvement in physical (shrinkage, optical, dielectrics and permeability), thermal (i.e. thermal expansion coefficient, flammability, decomposition and thermal stability) and mechanical (i.e. toughness, strength and modulus) properties [9–10]. PCNs are an emerging class of organic–inorganic hybrid materials consisting of nanometer-scale (layered and irregular-shaped) inorganic particles dispersed in an organic polymer matrix. Compared to conventional filled-polymers with micron-sized particles, they possess superior specific strength and stiffness, good fire retardant and enhanced barrier properties with the addition of small amount of nanoclay (5 wt.% or less) [10–12]. Many researchers have reported an enhancement in mechanical, thermal, and physical properties of polymeric matrix due to the addition of nanoclay [11–16].

* Corresponding author. Tel.: +61 8 9266 7544; fax: +61 8 9266 2377.
E-mail address: j.low@curtin.edu.au (I.M. Low).

In present study, a novel approach will be used to enhance the resistance of cellulose fibre reinforced polymer composites to water absorption by introducing a second phase that has good resistance to water diffusion such as nanoclay [8]. The incorporation of small amount of nanoclay usually increases the barrier properties of nanocomposites against oxygen, nitrogen, carbon dioxide, water vapor, gasoline and reduces the water uptake [7,11,17]. This improvement in the barrier properties is attributed to the large aspect ratio of the nanoclay layers, which increases the tortuous path of the gas and water molecules that permeate into the material as they diffuse into the nanocomposites.

This study is a part of a larger project on enhancing the mechanical, thermal and barrier properties of hybrid recycled cellulose fibre/nanoclay reinforced epoxy nanocomposites. In our earlier work, we studied the mechanical and thermal properties of hybrid RCF/nanoclay reinforced epoxy composites [18]. This work is focused on the effect of water absorption on the mechanical properties of hybrid RCF/nanoclay reinforced epoxy composites and to investigate the influence of nanoclay additives on water absorption.

2. Experimental procedure

2.1. Raw materials

General purpose low viscosity epoxy resin (FR-251) and epoxy hardener (isophorone-diamine) procured from Fibreglass & Resin Sales Pty Ltd, WA, Perth, Australia was used as a matrix. Recycled cellulose-fibre(RCF) papers with grade 200 GSM and 0.2 mm thickness supplied by Fuji Xerox Australia Pty. Limited, Belmont WA, Australia were used as the primary reinforcement. Finally, organoclay platelets (Cloisite 30B) which is a natural montmorillonite modified with methyl, tallow, bis-2-hydroxyethyl quaternary ammonium chloride provided by Southern Clay Products, United States based company were used as matrix modifier. The specifications and physical properties of Cloisite 30B are outlined in Table 1 [18].

2.2. Samples preparation

RCF reinforced epoxy/organoclay nanocomposites were prepared using RCF paper sheets with 30B nanoclay-filled epoxy. First, a mixture of nanoclay and epoxy were prepared by mixing the epoxy resin with three different weight percentages (1%, 3% and 5%) of nanoclay (Cloiste 30B) using a high speed mechanical mixer for 10 min with a rotation speed of 1200 rpm. After that, a hardener was added to the mixture and then stirred slowly to minimize the formation of air bubbles within the sample. The RCF sheets were heated at 70 °C for 60 min in order to get rid of the absorbent moisture. Then, RCF sheets were fully-soaked into the mixture of epoxy/nanoclay until they became entirely wetted by the mixture then laid down in a closed silicone mould under 8.2 kPa compressive pressure and left 24 h for curing at room temperature. The amount of RCF in the final products was ~50 wt.%.

Table 1
Physical properties of the nanoclay (Cloisite 30B).

Physical properties of Cloisite 30B	
Color	Off white
Density (g/cm^3)	1.98
d-Spacing (0 0 1) (nm)	1.85
Aspect ratio	200–1000
Surface area (m^2/g)	750
Mean particle size (μm)	6

2.3. Characterization

The micro-structure and the dispersion of Cloisite 30B organoclay into epoxy nanocomposites were studied by transmission electron microscopy (TEM). Fourier transforms infrared spectroscopy (FTIR) and Scanning electron microscopy (SEM)

Transmission electron microscopy imaging was done using a Titan Cryotwin (FEI Company) operating at 300 kV equipped with a 4 k × 4 k CCD camera (Gatan). Ultra-thin TEM specimens with thickness of (~80 nm) were prepared at room temperature using an ultramicrotome (Leica microsystem) and were recovered on a copper grid. TEM was carried out at King Abdullah University of Science and Technology (KAUST), Saudi Arabia.

Thin slices of RCF/epoxy composites and nanoclay filled RCF/epoxy nanocomposites were used for the collection of FTIR spectra. A Perkin Elmer Spectrum 100 FTIR spectrometer fitted with a single-bounce diamond/ZnSe ATR accessory was used to record the spectra in the range (4000–500 cm^{-1}) with a resolution of 2 cm^{-1} and 10 scans per sample.

The fracture surfaces and the crack propagation of fracture toughness specimens were investigated using scanning electron microscope (Zeiss Evo 40XVP). Fractured Specimens were coated with a thin layer of gold before the observation by SEM to avoid charging.

2.4. Physical property measurements

The apparent porosity P_a of the samples was studied to measure the ratio of open pores in the material to its bulk volume. The Australian Standard 1774.5, 2001 was used to determine the apparent porosity of samples using the following equation:

$$P_a = \left(\frac{m_s - m_d}{m_s - m_i}\right) \times 100 \tag{1}$$

where m_d is dry mass, m_i is mass of sample immersed in water and measured in water, and m_s is the mass of soaked sample and measured in air. Five specimens of each composition were used for porosity measurements.

Water absorption test was carried out by immersing samples with dimensions 10 mm × 10 mm × 3.5 mm in a water bath at room temperature. The weight gain of the samples was measured periodically. Each sample was dried using a tissue before weighing to remove excess water form sample's surfaces, immediately weighed, and then immersed again in the water bath for next measurement. The percentage of the moisture content (M_t) is determined using the following equation:

$$M_t(\%) = \left(\frac{W_t - W_o}{W_o}\right) \times 100 \tag{2}$$

where W_t is the weight of the sample at time t and W_o is the initial weight of the sample.

The water absorption behavior in the samples can be studied as Fickian behavior. Therefore, for short immersion times the following formula has been used [7,8]:

$$\frac{M_t}{M_\infty} = 4\left(\frac{Dt}{\pi h^2}\right)^{1/2} \tag{3}$$

where M_t is the moisture content at time t, M_∞ is the equilibrium moisture content, D is the diffusion coefficient and h is the sample thickness. Therefore, the diffusivity D can be determined from the initial slope of the moisture absorption versus the square root of time.

161

2.5. Mechanical property measurements

Five rectangular specimens of each composition with dimensions 60 mm × 10 mm × 6 mm were cut from the fully cured samples for mechanical tests.

Flexural strength, flexural modulus and fracture toughness were determined by using three-point bend tests [18]. A LLOYD Material Testing Machines – Twin Column Bench Mounted (5–50 kN) was used with a span of 40 mm and displacement rate of 1.0 mm/min to perform the three-point bend tests. Single edge notch bending (SENB) specimens were used to evaluate the fracture toughness. The ratio of notch length to width (a/w) was about (0.4). A sharp pre-crack was initiated in the notched specimens by tapping a sharp razor blade. Flexural strength (σ_F), flexural modulus (E_F) and fracture toughness (K_{IC}) were computed according to [18].

A Zwick Charpy impact testing with 1.0 J pendulum hammer was used to evaluate the impact strength and impact toughness. Samples were set edgewise for both impact strength and toughness tests. Un-notched samples were used to compute the impact strength using the following formula:

$$\sigma_I = \frac{E}{A} \tag{4}$$

where E is the impact energy to break a sample with a ligament of area A.

Samples of various notch lengths were used to determine the impact toughness of composites. In order to measure the impact toughness, the value of the critical strain energy release rate (G_{IC}) was evaluated as the slope of the fracture energy (U) versus the energy calibration factor (ϕ) as shown in the following equation [18]:

$$U = G_{IC}WD\phi + U_o \tag{5}$$

where U_o is the kinetic energy, W is the specimen width and D is the specimen thickness.

3. Results and discussion

3.1. Morphology of clay/epoxy nanocomposites

In a previous study [18], wide angle X-ray scattering (WAXS) and transmission electron microscopy (TEM) were used to investigate the dispersion of the nanoclay in the resulting epoxy/clay nanocomposites. Results showed an intercalation and homogeneous dispersion of nanoclay platelet with some agglomerations. Based on WAXS results, the basal spacing of (0 0 1) was 3.4 nm compared to 1.85 nm for nanoclay powder [18]. In this study we present more investigation on the nanocomposites structure that used as a matrix for RCF reinforced epoxy/clay nanocomposites. High magnification TEM images of epoxy reinforced with 1 and 5 wt.% nanoclay are shown in Fig. 1a and b. A combination of intercalated and exfoliated clay platelets in epoxy systems can be clearly observed. Fig. 1a shows the intercalation regions where a multi-layered structure of nanoclay is penetrated by the polymer chains as labeled by letter A, and also shows exfoliation regions where single layers of nanoclay are surrounded by the polymer chains (labeled by letter B). Fig. 1b reveals the basal spacing of nanoclay layers in the epoxy matrix. The measured d-spacing ranges from 2.65 to 7.98 nm compared to 1.8 nm of nanoclay platelet. This indicates that in general, the major structure of the nanoclay/epoxy matrix is intercalated with some exfoliated regions. Mixed of intercalated and exfoliated structure was also achieved by Zainuddin et al. [16] in their study of nanoclay/epoxy nanocomposites.

3.2. Porosity

Porosity values of RCF/epoxy and nanoclay filled RCF/epoxy composites are shown in Fig. 2. The dotted line in Fig. 2 represents the porosity of pure epoxy. A significant increase in porosity can be observed for all RCF composites when compared to pure epoxy. The addition of nanoclay shows no significant effect on the porosity of these composites. This significant increase in porosity is due to the presence of RCF which caused creation of fibre–matrix interfacial areas and thus the concomitant formation of voids in the sample [19].

3.3. Water absorption properties

Fig. 3 displays the water absorption results of nanoclay filled and unfilled RCF/epoxy composites. The weight gain of the samples is plotted as a function of square root of time. It can be seen from Fig. 3 that the water uptake continuously increased with the increase in time of immersion for all specimens. Typical Fickian diffusion behaviors are observed for all samples. Water uptake rate is linear and very rapid in the beginning of the exposure, after that, it slows down and reaches the saturation level [1,20].

The presence of RCF sheets dramatically increases the water absorption of RCF reinforced epoxy when compared to pure epoxy
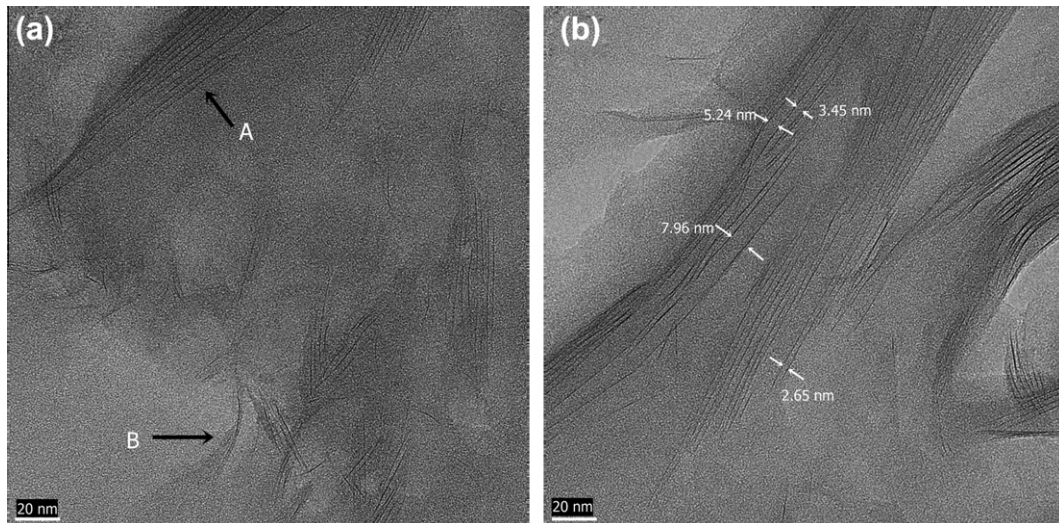
Fig. 1. TEM images of epoxy nanocomposites filled with (a) 1 wt.% and (b) 5 wt.% nanoclay. (Labels A and B indicate intercalated and exfoliated regions respectively.)
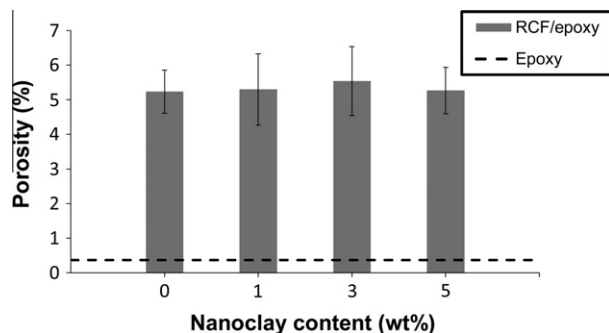
Fig. 2. The porosity of RCF/epoxy based nanocomposites as a function of nanoclay content.
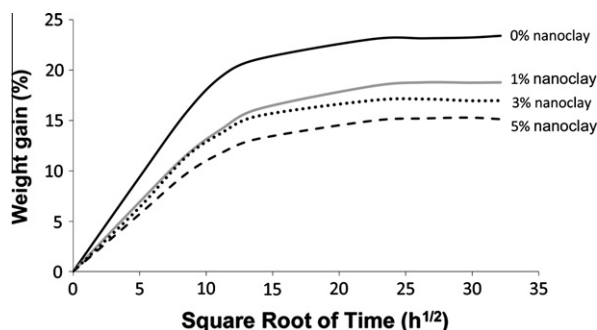
Fig. 3. Water absorption curves of RCF/epoxy and nanoclay filled composites.
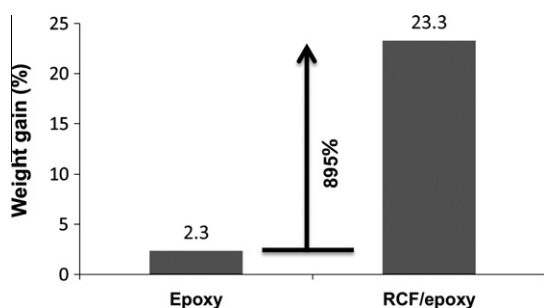
Fig. 4. Maximum water uptake of pure epoxy and RCF/epoxy composites.

(Fig. 4). This result was expected due to the hydrophilic nature of cellulose fibre , which leads to absorbing much water depending on the environmental condition. The chemical reason for this is due the presence of hydroxyl groups in the cellulose structure which attract water molecules, and bind with them through hydrogen bonding [20–22]. Similar observation has been made by Dhakal et al. [1] on hemp fibre reinforced unsaturated polyester composites. Results showed that water uptake increased as hemp fibre content increased.

However, the incorporation of nanoclay effectively decreases the water absorption for nanoclay-filled RCF/epoxy samples compared to unfilled RCF/epoxy samples. The maximum water uptake decreases continuously with increasing clay content. This phenomenon can be attributed to the presence of nanoclay in the RCF/epoxy composites which acts as a barrier medium that hinders the water flow into the composites from all direction, thus resulting in a decreased equilibrium water content as reported in the literature [23–25]. In addition, Mohan and Kanny [7] stated that the maximum water uptake depends on the rate of water flow into the composites rather than on water diffusion, which is measured

Table 2
Maximum water uptake and diffusion coefficient (D) of nanoclay filled RCF/epoxy composites.

Samples	Nanoclay content (wt.%)	$M\infty$ (%)	D (mm²/sec)
RCF/Epoxy	0	23.28	4.26×10^{-06}
RCF/Epoxy	1	18.78	3.52×10^{-06}
RCF/Epoxy	3	17.04	4.00×10^{-06}
RCF/Epoxy	5	15.39	3.66×10^{-06}

along the thickness direction of the sample. The maximum water absorptions and the diffusion coefficient values of unfilled composites and filled composites series are listed in Table 2. It can be observed that the maximum water uptake of RCF/epoxy decreased significantly by about 34% when 5 wt.% nanoclay was added. It can also be observed that the diffusivity of RCF/epoxy composites decreased by 17.4% and 14.1% after the addition of 1 and 5 wt.% nanoclay, respectively.

3.4. FTIR characterization

FTIR spectra of both dry and wet RCF/epoxy composite and 5 wt.% nanoclay filled RCF/epoxy nanocomposites are shown in Fig. 5. The FTIR spectra of all samples show a broad peak in the region between 3340 and 3290 cm^{-1}. This fundamental peak corresponds to the hydroxyl (OH) stretching vibration and is often divided into two peaks. The one with higher frequency is often due to the hydroxyl peak of liquid water and is attributed to un-associated water or loosely bound water, where water indirectly bonded to the hydroxyl groups through another water molecule [26,27]. However, the peak with lower frequency is usually related to strongly bound water, where water directly bonded to the hydroxyl group though hydrogen bonds [26,27]. Other signs of water absorption can be seen in the peaks at around 1642 ± 1 cm^{-1} and 692 cm^{-1}, which correspond to in plane (OH)
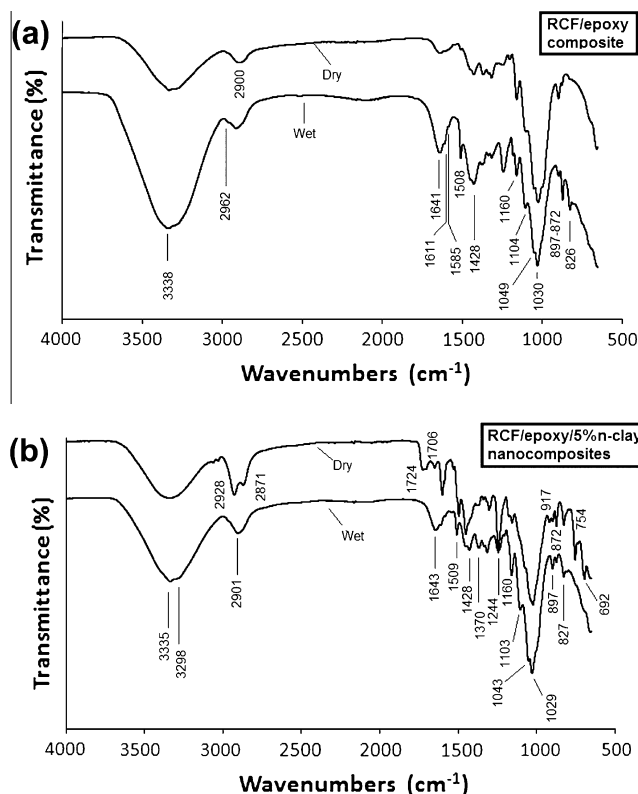
Fig. 5. FTIR analysis for dry and wet RCF/epoxy and 5 wt.% nanoclay filled RCF/epoxy composites.
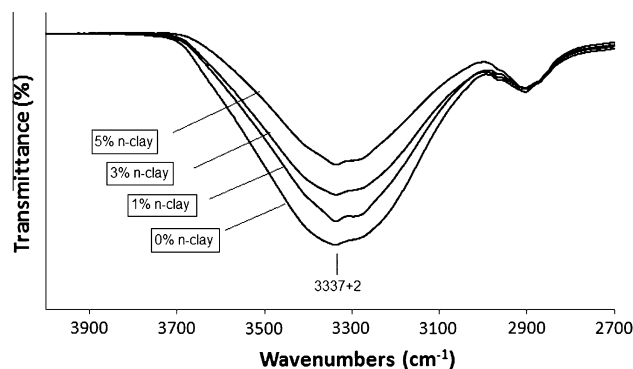
Fig. 6. FT–IR (4000–2700 cm^{-1}) of wet nanoclay filled RCF/epoxy composites.

Fig. 7. Typical stress–strain curves of RCF/epoxy composites filled with 0 and 5 wt.% nanoclay in dry and wet conditions.

bending vibration and out of plane vibrations of O—H group respectively [26,27]. The peak at 2902 ± 2 cm^{-1} is attributed to the (CH) stretching of cellulose fibre [28–30]. This peak is present in all RCF reinforced epoxy composites and nanocomposites due to the presence of CH in the chemical structure of cellulose fibre. The absorption band at 1428 cm^{-1} and 1370 cm^{-1} are assigned to CH$_2$ and CH$_3$ bending vibration of cellulose fibres respectively [26].

In addition, there are numbers of peaks are related to the presence of epoxy group in the composites. For example, the peaks at around 2928 and 2871 cm^{-1} may correspond to asymmetric and symmetric CH$_2$ and CH$_3$ of epoxy resin [31]. The carbonyl group if the epoxide ring produces a peak at 1724 cm^{-1} [28,32]. The FTIR bands at 1607, 1585 and 1508 cm^{-1} are due to the benzene ring of epoxy or C=C stretching of aromatic ring [32]. The peaks at 1243 and 918 cm^{-1} shows the epoxide ring vibration of epoxy resin, which belongs to the stretching absorption of C—O in the epoxide ring [31–33]. Peaks appear in the range of 1160 to 1029 cm^{-1} corresponds to C—O stretching of cellulose fibre and epoxy resin [23]. The 1,4-substitution of aromatic ring is observed at 826 cm^{-1} for epoxy resin [34,35]. Finally, the peak at 753 cm^{-1} is due Si—O—Al symmetric vibration which confirms the formation of nanocomposites (Fig. 5b) [36].

The main objective of using the FTIR spectroscopy was to investigate the effect of nanoclay addition on the water absorption behavior of RCF reinforced epoxy composites. Attention has been focused onto the fundamental OH stretching vibration centerd at 3337 ± 1 cm^{-1}, since this peak indicates the water content. It can be seen from Fig. 6 that the peak of interest at around 3337 cm^{-1} significantly increased for all wet composites due the immersion in water compared to dry composites. The presence of OH groups in the cellulose fibres attracts the water molecule, resulting in significant water absorption.

Fig. 6 illustrates the fundamental OH stretching vibration of wet RCF/epoxy composites filled with 0, 1, 3 and 5 wt.% nanoclay. It can be observed that unfilled RCF/epoxy composite displays the highest peak among other filled RCF/epoxy nanocomposites. The presence of nanoclay effectively reduces the water uptake for nanoclay filled RCF/epoxy composites.

The decrease in water uptake is the result of enhancement in the barrier properties of the nanocomposites due to the presence of high aspect ratio nanoclay platelets. Other interesting observation is that the intensity of the fundamental OH peak gradually decreases as nanoclay content increases with maximum reduction occurred at 5 wt.% nanoclay loading. This result is in agreement with the weight gain study of water absorption in the previous section.

3.5. Effect of moisture absorption on mechanical properties

Typical flexural stress–strain curves for unfilled RCF/epoxy and 5 wt.% nanoclay filled RCF/epoxy nanocomposites before and after
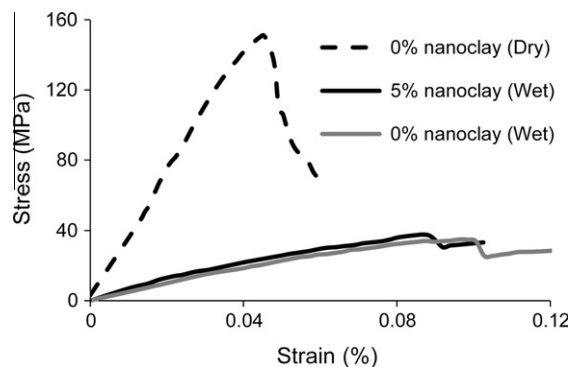
water treatment are shown in Fig. 7. It can be observed that maximum stress for both unfilled RCF/epoxy and nanoclay filled RCF/epoxy composites significantly decrease due to water treatment. This significant drop in stress can be attributed to the degradation in fibre–matrix interfacial bonding due to the water absorption [20]. However, Maximum bending strain of the composites is found to increase significantly due to water absorption. Water molecules act as a plasticizer agent in fibre reinforced composites leading to an increase in materials ductility, which results in increase in maximum strain [20]. The presence of nanoclay slightly enhances the maximum stress after water treatment.

Fig. 8 shows flexural strength for hybrid RCF reinforced epoxy/clay nanocomposites after placement in water medium. It can be seen from Fig. 7 significant drop in flexural strength for wet nanoclay filled and unfilled RCF/epoxy composites compared to dry unfilled RCF/epoxy. Flexural strength of RCF reinforced epoxy decreased by 77% from 152.3 to 35.1 MPa after immersing in water for 6 months. This significant reduction in flexural strength is due to the effect of water absorption in the degradation of fibre–matrix interface region, which in turn reduces stress transferring from matrix to fibres resulting in low flexural strength [1]. However, the presence of nanoclay has a positive effect on enhancing the flexural strength of water-immersed samples. Flexural strength of composites filled with 1 and 5 wt.% nanoclay increases by 11.4 and 6.7% respectively compared to unfilled wet composites.

Flexural modulus results are shown in Fig. 9. Exposure to moisture caused a considerable drop in flexural modulus for wet composites. Flexural modulus of wet RCF/epoxy composites decreased by 82.7% compared to dry RCF/epoxy composites. This reduction in modulus properties is due to the increase in composites ductility as a result of water absorption [24]. However, the incorporation of nanoclay leads to very slight enhancement in flexural modulus when compared to unfilled composites.
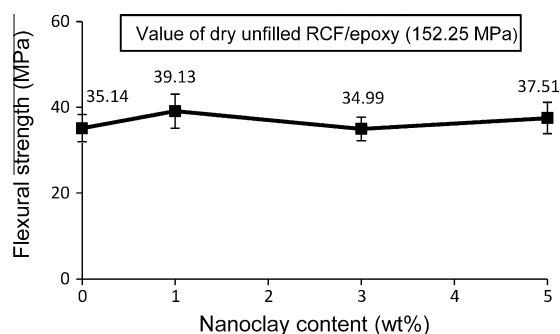
Fig. 8. Flexural strength of wet nanoclay filled RCF/epoxy composites.

164
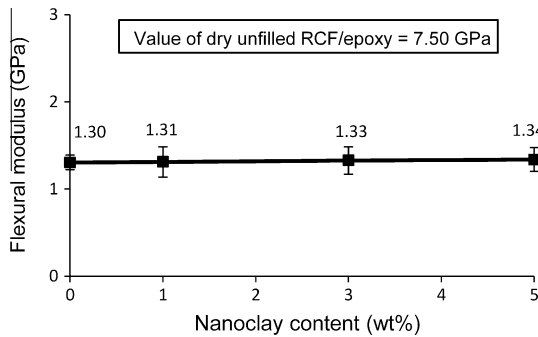
Fig. 9. Flexural modulus of wet nanoclay filled RCF/epoxy composites.
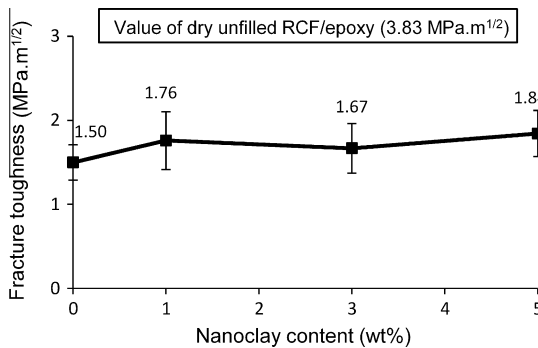
Fig. 11. Un-notched impact strength of wet nanoclay filled RCF/epoxy composites.

Fig. 10. Fracture toughness of wet nanoclay filled RCF/epoxy composites.

Fig. 12. Impact toughness of wet nanoclay filled RCF/epoxy composites.

Fracture toughness of wet RCF/epoxy composites filled with nanoclay is plotted in Fig. 10. Fracture toughness clearly decreased due to the effect of moisture absorption. The reduction in fracture toughness for RCF/epoxy filled with 0, 1, 3 and 5 wt.% nanoclay compared to dry unfilled RCF/epoxy composite is ∼61%, 54%, 56% and 52%, respectively. This substantial reduction in fracture toughness can be explained as, moisture absorption causes swelling of fibres, which could create micro-cracks in the sample and eventually could lead to failure in fracture toughness [1,37]. Moreover, water molecules can diffuse into the fibre–matrix interfaces through these micro-cracks, which result in debonding fibres and weakening the fibre–matrix interface, as proved by SEM images later on [7,20,37].

However, it can be observed that the addition of nanoclay reduced the effect of water absorption on facture toughness by displaying better improvement in toughness properties than those of unfilled RCF/epoxy composites. Fracture toughness of wet composites filled with 1, 3 and 5 wt.% nanoclay increases by 17.3%, 11.3% and 22.5% compared to unfilled wet composites. This enhancement in fracture toughness for wet samples filled with nanoclay can be attributed to the capability of well dispersed nanoclay platelets on crack deflection and stopping tiny cracks from propagation into the matrix [38]. In addition, the high aspect ratio of nanoclay platelet plays an essential role in decreasing water absorption in nanocomposites by introducing tortuous path for water molecules to diffuse and eventually minimizes the effect of moisture absorption on the mechanical properties of nanoclay filled composites.

Un-notched impact strength values of nanoclay filled RCF/epoxy composites after immersing in water are demonstrated in Fig. 11. Interestingly, all wet samples display better impact strength than dry unfilled RCF/epoxy sample. For examples, impact strength of unfilled RCF/epoxy composites increased by 28.6% after exposed to water for 6 months. Similar increase in Un-notched impact strength due to the immersing in water for 14 days of jute fibre/polypropylene composites was reported by Karmaker [39]. The
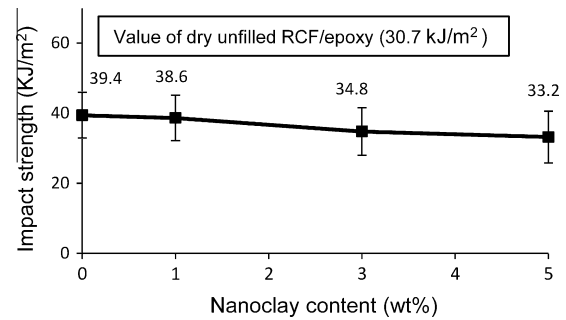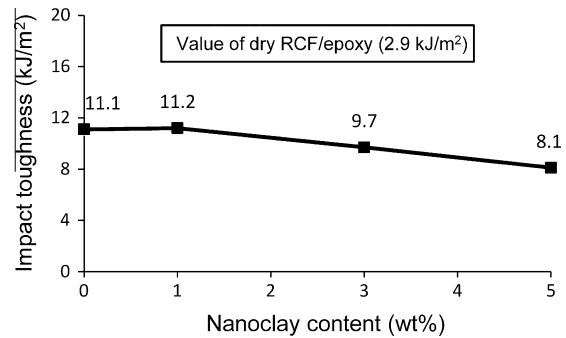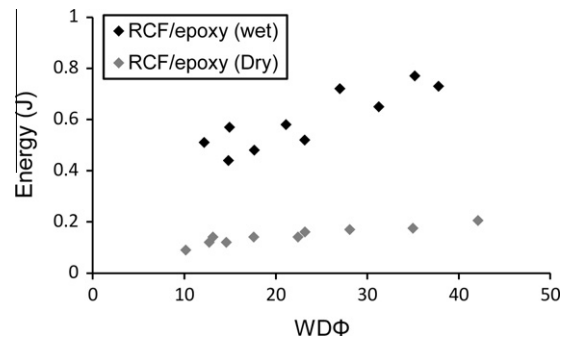
Fig. 13. Fracture energy versus WDΦ for dry and wet RCF/epoxy composites.

increase in impact strength of wet samples can be attributed to the plasticization effect of water absorption on RCF/epoxy composites [1,40]. However, after the addition of nanoclay, impact strength progressively decreases as nanoclay content increases. This result indicates that although the water absorption improves the overall impact energy of nanoclay filled and unfilled RCF/epoxy composite systems, the effect of water absorption on the impact energy is lower when nanoclay is added. This indicates that the presence of nanoclay platelet resists the influence of the plasticization effect of water absorption on composites mechanical properties.

Fig. 12 illustrates the effect of water absorption on impact toughness in terms of energy release rate (G_{IC}) of nanoclay filled RCF reinforced epoxy composites. Similar to impact strength results, impact toughness significantly increases for all samples after immersing in water for 6 months. This improvement in fracture toughness can be attributed to the water plasticization effect on RCF reinforced epoxy composites after the exposure to water. Moreover, water absorption can cause cellulose fibre swelling, which in turn increases fibre resistance to impact energy [1]. A

165
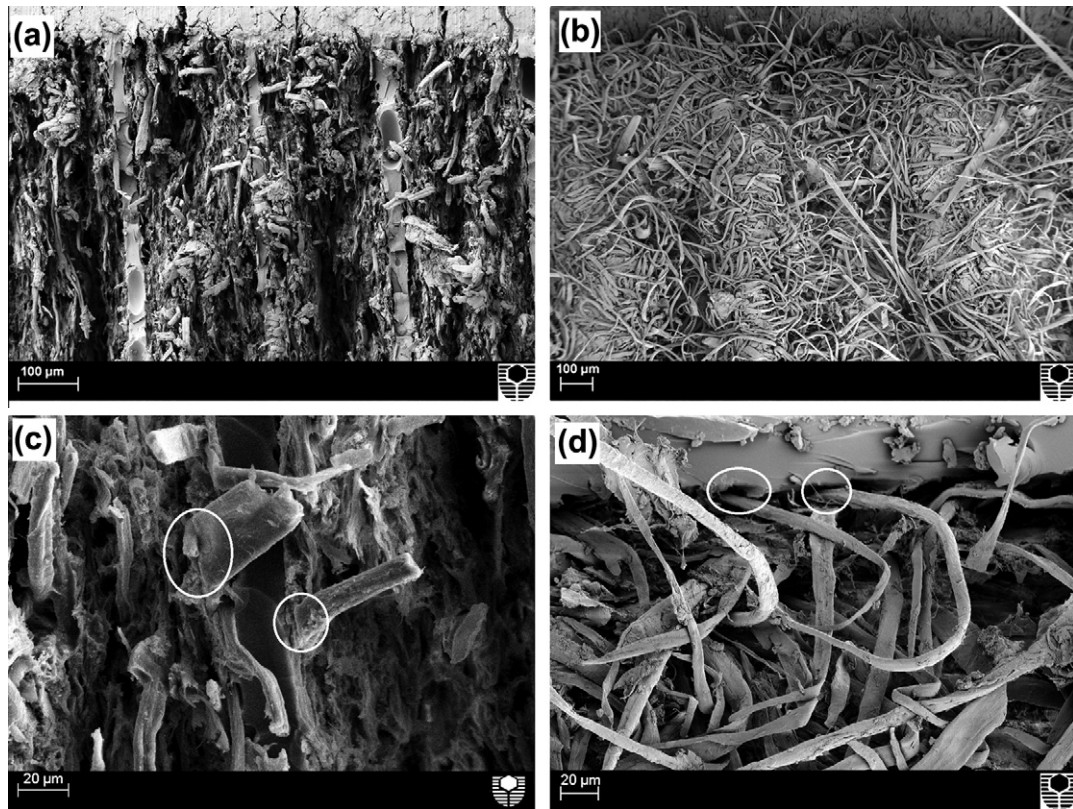
Fig. 14. SEM images of the fracture surface. (a) Dry RCF/epoxy/nanoclay 5 wt.%. (b) Wet RCF/epoxy/nanoclay 5 wt.%. (c) Dry RCF/epoxy. (d) Wet RCF/epoxy.
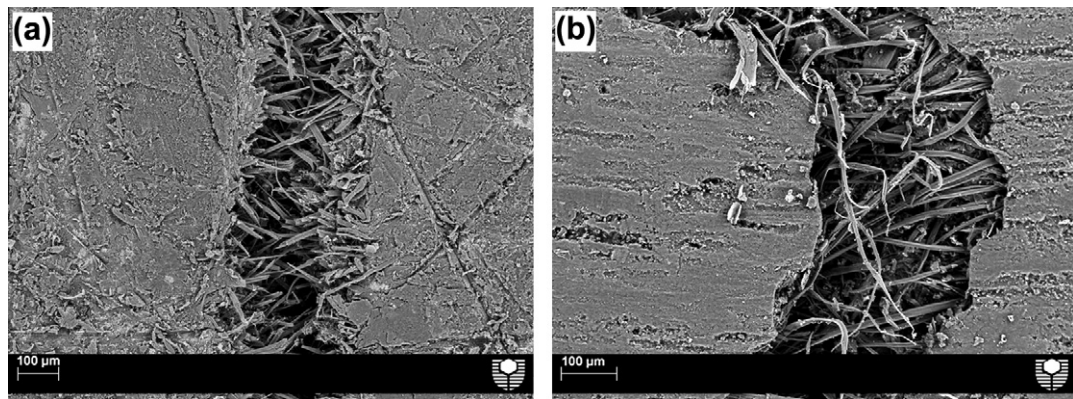
Fig. 15. SEM images of the crack propagation. (a) Dry RCF composites. (b) Wet RCF composites.

similar observation had been reported in an earlier work by Low and co-workers [40] in cellulose fibre reinforced epoxy composites. These authors reported a significant increase in both impact strength and toughness after immersing samples in seawater for two weeks. Fig 13 displays the fracture energy versus WDΦ for both dry and wet RCF/epoxy composites during impact toughness test. It can be clearly observed that water treated composites absorbed higher energy than dry composites. This indicates that water absorption increased the ability of RCF filled composites to withstand the impact force.

3.6. Fracture mechanisms

Fig. 14 illustrates the fracture surface micrograph of the composites before and after placement in water. Fig. 14a and b show the micrograph of dry and wet 5 wt.% nanoclay filled RCF/epoxy

composites. It can be clearly seen that dry composites show rougher fracture surface than wet composites. Fibres fracture can be easily observed in dry composites while it is hard to be seen in wet composites. However, the presence of unbroken fibres in wet composites after fracture test reveals that fibres were easily pulled out from the matrix, which indicates the lack of adhesion between fibre and matrix.

Fig. 14c and d displays high magnification image of dry and wet RCF/epoxy composites. Good fibre–matrix adhesion is observed for dry composites (no gap between fibre and matrix) while weak fibre–matrix interface is observed for wet composites, (indicated in white circles). This fibre debonding (characterized by the appearance of gap between fibre and matrix) is a clear evidence of weak fibre–matrix interfacial adhesion in the structure of wet composites. This observation is similar to that obtained by Mohan and Kenny [7]. In wet environment, water molecule penetrates into

the composites through micro-cracks and diffuses along the fibre–matrix interfaces causing debonding between fibre and matrix by replacing the matrix–fibre covalent bond with weaker hydrogen bonds [20,37].

Fig. 15a and b show a close observation of crack propagation for dry and wet composites. In the case of dry composites, an extensive fibre breakage is observed along the fibre propagation. Fibre breakage normally involves high energy to dissipate, which increases composite facture toughness properties. Fibre fracture can be an indicator of good fibre–matrix interaction [20].

However, in the case of wet composites, there is less fibre fracture, which indicates lower energy is involved for crack to propagate through the wet composites compared to dry composites. Moreover, a great number of smooth fibre pull-out, not broken is observed along the crack propagation. This confirms the poor adhesion between the fibre and the matrix, which results in low fracture toughness.

4. Conclusions

This study highlighted the impact of water absorption on the mechanical properties of cellulose fibre reinforced polymer composites and the influence of nanoclay incorporation on enhancing the barrier properties of nanoclay filled cellulose fibre/polymer nanocomposites. TEM results revealed that the dispersion of nanoclay was uniform with major intercalated structure and some exfoliated regions. Water absorption of RCF/epoxy composites was found to increase dramatically due to the presence of hydrophilic cellulose fibre. Water uptake decreased progressively due the incorporation of nanoclay. The addition of 5 wt.% nanoclay decreased the maximum water uptake of RCF/epoxy composites by about 34% compared to unfilled RCF/epoxy composites.

Exposure to moisture for long term resulted in significant reduction in flexural strength, flexural modulus and fracture toughness due to the degradation of the fibre–matrix interface. However, Comparing to dry composites, impact strength and impact toughness of wet composites surprisingly increased due to the plasticization effect of adsorbed water. The presence of nanoclay platelet was found to slightly minimize the effect of moisture on the mechanical properties of the composites by improving the flexural strength, flexural modulus and fracture toughness properties of the composites. Finally, SEM results showed that water absorption severely damaged the cellulose fibres and fibres–matrix interface in wet composites.

Acknowledgments

References

[1] Dhakal HN, Zhang ZY, Richardson MOW. Effect of water absorption on the mechanical properties of hemp fibre reinforced unsaturated polyester composites. Compos Sci Technol 2007;67:1674–83.
[2] Low IM, McGrath M, Lawrence D, Schmidt P, Lane J, Latella BA. Mechanical and fracture properties of cellulose fibre reinforced epoxy laminates. Composites: Part A 2007;38:963–74.
[3] Marsh G. Next step for automotive materials. Mater Today 2003;6:36–43.
[4] Sanadi A, Young R, Rowell R. Recycled newspaper fibres as reinforcing fillers in thermoplastics: Part I – Analysis of tensile and impact properties in polypropylene. J Reinforc Plast Compos 1994;13:54–67.
[5] Baroulaki I, Karakasi B, Pappa G, Tarantili P, Economides D, Magoulas K. Preparation and study of plastic compounds containing polyolefins and post used newspaper fibres. Composites: Part A 2006;37(10):1613–25.
[6] Wang B, Panigrahi S, Tabil L, Crerar W. Pre-treatment of Flax Fibre s for use in Rotationally Molded Biocomposites. J Reinf Plast Compos 2007;26(5):447–63.
[7] Mohan TP, Kanny K. Water barrier properties of nanoclay filled sisal fibre reinforced epoxy composites. Compos A Appl Sci Manuf 2011;42(4):385–93.
[8] Reddy CR, Sardashti AP, Simon LC. Preparation and characterization of polypropylene–wheat straw–clay composites. Compos Sci Technol 2010;70:1674–80.
[9] Ma J, Xu J, Ren JH, Yu ZZ, Mai YW. A new approach to polymer/montmorillonite nanocomposites. Polymer 2003;44(16):4619–24.
[10] Sinha SR, Okamoto M. Polymer/layered silicate nanocomposites: a review from preparation to processing. Prog Polym Sci 2003;28:1539–641.
[11] Alexandre B, Langevin D, Médéric P, Aubry T, Couderc H, Nguyen QT, et al. Water barrier properties of polyamide 12/montmorillonite nanocomposite membranes: Structure and volume fraction effects. J Membr Sci 2009;328:186–204.
[12] Qi B, Zhang QX, Bannister M, Mai YW. Investigation of the mechanical properties of DGEBA-based epoxy resin with nanoclay additives. Compos Struct 2006;75:514–9.
[13] Hwang SS, Liu SP, Hsu PP, Yeh JM, Chang KC, Lai YZ. Effect of organoclay on the mechanical/thermal properties of microcellular injection molded PBT–clay nanocomposites. Int Commun Heat Mass Transfer 2010;37:1036–43.
[14] Ha SR, Rhee KY, Park SJ, Lee JH. Temperature effects on the fracture behaviour and tensile properties of silane-treated clay/epoxy nanocomposites. Compos Part B: Eng 2010;41:602–7.
[15] Kaynak C, Nakas GI, Lsitman NA. Mechanical properties, flammability and char morphology of epoxy resin/ montmorillonite nanocomposites. Appl Clay Sci 2009;46:319–24.
[16] Zainuddin S, Hosura MV, Zhoua Y, Narteha AT, Kumarb A, Jeelani S. Experimental and numerical investigations on flexural and thermal properties of nanoclay–epoxy nanocomposites. Mater Sci Eng A 2010;527:7920–6.
[17] Zhang Y, Liu Q, Zhang Q, Lu Y. Gas barrier properties of natural rubber/kaolin composites prepared by melt blending. Appl Clay Sci 2010;50(2):255–9.
[18] Alamri H, Low IM, Alothman Z. Mechanical, thermal and microstructural characteristics of cellulose fibre reinforced epoxy/organoclay nanocomposites. Compos Part B: Eng 2012;43(7):2762–71.
[19] Alamri H, Low IM. Characterization and properties of recycled cellulose fibre-reinforced epoxy-hybrid clay nanocomposites. Mater Sci Forum 2010;654–656:2624–7.
[20] Kim HJ, Seo DW. Effect of water absorption fatigue on mechanical properties of sisal textile-reinforced composites. Int J Fatigue 2006;28:1307–14.
[21] Fraga AN, Frullloni E, de la Osa O, Kenny JM, Vázquez A. Relationship between water absorption and dielectric behaviour of natural fibre composite materials. Polym Testing 2006;25(2):181–7.
[22] Doan T, Brodowsky H, Mader E. Jute fibre/polypropylene composites II. Thermal, hydrothermal and dynamic mechanical behaviour. Compos Sci Technol 2007;67:2707–14.
[23] Deka BK, Maji TK. Study on the properties of nanocomposite based on high density polyethylene, polypropylene, polyvinyl chloride and wood. Composites: Part A 2011;42:686–93.
[24] Zhao H, Li RKY. Effect of water absorption on the mechanical and dielectric properties of nano-alumina filled epoxy nanocomposites. Composites: Part A 2008;39:602–11.
[25] Liu W, Hoa SV, Pugh M. Fracture toughness and water uptake of high-performance epoxy/nanoclay nanocomposites. Compos Sci Technol 2005;65:2364–73.
[26] Karbowiak T, Ferret E, Debeaufort F, Voilley A, Cayot P. Investigation of water transfer across thin layer biopolymer films by infrared spectroscopy. J Membr Sci 2011;370:82–90.
[27] Lasagabaster A, Abad MJ, Barral L, Ares A, Bouza R. Application of FTIR spectroscopy to determine transport properties and water–polymer interactions in polypropylene (PP)/poly(ethylene-co-vinyl alcohol) (EVOH) blend films: Effect of poly(ethylene-co-vinyl alcohol) content and water activity. Polymer 2009;50:2981–9.
[28] Sgriccia N, Hawley MC, Misra M. Characterization of natural fibre surfaces and natural fibre composites. Composites: Part A 2008;39:1632–7.
[29] Oh SY, Yoo DI, Shin Y, Seo G. FTIR analysis of cellulose treated with sodium hydroxide and carbon dioxide. Carbohydr Res 2005;340:417–28.
[30] Bledzki AK, Mamun AA, Volk J. Barley husk and coconut shell reinforced polypropylene composites: The effect of fibre physical, chemical and surface properties. Compos Sci Technol 2010;70:840–6.
[31] Shukla DK, Kasisomayajula SV, Parameswaran V. Epoxy composites using functionalized alumina platelets as reinforcements. Compos Sci Technol 2008;68:3055–63.
[32] Chozhan CK, Alagar M, Sharmila RJ, Gnanasundaram P. Thermo mechanical behaviour of unsaturated polyester toughened epoxy–clay hybrid nanocomposites. J Polym Res 2007;14:319–28.
[33] Rajasekaran R, Karikalchozhan C, Alagar M. Synthesis, characterization and properties of organoclaymodified polysulfone/epoxy interpenetrating polymer network nanocomposites. Chin J Polym Sci 2008;26(6):669–78.
[34] Khan R, Khare P, Baruah BP, Hazarika AK, Dey NC. Spectroscopic, kinetic studies of polyaniline–flyash composite. Adv Chem Eng Sci 2011;1:37–44.
[35] Nikolic G, Zlatkovic S, Cakic M, Cakic S, Lacnjevac C, Rajic Z. Fast fourier transform ir characterization of epoxy gy systems crosslinked with aliphatic and cycloaliphatic EH polyamine adducts. Sensors 2010;10:684–96.

[36] Sonawane SH, Chaudhari PL, Ghodke SA, Parande MG, Bhandari VM. Ultrasound assisted synthesis of polyacrylic acid–nanoclay nanocomposite and its application in sonosorption studies of malachite green dye. Ultrason Sonochem 2009;16:351–5.

[37] Athijayamani A, Thiruchitrambalam M, Natarajan U, Pazhanivel B. Effect of moisture absorption on the mechanical properties of randomly oriented natural fibres/polyester hybrid composite. Mater Sci Eng A 2009;517: 344–53.

[38] Dorigato A, Pegoretti A, Quaresimin M. Thermo-mechanical characterization of epoxy/clay nanocomposites as matrices for carbon/nanoclay/epoxy laminates. Mater Sci Eng A 2011;528:6324–33.

[39] Karmaker C. Effect of water absorption on dimensional stability and impact energy of jute fibre reinforced polypropylene. J Mater Sci Lett 1997;16:462–4.

[40] Low IM, Someers J, Kho HS, Davies IJ, Latella BA. Fabrication and properties of recycledcellulose fibre-reinforced epoxy composites. Compos Interfaces 2009;16:659–69.

4. CONCLUSIONS AND FUTURE WORK

4.1 Conclusions

4.1.1 Recycled Cellulose Fibre (RCF) Reinforced Epoxy Composites

a. RCF-reinforced epoxy composites with different fibre loadings have been prepared. The mechanical properties and water absorption were investigated as a function of fibre content. In addition, the effect of moisture absorption on the mechanical properties was studied. Results indicated that water absorption of RCF/epoxy composites increased as fibre content increased. The presence of RCF dramatically increased the water content of RCF/epoxy composites when compared to neat epoxy. The increase in water absorption was attributed to the hydrophilic nature of cellulose fibres. The mechanical properties (*i.e.* flexural strength, flexural modulus, fracture toughness and impact toughness) also increased as the fibre content increased. In comparison to neat epoxy, addition of about 52 wt% RCF increased flexural strength (by 160%), flexural modulus (by 760%), impact strength (by 444%), fracture toughness (by 350%) and impact toughness (by 263%). This significant increase in mechanical properties is attributed to the unique properties of cellulose fibres such as ability to withstand bending force and resist fracture force via number of energy absorbing events which include fibre pull-out, fibre fracture, fibre-debonding, crack-deflection and fibre-bridging. These micromechanisms of toughening were clearly observed by SEM on the fracture surface of RCF composites. These toughening mechanisms of RCF were the major factors of increasing fracture properties of samples reinforced with RCF when compared to neat epoxy. In addition, SEM results indicated an increase in energy dissipation events for composites filled with higher fibre content compared to their lower fibre content counterparts. In the case of thermal properties, the presence of RCF sheets accelerated the major degradation of epoxy filled with RCF compared to neat epoxy. This was as a result of reduction in the maximum decomposition temperature (T_{max}) by about 7.7 ^{o}C in epoxy filled with RCF as compared to neat epoxy. However, composites reinforced with RCF sheets showed better thermal stability than unfilled epoxy at elevated temperatures ($\geq$ 600 ^{o}C).

169

b. The effect of water absorption on the mechanical properties of RCF-reinforced epoxy composites was investigated and compared to dry composites for a short period (*i.e.* two weeks) and for a long period (*i.e.* six months). Exposure to moisture for two weeks caused a reduction in flexural strength (by 34.9%), flexural modulus (by 17.1%) and fracture toughness (by 23.9%) in epoxy reinforced with 46 wt% RCF. On the other hand, exposure to moisture for a long time resulted in severe reduction in flexural strength (by 77%), flexural modulus (by 82.7%) and fracture toughness (by 60.8%) for epoxy reinforced with 52 wt% RCF. This significant drop in mechanical properties was attributed to the degradation of bonding at the fibre–matrix interfaces as a result of water absorption. However, impact strength and impact toughness was found to increase after water absorption. The effect of water absorption on the mechanical properties was more pronounced at high fibre content as compared to low fibre content. SEM results showed that water absorption severely damaged the cellulose fibres and degraded the bonding along the fibres-matrix interfaces in wet composites.

4.1.2 Nano-Filler Reinforced Epoxy Nanocomposites

Epoxy nanocomposites reinforced with organo-clay platelets (Cloisite 30B), halloysite nanotubes (HNT) and nano-silicon carbide (n-SiC) were fabricated. The effect of nano-filler contents on the morphology, structure, mechanical, thermal and moisture barrier properties of epoxy nanocomposites was investigated. The effect of moisture absorption on the mechanical properties of these nanocomposites was also studied.

a. <u>Nanoclay (Cloisite 30B) reinforced epoxy nanocomposites</u>

A series of nanoclay/epoxy nanocomposites were fabricated with 1, 3 and 5 wt% of organoclay (Cloisite 30B). WAXS results showed an increase in the inter-layer distance between the clay platelets from 1.85 to 3.4 nm indicating that clay/epoxy nanocomposites with intercalated structure had been formed. Based on TEM results, the dispersion of nanoclay was uniform with some particle agglomerations. These particle clusters were found to increase as clay contents increased. Furthermore, TEM results confirmed that the major structure of nanoclay in the epoxy

matrix was intercalated with some exfoliated regions. The measured d-spacing ranged from 2.65 to 7.98 nm compared to 1.8 nm of nanoclay platelet.

The presence of nanoclay platelet was found to enhance the mechanical properties (*i.e.* flexural strength, flexural modulus impact strength, fracture toughness and impact toughness) of the epoxy resin. For example, the addition of 1 wt% nanoclay increased flexural strength (by 45.6%), flexural modulus (by 87.6%) fracture toughness (by 30%), and impact toughness (by 50%) compared to neat epoxy. However, the addition of more clay did not cause any further increase in these properties. This was attributed to the increase in matrix viscosity and formation of voids as well as poor dispersion of particles at higher clay contents.

With regard to thermal stability, the presence of nanoclay showed no effect on the thermal stability of epoxy resin at low temperatures (≤ 400 ^{o}C). The maximum decomposition temperatures of neat epoxy and its nanocomposites were found to be unchanged. However, the addition of only 5 wt% nanoclay slightly increased the char residue of epoxy at $700\,^{o}$C.

The fracture surface of neat epoxy and clay/epoxy nanocomposites were investigated by SEM. The fracture surface of epoxy was found to be smooth and featureless while epoxy filled with nanoclay displayed rougher fracture surface. This indicated the presence of crack deflection mechanisms which increase fracture toughness by increasing crack propagation length during deformation. Other fracture mechanisms such as crack pinning, particle debonding, plastic void growth, plastic deformation and particle pullouts were also observed for all types of nano-filler reinforced epoxy nanocomposites. Such toughness mechanisms can increase the energy dissipated by resisting crack propagation during deformation, which lead to an increase in fracture toughness values. Close observation on SEM images indicated that crack deflection and plastic deformation due to the presence of clay clusters were the dominant toughening mechanisms for nanocomposites filled with nanoclay.

b. HNTs/epoxy nanocomposites

A series of epoxy/HNTs nanocomposites were fabricated with different HNT contents (*i.e.* 1, 3 and 5 wt%). Based on TEM observations, homogeneous dispersion of HNTs with some

agglomerations was achieved by mixing the HNTs with the epoxy resin. Particle agglomerations increased as the HNT content increased.

The presence of only 1 wt% HNTs increased flexural strength (by 20.8%), flexural modulus (by 72.8%), fracture toughness (by 56.5%), and impact toughness (by 25.0%) over unmodified epoxy. However, adding more HNTs showed no further increase in flexural strength and fracture toughness properties due to the poor dispersion of HNTs at higher content. Impact strength and impact toughness were however found to increase as HNTs loading increased to 5 w%. As in the case of nanoclay thermal results, addition of HNTs into epoxy did not influence the maximum decomposition temperatures of epoxy matrix. However, epoxy modified with 3 and 5 wt% HNT loading showed better thermal stability than unmodified epoxy at high temperatures. SEM results showed that epoxy/HNT nanocomposites had a rougher fracture surface as compared to that of neat resin due to the presence of HNTs. Crack deflection and crack pinning and bowing were the main toughening mechanisms for nanocomposites filled with HNT.

c. N-SiC/epoxy nanocomposites

Silicon carbide nano-particles (n-SiC) have been used as reinforcing filler for epoxy matrix. A series of n-SiC/epoxy nanocomposites were made with 1, 3 and 5 wt% of n-SiC. The synchrotron radiation diffraction (SRD) results showed the formation of five sharp narrow diffraction peaks in the epoxy/n-SiC nanocomposites due to the presence of n-SiC particles. TEM results indicated that n-SiC particles were homogeneously dispersed inside the epoxy matrix except for some particle agglomerations, which were clearly seen at higher n-SiC loading due to the increase in matrix viscosity. In general, the inclusion of n-SiC particles led to an increase in most of the mechanical properties. For instance, the incorporation of only 1 wt% n-SiC increased flexural strength (by 21.5%), flexural modulus (by 83.9%), impact strength (by 33.2%), impact toughness (by 25.0%) and fracture toughness (by 89.4%). Impact strength and impact toughness reached their maximum value at 5 wt% n-SiC. Thermal stability of n-SiC/epoxy nanocomposites was determined using TGA and DTA. Results indicated that the addition of 3 and 5 wt% n-SiC accelerated the major degradation of epoxy nanocomposites compared to unfilled epoxy since nano-particles act as a catalyser in the degradation of polymer matrix. In contrast, epoxy filled

with 3 and 5 wt% n-SiC displayed better thermal properties than neat epoxy at temperatures above 500 ^{o}C.

SEM observation indicated that the presence of n-SiC particles increased the roughness of the fracture surface of epoxy nanocomposites compared to neat epoxy. Particle agglomerations and voids in micro-scale were observed for epoxy/n-SiC nanocomposites. Samples filled with 5 wt% n-SiC showed an increase in particle agglomerates and voids as compared to samples filled with 1 wt% n-SiC. The existence of micro-voids revealed that the plastic deformation of the matrix around the voids and the crack deflection due to the presence of these voids were primary toughening mechanisms.

d. Effect of water absorption on the mechanical properties of nano-filler reinforced epoxy nanocomposites

The effect of water absorption on the mechanical properties of nano-filler reinforced epoxy nanocomposites was investigated and compared to dry nanocomposites. Results indicated that, compared to dry nanocomposites, flexural strength and modulus of all types of nanocomposites decreased due to the plasticization effect of the water uptake. However, fracture toughness and impact strength were found to increase after water absorption due to increased ductility of the epoxy matrix.

The influence of the nano-fillers such as nanoclay platelets, HNTs and n-SiC on enhancing the mechanical and barrier properties of epoxy based nanocomposites in wet condition was investigated in terms of water absorption behaviour, flexural strength, flexural modulus, fracture toughness and impact strength. Results indicated that, as compared to unfilled epoxy, the incorporation of nano-fillers into epoxy matrix led to significant reduction in both water uptake and diffusion coefficients (*D*). This reduction was attributed to the tortuosity path created by the addition of the nano-fillers. Addition of nanoclay, HNT and n-SiC particles improved the mechanical properties of the nanocomposites after being exposed to water compared to neat epoxy under similar condition. Reinforcement with 1 wt% nano-filler showed better mechanical properties than other filler content. Enhanced barrier and mechanical properties of

nanocomposites were more pronounced for composites filled with n-SiC as compared to those filled with nanoclay platelets and halloysite nanotubes.

4.1.3 Nano-Filler Reinforced RCF/Epoxy Eco-Nanocomposites

A new class of epoxy eco-nanocomposites reinforced with nano-sized particles (*i.e.* nanoclay platelets, halloysite nanotubes or nano-silicon carbide) and recycled cellulose fibre sheets were successfully fabricated and investigated. The effects of these nano-fillers on the mechanical and thermal properties are summarised below.

a. Nanoclay filled RCF/epoxy eco-nanocomposites

The addition of nanoclay to RCF/epoxy composites showed no significant increase in flexural strength, flexural modulus and fracture toughness. In fact, addition of more than 1 wt% of clay led to a reduction in flexural strength as compared to unfilled RCF/epoxy composites. Flexural modulus and fracture toughness showed maximum values at 5 wt% nanoclay loading. For impact properties, the presence of 1% nanoclay significantly increased impact strength and impact toughness by 14.5% and 48.3%, respectively compared to RCF/epoxy composites. Adding more clay led to reduction in both impact strength and toughness.

Based on TGA results, the addition of nanoclay to RCF/epoxy composites increased the rate of decomposition by decreasing (T_{max}) by about 9 ^{o}C as compared to unfilled RCF/epoxy composites. However, the char residues at 700 ^{o}C of the RCF filled epoxy increased by 3.0% due to the presence of nanoclay.

b. HNTs filled RCF/epoxy eco-nanocomposites

The addition of HNTs to RCF/epoxy composites was found to slightly increase flexural strength, flexural modulus and fracture toughness. The optimum values of flexural strength and fracture toughness were obtained at 1 wt% HNTs while the optimum of flexural modulus was obtained at

174

5 wt% HNTs. On the other hand, the addition of HNTs to RCF/epoxy composites led to a reduction in impact strength. However, the presence of HNTs gradually increased impact toughness of RCF/epoxy composites with maximum enhancement reaching up to 27.6% at 5 wt% filler content.

TGA results showed that the addition of HNTs increased the thermal stability of RCF/epoxy composites at temperatures between 200-300 ^{o}C and between 500-700 ^{o}C. However, the presence of HNTs led to reduction in thermal stability at temperatures between 300-400 ^{o}C, where the major decomposition occurred.

c. N-SiC filled RCF/epoxy eco-nanocomposites

The incorporation of n-SiC to RCF/epoxy composites were found to increase flexural modulus, impact strength, fracture toughness and impact toughness compared to unfilled RCF/epoxy samples. Flexural strength increased after the addition of only 1 wt% n-SiC. However, increased addition of SiC caused a reduction in flexural strength. In comparison to unfilled RCF/epoxy composites, the addition of 5 wt% n-SiC displayed optimum increase in facture toughness (by 10.4%), impact strength (by 21.2%) and impact toughness (by 41.4%). In general, RCF/epoxy eco-nanocomposites filled with n-SiC displayed better mechanical properties than same composites filled with either HNTs or nanoclay.

The addition of n-SiC to RCF/epoxy composites was found to increase the thermal stability by increasing the char yield of composites at high temperatures. However, the rate of degradation increased after adding n-SiC to RCF/epoxy composites due to decreased maximum decomposition temperatures by about 8 ^{o}C. The reduction in thermal stability at low temperatures is due to the Hofmann elimination reaction, where nano-fillers act as a catalyser toward the degradation of the polymer matrix. However, at high temperatures, nano-fillers acted as insulators to the heat as well as barriers and hindered the diffusion of volatile decomposition products out from the nanocomposites resulting in an increase in thermal stability.

d. Investigation on the water absorption behaviour of nanolcay/RCF reinforced epoxy eco-nanocomposites

The effect of nanoclay on enhancing the mechanical and moisture barrier properties of nanoclay filled RCF/epoxy eco-nanocomposites in wet condition was investigated in terms of water absorption behaviour, flexural strength, flexural modulus, fracture toughness, impact strength and impact toughness. Results indicated that the addition of nanoclay to the RCF/epoxy composites led to significant reduction in water absorption compared to unfilled RCF/epoxy composites. A significant drop in flexural strength, flexural modulus and fracture toughness was observed as a result of water absorption. However, the presence of nanoclay platelet was found to slightly minimize the effect of moisture on the mechanical properties of the materials by improving the flexural strength, flexural modulus and fracture toughness of the eco-nanocomposites. Surprisingly, water absorption was found to increase the impact strength and impact toughness. Once again, the addition of nanoclay to RCF/epoxy was found to minimize the effect of water absorption on the impact properties by decreasing both impact strength and toughness.

e. Investigation on the water absorption behaviour of n-SiC/RCF reinforced epoxy eco-nanocomposites

The effect of water absorption on the mechanical properties of n-SiC filled RCF/epoxy eco-nanocomposites was studied. The influence of n-SiC particles on enhancing the mechanical and barrier properties of RCF/epoxy composites in wet condition was investigated. Results indicated that maximum water uptake of n-SiC filled RCF/epoxy eco-nanocomposites decreased with increasing n-SiC contents due to enhancement in composite barrier properties. Maximum reduction in water uptake and diffusivity occurred at 5 wt% n-SiC loading.

In comparison to dry eco-nanocomposites, exposing to water for six months was found to severely reduce flexural strength, flexural modulus and fracture toughness of n-SiC filled RCF/epoxy eco-nanocomposites. For example significant drop in flexural strength by 73.3%, flexural modulus by 81.5% and fracture toughness by 62.41% for composites filled with 5 wt% n-SiC compared to same composites in dry condition. This reduction was attributed to the

176

degradation of bonding at the fibre–matrix interfaces and to the damage in the fibre strength and structure.

The effect of n-SiC on enhancing the mechanical properties of RCF/epoxy composites in wet condition was investigated. In general, the addition of n-SiC was found to increase the flexural strength, modulus and fracture toughness of RCF/epoxy composites after water treatment. The addition of only 5 wt% n-SiC increased flexural strength by 14.4 %, flexural modulus by 7.5%, and fracture toughness by 6.1% over unfilled RCF/epoxy composites. The increase in these mechanical properties is due to the ability of n-SiC in enhancing the fibre-matrix interfacial bonding and increasing the crack propagation resistance by introducing toughness mechanisms such as crack pinning, crack bridging and particle debonding. On the other hand, the presence of n-SiC particles was found to decrease the impact strength of water-treated composites. SEM results showed clean pull out of cellulose fibres as a result of degradation in fibre-matrix interfacial bonding by water absorption. The presence of nano-filler was found to enhance the adhesion between the fibre and the matrix.

Finally, it can be concluded that epoxy matrix modified with n-SiC particles displayed better mechanical, thermal and barrier properties than those filled with nanoclay platelets and halloysite nanotubes.

4.2 Recommendations for Future Work

The primary objectives of this research have been achieved. The effect of recycled cellulose-fibre sheets, nano-fillers (*i.e.* nanoclay platelets, halloysite nanotubes and nano-silicon carbide) and both recycled cellulose fibre and nano-fillers dispersion on the microstructure, mechanical, thermal and barrier properties of epoxy resin was investigated and discussed. The research results provided a fundamental knowledge on the mechanism and performance of a new class of polymer eco-nanocomposites reinforced with nano-fillers and recycled cellulose fibres. Despite the significant improvement in mechanical properties for both RCF/epoxy composites and nano-filler reinforced epoxy nanocomposites, a very limited and slight improvement was achieved for nano-fillers filled RCF/epoxy eco-nanocomposites compared to unfilled RCF/epoxy composites. This leaves a wide scope for future investigators. Therefore, some recommendations for further research are as follows:

1- In this research no chemical or physical treatment has been used for cellulose fibre. Therefore, the use of coupling agents to improve fibre/epoxy interfacial bonding could be considered.

2- The dispersion of the nano-fillers in this research was fairly homogenous with some particle agglomerations with the use of only high speed mixture for 10 minutes. However, to get perfect dispersion for nano-fillers in polymer matrices is still challenge. Therefore, different methods and techniques as well as treatments are required to be investigated deeply to improve the nano-filler dispersion.

3- Advanced models are required to investigate the influence of nanostructures, such as shape and size distribution, orientation, aspect ratio, degree of spatial and interfaces on the physico-mechanical properties of eco-nanocomposites. Multi-scale mechanics models and numerical methods should be developed for better understanding of the enhanced mechanisms of eco-nanocomposites materials.

4- The effect of water absorption on the mechanical properties of nano-fillers reinforced polymer nanocomposites has received very limited attention in previous studies. This

research presents a number of interesting findings regarding to the effect of nano-fillers in enhancing the mechanical properties of epoxy resin and RCF/epoxy composites immersed in water for long period. However, more investigations are needed. Particularly, it would be interesting to study the effect of water absorption on the mechanical properties of the composites as a function of time. This might provide essential information on the role of water diffusion in influencing the mechanical properties of nanocomposites and eco-nanocomposites.

5- The mechanical properties of RCF/epoxy composites, nano-filler reinforced epoxy nanocomposites and nano-filler reinforced RCF/epoxy eco-nanocomposites were investigated and discussed in room temperature. Therefore, it is recommended to study the effect of temperature on the mechanical and fracture properties of these composites.

6- This project aimed to synthesize environmentally-friendly eco-nanocmposites reinforced with nano-fillers and recycled cellulose fibres. However, the use of epoxy as a matrix makes the resulted composites not fully green composites. Therefore, it is recommended to use biopolymer as a matrix to synthesize fully green nanocomposites reinforced with nanoclay and cellulose fibre.

5 APPENDICES

5.1 APPENDIX A

Effect of HNT Addition on Enhancing Barrier and Mechanical Properties of RCF/Epoxy Composites in Fully Wet Environment.

This work has been presented as an oral presentation in the 8th Asian-Australasian conference on Composite Materials (ACCM8). 6 – 8 Nov. Kuala Lumpur, Malaysia

The effect of halloysite nanotubes (HNT) on enhancing the barrier and mechanical properties of recycled cellulose fibre (RCF) reinforced epoxy composites in wet condition was investigated. Water treated specimens were subjected to water for about six months at room temperature.
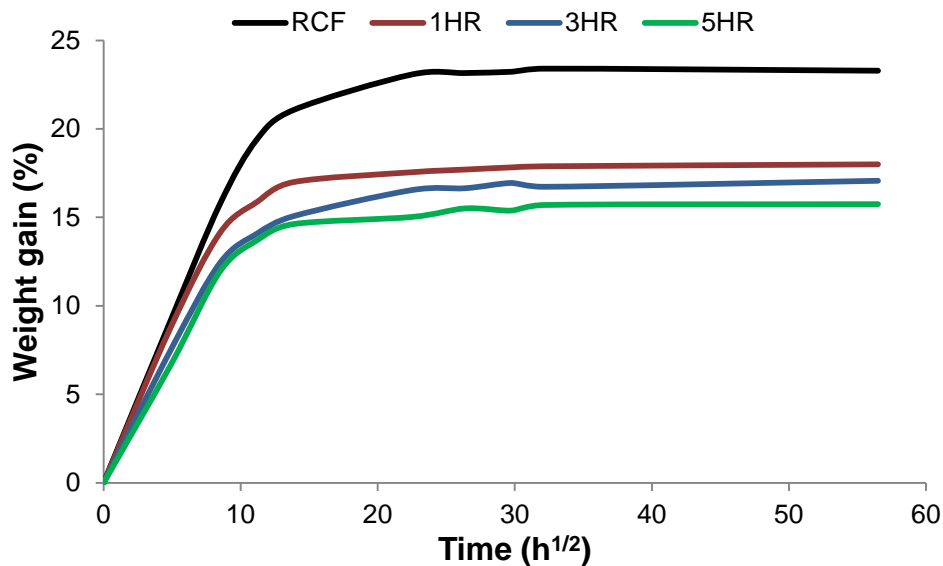
Figure 5.1. Water absorption curves of HNT filled RCF/epoxy eco-nanocomposites.

Table 5.1. Maximum water uptake and diffusion coefficient (D) of HNT filled RCF/epoxy eco-nanocomposites.

Samples	$M\infty$ (%)	$D \times 10^{-06}$ (mm²/sec)
RCF/epoxy	23.28	4.26
1% HNT/RCF/epoxy	17.99	5.95
3% HNT/RCF/epoxy	17.07	5.02
5% HNT/RCF/epoxy	15.75	5.27
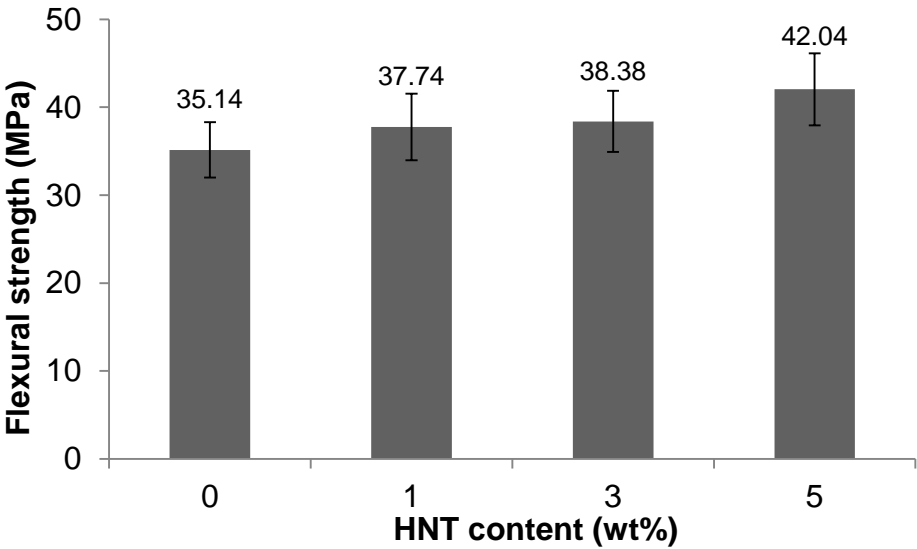
Figure 5.2. Effect of HNT addition on flexural strength of RCF/epoxy eco-nanocomposites in wet condition.
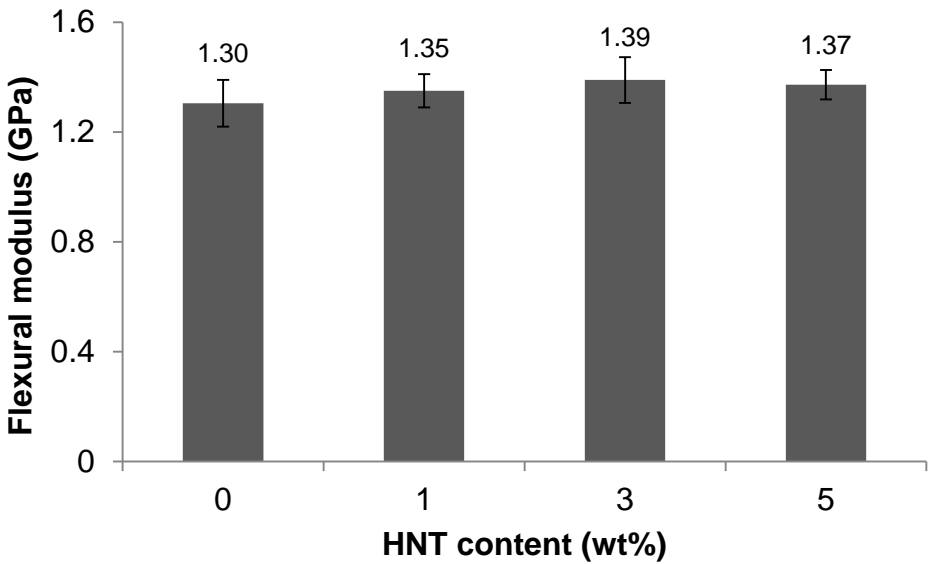
Figure 5.3. Effect of HNT addition on flexural modulus of RCF/epoxy eco-nanocomposites in wet condition.
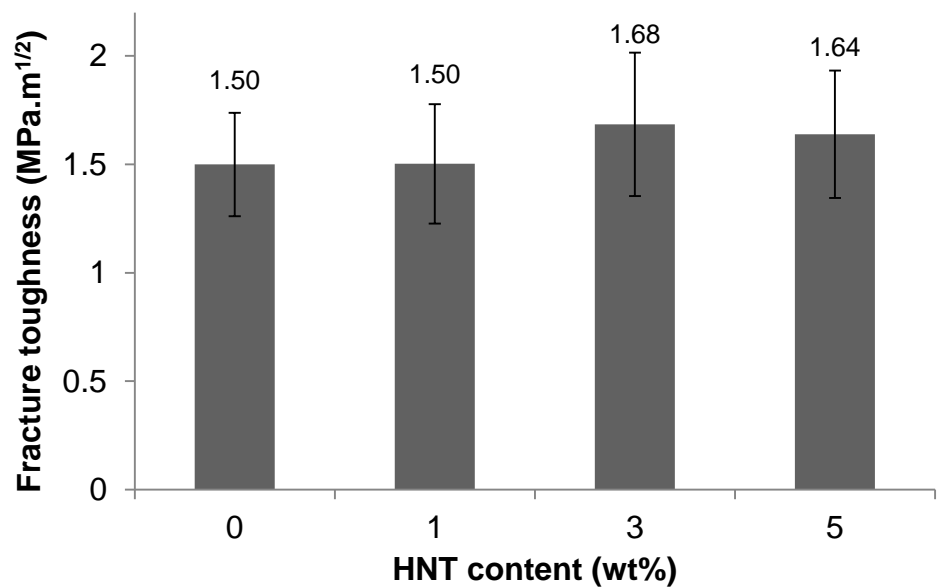
Figure 5.4. Effect of HNT addition on fracture toughness of RCF/epoxy eco-nanocomposites in wet condition.
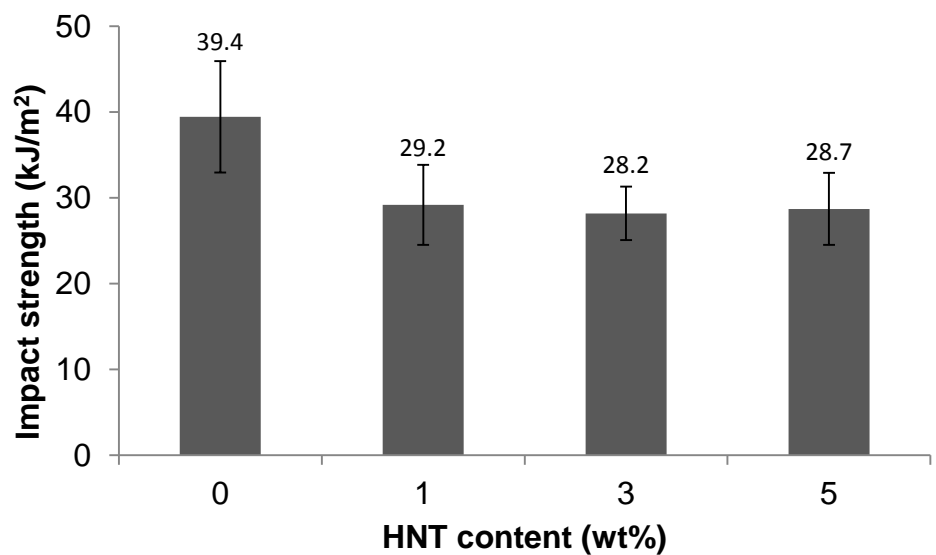
Figure 5.5. Effect of HNT addition on impact strength of RCF/epoxy eco-nanocomposites in wet condition.

5.2 APPENDIX B

Flame Retardancy Behaviour

The effect of nano-fillers such as nanoclay platelets (Cloisite 30B), halloysite nanotubes (HNT) and silicon carbide nano-particles (n-SiC) on enhancing the flammability properties of epoxy and RCF/epoxy composites was investigated as a function of nano-filler contents.

Flammability of the samples was determined via horizontal burning testing. In this work, five specimens with dimensions of 100mm × 10mm × 6mm were prepared for each composite and held horizontally at one end and a flame fuelled by natural gas at an angle of 45° to the horizontal was applied to light the free end of the specimens. The burning rate was calculated by measuring the time required for the flame to reach from a reference mark at 20mm from the free end to another reference mark at 80mm from the free end. The burning rate was measured in the units of mm/min using the following formula:

$$Burning\ rate = 60/(t_{80} - t_{20}) \tag{5.1}$$

where *60* is the length between mark 20mm and mark 80mm and $(t_{80} - t_{20})$ is the time for the flame to travel from mark 20 mm to mark 80 mm.

Figure 5.6 shows a schematic for horizontal burning testing, and Table 5.2 summarizes the burning test results.
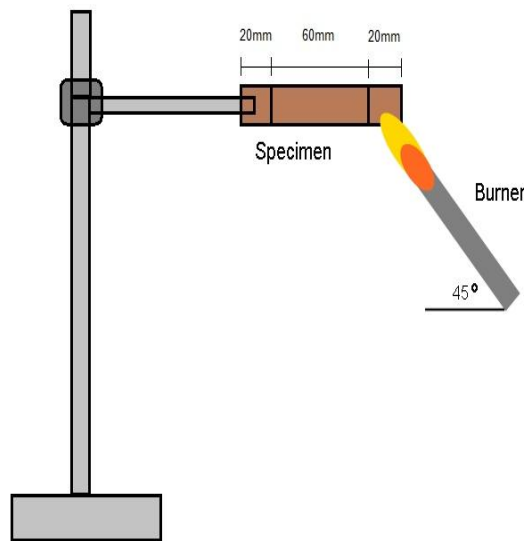
Figure 5.6. Schematic of horizontal burn test.

Table 5.2. Summary of horizontal burn test results for epoxy, epoxy filled nano-fillers, RCF/epoxy and RCF/epoxy filled nano-fillers.

Samples	Burning Rate (mm/min)	
	Without RCF sheets	With RCF sheets
Epoxy	26.2 ± 2.8	37.7 ± 1.8
Epoxy+nanoclay (1 wt%)	24.6 ± 2.4	36.0 ± 3.3
Epoxy+nanoclay (3 wt%)	23.3 ± 2.9	33.0 ± 3.2
Epoxy+nanoclay (5 wt%)	20.7 ± 1.6	31.5 ± 2.7
Epoxy+HNT (1 wt%)	24.5± 2.7	36.7 ± 2.4
Epoxy+HNT (3 wt%)	21.3± 2.2	34.1 ± 3.3
Epoxy+HNT (5 wt%)	20.8± 2.9	33.5 ± 2.6
Epoxy+n-SiC (1 wt%)	20.9±3.0	34.9 ± 2.6
Epoxy+n-SiC (3 wt%)	20.7±2.9	31.4 ± 2.2
Epoxy+n-SiC (5 wt%)	17.5±2.5	27.8 ± 2.3

Summary

- The presence of nano-fillers led to reduction in burning rate for both epoxy and RCF/epoxy composites.
- The flammability properties of composites were found to enhance as nano-filler content increased.
- The presence of RCF sheets increased the rate of burning for epoxy matrix.
- Nano-SiC particles displayed the best enhancement in flammability properties compared to nanoclay clay and HNT.

5.3 APPENDIX C

Glass Transition Temperature (T_g)

The effect of nano-fillers such as nanoclay platelets (Cloisite 30B), halloysite nanotubes (HNT) and silicon carbide nano-particles (n-SiC) as well as recycled cellulose fibres (RCF) on enhancing the T_g of epoxy matrix was investigated in both dry and wet conditions. Differential scanning calorimetry (DSC) analysis was performed on a Perkin Elmer (DSC 6000) in dry nitrogen atmosphere with heating rate of 10 ^oC/min. In this study, DSC was only conducted for neat epoxy, RCF/epoxy, epoxy filled with 5 wt% nano-filler and RCF/epoxy filled with 5 wt% nano-filler in both dry and wet conditions. Water treated specimens were subjected to water for about six months at room temperature.

Table 5.3. T_g of epoxy, epoxy filled with 5 wt% nano-filler, RCF/epoxy and RCF/epoxy filled with 5 wt% nano-filler in both dry and wet conditions.

Sample	T_g (^oC)	
	Dry	Wet
Epoxy	53.08	47.46
Epoxy + nanoclay (5wt%)	58.11	54.14
Epoxy + HNT (5wt%)	55.76	50.76
Epoxy + n-SiC (5wt%)	59.26	52.22
RCF/epoxy	61.36	------
RCF/epoxy + nanoclay (5wt%)	61.29	------
RCF/epoxy + HNT (5wt%)	58.58	------
RCF/epoxy + n-SiC (5wt%)	62.22	------

Summary

- The addition of both nano-fillers and RCF sheets led to an increase in T_g of epoxy system.

- The presence of nano-fillers in RCF/epoxy composites has slight effect on T_g.

- Exposing to water caused a reduction in T_g of epoxy system and its nanocomposites. However, the presence of nano-fillers led to an enhancement in T_g of nanocomposites compared to unfilled epoxy.
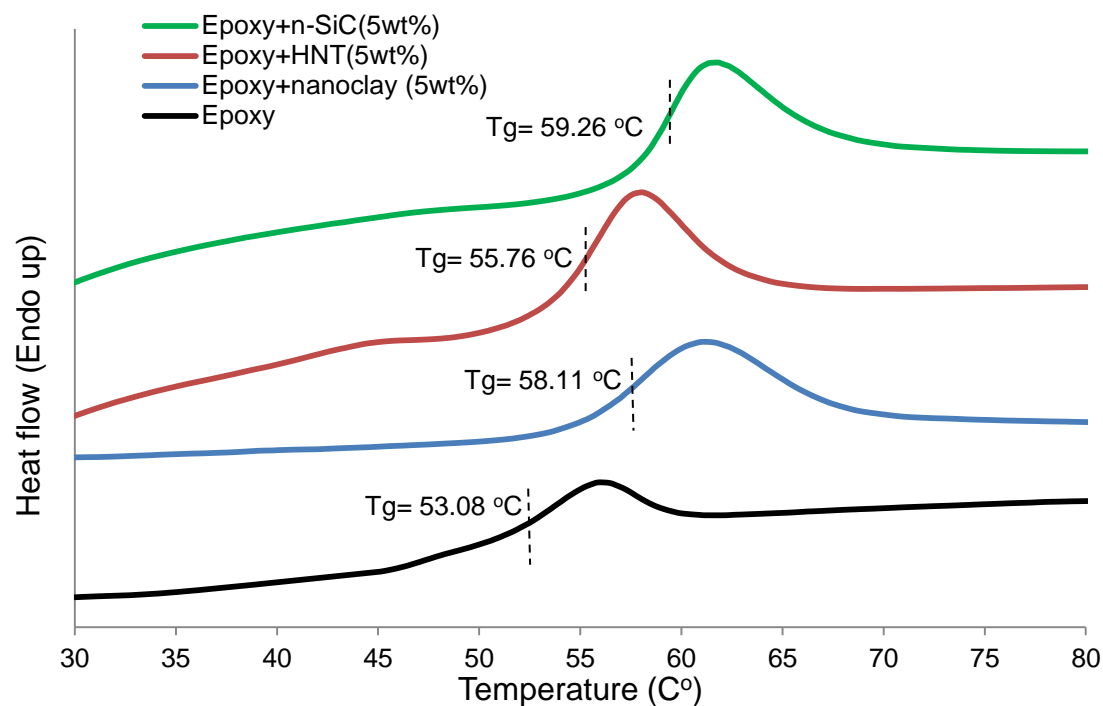
Figure 5.7. Effect of nano-fillers addition on enhancing T_g of epoxy system.
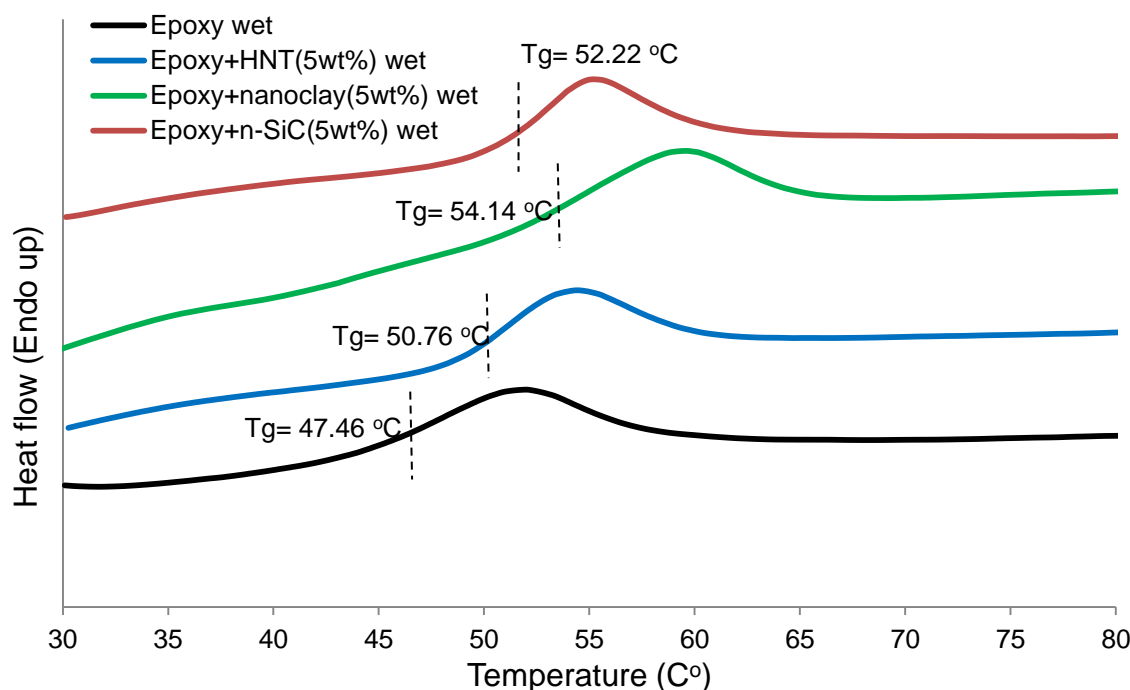
Figure 5.8. Effect of nano-fillers addition on enhancing T_g of epoxy system after water treatment.
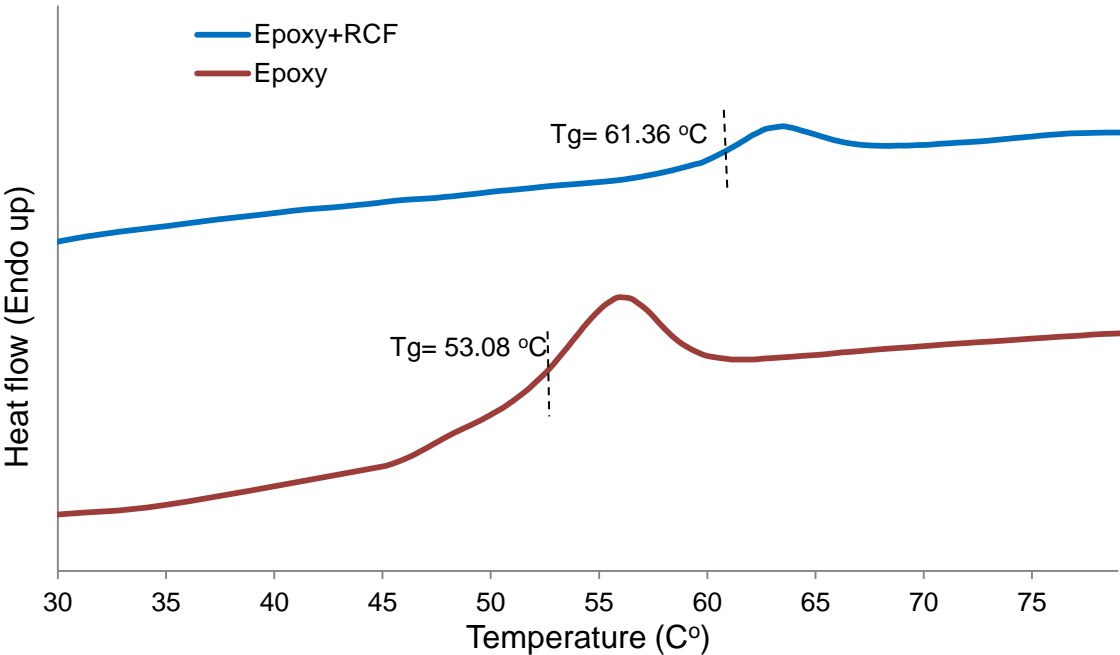
Figure 5.9. Effect of RCF sheets addition on enhancing T_g of epoxy system.
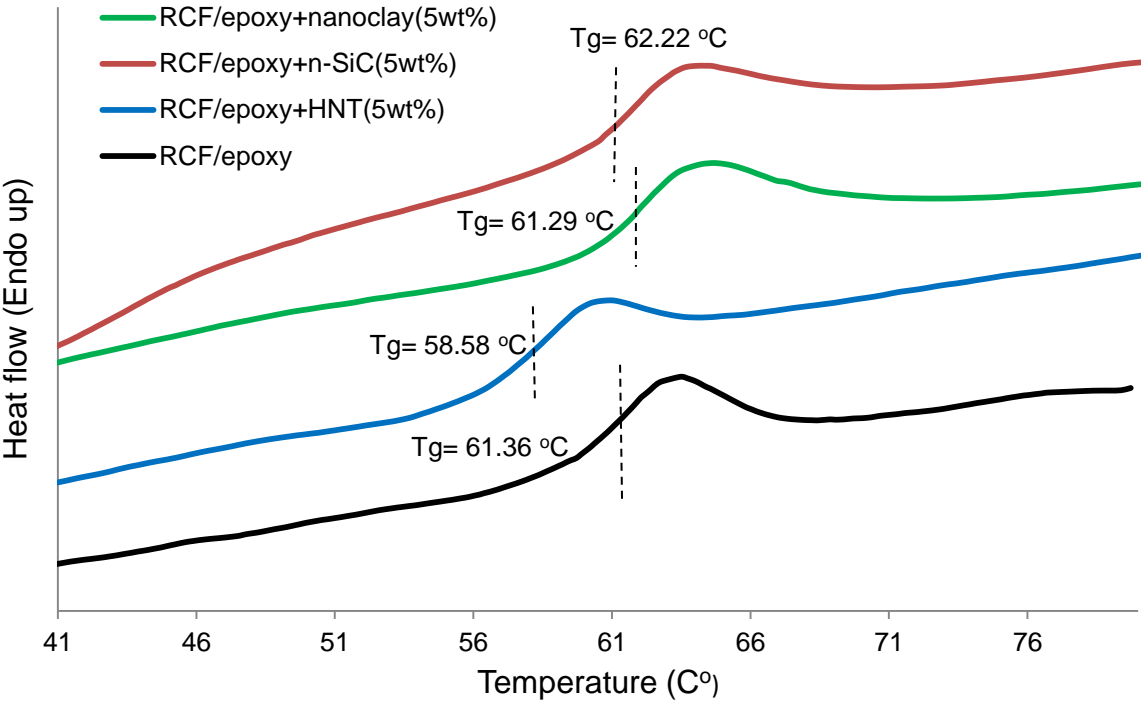
Figure 5.10. Effect of nano-fillers addition on enhancing T_g of RCF/epoxy composites.

5.4 APPENDIX D

Physical Properties

The physical properties such as bulk density (D_b) and apparent porosity (P_a) of neat epoxy, RCF/epoxy composites, nano-filler/epoxy nanocomposites and nano-filler filled RCF/epoxy eco-nanocomposites were determined using the Archimedes method as described in the Australian standard AS 1774.5-2001.

The bulk density and apparent porosity were calculated using the following equations,

a) Bulk density (D_b):

$$D_b = \frac{m_D}{m_s - m_i} \qquad (5.2)$$

b) Apparent porosity (P_a):

$$P_a = \frac{m_s - m_D}{m_s - m_i} \times 100 \qquad (5.3)$$

where m_D is the mass of dried sample, m_i is the mass of sample, saturated and immersed in water and m_s is the mass of sample, saturated and suspended in air. Five specimens of each composition were used for these measurements.

Table 5.4. Summary of bulk density and apparent porosity of neat epoxy, epoxy filled with nano-fillers, RCF/epoxy and RCF/ epoxy filled with nano-fillers.

Sample	Without RCF sheets		With RCF sheets	
	Bulk density (g/cm^3)	Apparent porosity (%)	Bulk density (g/cm^3)	Apparent porosity (%)
Epoxy	1.16 ± 0.06	0.26 ±0.14	1.26 ± 0.04	5.72 ± 0.80
+1wt% nanoclay	1.16 ± 0.04	0.20 ± 0.08	1.25 ± 0.02	5.19 ± 0.62
+3wt% nanoclay	1.16 ± 0.04	0.30 ± 0.12	1.26 ± 0.05	5.38 ± 1.22
+5wt% nanoclay	1.17 ± 0.03	0.25 ± 0.12	1.29 ± 0.04	4.73 ± 0.64
+1wt% HNT	1.17 ± 0.04	0.23 ± 0.14	1.23 ± 0.02	7.17 ± 0.86
+3wt% HNT	1.18 ± 0.06	0.26 ± 0.16	1.23 ± 0.04	6.28 ± 1.00
+5wt% HNT	1.19 ± 0.04	0.29 ± 0.14	1.26 ± 0.02	7.17 ± 0.86
+1wt% n-SiC	1.16 ± 0.03	0.25 ± 0.10	1.23 ± 0.06	6.87 ± 0.96
+3wt% n-SiC	1.17 ± 0.02	0.27 ± 0.12	1.23 ± 0.06	6.91 ± 0.46
+5wt% n-SiC	1.18 ± 0.05	0.30 ± 0.14	1.24 ± 0.04	6.78 ± 1.20

5.5 APPENDIX E

Effect of Process Variables on the Mechanical Properties of Nano-Filler Reinforced Epoxy Nanocomposites.

(Statistics Analysis)

The Taguchi design of experiment (DoE) method is a very familiar statistical approach that has been widely used in engineering analysis (Dong & Bhattacharyya 2008). This powerful method is used to minimize the experimental time, cost and numbers as well as to improve the quality of products and processes (Mirmohseni & Zavareh 2010). Moreover, the Taguchi approach is also used to determine the significant factors affecting the product performance (Dong & Bhattacharyya 2008).

In this work, the Taguchi method with Signal-to-Noise (S/N) ratio and Analysis of Variance (ANOVA) were used to statistically investigate the effect of operating variables (*i.e.* nano-filler type and nano-filler content) on the mechanical properties of nano-filler reinforced epoxy nanocomposites including flexural strength, flexural modulus, fracture toughness and impact strength. The main goal is to determine the most significant factor that influences each type of mechanical properties of such nanocomposites.

Design of experiments

In this work, two factors (*i.e.* nano-filler type and nano-filler content) with three levels are proposed in Taguchi design of experiment as seen in Table 5.5.

Table 5.5. Proposed factors with their levels.

Factors	Level 1	Level 2	Level 3
Nano-filler type (A)	nanoclay	HNT	n-SiC
Nano-filler content (B)	1 wt%	3 wt%	5 wt%

Taguchi L_9 orthogonal array is selected to analyse the experimental results of mechanical tests (Table 5.6).

Table 5.6. Taguchi L_9 orthogonal array

Trail	A	B
1	1	1
2	1	2
3	1	3
4	2	1
5	2	2
6	2	3
7	3	1
8	3	2
9	3	3

Signal-to-Noise (S/N) ratio

Signal-to-Noise (S/N) ratio "the-larger-the-better" is applied to the experimental results using the following equation.

$$S/N = -10 \log\left(\frac{1}{n}\sum_{i=1}^{n}\frac{1}{y_i^2}\right) \tag{5.4}$$

where y is the experimental observation, n is the number of observation in a trail. Five measurements were used for each trail.

The-large-the-better principle has been used in the calculation of S/N since our aim is to identify the most significant factor that causes maximum enhancement in flexural strength. The S/N of the experimental results for flexural strength is calculated and presented in Table 5.7.

Flexural Strength

Table 5.7. Experimental results for flexural strength and the corresponding S/N ratio.

Trail	Nano-filler type (A)	Nano-filler content (B)	Flexural strength (MPa)	S/N
1	nanoclay	1 wt%	85.23	38.60
2	nanoclay	3 wt%	58.72	35.32
3	nanoclay	5 wt%	61.16	35.69
4	HNT	1 wt%	70.71	36.89
5	HNT	3 wt%	68.20	36.51
6	HNT	5 wt%	64.48	36.12
7	n-SiC	1 wt%	71.11	37.01
8	n-SiC	3 wt%	66.33	36.41
9	n-SiC	5 wt%	61.89	35.80

Flexural strength is the average of five measurements. S/N ratio is the calculation of five measurements.

The response table of S/N for flexural strength is calculated and the result listed in Table 5.8.

An example of the calculation of the mean S/N ratio for each level of factor (A) is shown below:-

$$Level\ 1 = \frac{(38.60) + (35.32) + 35.69)}{3} = 36.54$$

$$Level\ 2 = \frac{(36.89) + (36.51) + 36.12)}{3} = 36.51$$

$$Level\ 3 = \frac{(37.01) + (36.41) + 35.80)}{3} = 36.41$$

Table 5.8. S/N response table for flexural strength.

Level	Nano-filler type (A)	Nano-filler content (B)
1	36.54	37.50
2	36.51	36.08
3	36.41	35.87
Max-Min	0.13	1.63

The most significant factor that affects the flexural strength can be identified by selecting the highest difference value from each factor (Joulazadeh & Navarchian 2010). Based on the results shown in the response table of S/N ratio, the most significant factor that has an effect on flexural strength is nano-filler content regardless the type of filler. Figure 5.11 shows the S/N response graph for flexural strength. Moreover, the best combination for the maximum enhancement in flexural strength can be identified by the selecting the highest S/N value from each factor. In this case, 1 wt% of nanoclay is the best option for optimizing flexural strength.
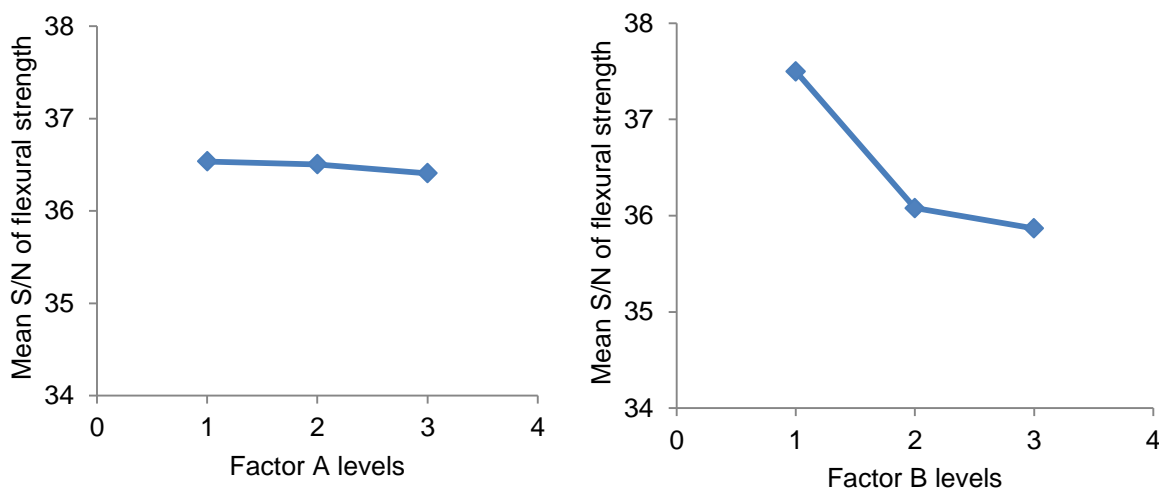
Figure 5.11. Mean S/N of flexural strength as a function of: a) Factor A levels; b) Factor B levels.

Analysis of Variance (ANOVA)

ANOVA is a statistical analysis that helps to determine the effect of each individual factor on the entire process by measuring the percentage contribution of each factor in the final result. Moreover, ANOVA can also determine the interaction between factors and their percentage contribution in the performance of the product.

In ANOVA analysis, we need to determine the degree of freedom (DF) for each factor. The total degree of freedom (DF_T), the degree of freedom for factor A (DF_A), the degree of freedom for factor B (DF_B) and the degree of freedom for the interaction AxB (DF_{AB}) can be calculated as follow:

$$DF_T = N - 1 \tag{5.5}$$

$$DF_A = a - 1 \tag{5.6}$$

$$DF_B = b - 1 \tag{5.7}$$

$$DF_{AB} = (a - 1)(b - 1) \tag{5.8}$$

where, N is number of trail, a is number of the level of factor A and b is number of the level of factor B.

To check if there is a possible interaction between factor A and B, we need to determine the S/N of factor A at each level of factor B as seen in Table 5.9. The significant interaction between factors A and B is seen in Figure 5.12.

Table 5.9. The factorial design of S/N for flexural strength.

	A1	A2	A3	Total
B1	38.60	36.89	37.01	**112.50**
B2	35.32	36.51	36.41	**108.24**
B3	35.69	36.12	35.80	**107.61**
Total	**109.61**	**109.52**	**109.22**	
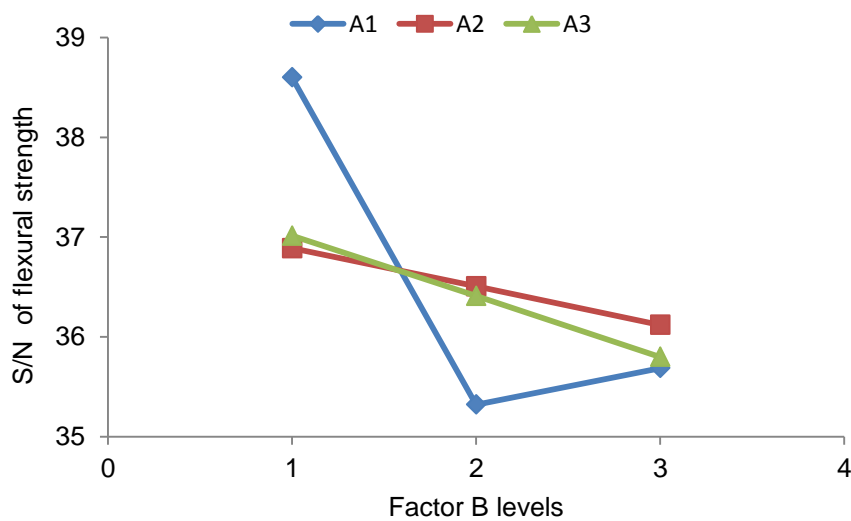
Figure 5.12. Two-way interaction plots of the S/N values for flexural strength.

The correction factor for total means S/N ratio (CF), the total sum of squares of mean S/N (SS_T), the sum of squares of mean S/N for factor A (SS_A), the sum of squares of mean S/N for factor B (SS_B), the sum of squares for the interaction AxB (SS_{AB}), and sum of squares of mean S/N for error (SS_e)

$$CF = \frac{(\sum_{i=1}^{n} y_i)^2}{n} \tag{5.9}$$

$$SS_T = \sum_{i=1}^{n} y_i^2 - CF \tag{5.10}$$

$$SS_A = \frac{\sum_{j=1}^{a} A_j^2}{b} - CF \tag{5.11}$$

$$SS_B = \frac{\sum_{k=1}^{b} B_k^2}{a} - CF \tag{5.12}$$

$$SS_{AB} = \sum_{k=1}^{b} \sum_{j=1}^{a} AB_{jk}^2 - SS_A - SS_B - CF \tag{5.13}$$

$$SS_e = SS_T - SS_A - SS_B - SS_{AB} \tag{5.14}$$

where y is the mean *S/N* observation for each trail (i), n is the total number of the trail (i), A_j is the mean *S/N* ratio of factor A at level j, B_k is the mean *S/N* ratio of factor B at level k, AB_{jk} is the mean *S/N* of factor A at level j and factor B at level k.

The mean of squares (MS) for each factor is calculated as follow:

$$MS_A = \frac{SS_A}{DF_A} \tag{5.15}$$

where MS_A is the mean of squares for factor A, DF_A is the degree of freedom for factor A.

The F-ratios are obtained by dividing the mean square of each factor (MS) by the mean square of error *(MS_e)* as follow:

$$F_A = \frac{MS_A}{MS_e} \tag{5.16}$$

Finally, the percentage of contributions (P) of each factor can be calculated as:

$$P_A = \frac{SS_A}{SS_T} \times 100 \tag{5.17}$$

ANOVA for the S/N ration of flexural strength is measured and listed in Table 5.10.

Table 5.10. ANOVA results for signal-to-noise (S/N) ratio for flexural strength.

Factors	DF	Sum of Sq	Mean Sq	F-ratio	P (%)
A	2	0.03	0.02	------	0.36
B	2	4.73	2.37	-----	62.88
A×B	4	2.77	0.69	------	36.76
Error	0	0	0	------	-------
Total	8	7.53	-------	------	100

ANOVA results indicate that factor B (nano-filler content) has the maximum influence in flexural strength with contributing (62.88 %) compared to the others. This means that flexural strength is very sensitive to the filler content. The results of S/N showed that the maximum flexural strength is obtained at low filler content (1 wt%). The interaction between filler content and filler type (A×B) has the second biggest contribution (36.77 %).

Flexural modulus

Signal-to-Noise (S/N) ratio

Table 5.11. Experimental results for flexural modulus and the corresponding S/N ratio.

Trail	Nano-filler type (A)	Nano-filler content (B)	Flexural modulus (GPa)	S/N
1	nanoclay	1 wt%	1.64	3.15
2	nanoclay	3 wt%	1.47	3.29
3	nanoclay	5 wt%	1.39	2.59
4	HNT	1 wt%	1.51	3.40
5	HNT	3 wt%	1.30	2.21
6	HNT	5 wt%	1.40	2.84
7	n-SiC	1 wt%	1.60	3.61
8	n-SiC	3 wt%	1.39	2.62
9	n-SiC	5 wt%	1.39	2.80

Flexural modulus is the average of five measurements. S/N ratio is the calculation of five measurements.

Table 5.12. S/N response table for flexural modulus.

Level	Nano-filler type (A)	Nano-filler content (B)
1	3.01	3.39
2	2.82	2.71
3	3.01	2.74
Max-Min	0.19	0.68
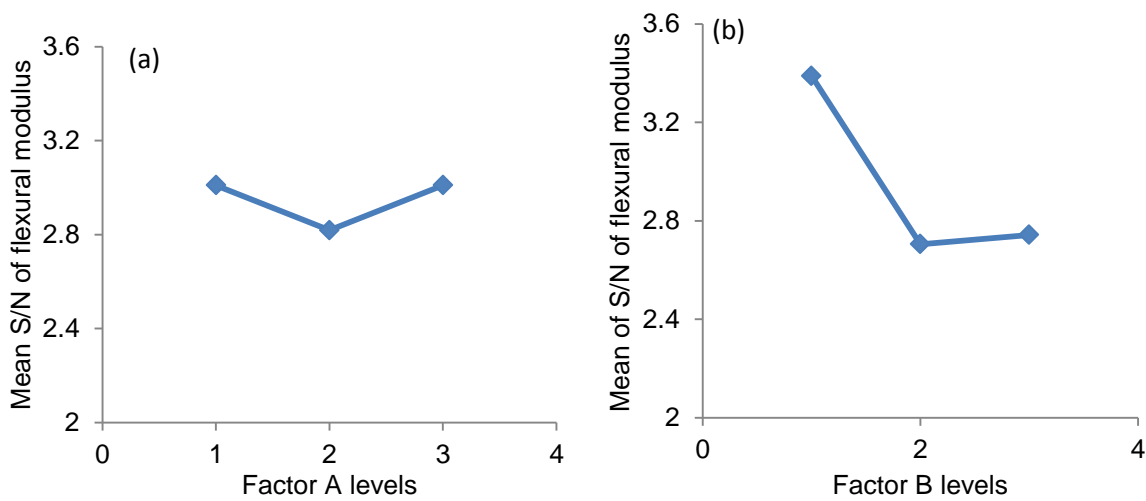
Figure 5.13. Mean S/N of flexural modulus as a function of: a) Factor A levels; b) Factor B levels.

Analysis of Variance (ANOVA)

Table 5.13. ANOVA results for signal-to-noise (S/N) ratio for flexural modulus.

Factors	DF	Sum of Sq	Mean Sq	F-ratio	P (%)
A	2	0.07	0.035	-----	4.53
B	2	0.89	0.45	-----	54.72
A×B	4	0.66	0.17	------	40.75
Error	0	0	0	------	------
Total	8	1.62	-------	------	100

Fracture toughness

Signal-to-Noise (S/N) ratio

Table 5.14. Experimental results for fracture toughness and the corresponding S/N ratio.

Trail	Nano-filler type (A)	Nano-filler content (B)	Fracture toughness $(MPa.m^{1/2})$	S/N
1	nanoclay	1 wt%	1.11	0.83
2	nanoclay	3 wt%	0.93	-0.71
3	nanoclay	5 wt%	0.98	-0.58
4	HNT	1 wt%	1.33	2.18
5	HNT	3 wt%	1.03	0.24
6	HNT	5 wt%	1.18	1.35
7	n-SiC	1 wt%	1.61	3.59
8	n-SiC	3 wt%	1.23	1.51
9	n-SiC	5 wt%	1.06	0.34

Fracture toughness is the average of five measurements. S/N ratio is the calculation of five measurements.

Table 5.15. S/N response table for fracture toughness.

| Level	Nano-filler type (A)	Nano-filler content (B)
1	-0.15	2.20
2	1.255	0.35
3	1.81	0.37
Max-Min	1.66	1.85
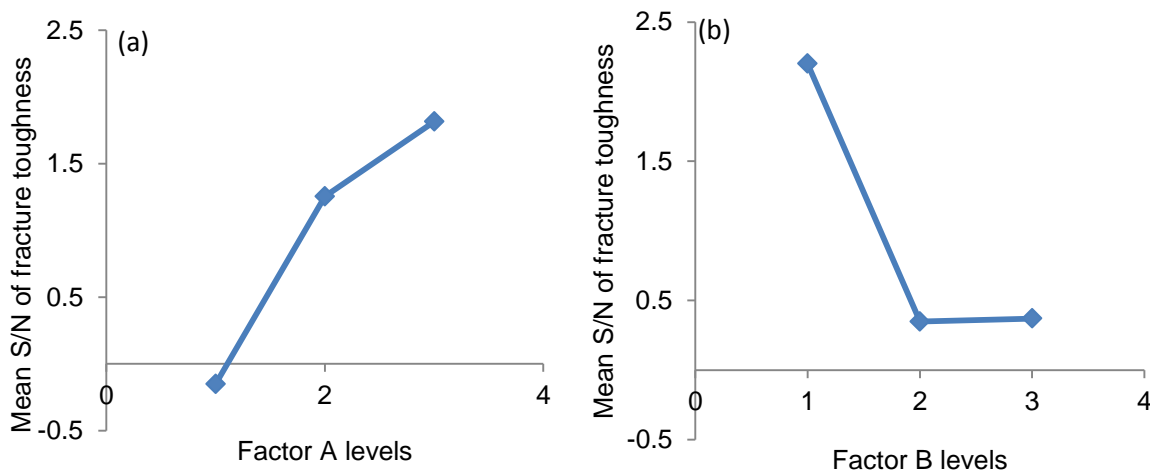
Figure 5.14. Mean S/N of fracture toughness as a function of: a) Factor A levels; b) Factor B levels.

Analysis of Variance (ANOVA)

Table 5.16. ANOVA results for signal-to-noise (S/N) ratio for fracture toughness.

Factors	DF	Sum of Sq	Mean Sq	F-ratio	P (%)
A	2	6.16	3.08	------	41.26
B	2	6.79	3.40	-----	45.45
A×B	4	1.98	0.50	------	13.29
Error	0	0	0	------	--------
Total	8	14.93	-------	------	100

Impact strength

Signal-to-Noise (S/N) ratio

Table 5.17. Experimental results for impact strength and the corresponding S/N ratio.

Trail	Nano-filler type (A)	Nano-filler content (B)	Impact strength (kJ/m^2)	S/N
1	nanoclay	1 wt%	6.11	15.00
2	nanoclay	3 wt%	6.86	16.30
3	nanoclay	5 wt%	7.78	16.81
4	HNT	1 wt%	5.61	14.46
5	HNT	3 wt%	6.38	15.95
6	HNT	5 wt%	6.96	16.64
7	n-SiC	1 wt%	7.51	17.25
8	n-SiC	3 wt%	6.96	16.68
9	n-SiC	5 wt%	7.63	17.36

Impact strength strength is the average of five measurements. S/N ratio is the calculation of five measurements.

Table 5.18. S/N response table for impact strength.

Level	Nano-filler type (A)	Nano-filler content (B)
1	16.04	15.57
2	15.68	16.31
3	17.10	16.94
Max-Min	1.42	1.37
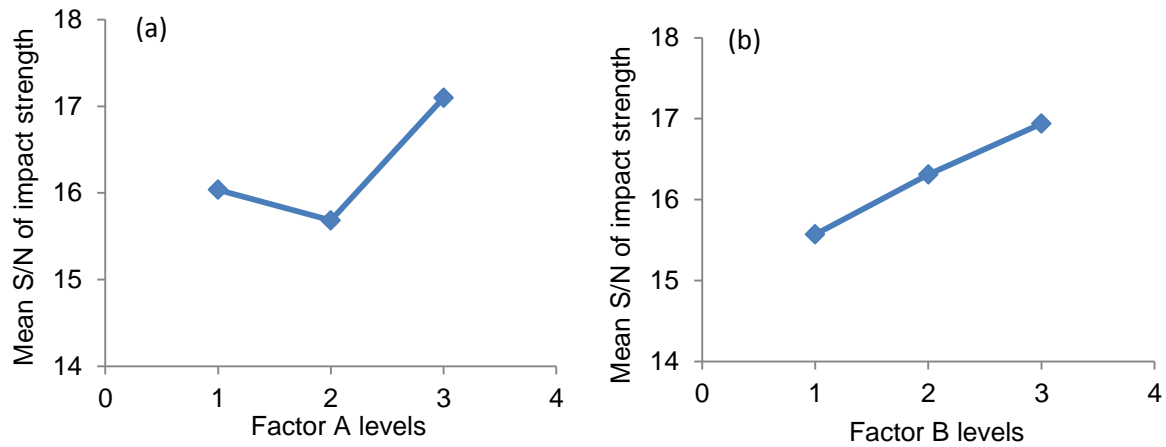
Figure 5.15. Mean S/N of impact strength as a function of: a) Factor A levels; b) Factor B levels.

Analysis of Variance (ANOVA)

Table 5.19. ANOVA results for signal-to-noise (S/N) ratio for impact strength.

Factors	DF	Sum of Sq	Mean Sq	F-ratio	P (%)
A	2	3.25	1.63	------	41.95
B	2	2.81	1.41	-----	36.31
A×B	4	1.68	0.42	------	21.74
Error	0	0	0	------	
Total	8	7.74	------	------	100

Summary of factors contribution on mechanical properties
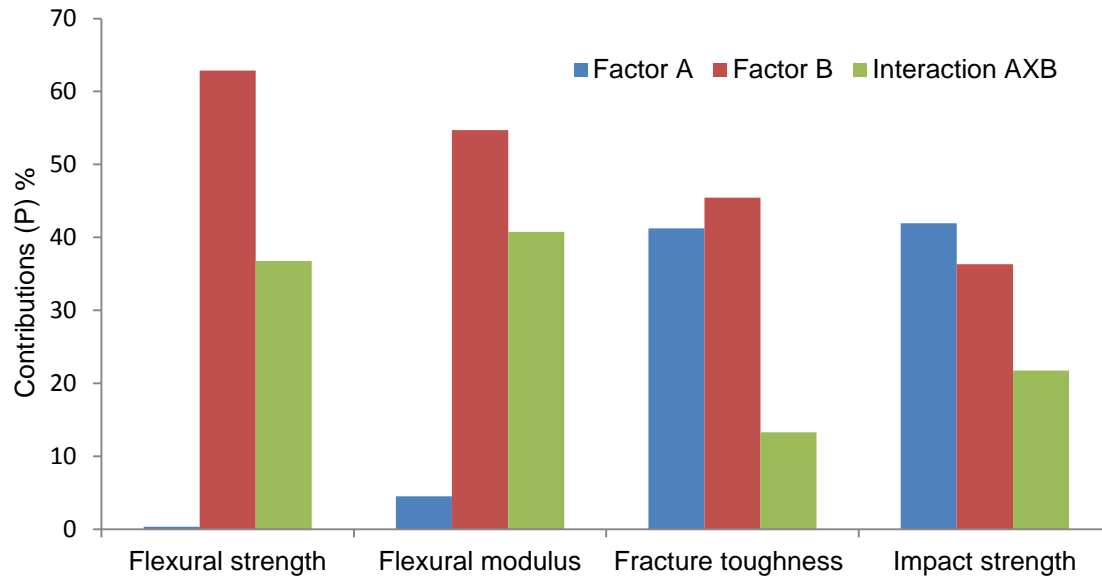
Figure 5.16. Summary of factors contribution for mechanical properties.

In summary, it can be observed from Figure 5.16 that nano-filler content has a strong effect on flexural strength (62.9% contributions) and flexural modulus (54.7% contributions) compared to nano-filler type.

However, there is no significant deference in the contribution of both nano-filler content and type for fracture toughness and impact strength. In the case of fracture toughness, filler content showed higher contributions than filler type. But in the case of impact strength, nano-filler type showed higher contributions than filler content.

5.6 APPENDIX F

Effect of Process Variables on the Mechanical Properties of RCF/Nano-Filler Reinforced Epoxy Eco-Nanocomposites.

(Statistics Analysis)

In this work, the Taguchi method with Signal-to-Noise (S/N) ratio and Analysis of Variance (ANOVA) were used to statistically investigate the effect of operating variables (*i.e.* nano-filler type, nano-filler content and RCF type) on the mechanical properties of RCF/nano-filler reinforced epoxy eco-nanocomposites including flexural strength, flexural modulus, fracture toughness and impact strength. The main goal was to determine the most significant factor that influences each type of mechanical properties of such eco-nanocomposites.

Design of experiments

In this work, three factors (*i.e.* nano-filler type, nano-filler content and RCF type) with three and two levels are proposed in Taguchi design of experiment as seen in Table 5.20

Table 5.20. Proposed factors with their levels.

Factors	Level 1	Level 2	Level 3
Nano-filler type (A)	nanoclay	HNT	n-SiC
Nano-filler content (B)	1 wt%	3 wt%	5 wt%
RCF type (C)	RCF with thickness 200 μ	RCF with thickness 600 μ	

Flexural Strength

Signal-to-Noise (S/N) ratio

Taguchi L_{27} orthogonal array was selected to analyse the experimental results of mechanical tests (Table 5.21).

Table 5.21. Experimental results for flexural strength and the corresponding S/N ratio.

Trail	Nano-filler type (A)	Nano-filler content (B)	RCF type (C)	Flexural strength (MPa)	S/N
1	1	1	1	156.46	43.88
2	1	2	1	151.41	43.58
3	1	3	1	149.30	43.45
4	2	1	1	156.06	43.84
5	2	2	1	154.51	43.75
6	2	3	1	153.69	43.67
7	3	1	1	156.06	43.81
8	3	2	1	151.55	43.59
9	3	3	1	150.38	43.52
10	1	1	2	90.62	39.11
11	1	2	2	76.23	37.61
12	1	3	2	78.31	37.83
13	2	1	2	80.01	38.06
14	2	2	2	67.00	36.35
15	2	3	2	68.60	36.70
16	3	1	2	81.11	38.17
17	3	2	2	81.66	38.22
18	3	3	2	81.65	38.18

Flexural strength is the average of five measurements. S/N ratio is the calculation of five measurements.

Table 5.22. S/N response table for flexural strength.

Level	Nano-filler type (A)	Nano-filler content (B)	RCF type (C)
1	40.91	41.14	43.68
2	40.39	40.52	37.80
3	40.91	40.56	------
Max-Min	0.52	0.62	5.88
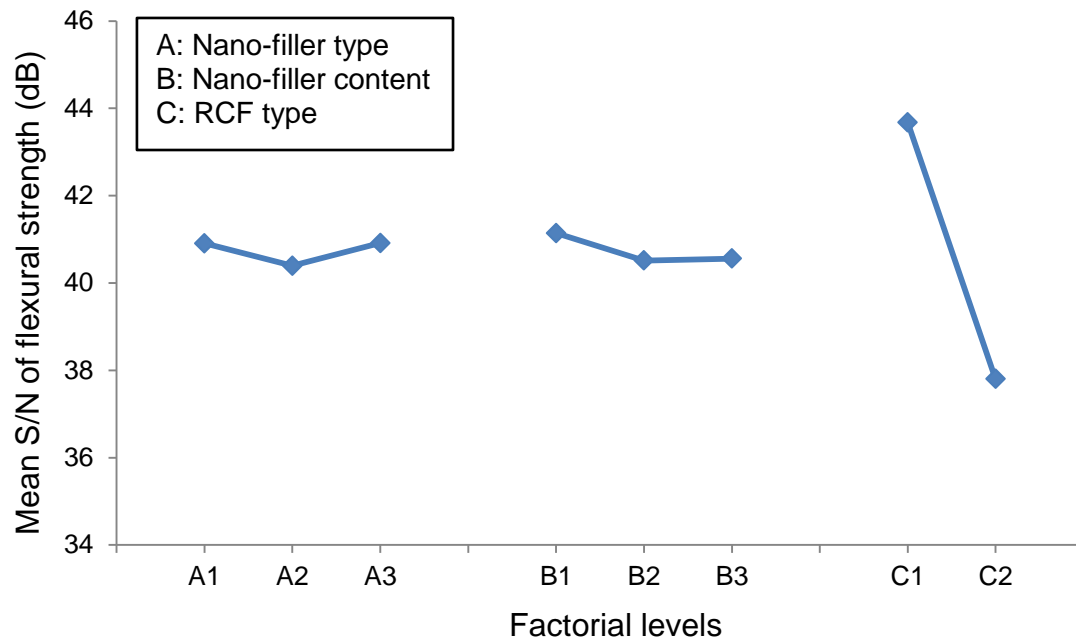
Figure 5.17. Mean S/N of flexural strength as a function of different factorial levels.

Analysis of Variance (ANOVA)

ANOVA for the S/N ration of flexural strength was measured and listed in Table 5.23.

Table 5.23. ANOVA results for signal-to-noise (S/N) ratio for flexural strength.

Factors	DF	Sum of Sq	Mean Sq	F-ratio	P (%)
A	2	1.07	0.54	1.59	0.67
B	2	1.47	0.74	2.18	0.91
A×B	4	0.51	0.13	0.38	0.31
C	1	155.29	155.29	456.74	96.42
Error	8	2.72	0.34		1.69
Total	17	161.06			100.00

Flexural Modulus

Signal-to-Noise (S/N) ratio

Table 5.24. Experimental results for flexural modulus and the corresponding S/N ratio.

Trail	Nano-filler type (A)	Nano-filler content (B)	RCF type (C)	Flexural modulus (GPa)	S/N
1	1	1	1	7.44	16.99
2	1	2	1	6.84	16.51
3	1	3	1	7.98	17.83
4	2	1	1	7.51	17.20
5	2	2	1	7.51	17.30
6	2	3	1	7.75	17.38
7	3	1	1	7.61	17.46
8	3	2	1	7.52	17.41
9	3	3	1	7.58	17.38
10	1	1	2	2.46	7.62
11	1	2	2	2.44	7.56
12	1	3	2	2.23	6.58
13	2	1	2	2.40	6.94
14	2	2	2	2.06	5.96
15	2	3	2	2.29	6.96
16	3	1	2	2.39	6.73
17	3	2	2	2.19	6.70
18	3	3	2	2.30	6.76

Flexural modulus is the average of five measurements. S/N ratio is the calculation of five measurements.

Table 5.25. S/N response table for flexural modulus.

Level	Nano-filler type (A)	Nano-filler content (B)	RCF type (C)
1	12.18	12.16	17.27
2	11.96	11.91	6.87
3	12.07	12.15	
Max-Min	0.22	0.25	10.40
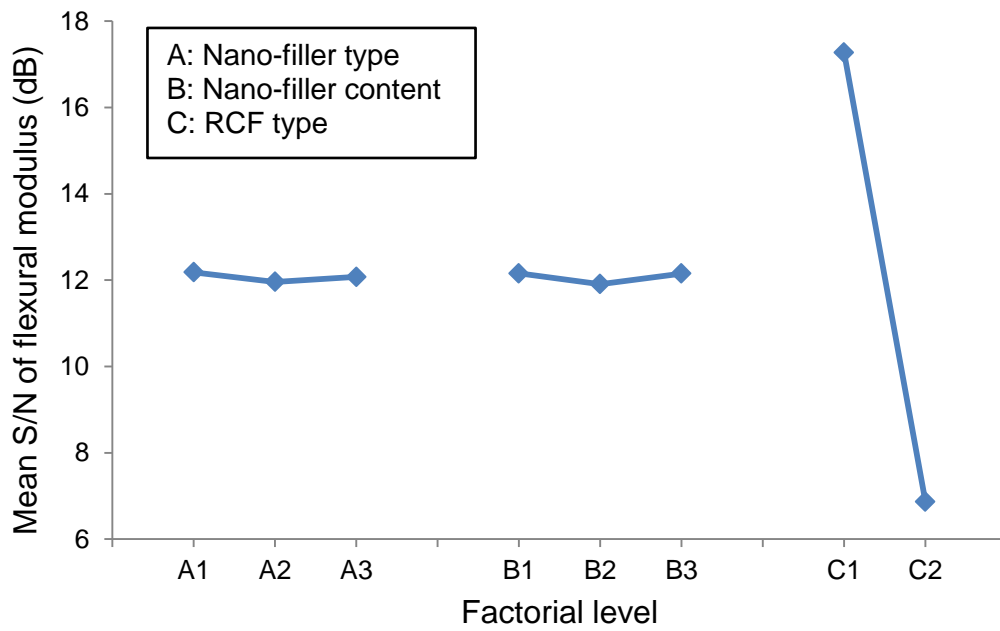
Figure 5.18. Mean S/N of flexural modulus as a function of different factorial levels.

Analysis of Variance (ANOVA)

Table 5.26. ANOVA results for signal-to-noise (S/N) ratio for flexural modulus.

Factors	DF	Sum of Sq	Mean Sq	F-ratio	P (%)
A	2	0.15	0.08	0.25	0.03
B	2	0.24	0.12	0.38	0.05
A×B	4	0.16	0.04	0.13	0.03
C	1	487.43	487.43	1523.22	99.37
Error	8	2.52	0.32		0.51
Total	17	490.50			100.00

Fracture toughness

Signal-to-Noise (S/N) ratio

Table 5.27. Experimental results for fracture toughness and the corresponding S/N ratio.

Trail	Nano-filler type (A)	Nano-filler content (B)	RCF type (C)	Fracture toughness (MPa.m$^{1/2}$)	S/N
1	1	1	1	3.84	11.57
2	1	2	1	3.89	11.75
3	1	3	1	3.87	11.72
4	2	1	1	4.12	12.04
5	2	2	1	3.88	11.59
6	2	3	1	3.96	11.80
7	3	1	1	3.85	11.45
8	3	2	1	4.10	12.08
9	3	3	1	4.23	12.36
10	1	1	2	2.32	7.19
11	1	2	2	2.30	6.82
12	1	3	2	2.02	5.96
13	2	1	2	2.41	7.42
14	2	2	2	2.37	6.96
15	2	3	2	2.33	7.29
16	3	1	2	2.42	6.67
17	3	2	2	2.21	6.35
18	3	3	2	2.18	6.32

Fracture toughness is the average of five measurements. S/N ratio is the calculation of five measurements.

Table 5.28. S/N response table for fracture toughness.

Level	Nano-filler type (A)	Nano-filler content (B)	RCF type (C)
1	9.17	9.39	11.82
2	9.51	9.26	6.78
3	9.21	9.24	
Max-Min	0.35	0.15	5.04
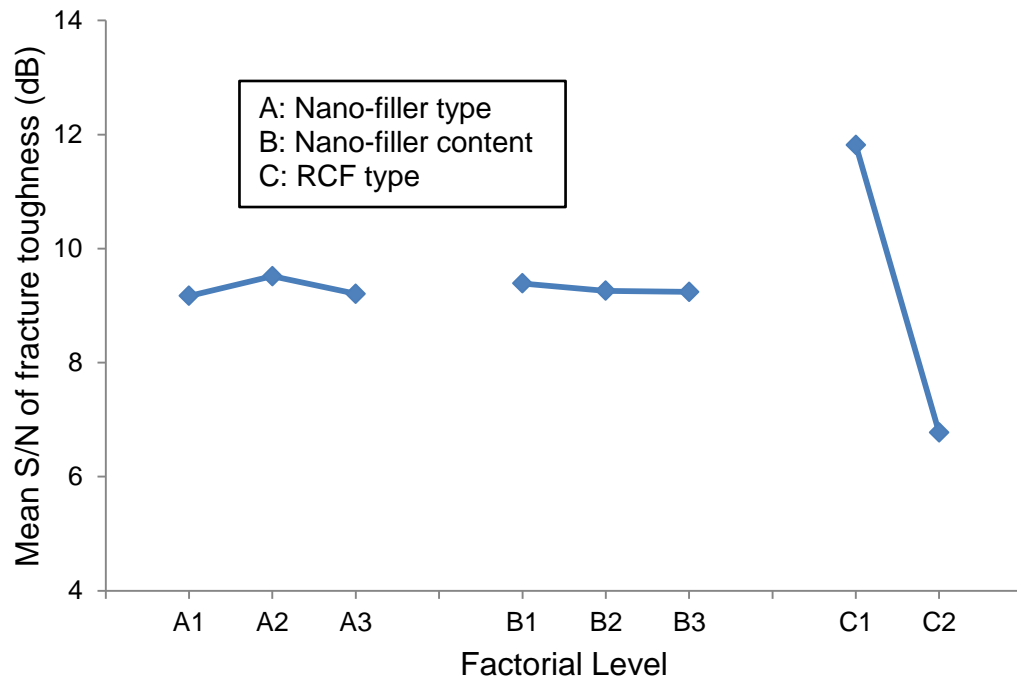
Figure 5.19. Mean S/N of fracture toughness as a function of different factorial levels.

Analysis of Variance (ANOVA)

Table 5.29. ANOVA results for signal-to-noise (S/N) ratio for fracture toughness.

Factors	DF	Sum of Sq	Mean Sq	F-ratio	P (%)
A	2	0.43	0.22	1.10	0.37
B	2	0.08	0.04	0.20	0.07
A×B	4	0.54	0.27	0.70	0.46
C	1	114.43	114.43	572.15	97.76
Error	8	1.56	0.20		1.34
Total	17	117.05			100.00

Impact strength

Signal-to-Noise (S/N) ratio

Table 5.30. Experimental results for impact strength and the corresponding S/N ratio.

Trail	Nano-filler type (A)	Nano-filler content (B)	RCF type (C)	Impact strength (kJ/m^2)	S/N
1	1	1	1	35.15	30.58
2	1	2	1	29.54	29.07
3	1	3	1	26.47	28.23
4	2	1	1	27.84	28.64
5	2	2	1	24.48	27.75
6	2	3	1	28.29	28.75
7	3	1	1	28.79	28.78
8	3	2	1	33.53	30.04
9	3	3	1	37.15	31.10
10	1	1	2	16.59	24.31
11	1	2	2	14.25	22.98
12	1	3	2	14.73	23.32
13	2	1	2	13.33	22.44
14	2	2	2	12.00	21.50
15	2	3	2	13.16	22.37
16	3	1	2	12.62	21.99
17	3	2	2	11.81	21.28
18	3	3	2	12.69	22.00

Flexural strength is the average of five measurements. S/N ratio is the calculation of five measurements.

Table 5.31. S/N response table for impact strength.

Level	Nano-filler type (A)	Nano-filler content (B)	RCF type (C)
1	26.42	26.12	29.22
2	25.24	25.44	22.47
3	25.87	25.96	
Max-Min	1.18	0.68	6.75
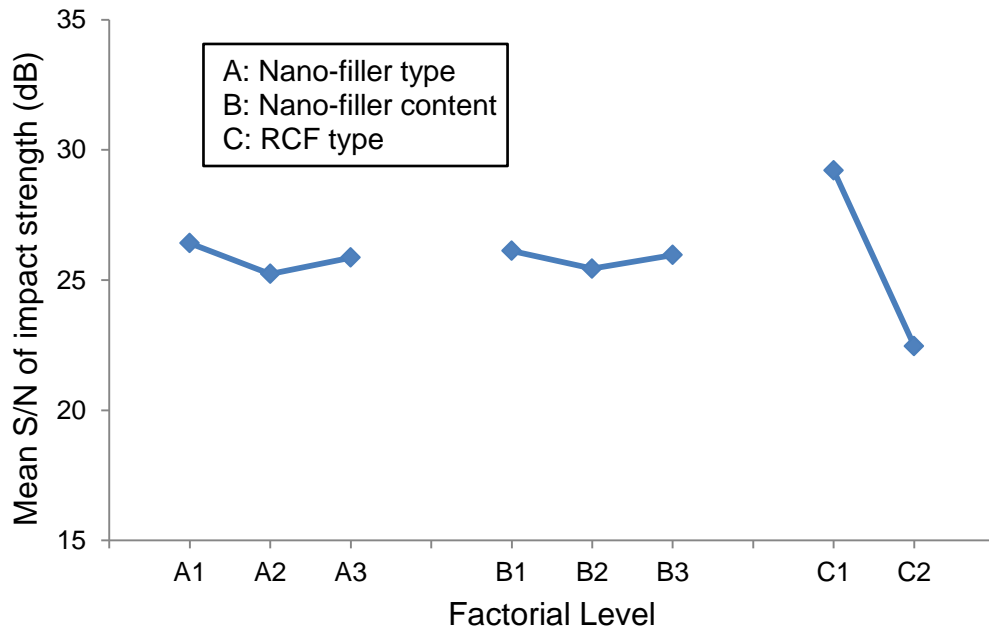
Figure 5.20. Mean S/N of impact strength as a function of different factorial levels.

Analysis of Variance (ANOVA)

Table 5.32. ANOVA results for signal-to-noise (S/N) ratio for impact strength.

Factors	DF	Sum of Sq	Mean Sq	F-ratio	P (%)
A	2	4.16	2.08	2.31	1.87
B	2	1.54	0.77	0.86	0.69
A×B	4	4.34	1.09	1.21	1.95
C	1	205.09	205.09	227.88	92.26
Error	8	7.17	0.90		3.23
Total	17	222.30			100.00

Summary of contributing factors on mechanical properties
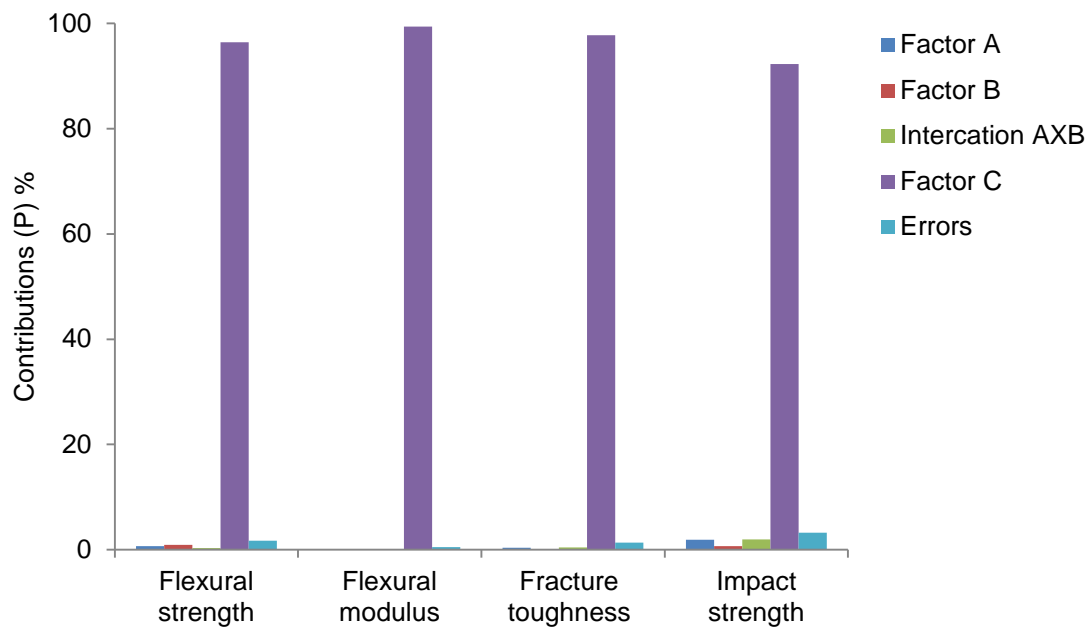
Figure 5.21. Summary of contributing factors for mechanical properties.

In Summary, it can be observed from Figure 5.21 that RCF type has very strong effect on all mechanical properties of RCF/nano-filler reinforced epoxy eco-nanocomposites. However, there is no significant effect of both nano-filler content and type on the mechanical properties of RCF/epoxy eco-nanocomposites.

5.7 APPENDIX G

Statement of Contributions of Others

5.7.1 Appendix G-1: Statement of Contribution of Others for "Mechanical Properties and Water Absorption Behaviour of Recycled Cellulose Fibre Reinforced Epoxy Composites".

Statement of Contribution of Others for "Mechanical Properties and Water Absorption Behaviour of Recycled Cellulose Fibre Reinforced Epoxy Composites".

13th June 2012

To Whom It May Concern

I, Prof. I.M. Low, contributed by project supervision and manuscript editing to the paper/publication entitled

Alamri, H., and I. M. Low. 2012. Mechanical properties and water absorption behaviour of recycled cellulose fibre reinforced epoxy composites. *Polymer Testing* 31(5): 620-628.

Undertaken with Hatem Alamri

(Signature of Co-Author)

I. M. Low

(Signature of First Author)

Hatem Alamri

5.7.2 Appendix G-2: Statement of Contribution of Others for "Mechanical, Thermal and Microstructural Characteristics of Cellulose Fibre Reinforced Epoxy/Organoclay Nanocomposites"

Statement of Contribution of Others for "Mechanical, Thermal and Microstructural Characteristics of Cellulose Fibre Reinforced Epoxy/Organoclay Nanocomposites".

12th June 2012

To Whom It May Concern

I, Prof. I.M. Low, contributed by project supervision and manuscript editing to the paper/publication entitled

Alamri, H., I. M. Low, and Z. Alothman. 2012. Mechanical, thermal and microstructural characteristics of cellulose fibre reinforced epoxy/organoclay nanocomposites. *Composites Part B: Engineering* 43: 2762-2771.

Undertaken with Hatem Alamri

(Signature of Co-Author)

I. M. Low

(Signature of First Author)

Hatem Alamri

Statement of Contribution of Other for "Mechanical, Thermal and Microstructural Characteristics of Cellulose Fibre Reinforced Epoxy/Organoclay Nanocomposites".

13th June 2012

To Whom It May Concern

I, Dr. Zeid. Alothman, contributed by specialist technical advice and instrument usage to the paper/publication entitled

Alamri, H., I. M. Low, and Z. Alothman. 2012. Mechanical, thermal and microstructural characteristics of cellulose fibre reinforced epoxy/organoclay nanocomposites. *Composites Part B: Engineering* 43: 2762-2771.

undertaken with Hatem Alamri

(Signature of Co-Author)

Zeid Alothman

(Signature of First Author)

Hatem Alamri

5.7.3 Appendix G-3: Statement of Contribution of Others for "Microstructural, Mechanical, and Thermal Characteristics of Recycled Cellulose Fibre-Halloysite-Epoxy Hybrid Nanocomposites".

Statement of Contribution of Others for "Microstructural, Mechanical, and Thermal Characteristics of Recycled Cellulose Fibre-Halloysite-Epoxy Hybrid Nanocomposites".

12th June 2012

To Whom It May Concern

I, Prof. I.M. Low, contributed by project supervision and manuscript editing to the paper/publication entitled

Alamri, H., and I. M. Low. 2012. Microstructural, mechanical, and thermal characteristics of recycled cellulose fibre-halloysite-epoxy hybrid nanocomposites. *Polymer Composites* 33(4): 589-600.

Undertaken with Hatem Alamri

(Signature of Co-Author)

I. M. Low

(Signature of First Author)

Hatem Alamri

5.7.4 Appendix G-4: Statement of Contribution of Others for "Characterization of Epoxy Hybrid Composites Filled with Cellulose Fibres and Nano-SiC".

Statement of Contribution of Others for "Characterization of Epoxy Hybrid Composites Filled with Cellulose Fibres and Nano-SiC".

11th June 2012

To Whom It May Concern

I, Prof. I.M. Low, contributed by project supervision and manuscript editing to the paper/publication entitled

Alamri, H., and I. M. Low. 2012. Characterization of epoxy hybrid composites filled with cellulose fibres and nano-SiC. *Journal of Applied Polymer Science* 126: 221-231.

Undertaken with Hatem Alamri

(Signature of Co-Author)

I. M. Low

(Signature of First Author)

Hatem Alamri

5.7.5 Appendix G-5: Statement of Contribution of Others for "Effect of Water Absorption on the Mechanical Properties of Nano-Filler Reinforced Epoxy Nanocomposites".

Statement of Contribution of Others for "Effect of Water Absorption on the Mechanical Properties of Nano-Filler Reinforced Epoxy Nanocomposites".

27th June 2012

To Whom It May Concern

I, Prof. I.M. Low, contributed by project supervision and manuscript editing to the paper/publication entitled

Alamri, H., and I. M. Low. 2012. Effect of water absorption on the mechanical properties of nano-filler reinforced epoxy nanocomposites. *Materials and Design* 42: 214-222.

Undertaken with Hatem Alamri

(Signature of Co-Author)

I. M. Low

(Signature of First Author)

Hatem Alamri

5.7.6 Appendix G-6: Statement of Contribution of Others for "Effect of Water Absorption on the Mechanical Properties of N-SiC Filled Recycled Cellulose Fibre Reinforced Epoxy Eco-Nanocomposites".

Statement of Contribution of Others for "Effect of Water Absorption on the Mechanical Properties of N-SiC Filled Recycled Cellulose Fibre Reinforced Epoxy Eco-Nanocomposites".

27th June 2012

To Whom It May Concern

I, Prof. I.M. Low, contributed by project supervision and manuscript editing to the paper/publication entitled

Alamri, H., and I. M. Low. 2012. Effect of water absorption on the mechanical properties of n-SiC filled recycled cellulose fibre reinforced epoxy eco-nanocomposites. *Polymer Testing* 31(6): 810-818.

Undertaken with Hatem Alamri

(Signature of Co-Author)

I. M. Low

(Signature of First Author)

Hatem Alamri

5.7.7 Appendix G-7: Statement of Contribution of Others for "Effect of Water Absorption on the Mechanical Properties of Nanoclay Filled Recycled Cellulose Fibre Reinforced Epoxy Hybrid Nanocomposites".

Statement of Contribution of Others for "Effect of Water Absorption on the Mechanical Properties of Nanoclay Filled Recycled Cellulose Fibre Reinforced Epoxy Hybrid Nanocomposites".

14th November 2012

To Whom It May Concern

I, Prof. I.M. Low, contributed by project supervision and manuscript editing to the paper/publication entitled

Alamri, H., and I. M. Low. 2013. Effect of water absorption on the mechanical properties of nanoclay filled recycled cellulose fibre reinforced epoxy hybrid nanocomposites. *Composites Part A: Applied Science and Manufacturing* 44: 23-31.

Undertaken with Hatem Alamri

(Signature of Co-Author)

I. M. Low

(Signature of First Author)

Hatem Alamri

5.8 APPENDIX H

Copyright Forms

5.8.1 Appendix H-1: Elsevier Journal Articles

Copyright information relating to;

Alamri, H., and I. M. Low. 2012. Mechanical properties and water absorption behaviour of recycled cellulose fibre reinforced epoxy composites. *Polymer Testing,* 31(5): 620-628.

Alamri, H., I. M. Low, and Z. Alothman. 2012. Mechanical, thermal and microstructural characteristics of cellulose fibre reinforced epoxy/organoclay nanocomposites. *Composites Part B: Engineering* 43: 2762-2771.

Alamri, H., and I. M. Low. 2012. Effect of water absorption on the mechanical properties of nano-filler reinforced epoxy nanocomposites. *Materials and Design* 42: 214-222.

Alamri, H., and I. M. Low. 2012. Effect of water absorption on the mechanical properties of n-SiC filled recycled cellulose fibre reinforced epoxy eco-nanocomposites. *Polymer Testing* 31(6): 810-818.

Alamri, H., and I. M. Low. 2013. Effect of water absorption on the mechanical properties of nanoclay filled recycled cellulose fibre reinforced epoxy hybrid nanocomposites. *Composites Part A: Applied Science and Manufacturing* 44: 23-31.

Available on

Authors' Rights & Responsibilities

At Elsevier, we are dedicated to protecting your rights as an author, and ensuring that any and all legal information and copyright regulations are addressed.

Whether an author is published with Elsevier or any other publisher, we hold ourselves and our colleagues to the highest standards of ethics, responsibility and legal obligation.

As a journal author, you retain rights for a large range of author uses of your article, including use by your employing institute or company. These rights are retained and permitted without the need to obtain specific permission from Elsevier.

What rights do I retain as a journal author*?

- the right to make copies (print or electronic) of the journal article for your own personal use, including for your own classroom teaching use;
- the right to make copies and distribute copies of the journal article (including via e-mail) to research colleagues, for personal use by such colleagues for scholarly purposes*****;
- the right to post a pre-print version of the journal article on Internet websites including electronic pre-print servers, and to retain indefinitely such version on such servers or sites for scholarly purposes***** (with some exceptions such as The Lancet and Cell Press. See also our information on ▭▸electronic preprints for a more detailed discussion on these points)*;
- the right to post a revised personal version of the text of the final journal article (to reflect changes made in the peer review process) on your personal or institutional website or server for scholarly purposes*, incorporating the complete citation and with a link to the Digital Object Identifier (DOI) of the article (but not in subject-oriented or centralized repositories or institutional repositories with mandates for systematic postings unless there is a specific agreement with the publisher. ▭▸Click here for further information);
- the right to present the journal article at a meeting or conference and to distribute copies of such paper or article to the delegates attending the meeting;
- for your employer, if the journal article is a 'work for hire', made within the scope of the author's employment, the right to use all or part of the information in (any version of) the journal article for other intra-company use (e.g. training);
- patent and trademark rights and rights to any process or procedure described in the journal article;
- **the right to include the journal article, in full or in part, in a thesis or dissertation**;
- the right to use the journal article or any part thereof in a printed compilation of your works, such as collected writings or lecture notes (subsequent to publication of the article in the journal); and
- the right to prepare other derivative works, to extend the journal article into book-length form, or to otherwise re-use portions or excerpts in other works, with full acknowledgement of its original publication in the journal.

Copyright information relating to;

Alamri, H., and I. M. Low. 2012. Microstructural, mechanical, and thermal characteristics of recycled cellulose fibre-halloysite-epoxy hybrid nanocomposites. *Polymer Composites* 33(4): 589-600.

Alamri, H., and I. M. Low. 2012. Characterization of epoxy hybrid composites filled with cellulose fibres and nano-SiC. *Journal of Applied Polymer Science* 126: 221-231.

**JOHN WILEY AND SONS LICENSE
TERMS AND CONDITIONS**

Mar 21, 2012

This is a License Agreement between Hatem Alamri ("You") and John Wiley and Sons ("John Wiley and Sons") provided by Copyright Clearance Center ("CCC"). The license consists of your order details, the terms and conditions provided by John Wiley and Sons, and the payment terms and conditions.

All payments must be made in full to CCC. For payment instructions, please see information listed at the bottom of this form.

License Number	2873500578829
License date	Mar 21, 2012
Licensed content publisher	John Wiley and Sons
Licensed content publication	Polymer Composites
Licensed content title	Microstructural, mechanical, and thermal characteristics of recycled cellulose fiber-halloysite-epoxy hybrid nanocomposites
Licensed content author	H. Alamri,I. M. Low
Licensed content date	Apr 1, 2012
Start page	589
End page	600
Type of use	Dissertation/Thesis
Requestor type	Author of this Wiley article
Format	Print and electronic
Portion	Full article
Will you be translating?	No
Order reference number	
Total	0.00 USD
Terms and Conditions	

TERMS AND CONDITIONS

This copyrighted material is owned by or exclusively licensed to John Wiley & Sons, Inc. or one of its group companies (each a "Wiley Company") or a society for whom a Wiley Company has exclusive publishing rights in relation to a particular journal (collectively WILEY"). By clicking "accept" in connection with completing this licensing transaction, you agree that the following terms and conditions apply to this transaction (along with the billing and payment terms and conditions established by the Copyright Clearance Center Inc., ("CCC's Billing and Payment terms and conditions"), at the time that you opened your Rightslink account (these are available at any time at http://myaccount.copyright.com)

Terms and Conditions

1. The materials you have requested permission to reproduce (the "Materials") are protected by copyright.

2. You are hereby granted a personal, non-exclusive, non-sublicensable, non-transferable, worldwide, limited license to reproduce the Materials for the purpose specified in the licensing process. This license is for a one-time use only with a maximum distribution equal to the number that you identified in the licensing process. Any form of republication granted by this licence must

JOHN WILEY AND SONS LICENSE
TERMS AND CONDITIONS

May 21, 2012

This is a License Agreement between Hatem Alamri ("You") and John Wiley and Sons ("John Wiley and Sons") provided by Copyright Clearance Center ("CCC"). The license consists of your order details, the terms and conditions provided by John Wiley and Sons, and the payment terms and conditions.

All payments must be made in full to CCC. For payment instructions, please see information listed at the bottom of this form.

License Number	2894630677406
License date	Apr 23, 2012
Licensed content publisher	John Wiley and Sons
Licensed content publication	Journal of Applied Polymer Science
Licensed content title	Characterization of epoxy hybrid composites filled with cellulose fibers and nano-SiC
Licensed content author	H. Alamri, I. M. Low
Licensed content date	Apr 6, 2012
Start page	n/a
End page	n/a
Type of use	Dissertation/Thesis
Requestor type	Author of this Wiley article
Format	Print and electronic
Portion	Full article
Will you be translating?	No
Order reference number	None
Total	**0.00 USD**

Terms and Conditions

TERMS AND CONDITIONS

This copyrighted material is owned by or exclusively licensed to John Wiley & Sons, Inc. or one of its group companies (each a "Wiley Company") or a society for whom a Wiley Company has exclusive publishing rights in relation to a particular journal (collectively WILEY"). By clicking "accept" in connection with completing this licensing transaction, you agree that the following terms and conditions apply to this transaction (along with the billing and payment terms and conditions established by the Copyright Clearance Center Inc., ("CCC's Billing and Payment terms and conditions"), at the time that you opened your Rightslink account (these are available at any time at http://myaccount.copyright.com)

Terms and Conditions

1. The materials you have requested permission to reproduce (the "Materials") are protected by copyright.

2. You are hereby granted a personal, non-exclusive, non-sublicensable, non-transferable, worldwide, limited license to reproduce the Materials for the purpose specified in the licensing process. This license is for a one-time use only with a maximum distribution equal to the number that you identified in the licensing process. Any form of republication granted by this licence must be completed within two years of the date of the grant of this licence (although copies prepared before may be distributed thereafter). The Materials shall not be used in any other manner or for any other purpose. Permission is granted subject to an appropriate acknowledgement given to the

BIBLIOGRAPHY

Abacha, N., M. Kubouchi, K. Tsuda, and T. Sakai. 2007. Performance of epoxy-nanocomposite under corrosive environment. *Express Polymer Letters* 1 (6): 364–369.

Adachi, T., M. Osaki, W. Araki, and S-C. Kwon. 2008. Fracture toughness of nano- and micro-spherical silica-particle-filled epoxy composites. *Acta Materialia* 56: 2101–2109.

Al-Kaabi, K., A. Al-Khanbashi, and A. Hammami. 2005. Date palm fibres as polymeric matrix reinforcement: DPF/polyester composite properties. *Polymer Composites* 26(5): 604-613.

Alamri, H., and I. M. Low. 2010. Characterization and properties of recycled cellulose fibre-reinforced epoxy-hybrid clay nanocomposites. *Materials Science Forum* 654-656: 2624-2627

Alamri, H., and I. M. Low. 2012a. Characterization of epoxy hybrid composites filled with cellulose fibres and nano-SiC. *Journal of Applied Polymer Science* 126: 221-231.

Alamri, H., and I. M. Low. 2012b. Mechanical properties and water absorption behaviour of recycled cellulose fibre reinforced epoxy composites. *Polymer Testing* 31 (5): 620-628.

Alamri, H., and I. M. Low. 2012c. Microstructural, mechanical, and thermal characteristics of recycled cellulose fibre-halloysite-epoxy hybrid nanocomposites. *Polymer composites* 33 (4): 589-600.

Alamri, H., I. M. Low, and Z. Alothman. 2012. Mechanical, thermal and microstructural characteristics of cellulose fibre reinforced epoxy/organoclay nanocomposites. *Composites Part B: Engineering* 43: 2762-2771.

Albano, C., J. González, M. Ichazo, and D. Kaiser. 1999. Thermal stability of blends of polyolefins and sisal fibre. *Polymer Degradation and Stability* 66 (2): 179-190.

Alexandre, B., D. Langevin, P. Médéric, T. Aubry, H. Couderc, Q. T. Nguyen, A. Saiter, and S. Marais. 2009. Water barrier properties of polyamide 12/montmorillonite nanocomposite membranes: Structure and volume fraction effects. *Journal of Membrane Science* 328 (1-2): 186-204.

Alexandre, M., and P. Dubois. 2000. Polymer-layered silicate nanocomposites: preparation, properties and uses of a new class of materials. *Materials Science and Engineering: R: Reports* 28 (1-2): 1-63.

Alexandre, M., P. Dubois, T. Sun, J. M. Garces, and R. Jérôme. 2002. Polyethylene-layered silicate nanocomposites prepared by the polymerization-filling technique: Synthesis and mechanical properties. *Polymer* 43 (8): 2123-2132.

Araújo, E. M., K. D. Araujo, R. A. Paz, T. R. Gouveia, R. Barbosa, and E. N. Ito. 2009. Polyamide 66/brazilian clay nanocomposites. *Journal of Nanomaterials* 2009: 5 pages.

Arbelaiz, A., B. Fernández, J. A. Ramos, A. Retegi, R. Llano-Ponte, and I. Mondragon. 2005. Mechanical properties of short flax fibre bundle/polypropylene composites: Influence of matrix/fibre modification, fibre content, water uptake and recycling. *Composites Science and Technology* 65 (10): 1582-1592.

Athijayamani, A., M. Thiruchitrambalam, U. Natarajan, and B. Pazhanivel. 2009. Effect of moisture absorption on the mechanical properties of randomly oriented natural fibres/polyester hybrid composite. *Materials Science and Engineering: A* 517 (1-2): 344-353.

Auad, M. L., S. R. Nutt, V. Pettarin, and P. M. Frontini. 2007. Synthesis and properties of epoxy-phenolic clay nanocomposites. *Express Polymer Letters* 1 (9): 629-639.

Bachtiar, D., S. M. Sapuan, and M. M. Hamdan. 2008. The effect of alkaline treatment on tensile properties of sugar palm fibre reinforced epoxy composites. *Materials & Design* 29 (7): 1285-1290.

Bader, M. G. 2001. Polymer composites in 2000: Structure, performance, cost and compromise. *Journal of Microscopy* 201 (2): 110-121.

Bahramian, A. R., and M. Kokabi. 2009. Ablation mechanism of polymer layered silicate nanocomposite heat shield. *Journal of Hazardous Materials* 166 (1): 445-454.

Baroulaki, I., O. Karakasi, G. Pappa, P. A. Tarantili, D. Economides, and K. Magoulas. 2006. Preparation and study of plastic compounds containing polyolefins and post used newspaper fibres. *Composites Part A: Applied Science and Manufacturing* 37 (10): 1613-1625.

Becker, O., R. J. Varley, and G. P. Simon. 2004. Thermal stability and water uptake of high performance epoxy layered silicate nanocomposites. *European Polymer Journal* 40 (1): 187-195.

Beyer, G. 2002. Nanocomposites: a new class of flame retardants for polymers. *Plastics, Additives and Compounding* 4 (10): 22-28.

Bismarck, A., S. Mishra, and T. Lampke. 2005. Plant fibres as reinforcement for green composites. In *Natural fibres, biopolymers, and biocomposites*, ed. A. K. Mohanty, M. Misra and L. T. Drzal, 37-108. Boca Raton, FL: CRC Press.

Blackman, B. R. K., A. J. Kinloch, J. Sohn Lee, A. C. Talor, R. Agarwal, G. Schueneman, and S. Sprenger. 2007. The fracture and fatigue behaviour of nano-modified epoxy polymers. *Journal of Materials Science* 42: 7049-7051.

Bledzki, A. K., and O. Faruk. 2004. Creep and impact properties of wood fibre–polypropylene composites: Influence of temperature and moisture content. *Composites Science and Technology* 64 (5): 693-700.

Bledzki, A. K., and J. Gassan. 1999. Composites reinforced with cellulose based fibres. *Progress in Polymer Science* 24 (2): 221-274.

Bledzki, A. K., A. A. Mamun, and J. Volk. 2010. Barley husk and coconut shell reinforced polypropylene composites: The effect of fibre physical, chemical and surface properties. *Composites Science and Technology* 70 (5): 840-846.

Bowen, C. R., A. C. Dent, L. J. Nelson, R. Stevens, M. G. Cain, and M. Stewart. 2006. Failure and volume fraction dependent mechanical properties of composite sensors and actuators. *Proc. I Mech E, Part C: Journal of Mechanical Engineering Science*, 220(11), 1655–1663

Bozkurt, E., E. Kaya, and M. Tanoğlu. 2007. Mechanical and thermal behavior of non-crimp glass fibre reinforced layered clay/epoxy nanocomposites. *Composites Science and Technology* 67 (15-16): 3394-3403.

Brouwer, W. D. 2001. *Natural fibre composites in structural components: alternative applications for sisal?* http://www.fao.org/DOCREP/004/Y1873E/y1873e0a.htm#fn30 (accessed 2011).

Brunner, A., A. Necola, M. Rees, P. Gasser, X. Kornmann, R. Thomann, and M. Barbezat. 2006. The influence of silicate-based nano-filler on the fracture toughness of epoxy resin. *Engineering Fracture Mechanics* 73 (16): 2336-2345.

Buehler, F. U., and J. C. Seferis. 2000. Effect of reinforcement and solvent content on moisture absorption in epoxy composite materials. *Composites Part A: Applied Science and Manufacturing* 31 (7): 741-748.

Callister, W. D. 2003. *Materials science and engineering: An introduction*. 6th ed. New York: John Wiley & Sons.

Callister, W. D. 2007. *Materials science and engineering: An introduction*. 7th ed. New York: John Wiley & Sons.

Cao, G. 2004. *Nanostructures and nanomaterials - synthesis, properties and applications*. London: Imperial College Press

Cauvin, L., D. Kondo, M. Brieu, and N. Bhatnagar. 2010. Mechanical properties of polypropylene layered silicate nanocomposites: Characterization and micro-macro modelling. *Polymer Testing* 29 (2): 245-250.

Chatterjee, A., and M. S. Islam. 2008. Fabrication and characterization of TiO2–epoxy nanocomposite. *Materials Science and Engineering: A* 487 (1-2): 574-585.

Chawla, K. K. 1998. *Composite materials: Science and engineering* 2nd ed. New York: Springer-Verlage

Chen, B., and J. R. G. Evans. 2009. Impact strength of polymer-clay nanocomposites. *Soft Matter* 5 (19): 3572-3584.

Chen, C., R. S. Justice, D. W. Schaefer, and J. W. Baur. 2008. Highly dispersed nanosilica–epoxy resins with enhanced mechanical properties. *Polymer* 49 (17): 3805-3815.

Cheung, H.-Y., M.-P. Ho, K.-T. Lau, F. Cardona, and D. Hui. 2009. Natural fibre-reinforced composites for bioengineering and environmental engineering. *Composites Part B: Engineering* 40 (7): 655-663.

Cho, J. W., and D. R. Paul. 2001. Nylon 6 nanocomposites by melt compounding. *Polymer* 42 (3): 1083-1094.

235

Choudalakis, G., and A. D. Gotsis. 2009. Permeability of polymer/clay nanocomposites: A review. *European Polymer Journal* 45 (4): 967-984.

Chow, C. P. L., X. S. Xing, and R. K. Y. Li. 2007. Moisture absorption studies of sisal fibre reinforced polypropylene composites. *Composites Science and Technology* 67 (2): 306-313.

Chozhan, C. K., M. Alagar, R. J. Sharmila, and GnanasundaramP. 2007. Thermo mechanical behaviour of unsaturated polyester toughened epoxy–clay hybrid nanocomposites. *Journal of Polymer Research* 14: 319–328.

Daud, W., H. E. N. Bersee, S. J. Picken, and A. Beukers. 2009. Layered silicates nanocomposite matrix for improved fibre reinforced composites properties. *Composites Science and Technology* 69 (14): 2285-2292.

De Rosa, I. M., C. Santulli, and F. Sarasini. 2010. Mechanical and thermal characterization of epoxy composites reinforced with random and quasi-unidirectional untreated Phormium tenax leaf fibres. *Materials & Design* 31 (5): 2397-2405.

Deka, B. K., and T. K. Maji. 2011. Study on the properties of nanocomposite based on high density polyethylene, polypropylene, polyvinyl chloride and wood. *Composites Part A: Applied Science and Manufacturing* 42 (6): 686-693.

Deng, S., J. Zhang, and L. Ye. 2009. Halloysite–epoxy nanocomposites with improved particle dispersion through ball mill homogenisation and chemical treatments. *Composites Science and Technology* 69 (14): 2497-2505.

Deng, S., J. Zhang, L. Ye, and J. Wu. 2008. Toughening epoxies with halloysite nanotubes. *Polymer* 49 (23): 5119-5127.

Dhakal, H., Z. Zhang, and M. Richardson. 2007. Effect of water absorption on the mechanical properties of hemp fibre reinforced unsaturated polyester composites. *Composites Science and Technology* 67 (7-8): 1674-1683.

Dittanet, P., and R. A. Pearson. 2012. Effect of silica nanoparticle size on toughening mechanisms of filled epoxy. *Polymer* 53: 1890-1905.

Doan, T., H. Brodowsky, and E. Mader. 2007. Jute fibre/polypropylene composites II. Thermal, hydrothermal and dynamic mechanical behaviour. *Composites Science and Technology* 67: 2707–2714.

Dong, Y. and D. Bhattacharyya. 2008. Effects of clay type, clay/compatibiliser content and matrix viscosity on the mechanical properties of polypropylene/organoclay nanocomposites. *Composites: Part A* 39: 1177–1191.

Dorigato, A., A. Pegoretti, and M. Quaresimin. 2011. Thermo-mechanical characterization of epoxy/clay nanocomposites as matrices for carbon/nanoclay/epoxy laminates. *Materials Science and Engineering A* 528: 6324–6333

Du, M., B. Guo, and D. Jia. 2006. Thermal stability and flame retardant effects of halloysite nanotubes on poly(propylene). *European Polymer Journal* 42 (6): 1362-1369.

Egusa, S. 1990. Anisotropy of radiation-induced degradation in mechanical properties of fabric-reinforced polymer-matrix composites. *Journal of Materials Science* 25 (3): 1863–1871.

El-Sakhawy, M., and M. L. Hassan. 2007. Physical and mechanical properties of microcrystalline cellulose prepared from agricultural residues. *Carbohydrate Polymers* 67 (1): 1-10.

Faruk,O., A.K. Bledzki, H-P. Fink, and M. Saind. 2012. Bio-composites reinforced with natural fibres: 2000–2010. *Progress in Polymer Science* 37: 1552– 1596.

Faruk, O., and L. M. Matuana. 2008. Nanoclay reinforced HDPE as a matrix for wood-plastic composites. *Composites Science and Technology* 68 (9): 2073-2077.

Ford, E. N. J., S. K. Mendon, J. W. Rawlins, and s. F. Thames. 2010. X-ray diffraction of cotton treated with neutralized vegetable oil-based macromolecular crosslinkers. *Journal of Engineered Fibres and Fabrics* 5(1): 10–20.

Fraga, A. N., E. Frullloni, O. de la Osa, J. M. Kenny, and A. Vázquez. 2006. Relationship between water absorption and dielectric behaviour of natural fibre composite materials. *Polymer Testing* 25 (2): 181-187.

Fu, S-Y., X-Q. Feng, B. Lauke, and Y-W. Mai. 2008. Effects of particle size, particle/matrix interface adhesion and particle loading on mechanical properties of particulate–polymer composites. *Composites: Part B* 39: 933–961.

Gañan, P., S. Garbizu, R. Llano-Ponte, and I. Mondragon. 2005. Surface modification of sisal fibres: Effects on the mechanical and thermal properties of their epoxy composites. *Polymer Composites* 26 (2): 121-127.

Gao, F. 2004. Clay/polymer composites: the story. *Materials Today* 7 (11): 50-55.

Gassan, J., and A. K. Bledzki. 1999. Possibilities for improving the mechanical properties of jute/epoxy composites by alkali treatment of fibres. *Composites Science and Technology* 59 (9): 1303-1309.

Georget, D. M. R., P. Cairns, A. C. Smith, and K. W. Waldron. 1999. Crystallinity of lyophilised carrot cell wall components. *International Journal of Biological Macromolecules* 26 (5): 325-331.

Ghosh, R., A. R. Krishna, G. Reena, and B. L. Raju. 2011. Effect of fibre volume fraction on the tensile strength of Banana fibre reinforced vinyl ester resin composites. *International Journal of Advanced Engineering Sciences and Technologies* 4 (1): 89–91.

Ha, S.-R., K.-Y. Rhee, S.-J. Park, and J. H. Lee. 2010. Temperature effects on the fracture behavior and tensile properties of silane-treated clay/epoxy nanocomposites. *Composites Part B: Engineering* 41 (8): 602-607.

Ha, S. R., K. Y. Rhee, H. C. Kim, and J. T. Kim. 2008. Fracture performance of clay/epoxy nanocomposites with clay surface-modified using 3-aminopropyltriethoxysilane. *Colloids and Surfaces A: Physicochemical and Engineering Aspects* 313-314 (0): 112-115.

Haghighat, M., A. Zadhoush, and S. N. Khorasani. 2005. Physicomechanical properties of α-cellulose–filled styrene–butadiene rubber composites. *Journal of Applied Polymer Science* 96 (6): 2203-2211.

Han, S. O., and L. T. Drzal. 2003. Water absorption effects on hydrophilic polymer matrix of carboxyl functionalized glucose resin and epoxy resin. *European Polymer Journal* 39 (9): 1791–1799.

Harish, S., D. P. Michael, A. Bensely, D. M. Lal, and A. Rajadurai. 2009. Mechanical property evaluation of natural fibre coir composite. *Materials Characterization* 60 (1): 44-49.

Hedicke-Höchstötter, K., G. T. Lim, and V. Altstädt. 2009. Novel polyamide nanocomposites based on silicate nanotubes of the mineral halloysite. *Composites Science and Technology* 69 (3-4): 330-334.

Holbery, J., and D. Houston. 2006. Natural-fibre-reinforced polymer composites in automotive applications. *JOM Journal of the Minerals, Metals and Materials Society* 58 (11): 80-86.

Hossain, M. K., K. A. Imran, M. V. Hosur, and S. Jeelani. 2011. Degradation of mechanical properties of conventional and nanophased carbon=epoxy composites in seawater. *Journal of Engineering Materials and Technology* 133 (4): 41004.

Hughes, M., J. Carpenter, and C. Hill. 2007. Deformation and fracture behaviour of flax fibre reinforced thermosetting polymer matrix composites. *Journal of Materials Science* 42 (7): 2499-2511.

Hughes, M., C. A. S. Hill, and J. R. B. Hague. 2002. The fracture toughness of bast fibre reinforced polyester composites. Part 1 evaluation and analysis. *Journal of Materials Science* 37 (21): 4669-4676.

Hussain, F., M. Hojjati, M. Okamoto, and R. E. Gorga. 2006. Review article: Polymer-matrix Nanocomposites, Processing, Manufacturing, and Application: An Overview. *Journal of Composite Materials* 40 (17): 1511-1575.

Hwang, S.-s., S.-p. Liu, P. P. Hsu, J.-m. Yeh, K.-c. Chang, and Y.-z. Lai. 2010. Effect of organoclay on the mechanical/thermal properties of microcellular injection molded PBT–clay nanocomposites. *International Communications in Heat and Mass Transfer* 37 (8): 1036-1043.

Imai, Y., S. Nishimura, E. Abe, H. Tateyama, A. Abiko, A. Yamaguchi, T. Aoyama, and H. Taguchi. 2002. High-modulus poly(ethylene terephthalate)/expandable fluorine mica nanocomposites with a novel reactive compatibilizer. *Chemistry of Materials* 14 (2): 477-479. http://dx.doi.org/10.1021/cm010408a (accessed 2011/09/27).

Ismail, H., P. Pasbakhsh, M. N. A. Fauzi, and A. Abubakar. 2008. Morphological, thermal and tensile properties of halloysite nanotubes filled ethylene propylene diene monomer (EPDM) nanocomposites. *Polymer Testing* 27 (7): 841-850.

John, M. J., R. D. Anandjiwala, and S. Thomas. 2009. Lignocellulosic fibre reinforced rubber composites. In *Natural fibre reinforced polymer composites: Macro to nanoscale*, ed. S. Thomas and L. A. Pothan, 252-269. philadelphia: Old City Publishing.

John, M. J., and S. Thomas. 2008. Biofibres and biocomposites. *Carbohydrate Polymers* 71 (3): 343-364.

Johnsen, B. B., A. J. Kinloch, R. D. Mohammed, A. C. Taylor, and S. Sprenger. 2007. Toughening mechanisms of nanoparticle-modified epoxy polymers. *Polymer* 48 (2): 530-541.

Jonoobi, M., J. Harun, P. Tahir, L. Zaini, S. SaifluAzry, and M. Makinejad. 2010. Characteristics of nanofibres extracted from kenaf core. *Bio-Resources* 5 (4): 2556-2566.

Joseph, P. V., K. Joseph, and S. Thomas. 1999. Effect of processing variables on the mechanical properties of sisal-fibre-reinforced polypropylene composites. *Composites Science and Technology* 59 (11): 1625-1640.

Joulazadeh, M. Navarchian, A. 2010. Effect of process variables on mechanical properties of polyurethane/clay nanocomposites. *Polymers for Advanced Technology* 21: 263–271.

Kabir, M. M., H. Wang, T. Aravinthan, F. Cardona, and K-T. Lau. 2011. Effects of natural fibre surface on composite properties: a review. *Proc. 1st International Postgraduate Conference on Engineering, Designing and Developing the Built Environment for Sustainable Wellbeing*, Brisbane, Australia, 27-29 Apr: 94-99.

Karbowiak, T., E. Ferret, F. Debeaufort, A. Voilley, and P. Cayot. 2011. Investigation of water transfer across thin layer biopolymer films by infrared spectroscopy. *Journal of Membrane Science* 370 (1–2): 82-90.

Kardos, J. L. 1985. Critical issues in achieving desirable mechanical properties for short fibre composites. *Pure and Applied Chemistry* 57(11): 651-1657.

Karmaker, C. 1997. Effect of water absorption on dimensional stability and impact energy of jute fibre reinforced polypropylene. *Journal of Materials Science Letters* 16: 462–464.

Kaynak, C., G. I. Nakas, and N. A. Isitman. 2009. Mechanical properties, flammability and char morphology of epoxy resin/montmorillonite nanocomposites. *Applied Clay Science* 46 (3): 319-324.

Ke, Z., and B. Yongping. 2005. Improve the gas barrier property of PET film with montmorillonite by in situ interlayer polymerization. *Materials Letters* 59 (27): 3348-3351.

Khan, R., P. Khare, B. P. Baruah, A. K. Hazarika, and N. C. Dey. 2011. Spectroscopic, kinetic studies of polyaniline-flyash composite. *Advances in Chemical Engineering and Science* 1: 37–44.

Khan, S. U., K. Iqbal, A. Munir, and J.-K. Kim. 2011. Quasi-static and impact fracture behaviors of CFRPs with nanoclay-filled epoxy matrix. *Composites Part A* 42: 253-264.

Kiliaris, P., and C. D. Papaspyrides. 2010. Polymer/layered silicate (clay) nanocomposites: An overview of flame retardancy. *Progress in Polymer Science* 35 (7): 902-958.

Kim, B. C., S. W. Park, and D. G. Lee. 2008. Fracture toughness of the nano-particle reinforced epoxy composite. *Composite Structures* 86 (1–3): 69-77.

Kim, H. J., and D. W. Seo. 2006. Effect of water absorption fatigue on mechanical properties of sisal textile-reinforced composites *International Journal of Fatigue* 28: 1307–1314

Kim, J.-K., C. Hu, R. S. C. Woo, and M.-L. Sham. 2005. Moisture barrier characteristics of organoclay–epoxy nanocomposites. *Composites Science and Technology* 65 (5): 805-813.

Knauert, S. T., J. F. Douglas, and F. W. Starr. 2007. The effect of nanoparticle shape on polymer-nanocomposite rheology and tensile strength. *Journal of Polymer Science: Part B: Polymer Physics* 45: 1882–1897.

Kojima, Y., A. Usuki, M. Kawasumi, A. Okada, Y. Fukushima, T. Kurauchi, and O. Kamigaito. 1993. Mechanical properties of nylon 6-clay hybrid. *Journal of Materials Research* 8: 1185-1189.

Kornmann, X. 2000. Synthesis and characterization of thermoset-clay nanocomposites. PhD diss, Lulea University of Technology, Sweden.

Krishnamoorti, R., J. Ren, and A. S. Silva. 2001. Shear response of layered silicate nanocomposites. *Journal of Chemical Physics* 114 (11): 4968-4973.

Krishnamoorti, R., and K. Yurekli. 2001. Rheology of polymer layered silicate nanocomposites. *Current Opinion in Colloid & Interface Science* 6 (5-6): 464-470.

Ku, H., H. Wang, N. Pattarachaiyakoop, and M. Trada. 2011. A review on the tensile properties of natural fibre reinforced polymer composites. *Composites Part B: Engineering* 42(4): 856–873.

Lasagabáster, A., M. J. Abad, L. Barral, A. Ares, and R. Bouza. 2009. Application of FTIR spectroscopy to determine transport properties and water–polymer interactions in polypropylene (PP)/poly(ethylene-co-vinyl alcohol) (EVOH) blend films: Effect of poly(ethylene-co-vinyl alcohol) content and water activity. *Polymer* 50 (13): 2981-2989.

Le Guen, M. J., and R. H. Newman. 2007. Pulped phormium tenax leaf fibres as reinforcement for epoxy composites. *Composites: Part A* 38: 2109–2115.

Le Pluart, L., J. Duchet, and H. Sautereau. 2005. Epoxy/montmorillonite nanocomposites: influence of organophilic treatment on reactivity, morphology and fracture properties. *Polymer* 46: 12267–12278.

Lee, J. H., K. Y. Rhee, and J. H. Lee. 2010. Effects of moisture absorption and surface modification using 3-aminopropyltriethoxysilane on the tensile and fracture characteristics of MWCNT/epoxy nanocomposites. *Applied Surface Science* 256 (24): 7658-7667.

Leman, Z., S. M. Sapuan, A. M. Saifol, M. A. Maleque, and M. M. H. M. Ahmad. 2008. Moisture absorption behavior of sugar palm fibre reinforced epoxy composites. *Materials and Design* 29 (8): 1666-1670.

Li, Y., Y-W. Wing, and L. Ye. 2000. Sisal fibre and its composites: a review of recent developments. *Composites Science and Technology* 60: 2037-2055

Liang, Y.L., and R.A. Pearson. 2010. The toughening mechanism in hybrid epoxy-silica-rubber nanocomposites (HESRNs). *Polymer* 51: 4880-4890.

Liao, C. Z., S. P. Bao, and S. C. Tjong. 2011. Effect of Silicon Carbide Nanoparticle Additions on Microstructure and Mechanical Behavior of Maleic Anhydride Compatibilized High Density Polyethylene Composites. *Composite Interfaces* 18 (2): 107-120.

Lim, S. H., K.Y. Zenga, and C.B. He. 2010. Morphology, tensile and fracture characteristics of epoxy-alumina nanocomposites. *Materials Science and Engineering A* 527: 5670–5676.

Liu, M., B. Guo, M. Du, X. Cai, and D. Jia. 2007. Properties of halloysite nanotube-epoxy resin hybrids and the interfacial reactions in the systems. *Nanotechnology* 18 (45): 455703-455712.

Liu, Q., and M. Hughes. 2008. The fracture behaviour and toughness of woven flax fibre reinforced epoxy composites. *Composites Part A: Applied Science and Manufacturing* 39 (10): 1644-1652.

Liu, W., S. V. Hoa, and M. Pugh. 2005a. Fracture toughness and water uptake of high-performance epoxy/nanoclay nanocomposites. *Composites Science and Technology* 65 (15-16): 2364-2373.

Liu, W., S. V. Hoa, and M. Pugh. 2005b. Organoclay-modified high performance epoxy nanocomposites. *Composites Science and Technology* 65 (2): 307-316.

Liu, W., S. V. Hoa, and M. Pugh. 2008. Water uptake of epoxy–clay nanocomposites: Model development. *Composites Science and Technology* 68 (1): 156-163.

Low, I. M., and Y. W. Mai. 1992. Fracture properties and failure mechanisms in pure and toughened epoxy resins. In *Handbooks of ceramics & composite materials*, ed. N. P. Cheremisinoff, 105-160. New York: Marcel Dekker Publishers.

Low, I. M., M. McGrath, D. Lawrence, P. Schmidt, J. Lane, and B. A. Latella. 2007. Mechanical and fracture properties of cellulose-fibre-reinforced epoxy laminates. *Composites: Part A* 38: 963-974.

Low, I. M., J. Somers, H. S. Kho, I. J. Davies, and B. A. Latella. 2009. Fabrication and properties of recycled cellulose fibre-reinforced epoxy composites. *Composite Interfaces* 16: 659–669.

Lu, C., and Y.-W. Mai. 2007. Permeability modelling of polymer-layered silicate nanocomposites. *Composites Science and Technology* 67 (14): 2895-2902.

Lu, C., and Y. W. Mai. 2005. Influence of aspect ratio on barrier properties of polymer-clay nanocomposites. *Physical Review Letters* 95: 088303.

Lu, S.-R., Y.-M. Jiang, and C. Wei. 2009. Preparation and characterization of EP/SiO2 hybrid materials containing PEG flexible chain. *Journal of Materials Science* 44 (15): 4047-4055.

Luo, J.-J., and I. M. Daniel. 2003. Characterization and modeling of mechanical behavior of polymer/clay nanocomposites. *Composites Science and Technology* 63 (11): 1607-1616.

Ma, J., M.-S. Mo, X.-S. Du, P. Rosso, K. Friedrich, and H.-C. Kuan. 2008. Effect of inorganic nanoparticles on mechanical property, fracture toughness and toughening mechanism of two epoxy systems. *Polymer* 49 (16): 3510-3523.

Ma, J., J. Xu, J.-H. Ren, Z.-Z. Yu, and Y.-W. Mai. 2003. A new approach to polymer/montmorillonite nanocomposites. *Polymer* 44 (16): 4619-4624.

Madaleno, L., J. Schjødt-Thomsen, and J. C. Pinto. 2010. Morphology, thermal and mechanical properties of PVC/MMT nanocomposites prepared by solution blending and solution blending and solution blending + melt compounding. *Composites Science and Technology* 70 (5): 804-814.

Majewski, P., N. R. Choudhury, D. Spori, E. Wohlfahrt, and M. Wohlschloegel. 2006. Synthesis and characterisation of star polymer/silicon carbide nanocomposites. *Materials Science and Engineering A* 434: 360–364.

Maleque, M. A., F. Y. Belal, and S. M. Sapuan. 2007. Mechanical properties study of pseudo-stem banana fibre reinforced epoxy composite. *The Arabian Journal for Science and Engineering* 32 (2B): 359-364.

Malik, H. K., and A. K. Singh. 2010. *Engineering Physics*. Delhi: Tata McGraw Hill Education Private Limited.

Mallick, P. K. 2007. *Fibre-reinforced composites: Materials, manufacturing, and design* 3rd ed. Boca Raton, FL: CRC Taylor & Francis.

Manfredi, L. B., H. De Santis, and A. Vázquez. 2008. Influence of the addition of montmorillonite to the matrix of unidirectional glass fibre/epoxy composites on their mechanical and water absorption properties. *Composites Part A: Applied Science and Manufacturing* 39 (11): 1726-1731.

Marsh, G. 2003. Next step for automotive materials. *Materials Today* 6 (4): 36-43.

Masirek, R., Z. Kulinski, D. Chionna, E. Piorkowska, and M. Pracella. 2007. Composites of poly(L-lactide) with hemp fibres: Morphology and thermal and mechanical properties. *Journal of Applied Polymer Science* 105 (1): 255-268.

Mazumdar, S. K. 2002. *Composites manufacturing: materials, product, and process engineering*. Boca Raton, FL: CRC press.

McGrath, M., W. Vilaiphand, S. Vaihola, A. Lopez, I. M. Low, and B. A. Latella. 2004. Synthesis and properties of clay-ZrO2-cellulose fibre-reinforced polymeric nanohybrids. In *Structural integrity and fracture international conference (SIF'04)*, edited by A. Atrens, J. N. Boland, R. Clegg and J. R. Griffiths. Brisbane, Australia.

McNally, T., W. Raymond Murphy, C. Y. Lew, R. J. Turner, and G. P. Brennan. 2003. Polyamide-12 layered silicate nanocomposites by melt blending. *Polymer* 44 (9): 2761-2772.

Messersmith, P. B., and E. P. Giannelis. 1995. Synthesis and barrier properties of poly(ε-caprolactone)-layered silicate nanocomposites. *Journal of Polymer Science Part A: Polymer Chemistry* 33 (7): 1047-1057.

Mirmohseni, A., and S. Zavareh. 2010. Preparation and characterization of an epoxy nanocomposite toughened by a combination of thermoplastic, layered and particulate nano-fillers. *Materials and Design* 31 (6): 2699-2706.

Mishra, S., A. K. Mohanty, L. T. Drzal, M. Misra, S. Parija, S. K. Nayak, and S. S. Tripathy. 2003. Studies on mechanical performance of biofibre/glass reinforced polyester hybrid composites. *Composites Science and Technology* 63 (10): 1377-1385.

Mitchell B. S. 2004. *An introduction to materials engineering and science: for chemical and materials engineers*. Hoboken, NJ, USA: John Wiley & Sons.

Mittal, A., R. Katahira, M. E. Himmel, and D. K. Johnson. 2011. Effects of alkaline or liquid-ammonia treatment on crystalline cellulose: changes in crystalline structure and effects on enzymatic digestibility. *Biotechnology for Biofuels* 4: 41-57.

Moeini, M. H., S. H. Heidary, I. Amiri, and A. Payami. 2009. Wood–polyvinyl chloride composite for insulation of electrical wires: Fabrication and investigation of properties. *Journal of Reinforced Plastics and Composites* 29 (6): 899-908

Mohan, T. P., and K. Kanny. 2011. Water barrier properties of nanoclay filled sisal fibre reinforced epoxy composites. *Composites Part A: Applied Science and Manufacturing* 42 (4): 385-393.

Mohanty, A. K., M. Misra, L. T. Drzal, S. Selke, B. Harte, and G. Hinrichsen. 2005. Natural fibres, biopolymers, and biocomposites: An introduction. In *Natural fibres, biopolymers, and biocomposites*, ed. A. K. Mohanty, M. Misra and L. T. Drzal, 1-30. Boca Raton, FL: CRC Press.

Morgan, A. B., and J. W. Gilman. 2003. Characterization of polymer-layered silicate (Clay) nanocomposites by transmission electron microscopy and x-ray diffraction: A comparative study. *Journal of Applied Polymer Science* 87 (8): 1329-1338.

Morgan, A. B., and J. D. Harris. 2004. Exfoliated polystyrene-clay nanocomposites synthesized by solvent blending with sonication. *Polymer* 45 (26): 8695-8703.

Mwaikambo, L. Y., and M. P. Ansell. 2002. Chemical modification of hemp, sisal, jute, and kapok fibres by alkalization. *Journal of Applied Polymer Science* 84: 2222–2234.

Nair, S. S., S. Wang, and D. C. Hurley. 2010. Nanoscale characterization of natural fibres and their composites using contact-resonance force microscopy. *Composites Part A: Applied Science and Manufacturing* 41 (5): 624-631.

Nickel, J., and U. Riedel. 2003. Activities in biocomposites. *Materials Today* 6 (4): 44-48.

Nikolic, G., S. Zlatkovic, M. Cakic, S. Cakic, C. Lacnjevac, and Z. Rajic. 2010. Fast Fourier transform IR characterization of epoxy GY systems crosslinked with aliphatic and cycloaliphatic EH polyamine adducts. *Sensors* 10: 684–696.

Ogasawara, T., Y. Ishida, T. Ishikawa, T. Aoki, and T. Ogura. 2006. Helium gas permeability of montmorillonite/epoxy nanocomposites. *Composites Part A: Applied Science and Manufacturing* 37 (12): 2236-2240.

Oh, S. Y., D. I. Yoo, Y. Shin, and G. Seo. 2005. FTIR analysis of cellulose treated with sodium hydroxide and carbon dioxide. *Carbohydrate Research* 340: 417–428.

Okada, A., M. Kawasumi, A. Usuki, Y. Kojima, T. Kurauchi, and O. Kamigaito. 1990. Nylon 6-clay hybrid. *Material resource society proceedings* 171: 45–50.

Ou, Y., F Yang, and Z-Z Yu. 1998. A new conception on the toughness of nylon 6/silica nanocomposite prepared via in situ polymerization. *Journal of Polymer Science: Part B: Polymer Physics* 36: 789–795

Park, S., J. O. Baker, M. E. Himmel, P. A. Parilla, and D. K. Johnson. 2010. Cellulose crystallinity index: measurement techniques and their impact on interpreting cellulose performance. *Biotechnology for Biofuels* 3: 1-10.

Pasbakhsh, P., H. Ismail, M. N. A. Fauzi, and A. A. Bakar. 2010. EPDM/modified halloysite nanocomposites. *Applied Clay Science* 48 (3): 405-413.

Patel, H. A., R. S. Somani, H. C. Bajaj, and R. V. Jasra. 2006. Nanoclays for polymer nanocomposites, paints, inks, greases and cosmetics formulations, drug delivery vehicle and waste water treatment. *Bulletin of material science* 29 (2): 133-145.

Paul, M. A., M. Alexandre, P. Dege´e, C. Henrist, A. Rulmont, and P. Dubois. 2003. New nanocomposite materials based on plasticized poly(L-lactide) and organo-modified montmorillonites: thermal and morphological study. *Polymer* 44: 443–450.

Pavlidou, S., and C. D. Papaspyrides. 2008. A review on polymer–layered silicate nanocomposites. *Progress in Polymer Science* 33 (12): 1119-1198.

Peltola, P., E. Välipakka, J. Vuorinen, S. Syrjälä, and K. Hanhi. 2006. Effect of rotational speed of twin screw extruder on the microstructure and rheological and mechanical properties of nanoclay-reinforced polypropylene nanocomposites. *Polymer Engineering & Science* 46 (8): 995-1000.

Phang, I. Y., T. Liu, A. Mohamed, K. P. Pramoda, L. Chen, L. Shen, S. Y. Chow, C. He, X. Lu, and X. Hu. 2005. Morphology, thermal and mechanical properties of nylon 12/organoclay nanocomposites prepared by melt compounding. *Polymer International* 54 (2): 456-464.

Pothan, L. A., Z. Oommen, and S. Thomas. 2003. Dynamic mechanical analysis of banana fibre reinforced polyester composites. *Composites Science and Technology* 63 (2): 283-293.

Prashantha, K., M. F. Lacrampe, and P. Krawczak. 2011. Processing and characterization of halloysite nanotubes filled polypropylene nanocomposites based on a masterbatch route: effect of halloysites treatment on structural and mechanical properties. *eXPRESS Polymer Letters* 5 (4): 295–307.

Qi, B., Q. X. Zhang, M. Bannister, and Y. W. Mai. 2006. Investigation of the mechanical properties of DGEBA-based epoxy resin with nanoclay additives. *Composite Structures* 75 (1-4): 514-519.

Rai, U. S., and R. K. Singh. 2004. Synthesis and mechanical characterization of polymer-matrix composites containing calcium carbonate/white cement filler. *Materials Letters* 58 (1-2): 235-240.

Rajasekaran, R., C. Karikalchozhan, and M. Alagar. 2008. Synthesis, characterization and properties of organoclaymodified polysulfone/epoxy interpenetrating polymer network nanocomposites. *Chinese Journal of Polymer Science* 26 (6): 669–678.

Ramadan, A. R., A. M. K. Esawi, and A. A. Gawad. 2010. Effect of ball milling on the structure of Na+-montmorillonite and organo-montmorillonite (Cloisite 30B). *Applied Clay Science* 47 (3–4): 196-202.

Ramesh, K. T. 2009. Nanoscale mechanics and materials: Experimental techniques. In *Nanomaterials mechanics and mechanisms*, 61-93. Springer US.

Rashdi, A., S. Sapuan, M. Ahmad, and A. Khalina. 2009. Water absorption and tensile properties of soil buried kenaf fibre reinforced unsaturated polyester composites (KFRUPC). *Journal of Food, Agriculture & Environment* 7 (3&4): 9 0 8 - 9 1 1

Ratna, D., N. R. Manoj, R. Varley, R. K. Singh Raman, and G. P. Simon. 2003. Clay-reinforced epoxy nanocomposites. *Polymer International* 52 (9): 1403-1407.

Ray, D., and J. Rout. 2005. Thermoset biocomposites. In *Natural fibres, biopolymers, and biocomposites*, ed. A. K. Mohanty, M. Misra and L. T. Drzal, 298-355. Boca Raton, FL: CRC Press.

Reddy, C. R., A. P. Sardashti, and L. C. Simon. 2010. Preparation and characterization of polypropylene–wheat straw–clay composites. *Composites Science and Technology* 70 (12): 1674-1680.

Reddy, M., R. Gupta, S. Bhattacharya, and R. Parthasarathy. 2007. Structure-property relationship of melt intercalated maleated polyethylene nanocomposites. *Korea-Australia Rheology Journal* 19 (3): 133-139.

Riedel, U., and J. Nickel. 2005. Applications of natural fibre composites for constructive parts in aerospace, automobiles, and other Areas. In *Biopolymers Online*: Wiley-VCH Verlag GmbH & Co. KGaA.

Rodgers, R. M., H. Mahfuz, V. K. Rangari, N. Chisholm, and S. Jeelani. 2005. Infusion of SiC nanoparticles into SC-15 epoxy: an investigation of thermal and mechanical response. *Macromolecular Materials and Engineering* 290 (5): 423-429.

Roncero, M. B., A. L. Torres, J. F. Colom, and T. Vidal. 2005. The effect of xylanase on lignocellulosic components during the bleaching of wood pulps. *Bioresource Technology* 96 (1): 21-30.

Rong, M. 2001. The effect of fibre treatment on the mechanical properties of unidirectional sisal-reinforced epoxy composites. *Composites Science and Technology* 61 (10): 1437-1447.

Rösler, J., H. Harders, and M. Bäker. 2007. *Mechanical behaviour of engineering materials metals, ceramics, polymers, and composites*. Berlin Heidelberg: Springer-Verlag.

Rowell, R., A. R. Sanadi, D. F. Caulfield, and R. E. Jacobson. 1997. Utilization of natural fibres in plastic composites: Problems and opportunities. In *Lignocellulosic-plastics composites*, ed. A. L. Leao, F. X. Carvalho, and E. Frollini, 23-51. Sao Paulo, Brazil: Universidade de Sao Paulo Press.

Ruoyuan, S., K. Teruo, and I. Haruhiro. 2010. Papermaking from waste silk and its application as reinforcement of green composites. *Journal of Textile Engineering* 56(3): 71-76.

Saari, P., H. Heikkilä, and M. Hurme. 2010. Adsorption equilibria of arabinose, fructose, galactose, glucose, mannose, rhamnose, sucrose, and xylose on ion-exchange resins. *Journal of Chemical & Engineering Data* 55 (9): 3462-3467.

http://dx.doi.org/10.1021/je100165v (accessed 2011/09/28).

Sanadi, A. R., R. A. Young, C. Clemons, and R. M. Rowell. 1994. Recycled newspaper fibres as reinforcing fillers in thermoplastics: Part I-analysis of tensile and impact properties in polypropylene. *Journal of Reinforced Plastics and Composites* 13 (1): 54-67.

Sánchez-Soto, M., P. Pagés, T. Lacorte, K. Briceño, and F. Carrasco. 2007. Curing FTIR study and mechanical characterization of glass bead filled trifunctional epoxy composites. *Composites Science and Technology* 67 (9): 1974-1985.

Satapathy, A., J. Alok Kumar, S. Mantry, S. K. Singh, and A. Patnaik. 2009. Processing and characterization of jute-epoxy composites reinforced with SiC derived from rice husk. *Journal of Reinforced Plastics and Composites* 29 (18): 2869-2878.

Sgriccia, N., M. C. Hawley, and M. Misra. 2008. Characterization of natural fibre surfaces and natural fibre composites. *Composites Part A: Applied Science and Manufacturing* 39 (10): 1632-1637.

Shenoy, M. A., and D. J. D'Melo. 2009. Effect of water on mechanical properties of unsaturated polyester-acetylated hydroxypropyl guar gum composites. *Journal of Reinforced Plastics and Composites* 28: 2561-2576.

Shih, Y.-F. 2007. Mechanical and thermal properties of waste water bamboo husk fibre reinforced epoxy composites. *Materials Science and Engineering: A* 445–446 (0): 289-295.

Shokrieh, M. M., A. R. Kefayati, and M. Chitsazzadeh. 2012. Fabrication and mechanical properties of clay/epoxy nanocomposite and its polymer concrete. *Materials & Design* 40 (0): 443-452.

Singh, R. P., M. Zhang, and D. Chan. 2002. Toughening of a brittle thermosetting polymer: Effects of reinforcement particle size and volume fraction. *Journal of Materials Science* 37: 781– 788.

Sonawane, S. H., P. L. Chaudhari, S. A. Ghodke, M. G. Parande, and V. M. Bhandari. 2009. Ultrasound assisted synthesis of polyacrylic acid–nanoclay nanocomposite and its application in sonosorption studies of malachite green dye. *Ultrasonics Sonochemistry* 16: 351–355

Shukla, D. K., S. V. Kasisomayajula, and V. Parameswaran. 2008. Epoxy composites using functionalized alumina platelets as reinforcements. *Composites Science and Technology* 68 (14): 3055-3063.

Sinha Ray, S., and M. Okamoto. 2003. Polymer/layered silicate nanocomposites: A review from preparation to processing. *Progress in Polymer Science* 28 (11): 1539-1641.

Sombatsompop, N., and K. Chaochanchaikul. 2004. Effect of moisture content on mechanical properties, thermal and structural stability and extrudate texture of poly(vinyl chloride)/wood sawdust composites. *Polymer International* 53 (9): 1210-1218.

Stadtländer, C. T. K.-H. 2007. Scanning electron microscopy and transmission electron microscopy of mollicutes: Challenges and opportunities. In *Modern research and educational topics in microscopy*, ed. A. Méndez-Vilas and J. Díaz, 122-131. Spain: Formatex.

Stamboulis, A., C. A. Baillie, and T. Peijs. 2001. Effects of environmental conditions on mechanical and physical properties of flax fibres. *Composites Part A: Applied Science and Manufacturing* 32 (8): 1105-1115.

Taib, R.M. 1998. Cellulose fibre-reinforced thermoplastic composites: Processing and products characteristics. *M.S Thesis*. Virginia Tech, Blacksburg. Virginia.

Taj, S., M. A. Munawar, and S. Khan. 2007. Review natural fibre-reinforced polymer composites. *Proceedings of the Pakistan Academy of Sciences* 44 (2): 129-144.

Tang, Y., S. Deng, L. Ye, C. Yang, Q. Yuan, J. Zhang, and C. Zhao. 2011. Effects of unfolded and intercalated halloysites on mechanical properties of halloysite–epoxy nanocomposites. *Composites Part A: Applied Science and Manufacturing* 42 (4): 345-354.

Technical Information of Imerys Tableware Asia Limited. 2011.

http://www.nzcc.co.nz/technical1.htm (accessed July, 2011).

Technical Information of Sigma-Aldrich. LLC. 2011.

http://www.sigmaaldrich.com/australia.html (accessed August, 2011).

Tjong, S. C. 2006. Structural and mechanical properties of polymer nanocomposites. *Materials Science and Engineering: R: Reports* 53 (3-4): 73-197.

Tserki, V., N. E. Zafeiropoulos, F. Simon, and C. Panayiotou. 2005. A study of the effect of acetylation and propionylation surface treatments on natural fibres. *Composites Part A: Applied Science and Manufacturing* 36 (8): 1110-1118.

Usuki, A., Y. Kojima, M. Kawasumi, A. Okada, Y. Fukushima, T. Kurauchi, and O. Kamigaito. 1993. Synthesis of nylon 6-clay hybrid. *Journal of Materials Research* 8: 1179-1184

Valera-Zaragoza, M., E. Ramírez-Vargas, F. J. Medellín-Rodríguez, and B. M. Huerta-Martínez. 2006. Thermal stability and flammability properties of heterophasic PP–

EP/EVA/organoclay nanocomposites. *Polymer Degradation and Stability* 91 (6): 1319-1325.

Wada, M., L. Heux, and J. Sugiyama. 2004. Polymorphism of cellulose I family: Reinvestigation of cellulose IV$_I$. *Biomacromolecules* 5: 1385-1391.

Wambua, P., J. Ivens, and I. Verpoest. 2003. Natural fibres: can they replace glass in fibre reinforced plastics? *Composites Science and Technology* 63 (9): 1259-1264.

Wang, B., S. Panigrahi, L. Tabil, and W. Crerar. 2007. Pre-treatment of flax fibres for use in rotationally molded biocomposites. *Journal of Reinforced Plastics and Composites* 26 (5): 447-463.

Wang, H., K. C. Sheng, T. Lan, M. Adl, X. Q. Qian, and S. M. Zhu. 2010. Role of surface treatment on water absorption of poly(vinyl chloride) composites reinforced by Phyllostachys pubescens particles. *Composites Science and Technology* 70 (5): 847-853.

Wang, L., K. Wang, L. Chen, C. He, and Y. Zhang. 2006. Hydrothermal effects on the thermomechanical properties of high performance epoxy/clay nanocomposites. *Polymer Engineering & Science* 46 (2): 215-221.

Wang, Y., J. Gao, Y. Ma, and U. S. Agarwal. 2006. Study on mechanical properties, thermal stability and crystallization behavior of PET/MMT nanocomposites. *Composites Part B: Engineering* 37 (6): 399-407.

Wetzel, B., P. Rosso, F. Haupert, and K. Friedrich. 2006. Epoxy nanocomposites – fracture and toughening mechanisms. *Engineering Fracture Mechanics* 73 (16): 2375-2398.

White J. R., and S. K. De. 1996. Survey of short fibre-polymer composites. In *Short fibre-polymer composites*, ed. S. K. De and J. R. White, 1-19. Cambridge: Woodhead Publishing.

Wypych, F., and K. G. Satyanarayana. 2005. Functionalization of single layers and nanofibres: a new strategy to produce polymer nanocomposites with optimized properties. *Journal of Colloid and Interface Science* 285 (2): 532-543.

Xu, Y., and S. V. Hoa. 2008. Mechanical properties of carbon fibre reinforced epoxy/clay nanocomposites. *Composites Science and Technology* 68 (3-4): 854-861.

Yasmin, A., J. L. Abot, and I. M. Daniel. 2003. Processing of clay/epoxy nanocomposites by shear mixing. *Scripta Materialia* 49 (1): 81-86.

Yasmin, A., J. J. Luo, J. L. Abot, and I. M. Daniel. 2006. Mechanical and thermal behavior of clay/epoxy nanocomposites. *Composites Science and Technology* 66 (14): 2415-2422.

Ye, Y., H. Chen, J. Wu, and C. M. Chan. 2011. Evaluation on the thermal and mechanical properties of HNT-toughened epoxy/carbon fibre composites. *Composites Part B: Engineering* 42 (8): 2145-2150.

Ye, Y., H. Chen, J. Wu, and L. Ye. 2007. High impact strength epoxy nanocomposites with natural nanotubes. *Polymer* 48 (21): 6426-6433.

Yeh, J.-M., H.-Y. Huang, C.-L. Chen, W.-F. Su, and Y.-H. Yu. 2006. Siloxane-modified epoxy resin–clay nanocomposite coatings with advanced anticorrosive properties prepared by a solution dispersion approach. *Surface and Coatings Technology* 200 (8): 2753-2763.

Yeoman, B., and L. Paisley. 2005. *Raging inexorable thunderlizard for change: out, out, brown spot; or, ceiling tile alternatives*.

http://heasc.aashe.org/sites/heasc1.drupalgardens.com/files/2005%20Spring%20Out%20out%20Brown%20spot.pdf (accessed May 2011).

Yong, V., and H. T. Hahn. 2009. Monodisperse SiC/vinyl ester nanocomposites: Dispersant formulation, synthesis, and characterization. *Journal of Materials Research* 24 (4): 1553-1558.

Yudin, V. E., J. U. Otaigbe, V. M. Svetlichnyi, E. N. Korytkova, O. V. Almjasheva, and V. V. Gusarov. 2008. Effects of nanofiller morphology and aspect ratio on the rheo-mechanical properties of polyimide nanocomposites. *Express Polymer Letters* 2, (7): 485–493.

Zainuddin, S., M. V. Hosur, Y. Zhou, A. T. Narteh, A. Kumar, and S. Jeelani. 2010. Experimental and numerical investigations on flexural and thermal properties of nanoclay–epoxy nanocomposites. *Materials Science and Engineering: A* 527 (29-30): 7920-7926.

Zaman, H. U., M. A. Khan, and R. A. Khan. 2011. A comparative study on the mechanical and degradation properties of plant fibres reinforced polyethylene composites. *Polymer Composites* 32 (10): 1552-1560.

Zanetti, M., and L. Costa. 2004. Preparation and combustion behaviour of polymer/layered silicate nanocomposites based upon PE and EVA. *Polymer* 45 (13): 4367-4373.

Zhang, Y., Q. Liu, Q. Zhang, and Y. Lu. 2010. Gas barrier properties of natural rubber/kaolin composites prepared by melt blending. *Applied Clay Science* 50 (2): 255-259.

Zhao, C., H. Qin, F. Gong, M. Feng, S. Zhang, and M. Yang. 2005. Mechanical, thermal and flammability properties of polyethylene/clay nanocomposites. *Polymer Degradation and Stability* 87 (1): 183-189.

Zhao, H., and R. K. Y. Li. 2008. Effect of water absorption on the mechanical and dielectric properties of nano-alumina filled epoxy nanocomposites. *Composites Part A: Applied Science and Manufacturing* 39 (4): 602-611.

Zhao, S., L. Schadler, H. Hillborg, and T. Auletta. 2008. Improvements and mechanisms of fracture and fatigue properties of well-dispersed alumina/epoxy nanocomposites. *Composites Science and Technology* 68 (14): 2976-2982.

Zhou, T., X. Wang, G. U. Mingyuan, and X. Liu. 2008. Study of the thermal conduction mechanism of nano-SiC/DGEBA/EMI-2,4 composites. *Polymer* 49 (21): 4666-4672.

Zulfli, N. H. M., and C. W. Shyang. 2010. Flexural and morphological properties of epoxy/ glass fibre/silane-treated organo montmorillonite composites. *Journal of Physical Science* 21 (2): 41–50.

Hatem Alamri

Signature

Date: 13th July 2012